TARGETING HAMMERHEAD RIBOZYMES AGAINST HEPATITIS B VIRUS

RICHARD SMITH

A THESIS PRESENTED FOR THE DEGREE OF

DOCTOR OF PHILOSOPHY

in

THE INSTITUTE OF BIOMEDICAL AND LIFE SCIENCES,

THE FACULTY OF SCIENCE, UNIVERSITY OF GLASGOW

Division of Virology,
Church Street,
Glasgow,
G11 5JR.

February 1998

ProQuest Number: 13818628

All rights reserved

INFORMATION TO ALL USERS
The quality of this reproduction is dependent upon the quality of the copy submitted.

In the unlikely event that the author did not send a complete manuscript
and there are missing pages, these will be noted. Also, if material had to be removed,
a note will indicate the deletion.

ProQuest 13818628

Published by ProQuest LLC (2018). Copyright of the Dissertation is held by the Author.

All rights reserved.
This work is protected against unauthorized copying under Title 17, United States Code
Microform Edition © ProQuest LLC.

ProQuest LLC.
789 East Eisenhower Parkway
P.O. Box 1346
Ann Arbor, MI 48106 – 1346

GLASGOW UNIVERSITY
LIBRARY
11330 (copy 1)

UNIVERSITY OF GLASGOW

THESIS ACCESS DECLARATION

Candidate's Name (BLOCK LETTERS) ....

Thesis title TARGETING HAMMERHEAD RIBOZYMES AGAINST HEPATITIS B VIRUS

I understand that in the interests of good scholarship, theses of the University are normally made freely available for consultation in the University Library, or within another library, immediately after deposit but that a candidate may stipulate a period of either one or three years after deposit during which his or her written consent must be sought before such access is given. (A candidate is usually advised by the supervisor if commercial or patent reasons make this restriction desirable).

I therefore agree to grant access and permit copies to me bade for other libraries or individuals without my specific authorisation:

*A	Immediately on deposit	OR
*B	One year after deposit	OR
*C	Three years after deposit	

I further accept that candidates who stipulate written consent but from whom no reply has been received within three months of a request from the University Library posted to their last known address will be assumed to have ceded this power to the Library Committee, to be exercised in consultation with the Higher Degrees Committee of the Faculty.

Signed

Date

GUL
07 JAN 1999
11330

* PLEASE CIRCLE **either** A **or** B **or** C ABOVE

SUMMARY

Hammerhead ribozymes are RNA motifs found in a number of plant viroids which possess an autocatalytic function for cleaving intramolecular phosphodiester bonds. The hammerhead motif consists of a conserved catalytic core of 22 nucleotides which is flanked by sequences of varying length which hybridise to the target region of the substrate RNA through Watson-Crick base-pair interactions. The flanking sequences can be manipulated to enable the hammerhead motif to function in a *trans*-conformation and cleave any RNA molecule after a triplet motif with the consensus sequence 'NUX', where N can be any nucleotide and X any nucleotide with the exception of guanosine. There has been considerable interest in the potential of hammerhead ribozymes as therapeutic gene silencing agents for the treatment of dominant-negative genetic disorders, tumours and chronic viral infections. The current study has focused on hammerhead ribozymes targeted against hepatitis B virus (HBV). The ribozyme-mediated cleavage reaction has been split into two components: hybridisation and phosphodiester bond cleavage. The influence of substrate RNA secondary structure on both of these steps has been investigated.

A potential stem-loop in the HBV core protein open reading frame was identified by computer modelling. Five hammerhead ribozymes with total flanking sequences of 16 bases were targeted against NUX triplets in this stem-loop. Ribozyme-substrate hybridisation was studied by gel-shift assay utilising radiolabelled ribozymes with an unlabelled excess of either a 60-base truncated substrate corresponding to the stem-loop, or a 639-base substrate corresponding to the entire core protein open reading frame. The ribozymes were shown to bind more strongly to the 639-base substrate. This was thought to be due to the 60-base substrate forming aggregates in which the ribozyme binding sites were inaccessible. Increasing the length of the ribozyme flanking sequences from 16 to 59 bases increased the strength of binding. The strength of ribozyme-substrate hybridisation was not related to the predicted extent of double-stranded RNA in the target region of the substrate.

The rate of ribozyme-mediated cleavage was determined under single-turnover conditions, with radiolabelled 60-base substrate and an excess of unlabelled ribozyme. Strong hybridisation did not necessarily confer a rapid rate of cleavage. Two ribozymes, RZ572 and RZ572B, targeted against the same NUX triplet, had different flanking sequences (RZ572, total flanking sequence of 16 bases; RZ572B, total flanking sequence of 59 bases). Although RZ572B has a seven-fold higher affinity for the substrate than RZ572, RZ572 has a five-fold higher cleavage rate. It is thought that this is due to changes in the substrate secondary structure influenced by the binding of the ribozyme flanking sequences. It is proposed that a highly structured substrate RNA promotes rapid ribozyme-mediated cleavage as a result of increased torsional stress within the phosphodiester bonds. However,

the substrate secondary structure should not prevent the ribozyme and substrate from hybridising.

The activity of the ribozymes in the rabbit reticulocyte lysate cell-free translation system was determined. Only one ribozyme, RZ534, when transcribed *in situ*, induced a decrease of 20% in core protein production relative to a luciferase control. This ribozyme did not demonstrate any cleavage activity in the earlier *in vitro* studies. Primer extension analysis of RNA extracted from the reticulocyte lysate reactions showed that no cleavage products were generated by any of the ribozymes used, suggesting that the inhibition seen with RZ534 was the result of an antisense mechanism. Repeating the experiment with *in vitro* synthesized ribozyme RNA did not result in any inhibition of protein synthesis, suggesting that the antisense inhibition previously seen was caused by the RZ534 DNA transcription template.

The disparity between the results obtained with the 60-base and 639-base substrates, and between the purified RNA and cell-free translation experiments, and the large inaccuracies seen in the techniques used raises concerns about the validity of this and many other earlier *in vitro* studies, and their relevance to *in vivo* conditions. It may be better to discard such methodologies, replacing them with intracellular screening and *in vitro* evolution of RNA libraries.

CONTENTS

ABBREVIATIONS

ε	Encapsidation signal
2'5'OAS	2'5'-oligoadenylate synthase
3TC	3'-thiacytidine (lamivudine)
A	Adenosine
Ab	Antibody
ABTS	2,2-azino-di-[3-ethylbenzthiazoline sulfonate]
Ag	Antigen
ALT	Alanine aminotransferase
AMP	Adenosine monophosphate
ARA-A	Adenosine arabinoside
ARA-AMP	Adenosine arabinoside mono-phosphate
ASBV	Avocado sunblotch viroid
ATP	Adenosine triphosphate
BIO	Biotin
C	Cytosine
CTP	Cytosine triphosphate
cccDNA	Covalently closed circular DNA
C/EBP	CCAAT/ enhancer binding protein
CTL	Cytotoxic T-lymphocyte
dA	Deoxyadenosine
dC	Deoxycytosine
dG	Deoxyguanosine
dT	Deoxythymidine
dU	Deoxyuridine
ddA	Dideoxyadenosine
ddC	Dideoxycytosine
ddG	Dideoxyguanosine
ddT	Dideoxythymidine
ddU	Dideoxyuridine
DEPC	Diethylpyrocarbonate
DHBV	Duck hepatitis B virus
DIG	Digoxigenin
DNA	Deoxyribonucleic acid
dNTP	Deoxynucleotide triphosphate
ds	Double-stranded
DTT	Dithiothreitol
EDTA	Ethylenediaminetetra-acetate
EGS	External guide sequence
ELISA	Enzyme-linked immunosorbant assay
Enh	Enhancer
ER	Endoplasmic reticulum
G	Guanosine
GTP	Guanosine triphosphate
HBcAg	Core antigen
HBeAg	e-antigen
HBsAg	Surface antigen
HBx	X protein
HBV	Hepatitis B virus
HCC	Human hepatocellular carcin-oma
HCV	Hepatitis C virus
HDV	Hepatitis delta virus
HIV	Human immunodeficiency virus
HLA	Human leucocyte antigen
HNF	Hepatocyte nuclear factor
IFN	Interferon
IL	Interleukin
LHBs	Large surface protein
LTR	Long terminal repeat
MHBs	Middle surface protein
MHC	Major histocompatability complex

mRNA	Messenger RNA
NA	Nucleic acid
nt	Nucleotide
OD	Optical density
ORF	Open reading frame
PAGE	Polyacrylamide gel electrophoresis
P-AP	Peroxidase-anti-peroxidase
PCR	Polymerase chain reaction
pgRNA	Pre-genomic RNA
PKR	Protein kinase R
PNA	Peptide nucleic acid
R	Purine
RNA	Ribonucleic acid
RNase	Ribonuclease
rpm	Revolutions per minute
rRNA	Ribosomal RNA
RT	Reverse transcriptase
SDS	Sodium dodecyl sulphate
SHBs	Small surface protein
SIV	Simian immunodeficiency virus
ss	Single-stranded
T	Thymidine
TdT	Terminal deoxynucleotidyl transferase
TTP	Thymidine triphosphate
TFO	Triplex-forming oligonucleotide
Th	T-helper cell
TNF	Tumour necrosis factor
tRNA	Transfer RNA
U	Uridine
UTP	Uridine triphosphate
UV	Ultraviolet
WHV	Woodchuck hepatitis virus
Y	Pyrimidine

LIST OF FIGURES

LIST OF TABLES

ACKNOWLEDGEMENTS

I am grateful to Dr. H. Marsden, and Professors J. B. Clements and D. McGeogh, who have contributed by running the Institute of Virology.

I would like to thank my supervisor, Dr. Bill Carman, for his support and boundless enthusiasm throughout this project, even when it looked like the ribozymes would never work, and for many fascinating 'lab meetings' (*e.g.* 'The Lion King', 'Independence Day', 'Star Wars' etc.).

All the members of lab 109, past and present, deserve many thanks for making my time in Glasgow so much fun. Special mentions have to go to Dr. Lesley Wallace, without whom lab 109 would cease to function, Winnie Boner, Mahmuda Yasmin and David Williams for showing me that doing a PhD isn't impossible, and Ricky van Deursen and Ed Dornan for being great travelling companions through Italy and France. Thanks also go to everyone in the washroom, media, stores and front office for all their help and good humour.

Special thanks have to go to Dr. Georg Sczakiel and his laboratory at the Deutscheskrebsforschungzentrum, Heidelberg, in particular Wolfgang Nedbal, Robert Hormes, Volke Patzel and Sigrid Eckhardt, for helping get my project working, and for making me so welcome.

I am very grateful to the many great friends I have made in my time in Glasgow, in particular Ross Reid and Russell Thompson, and all the hillwalking crowd, especially Paul Hodge, and Terry Collins for teaching me everything he knows about hillwalking (though I still haven't got lost or seriously injured yet). A big thank you to Kathy Williams, Marie Anderson, and Liz Homer for two great Hogmanays up on the Isle of Lismore. I am especially grateful to Meeta Kathoria for always being there when things weren't going well, putting up with my bad moods, and for being willing to proof-read this thesis.

I have to especially give thanks to Helen Attrill, for making the time I spent writing up a lot more enjoyable, and for being incredibly supportive.

Finally I have to thank my family, especially my parents, for their love, support and encouragement over the years, without which none of this would have been possible.

The author was the recipient of a Wellcome Trust Prize Studentship. Unless otherwise stated, all of the work presented in this thesis was carried out by the author.

Richard Smith February 1998

Basic research is what I am doing when I don't know what I'm doing.

Wernher von Braun.

The most exciting phrase to hear in science, the one that heralds the most discoveries, is not 'Eureka!' (I found it!), but 'That's funny.....'

Isaac Asimov.

CHAPTER 1 INTRODUCTION

1.1 HEPATITIS B INFECTION

The World Health Organisation estimates that approximately two billion people have been infected with hepatitis B virus (HBV). Most of these patients have an acute infection, defined as clearing the virus in less than six months after infection. However, approximately 350 million persons are chronically infected, with infection lasting more than six months. Fifty percent of these patients will eventually clear the virus or suffer a subclinical infection, but the other fifty percent will die prematurely from viral-induced cirrhosis or primary hepatocellular carcinoma. HBV is the prototype virus of the family *Hepadnaviridae*, which also includes viruses which infect duck, heron, ground squirrel and woodchuck. Hepadnaviruses are not thought to be cytopathic; both acute and chronic hepatitis B result from the immune response eliminating HBV infected cells. The pathogenesis of chronic carriage is explained by an individual's immune status; note that neonates and the immunocompromised develop a chronic infection. Despite an intensive vaccination programme, over one million people a year die as a result of HBV infection. Current antivirals have limited efficacy either because of specific immune deficits or because of viral resistance. They are also too expensive for widespread use in the developing world. To understand their antiviral mechanisms, we first need to examine the molecular biology of the virus.

1.2 HEPATITIS B VIRUS

HBV is the smallest known human virus. The virion, or Dane particle, has a diameter of 42nm, containing within its 7nm thick outer lipid envelope an icosahedral capsid with a diameter of 21nm and a partially double stranded circular genome of 3.2kb (figure 1.1). The genome contains four overlapping open reading frames (ORFs) encoding the viral polymerase, the surface envelope glycoproteins (LHBs, MHBs and SHBs), the core capsid protein (HBc), the secreted e-antigen (HBeAg), and the poorly characterised X protein (HBx). In addition to the viral proteins, the virion also includes a cellular protein kinase (Kann *et al.*, 1993).

1.2.1 HBV polymerase

The 90kDa HBV polymerase can be divided into four domains.

1) The N-terminal primase domain. This region is covalently linked via a tyrosine residue to the 5' end of the minus-strand of the virion DNA and is necessary for priming minus-strand synthesis.
2) The spacer or tether domain which, despite being necessary for polymerase function, has no specific function of its own.

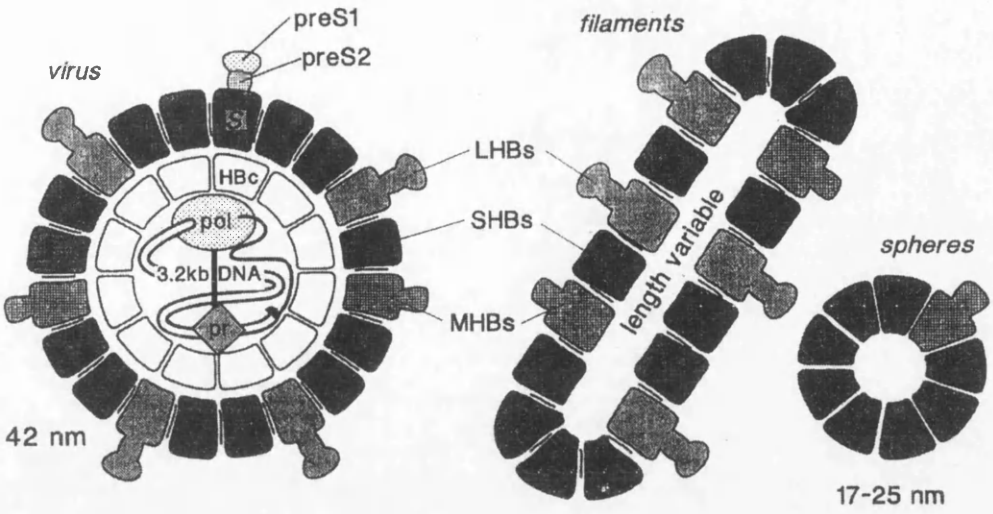

Figure 1.1a. The HBV virion (or Dane particle) and non-infectious filaments. The nucleocapsid (consisting of HBcAg) contains the relaxed, circular DNA and polymerase, which are covalently linked via the polymerase terminal (primase) domain. The nucleocapsid is surrounded by a lipid envelope derived from hepatocytes, in which is embedded the L, M and S forms of HBsAg. The non-infectious filaments and spheres are composed of just the three surface proteins. Taken from Gerlich, (1993a)

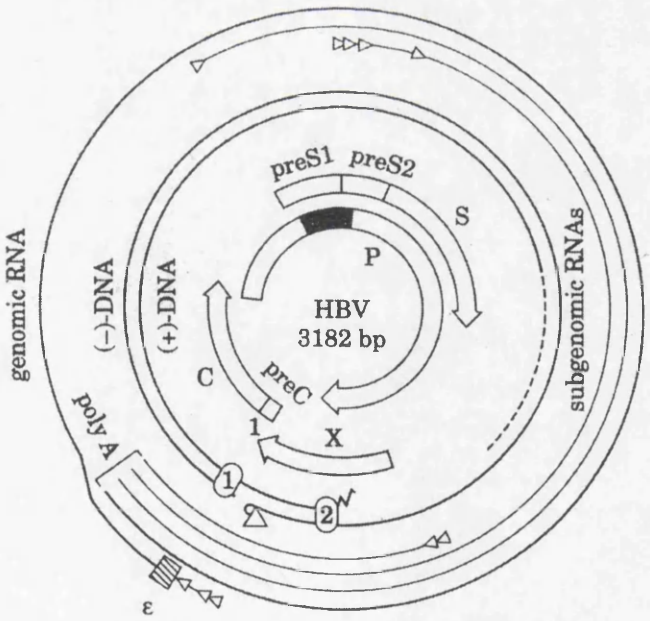

Figure 1.1b HBV genome organization. The outer lines represent the various classes of RNA transcripts, with the encapsidation signal, ε, indicated. The viral promoters are indicated as triangles The inner lines represent the partially double-stranded DNA genome, with the repeats DR1 and DR2 indicated as boxes 1 and 2 respectively. The central arrows represent the four major ORFs, pre-core (pre-C)/core (C), surface (pre-S1/preS-2/S), polymerase (P) and X. Taken from Gerlich, (1993a).

3) The reverse transcriptase domain, encoding the nucleic acid-dependent polymerase activity.
4) The C-terminal RNase H domain, responsible for digesting the RNA strand of the pregenomic (pg) RNA-minus strand DNA hybrid (Radziwill *et al.*, 1990).

Although recombinant polymerase is active in the absence of pgRNA and HBc (Seifer & Standring, 1993), the polymerase is only packaged in the presence of pgRNA which only carries one functional encapsidation signal. It is thought that only one polymerase molecule is packaged per virion. However, it is possible that the polymerase could be packaged as a multimer. The polymerase has been targeted with a range of antiviral nucleoside analogues (see section 1.8).

1.2.2 Envelope proteins

The pre-S1/pre-S2/S ORF encodes three glycoproteins, translated from three different start codons, but all having identical carboxy termini. The small HBs (SHBs) protein (24 kD) is encoded by the S region of ORF S and is translated from the third AUG. The N termini of the large (LHBs, 39 kD) and medium (MHBs, 33 kD) surface proteins are encoded by the pre-S1 and pre-S2 regions respectively (Heermann *et al.*, 1984, Stibbe & Gerlich, 1983a). In carriers with high viraemia, non-infectious particles composed of excess HBsAg can be found in the serum. The morphology of these particles varies from spheres with a diameter of 17 to 25 nm to less numerous filaments with a 20 nm diameter and variable length. When the LHBs protein is overexpressed relative to the two smaller proteins, HBsAg accumulates in the ER (endoplasmic reticulum). The ER dilates and the hepatocytes appear opaque when examined by light microscopy, becoming known as 'ground glass' cells (Chisari *et al.*, 1987, Gallina *et al.*, 1994).

SHBs is very rich in hydrophobic residues. Computer modelling suggests that these hydrophobic domains form four α–helical transmembrane domains (Berting *et al.*, 1995, Stirk *et al.*, 1992). Helices III and IV are amphipathic. It is predicted that this polarity will allow SHBs to multimerize within the lipid bilayer, potentiating the budding of HBs particles into the ER lumen (Simon *et al.*, 1988). This is supported by studies which have shown that HBs with helices III and IV deleted cannot escape from the ER. It also has an unusually high number of 14 cysteines, all of which are crosslinked. Treatment of SHBs particles with dithiothreitol breaks the disulphide bonds and can render these particles non-immunogenic . A signal for N-linked glycosylation is found at asparagine-146 (Peterson *et al.*, 1982).

The MHBs protein is a minor virion component, with its N-terminal 55 amino acids being derived from the pre-S2 domain. The pre-S2 domain is exposed on the outside of the virion and is susceptible to protease degradation (Stibbe & Gerlich, 1983b). The asparagine at position 4 is glycosylated. The epitopes in this region are not conformation dependent, suggesting this region is very flexible (Heermann *et al.*, 1987). Peptides with the N-terminal

pre-S2 sequence have been shown to induce protective immunity. This has led to considerable interest in incorporating the pre-S1 and pre-S2 regions into the HBV vaccine, which only comprises of the SHBs protein in commercially available vaccines.

In the LHBs protein, the pre-S1 domain masks the pre-S2 domain. This prevents the glycosylation of asparagine 4 in pre-S2. However, the pre-S1 domain becomes myristoylated at the N terminus, anchoring it in the membrane. Myristoylation is essential for virus infectivity *in vitro* (Bruss *et al.*, 1996b). Although LHBs is inserted into the membrane cotranslationally, its topology is believed to alter after translation is complete (Bruss *et al.*, 1994)

1.2.3 HBc protein

The HBc protein has either 183 or 185 amino acids, depending on the virus genotype. Translation begins from the second start codon of ORF C, 29 codons downstream of the first . This upstream region is termed pre-core, and forms the N-terminal of the secreted form of HBc, called the e antigen (HBeAg).

HBc contains many charged amino acids. The only post-translational modification is phosphorylation when it is expressed in eukaryotic cells (Machida *et al.*, 1991, Roossinck & Siddiqui, 1987). The dynamics of capsid assembly have been studied in *Xenopus* oocytes (Zhou *et al.*, 1992, Zhou & Standring, 1991). Once synthesised in the cytoplasm, HBc is translocated to the nucleus where it first dimerizes (Zhou & Standring, 1992a). Once the concentration of dimers reaches 0.8μM, they self-assemble into isometric particles with T3 symmetry containing 180 HBc subunits. These particles contain the pgRNA, the viral polymerase and a cellular protein kinase C, though empty particles are also observed (Pasek *et al.*, 1979). Once assembled the particles are stabilised by disulphide bonds (Nassal, 1992b, Zhou & Standring, 1992b).

HBc contains two distinct domains which have been defined by mutational analysis. The first 147 or 149 amino acids form a protease resistant hydrophobic domain which is necessary for core particle formation (Seifer & Standring, 1995). The key motif in this region is thought to be a heptad repeat of hydrophobic residues which may form a leucine zipper-like domain. Deletion analysis has shown that a minimum of the first 139 amino acids is required for core particle formation. The final 36 residues are protease sensitive, and are therefore not thought to have any tight structure; this protamine-like domain is extremely arginine-rich (Gallina *et al.*, 1989). The arginines are clustered in four blocks, three of which have the sequence SPRRR(R), and are thought to be involved in binding nucleic acids (Nassal, 1992a). Effective encapsidation requires at least the first 164 amino acids. However, virus variants in which the core polypeptide ends at residue 164 have severely impaired ability to complete positive strand DNA synthesis, making HBc a vital component in virus genome replication. Deletion of the first 10 residues at the N-terminal end prevents

formation of core particles, though substitution of core sequence at the C-terminal and in the epitope regions does not impair particle formation (Seifer & Standring, 1995). The minimal assembly domain lies between residues 10 and 144 (Birnbaum & Nassal, 1990).

A number of deletions in the central portion of the core ORF have been detected in clinical samples. The importance of these deletions is unclear; they are unable to form hybrid particles with wild-type HBcAg (Williams, 1997). The presence of these deletions is sometimes associated with increased severity of disease. Wild-type HBcAg shows cell-cycle dependent intracellular localisation. The protein is present in the nucleus in G1 and G2, but is found in the cytoplasm during S phase. The deletions described here show distribution throughout the nucleus and cytoplasm, possibly resulting from the deletion lying just upstream of the nuclear localisation signal. Although the relevance of these observations is unclear, they may be linked to the severe chronic disease seen in these patients.

1.2.4 HBe antigen

The pre-core region of ORF C encodes a hydrophobic α-helix which functions as a secretion signal, allowing HBeAg to be translocated into the ER lumen in its unprocessed form as p25e (Ou *et al.*, 1986). Following translocation, 19 of the 29 pre-core amino acids are removed by host signal peptidase to give p23e. The remaining 10 amino acids prevent HBeAg assembling into particles (Wasenauer *et al.*, 1992). p23e is either secreted, becomes embedded in the plasma membrane (Bruss & Gerlich, 1988), or undergoes further cleavage in the C-terminal protamine-like domain to give three truncated proteins, p16e, p18e and p20e, all of which are secreted . Sometimes uncleaved p25e can be found remaining in the cytoplasm (Garcia *et al.*, 1988).

HBeAg is not essential for the viral life cycle (Schlicht & Schaller, 1988). Mutations in the pre-core region can yield viable virus which does not produce HBeAg during chronic or acute infection (see section 1.4.2) (Carman *et al.*, 1989). This can complicate monitoring of disease progression, as HBeAg has been used as a marker of viral replication, with loss of HBeAg along with the appearance of anti-HBe antibodies being taken as an indicator of resolution of disease (loss of HBeAg indicates a good prognosis during interferon treatment). However, there are patients, particularly of Far Eastern or Mediterranean origin, for whom loss of HBeAg leads to more severe disease. It is also important to note that patients who are anti-HBe positive fail to respond as well to interferon as HBeAg positive patients. There have been reports of patients in which HBeAg was undetectable by serological methods following interferon treatment, but DNA sequencing revealed wild-type virus. It is speculated in these cases that HBeAg is still being produced, but is contained entirely within immune complexes.

HBeAg is believed to induce tolerance (Milich *et al.*, 1993b), particularly in neonatal infections, by stimulating a Th2 response, which downregulates the CTL response which

would otherwise cause disease (see section 1.4.2). It has also been suggested that HBeAg may enter the thymus of neonates, and promote the deletion of HBeAg/HBcAg reactive T-helper clones. However, the role of HBeAg in adult infections, of which only 5% become chronic, is unclear (Aldershvile *et al.*, 1980). Transient overexpression of HBeAg has been shown to suppress viral replication through the interaction of p23e with HBcAg, to form hybrid core particles which are unable to support encapsidation (Guidotti *et al.*, 1996b, Scaglioni *et al.*, 1997).

1.2.5 HBx protein

The HBx protein is produced at extremely low abundance. Its role has yet to be determined in HBV. It has been thought that it may play no useful role in infection, as avian hepadnaviruses lack an equivalent to HBx. *In vitro* experiments with HBV HBx have implied that HBx is not necessary for infectivity (Blum *et al.*, 1992). However, experiments in the woodchuck, using viruses in which the X ORF is disrupted by a nonsense mutation, show that the X protein is essential for the establishment of infection (Zoulim *et al.*, 1994).

In vitro experiments have suggested a role for HBx in gene transactivation (Arii *et al.*, 1992), with interactions with ras and rel signalling proteins having been reported (Klein & Schneider, 1997). HBx has been shown to bind indirectly to HBV enhancer I (Enh-I) via the AP-1 and CREB transcription factors (Benn *et al.*, 1996). Over-expression experiments in cell culture have suggested interactions with p53 (Truant *et al.*, 1995) and protein kinase C, as well as suggesting HBx may induce apoptosis (Su & Schneider, 1997). Other cell culture experiments have implied that HBx is tumourigenic (Seifer *et al.*, 1991), whilst transgenic mice over-expressing HBx develop hepatocellular carcinoma (Koike *et al.*, 1994). However, the implications of these experiments must be carefully considered, as they all involve levels of HBx many times greater than that found in a normal infection. Other activities attributed to HBx include serine/threonine kinase (Wu *et al.*, 1990), AMP kinase (Dopheide & Azad, 1996) and kunitz-type serine protease inhibitor activities. The latter activity may be significant when the interaction between HBx and the proteasome complex is considered (Fischer *et al.*, 1995).

1.3 VIRAL LIFE CYCLE

The HBV lifecycle can be split into several stages (figure 1.2). These are attachment to the host cell surface, penetration of the host cell, viral gene expression, genome replication and the production and release of new virion particles.

1.3.1 Attachment to the cell membrane

This is the first stage in determining the host range and tissue tropism of a virus (Gerlich *et al.*, 1993b). Identification of the HBV receptor has been slowed by the lack of a

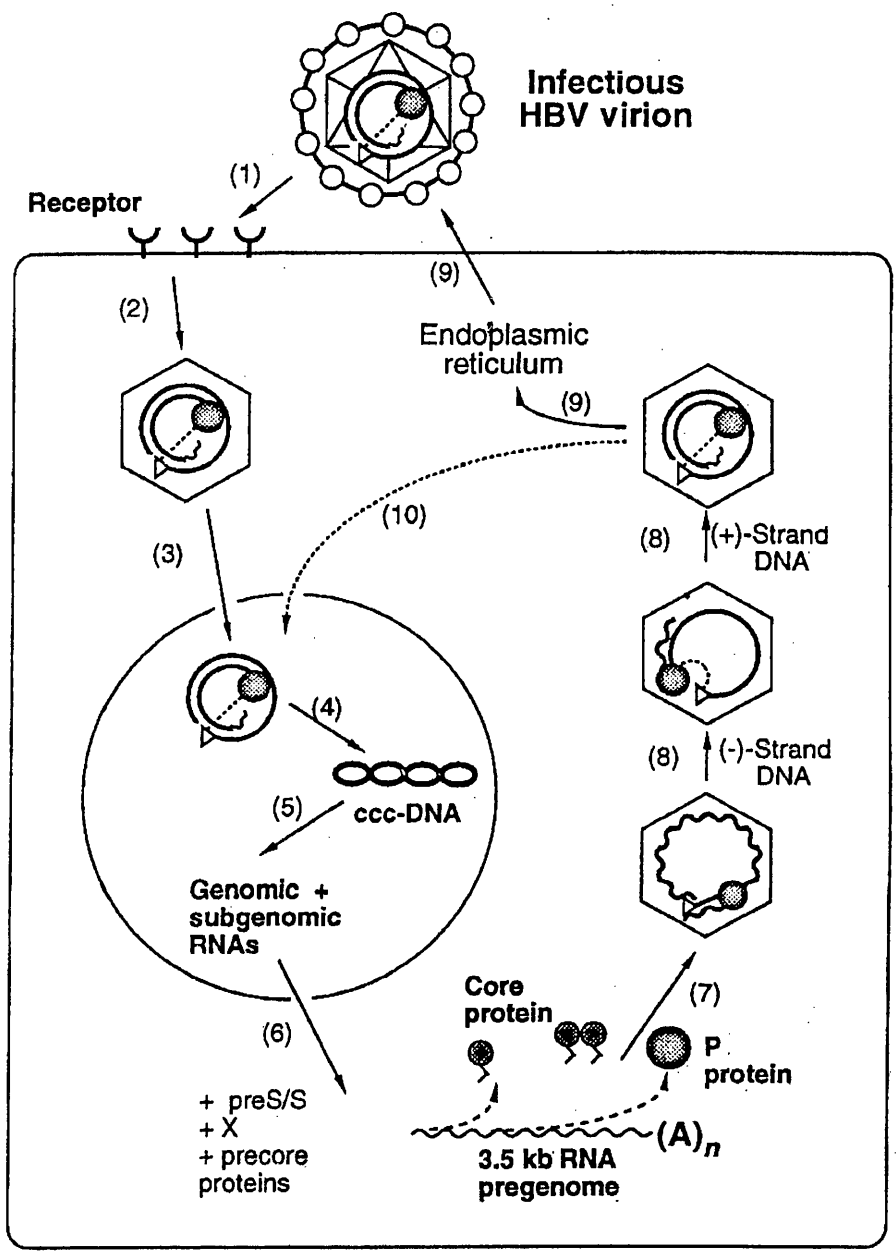

Figure 1.2. A diagrammatic representation of the HBV lifecycle, with key stages indicated. **(1)** Binding to the receptor; **(2)** penetration of the hepatocyte; **(3)** entry into the nucleus; **(4)** formation of cccDNA; **(5)** transcription of viral RNAs; **(6)** translation of viral mRNAs; **(7)** encapsidation of pgRNA; **(8)** DNA synthesis; **(9)** release of new virions from the hepatocyte; **(10)** retention of some genomes in the nucleus for further rounds of replication. Taken from Nassal & Schaller, (1996)

tissue culture system. Human hepatocellular carcinoma (HCC) cell lines have been used to show that the pre-S domains bind to the membranes of these cells, but not to animal hepatocytes or human carcinomas from outside the liver. SHBs is indispensable for viral infectivity (Neurath *et al.*, 1986). It has recently been shown to bind in a Ca^{2+} dependent fashion to a phospholipid binding protein, annexin V, which is present on human liver

plasma membranes (Leenders *et al.*, 1992, Debruin *et al.*, 1995). Despite 90% sequence homology, rat liver annexin V does not bind SHBs. Transfection of a non-permissive rat HCC cell line with annexin V allows these cells to be infected with HBV, lending more support to annexin V being the receptor for HBV (Gong *et al.*, 1997). A role for serum proteins has been implied, as both interleukin-6 (Neurath *et al.*, 1992) and monomeric and polymerized serum albumin have both been shown to bind HBs (Ishihara *et al.*, 1987, Hu & Peterson, 1988, Krone *et al.*, 1990).

1.3.2 Penetration of the host cell

Although there is evidence from DHBV that the capsid enters cells by pH independent mechanisms (Rigg & Schaller, 1992), it is still unclear how hepadnaviruses penetrate hepatocytes. In DHBV, covalently closed circular (ccc) DNA has been found in the nucleus 24 hours after infection (Tuttleman *et al.*, 1986). Although core particles are found in the nuclei it is not known if they deliver the DNA or if free DNA enters the nucleus on its own. HBc does have a nuclear localisation signal (Yeh *et al.*, 1990), and the diameter of core particles is at the functional limit of the nuclear pore (Feldherr *et al.*, 1984).

1.3.3 Viral gene expression

Viral transcription occurs from a limited number of cccDNAs in the host cell nucleus. Expression is controlled from two enhancers, with mRNAs being initiated from four promoters, but all terminating at the same polyadenylation signal (Schaller & Fischer, 1991) (Siddiqui *et al.*, 1987). Note that the quoted nucleotide positions in this thesis are measured from the HBV unique *Eco*RI restriction site in pre-S2.

1) *3.5kb RNAs.* This is the major transcription product, and covers the entire genome, with some redundancy at the ends (Seeger *et al.*, 1991). Transcription is driven from the core promoter to generate two RNAs (Yaginuma & Koike, 1989). The slightly shorter pgRNA (initiating at nt 1818) functions as the template for the viral reverse transcriptase, as it generates new viral genomes, as well as mRNA for the core and polymerase genes. The pre-core RNA initiates 20 to 30 bases upstream of the pre-core ORF (between nts 1783 and 1790) and serves as mRNA for HBeAg (Yaginuma *et al.*, 1987).
2) *2.4kb RNA.* A low abundance RNA, which functions as the mRNA for LHBs. Transcription is controlled from the SP-I promoter element.
3) *2.1kb RNAs.* These RNAs with heterogeneous 5' ends serve as the mRNAs for production of MHBs and SHBs. Transcription is controlled from the SP-II promoter (Cattaneo *et al.*, 1983).
4) *0.9kb RNA.* The mRNA for X-gene expression. Transcription is repressed under conditions supporting viral growth, reflecting the extremely low abundance of HBx.

The typical eukaryotic promoter has a TATA-box approximately 30 nt upstream of the transcription initiation point. This motif binds transcription factor IID, which forms the core of the transcription pre-initiation complex which recruits RNA polymerase II to a precise point for starting transcription. Therefore transcripts produced from TATA-box promoters have a precise 5' end. Only the SP-I promoter in HBV has a TATA-box; the remaining three promoters are TATA-less and produce mRNAs with variable 5' ends (Schaller & Fischer, 1991).

All four HBV promoters are more active in liver cells than in non-liver cells, with the SP-II and X promoters being active in all mammalian cell types (Seifer *et al.*, 1990). Maximum transcriptional activity requires binding of hepatocyte-specific transcription factors. SP-I requires hepatocyte nuclear factor-I (HNF-I), whilst the pre-core/core promoter requires HNF-III (Chen *et al.*, 1994) and C/EBP (CCAAT/enhancer binding protein) for its activation (Yuh & Ting, 1991).

Promoter activities are frequently controlled by enhancers. These are elements which are usually situated upstream (though also occasionally downstream) of promoters which also bind transcription factors to increase the activity of the promoters under their control. HBV has two enhancers. The first, Enh-I, is located 450nt upstream of the pre-core/core promoter between nts 1080 and 1234 (Dikstein *et al.*, 1990a). It has been shown to upregulate the activity of the pre-core/core, surface and X promoters, and to also increase the tissue specificity of the surface promoter (Bulla & Siddiqui, 1988, Roossinck & Siddiqui, 1987). A number of factors bind to Enh-I, though only C/EBP (Dikstein *et al.*, 1990b) and the poorly defined hepatitis B liver factor (Guo *et al.*, 1993) are hepatocyte specific. Amongst the other factors are AP-1 and CREB , which mediate transactivation of Enh-I by HBx (Jameel & Siddiqui, 1986).

A second enhancer is located between nts 1685 and 1773, overlapping the core promoter (Yuh & Ting, 1990, Yuh *et al.*, 1992). This is highly tissue specific, having only been shown to function in highly differentiated hepatoma cell lines (Yuh & Ting, 1993). It has been shown to drive both the SP-I and SP-II promoters. Clusters of mutations have been found in Enh-II which are associated with fulminant hepatitis (Yasmin, 1997). Gel shift experiments have shown that these mutations prevent the binding of an uncharacterised nuclear component, whilst reporter gene assays show that the mutated Enh-II has an increased transactivational ability. This has led to the hypothesis that these mutations prevent the binding of an inhibitory factor, or disrupt a negative regulatory element in Enh-II (Lo & Ting, 1994), leading to increased viral transcription which contributes to the development of fulminant hepatitis.

The transcription termination signal is situated just after the pregenomic RNA initiation site (Ganem & Varmus, 1987). However, it can only function as a terminator when it is more than 400 bases away from the start of transcription (Cherrington *et al.*,

1992), enabling RNA polymerase II to ignore it during the first pass from the 3.5kb RNA start point. All HBV RNAs are capped and polyadenylated. Some splice variants have been observed in HCCs and infected livers, though their function is unknown in humans (Su *et al.*, 1989). Site-directed mutagenesis of these splice sites does not affect viral replication in cell culture. A novel genetic element similar to the *rev* response element from HIV-1 has been found 3' to the S gene, which is believed to suppress splicing (Huang & Yen, 1995). However, in ducks, it has been shown that splice variants are needed for the production of LHBs (Obert *et al.*, 1996).

1.3.4 Genome replication

The hepadnaviruses are similar to retroviruses in that both groups use reverse transcriptase in the replication of their genomes. Whilst retroviruses have an RNA genome and replicate via a DNA intermediate (the provirus, which must be integrated into the host cell DNA), the hepadnaviruses have a DNA genome and replicate via an RNA intermediate, the 3.5kb pgRNA. Although the pgRNA is generated in the cell nucleus, DNA synthesis does not occur until the pgRNA has been encapsidated. This process is described in figure 1.3 and reviewed in detail by Nassal & Schaller, (1996).

1.3.5 Formation of new virions

Formation of new virions begins with the association of the polymerase with the ε encapsidation signal at the 5' end of the pgRNA (Bartenschlager *et al.*, 1990, Bartenschlager & Schaller, 1992). The ε signal is a highly structured region which is sensitive to mutations. This region lies in the pre-core region of the mRNA. Mutations in this region are very important during HBeAg to anti-HBe seroconversion in chronic infection (section 1.4.2). Because the structure must be maintained, only a limited number of mutations can occur (figure 1.4) (Knaus & Nassal, 1993, Pollack & Ganem, 1993).

Core particle assembly and genome maturation occur in the cytoplasm. As described previously core particles spontaneously dimerize and when at a sufficiently high concentration these dimers assemble around the pregenomic RNA and polymerase to form capsids, or core particles.

As the surface proteins are translated the two signal peptides in the S domain insert the growing polypeptides into the ER membrane. Core particles show an affinity for ER membranes containing LHBs protein (Bruss *et al.*, 1996a), and bud through the ER membrane picking up a membrane envelope containing a mixture of all three surface proteins. As the virions pass through the Golgi apparatus the glycoside chains on the surface proteins are modified and the HBc and LHBs subunits are linked by disulphide bridges (Ganem, 1991). Release of the finished virion particles does not require any specific signals.

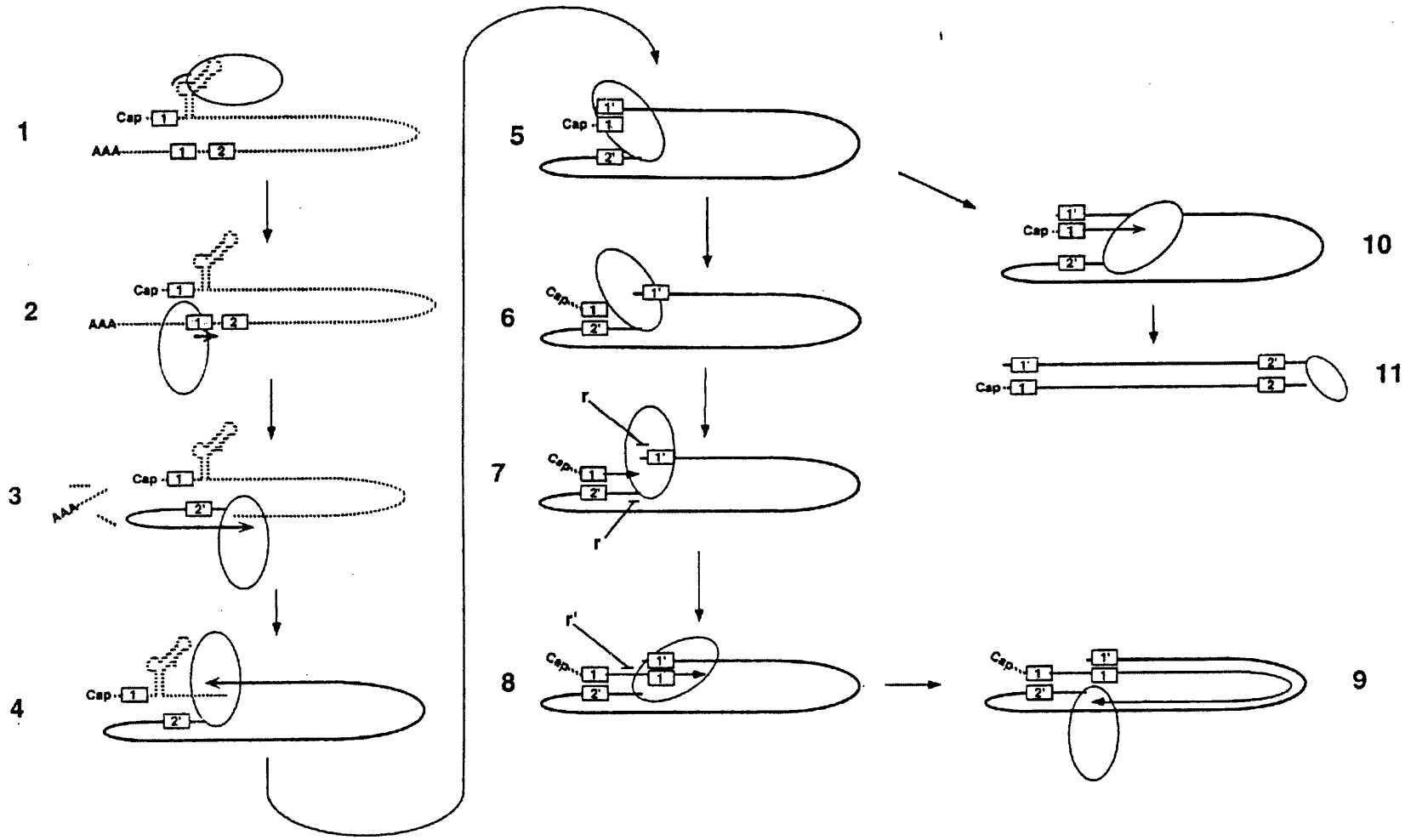
1
Cap
1
AAA
1
2
2
Cap
1
AAA
1
2
3
Cap
1
AAA
2'
4
Cap
1
2'
5
Cap
1'
1
2'
6
Cap
1
1'
2'
7
r
Cap
1
1'
2'
r'
8
r'
Cap
1
1'
1
2'
9
Cap
1'
1
2'
10
Cap
1'
1
2'
11
Cap
1'
1
2'
2

Figure 1.3. Encapsidation is facilitated by the polymerase, which binds to the 5' ε (encapsidation) signal **(1)**. Four nucleotides of the minus DNA strand are synthesized from the bulge region, and are covalently attached to the polymerase via a tyrosine residue in the polymerase's primase region. The polymerase-tetrenucleotide complex is translocated to complementary sequences in the 3' copy of DR1, and minus strand synthesis continues **(3)**. As minus strand DNA is synthesized the pgRNA is degraded by the polymerase's RNase H activity **(4)**. The first 18 nucleotides of the pgRNA (from the cap to the 3' end of DR1) remain following RNase H digestion **(5)**. This fragment forms the plus strand primer, which anneals to DR2, which is juxtaposed to DR1 on completion of minus strand synthesis **(6)**. Plus strand synthesis begins **(7)**, but stops when 50 nucleotides have been synthesized. This 50 nucleotide fragment is transposed to the 3' end of the minus strand DNA **(8)** as a result of the minus strand terminal redundancy (labelled 'r'). Plus strand elongation continues to finally give a relaxed circular DNA **(9)**. Alternatively, a fraction of plus strands may initiate at DR1 rather than DR2 as a result of the plus strand primer failing to be transposed **(10 and 11)**. This produces a linear double-stranded DNA. In both cases the positive strand is only approximately 50% complete. This is thought to be due to a limited availablity of nucleotides within the capsid where DNA synthesis occurs. From Loeb *et al.*, (1997).

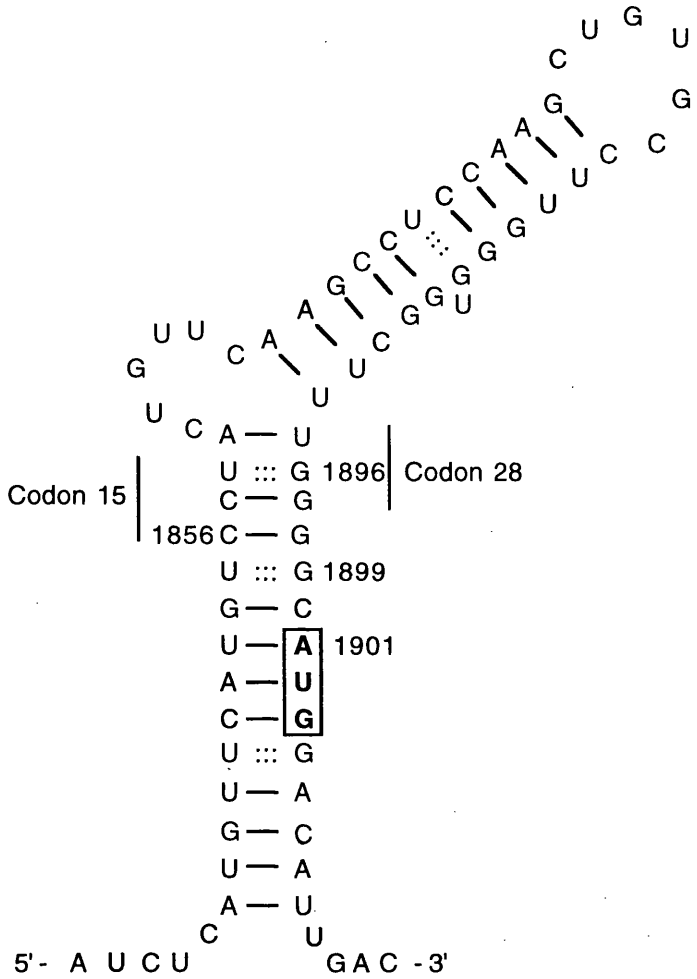

Figure 1.4. The predicted secondary structure of the HBV encapsidation signal. The HBcAg start codon (AUG) is highlighted in bold and boxed. The bulge above codon 15 is where the negative strand primer is synthesised (section 1.3.4). This structure must be maintained for effective encapsidation of the pgRNA; only mutations which do not disrupt the structure can be selected for. Commonly observed mutations are G1896A and G1899A. (Kindly supplied by D. Williams, Institute of Virology.)

1.4 HBV PATHOLOGY

1.4.1 Epidemiology and transmission

HBV infection has a broad spectrum of outcomes, ranging from subclinical infection to acute, self limiting hepatitis and rarely fulminant hepatitis, which is frequently fatal (figure 1.5). 50% of infected adults develop a subclinical infection with no visible symptoms. 90% of adults with a clinical infection develop acute hepatitis, with only 10% becoming chronic carriers. This situation is reversed in patients infected perinatally. There are over 350 million chronic carriers unevenly distributed around the world. In Northern Europe only

0.1-0.2% of the population are HBsAg carriers. This rises to 3% in the Mediterranean and 10-15% in Africa and the Far East. Even higher rates of incidence can be found in some communities of Inuit and Australian Aborigines. In endemic areas with carrier incidence of up to 20%, over 85% of the population are positive for anti-HBs and/or anti-HBc antibodies.

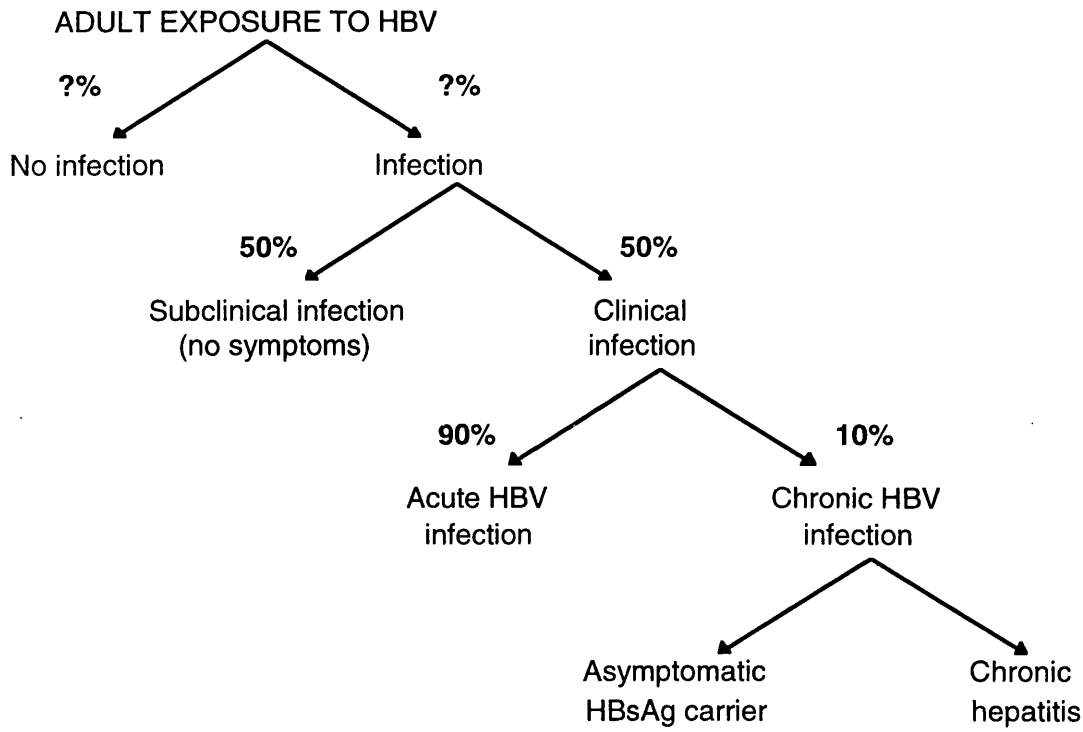

Figure 1.5. HBV infection disease phenotypes. Disease progression can be represented as a series of pairs of possible outcomes through which a patient may progress.

The main route of transmission is by percutaneous exposure. Before the introduction of HBsAg screening infection commonly occurred following blood transfusion or the administration of blood products. Today a more common transmission route is via needles shared by intravenous drug abusers. Transmission can also occur via acupuncture, tattooing and body piercing as well as by seemingly innocuous routes such as sharing razors and toothbrushes.

Many adult infections in low prevalence countries occur sexually. Experiments in non-human primates have demonstrated infection with contaminated semen, but not with saliva. Homosexual men are at particularly increased risk (Karayiannis *et al.*, 1985).

The most important mechanism in endemic areas is from mother to child. Transmission does not usually occur *in utero*, but during birth and the period immediately after in Asia, whilst in Africa infection usually occurs in early childhood. Almost all women who are HBeAg positive infect their child, whilst transmission is less common from mothers who are anti-HBe positive (Delcanho *et al.*, 1994, Zhu *et al.*, 1997).

1.4.2 Immunopathogenesis

Acute hepatitis is characterised by viral clearance as a result of CTL-mediated killing or apoptosis of infected hepatocytes. Although there is evidence from transgenic mouse models that CTL can block HBV replication by a non-cytolytic mechanism mediated by tumour necrosis factor (TNF)-α and interferon-γ (Guidotti *et al.*, 1996a), the high levels of serum ALT observed during active hepatitis tie in with the cytolytic mechanism. The acute response is broad, strong and polyclonal, and possibly involves natural killer cells. Clearance may never be 100% as virus can be found peripherally which can restimulate CTL (Michalak *et al.*, 1994a, Michalak *et al.*, 1994b). It is not clear if this residual virus comes from a reservoir in the lymphocytes (StollBecker *et al.*, 1997). A strong memory T-cell response is also found after clearance (Penna *et al.*, 1996, Rehermann *et al.*, 1996). In contrast to the acute infection, what little CTL response there is in a chronic infection is weak and limited to a small number of epitopes.

What factors are involved in producing a chronic infection? It is obviously to the virus's advantage to persist in the host for as long as possible. HBV is believed to induce tolerance by producing high levels of serum HBeAg and HBsAg (Milich *et al.*, 1993a). The hypothesis that HBsAg induces tolerance is based on circumstantial evidence (Mishra *et al.*, 1992); the long period of HBsAg positivity that is observed following seroconversion to anti-HBe does suggest some degree of tolerance. HBeAg has been shown in mice to cross the placenta and induce tolerance in the foetus . This parallels what is observed in babies born to HBeAg positive mothers, where there is a 90% rate of establishment of chronicity (Milich *et al.*, 1993b). However this tolerance is eventually lost in both mice and humans, though it is not known why this occurs. How does HBeAg induce tolerance and prevent active disease? HBeAg preferentially stimulates Th2 cells, which mediate the antibody response, and downregulates Th1 cells, which mediate CTL activity. This is puzzling as HBcAg, which shares many epitopes with HBeAg, does not induce tolerance, but instead stimulates the Th1 response, leading to active disease (Franco *et al.*, 1996). This is probably due to the different structures of HBeAg and HBcAg, and the key epitopes being conformational (Milich *et al.*, 1995). This observation also explains why patients infected with viruses which do not produce HBeAg often go on to develop severe acute, and sometimes fulminant, hepatitis. However, it does not explain the large number of cases in adults of acute hepatitis caused by HBeAg producing strains. It is believed that the establishment of chronic infection in adults is primarily a result of host factors.

HLA class II alleles have been associated with viral clearance; a study in the Gambia showed a link between the class II alleles DR1301/1302 and the ability to clear virus (Thursz *et al.*, 1995). This link is not perfect, and other factors such as mannose binding protein (which binds to the carbohydrate moieties on the viral particles) (Summerfield *et al.*, 1995) and TNF-α alleles may also be important (Thursz, 1997).

As chronic infection proceeds, the virus accumulates mutations (Marinos *et al.*, 1996). At an early stage pre-core mutants appear which lead to an inability to produce HBeAg. The most frequently observed is the G to A substitution at position 1896, which produces a stop codon. HBeAg is lost from 5% of chronic carriers per year, resulting either in remission or more severe disease. This dichotomy is linked to further mutations arising in HBcAg. HBeAg-negative strains have occasionally been reported in patients with non-fulminant acute hepatitis. Evidence from sequence analysis has shown that such HBeAg-negative viruses are transmissible (Mphahlele *et al.*, 1997). Patients with continuing disease show an accumulation of amino acid substitutions in the B-cell epitopes (Carman *et al.*, 1995, Carman *et al.*, 1997a). This is proposed to lead to an ineffective anti-HBc B-cell response. In contrast, those patients who enter clinical remission carry viruses with amino acid substitutions in the T-helper epitopes of HBcAg. This is thought to permit immune escape and reduces immune-mediated disease, with mutant epitopes perhaps acting as antagonists against T-cells responsive to wild-type epitopes (Bertoletti *et al.*, 1994).

More and more mutations are selected by the constantly evolving host immune response, leading ultimately to the virus being overwhelmed, and full seroconversion occurring. The viruses in the late stage of a chronic infection are believed to be considerably weaker in terms of infectivity and replication competence than the original wild-type strain. Some patients with no serological markers indicating HBV infection have been found to be carrying replication-defective HBV genomes (Hiller *et al.*, 1995). It is believed that most transmission usually occurs in the acute or HBeAg positive phases of an infection. Although this ongoing evolution suggests that the immune system will eventually defeat the virus, 50% of patients die before this can happen from cirrhosis or primary hepatocellular carcinoma.

1.5 VACCINATION

The original HBV vaccine consists of HBsAg particles taken from the plasma of chronic carriers. This vaccine is still widely used in Africa and the Far East, but has been superseded by a recombinant vaccine in Europe and North America as a result of safety concerns. The recombinant vaccine is produced in yeast and is currently the only recombinant vaccine licensed for use in humans (Bitter *et al.*, 1988). Both vaccines are equally efficacious, though the plasma derived vaccine has the advantage of possibly containing small amounts of LHBs and MHBs, as well as having the proper post-translational glycosylation. The presence of these components may help to recruit T-cell help for antibody production.

The vaccine is administered in three doses at 0, 1 and 6 months and has an 85% seroconversion rate. This rises to 90 to 95% after non-responders have received a fourth booster shot. There is some controversy as to whether booster shots are required. This is

due to disagreement over what is a protective level of anti-HBs antibodies, as well as discordance between the variety of diagnostic tests available for measuring anti-HBs titres. Although an anti-HBs titre of 10mIu/ml will give protection, such low titres may favour the selection of escape mutants.

A number of vaccine escape mutants have been observed, with the best characterised being the G145R (Carman *et al.*, 1990a, Carman *et al.*, 1990b). This is situated in the 'a' determinant region of HBs, a key region in determining virus serotype. This variant has been observed in vaccinated children with low titres of anti-HBs. Chimpanzee experiments have shown that high titres of anti-HBs can protect against infection with this variant. This is probably because other epitopes are shared between 145G and 145R, and high titres of polyclonal anti-HBs may be capable of responding to these other epitopes. The importance of these variants is under study using computer modelling to see how the variants are likely to spread. A key factor in this work is determining how fast the variants can spread. The incidence of new HBV infections is low, as the spread of HBV is dependent on chronic infection generating new infections over a period of decades. It is also unknown whether these new variants are spread sexually or vertically; this will have to wait for the cohort of infected children to reach sexual maturity. It is also important to know the natural incidence of HBsAg variants. Many examples have been reported. Studies of unvaccinated populations in Papua New Guinea, Sardinia and South Africa using two different HBsAg assays failed to detect some variants (Carman *et al.*, 1997b). The clinical importance of HBsAg variants has recently been reviewed by Wallace & Carman, (1997). Initial mathematical models do indicate that, with current vaccination policies, vaccine escape mutants will become the dominant form of HBV by the mid-21st century (Wilson *et al.*, 1997).

In the light of the potential problems with variants a number of options are being considered for the next generation of HBV vaccines. In the short term the best option for dealing with escape mutants may be to use a hybrid vaccine containing both 145G and 145R HBsAg particles. The addition of pre-S and HBc epitopes to the vaccine may increase efficacy by recruiting T-cell help, as well as generating a broad polyclonal response similar to that seen in an acute infection (Kuhrober *et al.*, 1997). Recent studies have shown that a vaccine containing pre-S1 and pre-S2 produced a 64% seroconversion rate in people who failed to respond to the traditional vaccine (Hourvitz *et al.*, 1996). Such vaccines will probably supplant the use of HBIg (hyperimmunoglobulin) in neonates born to HBeAg positive mothers (Delcanho *et al.*, 1994). DNA vaccines are also being studied (Davis, 1996, Davis *et al.*, 1997). These are based on the surprising discovery that plasmid DNA injected intramuscularly can be expressed and produce immunogenic proteins (Wolff *et al.*, 1990). DNA vaccination induces a strong CTL response as well as T-helper and B-cell reponses (Schirmbeck *et al.*, 1995). These responses are against a broad range of epitopes,

thus mimicking the natural immune response in acute hepatitis. DNA vaccination also appears to bypass HLA restriction; mice which fail to respond to a protein vaccine can mount a good CTL response after DNA vaccination (Geissler *et al.*, 1997). The mechanism by which this occurs is unknown. Another important consideration for using DNA vaccines is that plasmid DNA is much cheaper and easier to produce than traditional protein vaccines. Other recent developments include the development of oral vaccines. Approaches being investigated include using attenuated salmonella bacteria modified to express HBV proteins (Schodel *et al.*, 1990, Schodel *et al.*, 1993), and bananas engineered to produce HBsAg (Anon., 1997). These approaches are still at an early stage of development.

Who should receive HBV vaccine ? Over 100 countries, including the United States (Holland, 1996), have implemented a programme of universal childhood vaccination. The United Kingdom has controversially failed to follow this lead, restricting vaccination to high risk groups. It is generally considered that universal vaccination is the only way that HBV will be eventually eradicated.

1.6 CURRENT ANTIVIRAL STRATEGIES

As described earlier, most people infected with HBV develop a clinical or sub-clinical acute hepatitis, with the cytotoxic arm of the immune system clearing infected hepatocytes and the humoral response neutralising circulating virions and protecting against future infection. No antiviral therapies are required for these patients who usually go on to make a complete recovery. The situation is not as straightforward for patients with a chronic infection, where the host immune response is either insufficiently strong to clear the virus, or has been made tolerant to the virus (see section 1.4.2). Many studies have looked at HBeAg positive patients, where seroconversion to anti-HBe is linked to a reduction in hepatic inflammation and a long-lasting histological improvement in 95% of patients. However, many of these studies have failed to take into account the natural rate of spontaneous seroconversion from HBeAg to anti-HBe (approximately 5% per annum), making interpretation of results difficult.

The end points used to assess efficacy of treatment of chronic HBV infection are as follows.

1) *Suppression of HBV replication.*

   Clearance of HBV DNA from serum measured by the relatively insensitive hybridisation assay.

   Clearance of HBeAg/ detection of anti-HBe.

2) *Improvement in liver disease.*

   Normalisation of serum aminotransferase levels.

   Decrease in necroinflammatory activity on liver biopsies.

The following are long term assessments.

3) *Eradication of HBV.*
   Clearance of HBsAg/ detection of anti-HBs.
   Clearance of HBV DNA from serum, measured by PCR.
4) *Prevention of cirrhosis and hepatocellular carcinoma.*
   No data yet available. As these are the end stages of chronic HBV infection it will be another one to two decades before the effects of current antivirals on their development can be assessed.

Current antiviral agents can be divided into two groups. The first group, the immune modulators, includes interferon and other cytokines, as well as therapeutic vaccination. These agents aim to stop viral replication indirectly by directing the immune system against infected cells. The second group, the enzyme inhibitors, are designed to block viral replication directly by inhibiting the viral polymerase.

1.6.1 Model systems

Before any treatment can enter clinical trials in humans its safety must be determined by *in vitro* and animal experiments. HBV is particularly difficult to study because of its tight species specificity, and the difficulties in culturing primary human hepatocytes. In any model system a number of markers must be detected in order to establish whether HBV infection and replication has occurred.

1) Detection of secreted HBsAg and HBeAg.
2) Detection of HBcAg in hepatocytes.
3) Detection of RNA transcripts of the correct size (see section 1.3.3).
4) Detection of DNA replication intermediates. These include cccDNA and negative and positive strand intermediates.

Hepatoma cell lines grow well in cell culture. Transfection of a rat hepatoma line with head-to-tail dimers of the HBV genome has been shown to result in the generation of 42nm Dane-like particles and subviral spheres and filaments of HBsAg, as well as HBV specific transcripts and HBV DNA polymerase activity. This work suggests that HBV species specificity occurs at the stage of binding and entry into the host cell. Similar work has been done with the human hepatoma cell line HepG2. These cells have been shown to permit virus entry, but there are contradictory results regarding the detection of replication markers. Bchini et al (1990) claimed to have detected cccDNA, viral transcripts and secreted particles following infection of HepG2 cells with HBV obtained from the serum of a chronic HBsAg carrier. In contrast Qiao *et al.* (1994) failed to detect any intermediates, though they show that virions were internalised by HepG2 cells, but the core particles failed to disassemble to release the genome. Infectivity of HepG2 cells has been increased by pre-treating virions with V8 protease, which removes a portion of the pre-S domain (Lu *et al.*,

1996). Many enveloped viruses require cleavage of part of a surface protein before they can enter their target cell. It is hypothesised that HepG2 cells lack a specific protease which HBV requires for entry.

It would be more desirable to use primary hepatocytes as a model system. However, primary hepatocytes are very difficult to grow in culture as they are not completely differentiated. This causes them to rapidly change phenotype and become fibroblasts after a short period in culture. There has been some success in maintaining primary hepatocytes in culture, though the exact details of how this has been achieved have not yet been published. Primary hepatocytes have been shown to internalise sHBsAg particles (Debruin *et al.*, 1995). Both foetal and adult hepatocytes have been used in infection experiments (Gripon *et al.*, 1988, Ochiya *et al.*, 1989). In both cases replication markers were detected, though the efficiency was low (HBcAg detected in 3% of adult cells and 12% of foetal cells). These results were highly variable, though the efficiency of infection can be increased by treating the cells with dimethylsulphoxide. An alternative is to try and identify the viral receptor and over-express it in cultured cells (see section 1.3.1). This has been done by transfecting annexin V into rat hepatocytes. This has allowed entry and replication of the virus.

Although cell systems are potentially useful for testing antivirals which directly inhibit a virus component, they are not useful for studying immune modulators. This requires an animal model. A considerable amount of work has been done using transgenic mice either encoding the whole virus or particular components. These mice have given many insights into HBV immunopathogenesis, replication strategies and the development of hepatocellular carcinoma (Chisari, 1996). The results of many of these studies are summarised in table 1.1. It is important to consider the effects of the different promoters used, as this could lead to changes in outcome. For example, expression of HBx from the HBV promoter leads to HCC, whilst expression from the α_1-anti-trypsin promoter does not.

As the transgenic mouse systems are based on randomly integrated genomes, they do not mimic a natural infection with HBV (where integration into the host cell's DNA is not a necessary step in the life-cycle, and so does not always occur). Therefore an infectable animal model is required. The only other species which HBV infects is the chimpanzee (Fowler *et al.*, 1982, Thomas *et al.*, 1982). However, there are strong moral and economic objections to the use of chimps in biomedical research, and the course of disease in chronically infected chimps differs from humans. There are a number of other hepadnaviruses in other species which can be used as model systems. Both the heron and the duck are infected by hepadnaviruses, though they do differ from HBV (Ishikawa & Ganem, 1995). Avian hepadnaviruses lack an HBx protein, and their core protein appears to differ functionally. Core proteins from HBV and mammalian hepadnaviruses can form mixed hybrid core particles, whilst avian core proteins cannot interact with human HBc in this way. This could have implications for encapsidation and DNA synthesis.

Promoter	Genes expressed	Characteristics	Reference
HBV	All HBV ORFs	Viral replication	(Araki *et al.*, 1989)
		CTL inhibit viral replication (non-cytolytic mechanism)	(Guidotti *et al.*, 1996a)
		CTL induced hepatitis	(Guidotti *et al.*, 1994a)
HBV	SHBs	Developmental and hormonal regulation	(Farza *et al.*, 1987)
		CTL and cytokine regulation of HBV gene expression	(Guidotti *et al.*, 1994a)
		Small S is not cytopathic	(Chisari *et al.*, 1985)
		CTL induced hepatitis	(Moriyama *et al.*, 1990)
MT + HBV	LHBs and SHBs	SHBs forms rapidly secretable spherical particles	(Chisari *et al.*, 1986)
		LHBs forms HBsAg filaments that are retained in the ER forming 'ground-glass' cells	
ALB + HBV	LHBs and SHBs	HBsAg storage disease	(Chisari, 1989)
		Cytokine induced hepatitis	(Gilles *et al.*, 1992)
		CTL induced hepatitis	(Moriyama *et al.*, 1990)
		HCC	(Chisari, 1989)
HBV	HBx	HCC	(Koike *et al.*, 1994)
α_1AT	HBx	No HCC	(Lee *et al.*, 1990)
MUP	HBc	Core particles do not cross the nuclear membrane	(Guidotti *et al.*, 1994b)
MUP	HBeAg	HBeAg is secreted, not cytoplasmic or nuclear	(Chisari, 1996)
		HBeAg is not cytopathic	
MT	HBc	Immunological tolerance	(Milich *et al.*, 1994)
MT	HBeAg	Immunological tolerance	(Milich *et al.*, 1990)

Table 1.1. HBV transgenic mice. Promoters used include; HBV (hepatitis B virus), MT (metallothionein), ALB (albumin), α_1AT (α_1-anti-trypsin), MUP (mouse major urinary protein). Taken from (Chisari, 1996)

The animal system most closely resembling human HBV infection is the woodchuck. The woodchuck is a native of the United States, and is infected by the hepadnavirus woodchuck hepatitis virus (WHV). This system has been well characterised and appears to have a similar natural history to HBV, causing a chronic infection which can progress to cirrhosis or hepatocellular carcinoma. WHV allows studies of infection, pathogenesis, superinfection with HDV and antiviral treatment, and is currently probably the most reliable model system (reviewed in Roggendorf & Tolle, 1995).

1.7 IMMUNE SYSTEM MODULATORS

1.7.1 Interferon

1.7.1a What are interferons?

Interferons (IFN) were first described in 1957 as proteins with the ability to interfere with viral infections (Isaacs & Lindenmann, 1957). The IFN family can be divided in two. Type I IFNs, α and β, primarily have antiproliferative and antiviral effects, while type II, or γ, IFN functions as an immune modulator. All three types of IFN act at the cell surface, with their stimulatory signals being propagated within the cell by protein kinase cascades.

The type of IFN produced during a viral infection depends on the type of cell involved. IFN-α is produced primarily by leucocytes, whilst IFN-β is synthesised by fibroblasts. Within the groups of IFN-α and β are numerous subtypes produced from two clusters of a total of 23 genes on chromosome 9. In contrast, IFN-γ production is induced in lymphocytes by mitogenic cytokines. IFN-α is the most widely used in therapy either obtained from leucocytes or in recombinant form. Recombinant, or 'consensus', IFN-α is based on a consensus sequence of the commonest forms of naturally occurring IFN-α.

IFN receptors are heterodimers embedded in the plasma membrane, with a cytoplasmic tyrosine kinase domain. IFN-α and β both act through the same receptor, whilst IFN-γ has its own receptor. IFNs make the intracellular environment less hospitable for viruses, as well as boosting the immune response.

1.7.1b Antiviral action

Two arms of IFN's antiviral action involve double-stranded RNA-dependent enzymes (figure 1.6). Many viral RNAs, in contrast to host mRNAs, contain extensive double stranded regions.

The (2'-5') oligoadenylate synthetase (2'5'OAS) is induced early in response to IFN-α to generate oligonucleotides with the general structure $ppp(A2'p)_nA$. These oligonucleotides activate the latent cellular nuclease RNase L, which preferentially cleaves double-stranded RNA (Fischer *et al.*, 1996).

A second double-stranded RNA-dependent enzyme, p1/eIF2α serine/threonine protein kinase, or protein kinase R (PKR), is induced by IFN-α and β in human epithelial

cells. Following synthesis, PKR autophosphorylates, associates with the ribosome and goes on to phosphorylate the α subunit of elongation initiation factor 2. This blocks any further protein synthesis.

IFN also has immunomodulatory effects which play an important role in limiting viral infection (Guidotti *et al.*, 1994a). Most significant of these is the upregulation of MHC class I expression on the surface of infected cells, thus increasing the likelihood of these cells being removed by the cytotoxic immune response. In addition to this, IFN also activates antigen processing cells and regulates the production of cytokines to enhance cytotoxic T-cell and natural killer cell activities (Akbar *et al.*, 1996).

1.7.1c IFN in the treatment of chronic HBV infection

IFN-α obtained from buffy coat leucocytes was initially used in the mid 1970s to treat HBV. However studies were limited in size and number until recombinant IFN-α became available, though these early studies did demonstrate that IFN-α can suppress HBV replication. Over the past decade it as become clear that only a third of patients with HBeAg-positive chronic HBV respond to treatment with a sustained loss of viral replication markers from serum (figure 1.7). This is accompanied by a flare in serum ALT levels which then return to normal, seroconversion to anti-HBe (Brunetto *et al.*, 1991), as well as histological evidence of an improvement in liver disease. Successful treatment requires three to six months administration of thrice-weekly intramuscular or subcutaneous injection of 5 to 10 MU of IFN-α. IFN-α is currently the most widely used therapy for chronic HBV infection.

IFN-β obtained from fibroblast cultures has been shown to have minimal effect on HBV replication (Capalbo *et al.*, 1992). There are limited data regarding recombinant IFN-β, though this is slightly more encouraging.

IFN-γ does suppress HBV replication, though not to the same extent as IFN-α (Kakumu *et al.*, 1991). There is no advantage in using IFN-γ in combination with IFN-α or β, as there is no increase in seroconversion rates and there are more serious side effects, such as granulocytopenia and hepatic decompensation (Gilles *et al.*, 1992).

1.7.1d What factors influence IFN response?

Why do only a third of patients respond to IFN? It is important to answer this question as it could give an insight into how IFN's antiviral effect could be improved, as well as predicting which patients will not respond, thus sparing them the side effects of prolonged IFN treatment and being more cost effective. The most important factors predicting a favourable response are elevated ALT (but not too elevated, otherwise decompensation may occur) and low, but not negative, serum HBV DNA levels. Raised ALT suggests the presence of some immune response against HBV (Bayraktar *et al.*, 1996), which can be boosted by IFN. Concurrent infection with HIV (Dimartino *et al.*, 1996) or

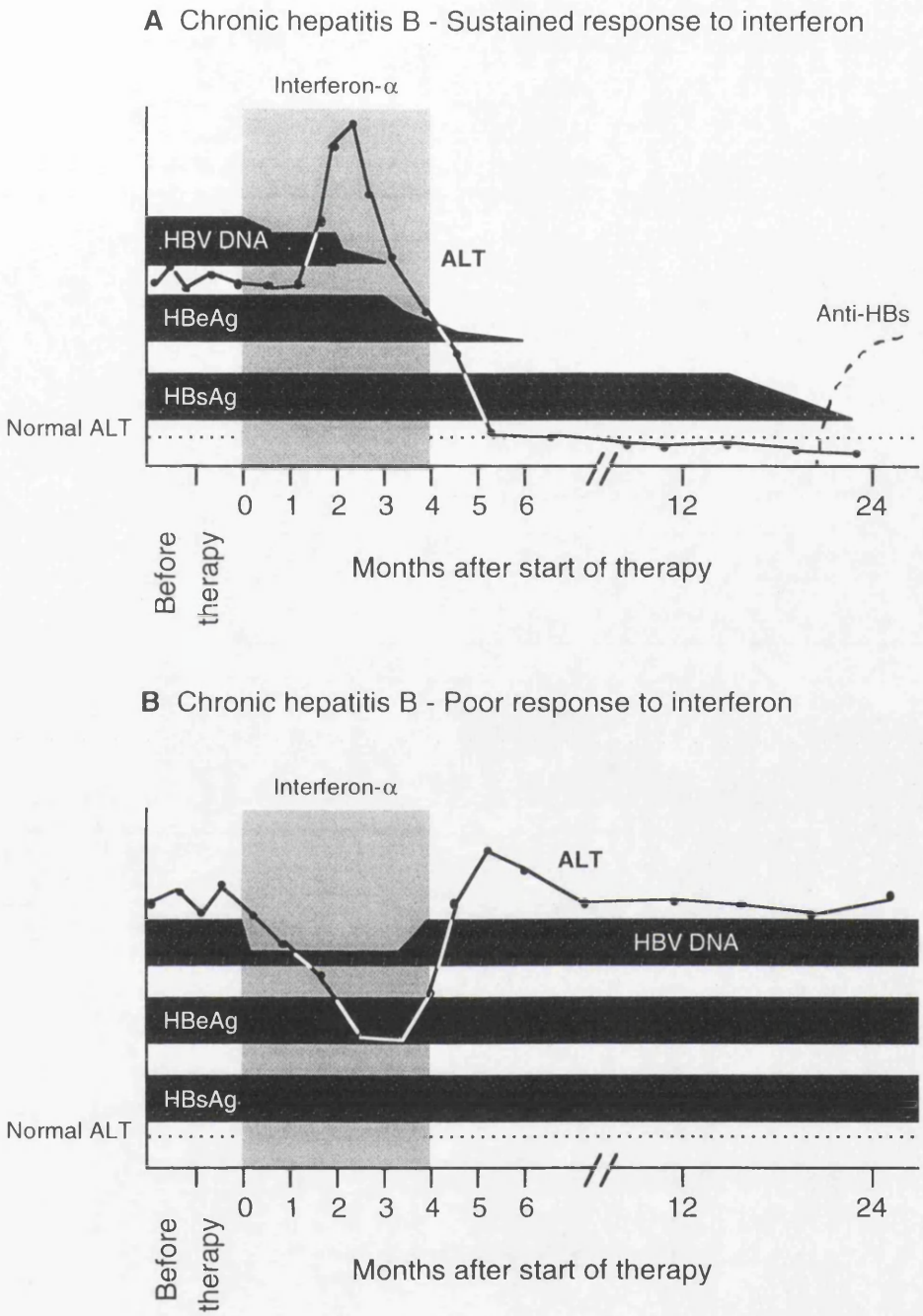

Figure 1.7. Serum ALT levels and viral markers in patients with chronic HBV infection before, during and after a four month course of IFN-α therapy. The top diagram shows a typical response to IFN, where HBV DNA is lost before HBeAg, whilst the lower diagram shows the course of a poor response. The solid bars represent the levels of three viral markers; HBV DNA, HBeAg, and HBsAg, which are used to follow disease progression. The peak of ALT in the top panel is the result of a burst of IFN-α stimulated CTL, which clears the bulk of the infected hepatocytes. Taken from Hoofnagle & Di Bisceglie (1997).

HCV (Zignego *et al.*, 1997) does not favour a good response. HBeAg-negative chronic carriers have a reduced response rate to IFN. Reactivation in these patients is more likely when cirrhosis is present, when disease has been long-term, and if the pre-core mutant of HBV has become the predominant circulating virus.

Some studies have looked at peripheral blood cells in non-responders. These have shown that levels of IFN receptors do not vary between responders and non-responders, though levels of 2'5'OAS do appear to be elevated in responders (Solinas *et al.*, 1993). However, the relevance of these studies is questionable, as it is not known how these observations relate to what is happening in the liver.

A major concern clouding the use of IFN is that is has been widely reported to have poor efficacy in Oriental patients, who constitute over 80% of patients with chronic HBV. This is likely to be because most Oriental patients are infected perinatally, leading to immune tolerance and the presence of integrated HBV DNA in the host genome. The development of immune tolerance could explain why a large proportion of Oriental patients have normal ALT levels. Those patients who have elevated ALT respond at rates comparable to Caucasian patients. The main reason for long-term failure to respond is the high frequency (47%) of reactivation. This could be related to the reported high prevalence of anti-IFN-α2a antibodies in Oriental patients compared to Caucasians treated in a multicentre trial (Lok *et al.*, 1990), though other studies have failed to support this observation. Neutralising antibodies are not detected when IFN-α2b is used instead. It has been suggested that ethnic variation in the distribution of IFN-α2 alleles leads to Oriental patients recognising recombinant IFN-α2a as foreign. However, only 50% of patients lacking the IFN-α2a gene develop neutralising antibodies; HLA type may play a role in this.

1.7.1e Long term outcome in patients treated with IFN

Few studies have examined responses later than 12 to 18 months after the start of IFN treatment, though those that have do report good responses (Korenman *et al.*, 1991, Villeneuve & Willems, 1996). However, delayed reactivation of viral replication occurs in up to 50% of responders. This is due to either incomplete suppression of HBV replication during the course of treatment, or the development of anti-IFN antibodies.

In 50 to 100% of patients who clear both HBsAg and HBeAg serum HBV DNA drops to levels undetectable by PCR. However it has been reported that residual HBV DNA can be found in peripheral blood mononuclear cells and in the liver of these patients (StollBecker *et al.*, 1997). It is not certain as to whether this comes from integrated genomes which are incapable of replication, or whether such small quantities of HBV DNA are clinically relevant.

1.7.2 Prednisolone

Acting via the glucocorticoid response element (Turkaspa *et al.*, 1988) and indirectly as an immunosuppressor, prednisolone enhances HBV replication (Chou *et al.*, 1992, Lau *et al.*, 1992). It may seem strange to use such an agent to treat HBV infection, but withdrawal of chronic HBV patients from steroid therapy has been shown to cause an ALT flare and spontaneous HBe seroconversion (Daikoku *et al.*, 1995). This has been attributed to a rebound increase in immune function above its previous state. This can be further enhanced by following prednisolone priming with IFN-α therapy, though this finding has not been observed in all trials (Krogsgaard *et al.*, 1996).

1.7.3 Thymosin α_1

Thymosin-α_1 is a 28 amino acid peptide purified from bovine thymus which promotes IFN-α, IFN-γ and IL-2 production, and enhances T-cell function and IL-2 receptor expression. An initial pilot study showed 86% of patients responded to thymosin-α_1 treatment in the first year (measured by DNA clearance) compared to 25% of patients receiving a placebo (Andreone *et al.*, 1993). 78% of the patients who responded maintained a response up to three and a half years after the treatment. Thymosin-α_1 is well tolerated, and has been shown to be effective when used in combination with a low dose of IFN-α. In this trial 55% of patients who failed to respond to the standard IFN-α treatment responded to the thymosin-α_1-IFN-α combination (Rasi *et al.*, 1996). A more recent study in China has showed an overall rate of HBeAg to anti-HBe seroconversion rate of 70.3% in patients treated with thymosin-α_1-IFN-α compared to 46.3% seroconversion in patients treated with thymosin-α_1 alone. This is particularly significant as it demonstrates the successful use of immunomodulators in an Oriental population. A successful response requires less than 2500pg/ml of viral DNA in serum (Naylor *et al.*, 1996).

As well as having immunomodulatory functions, thymosin-α_1 has also been shown to inhibit the growth of non-small cell lung carcinoma and to specifically inhibit the anchorage-independent growth of HBV transfected HepG2 cells (Moshier *et al.*, 1996). The mechanisms by which thymosin-α_1 does this are unknown.

1.7.4 Levamisole

Levamisole is a synthetic, orally administered T-cell stimulant. It has been shown in a randomised, double blind trial to increase the number of patients becoming HBV DNA negative (Fattovich *et al.*, 1994). However, the rate of HBeAg loss was the same in the treated and control groups. Combination therapy with IFN-α is inferior to treatment with IFN-α alone, and has more severe side-effects (Bosch *et al.*, 1993).

1.7.5 Granulocyte-macrophage colony-stimulating factor (GM-CSF)

GM-CSF is used to improve immune function in immunosuppressed patients, and has been shown to decrease serum HBV DNA in chronic HBV patients. The major role for GM-CSF is in patients with leucopenia. These patients cannot be safely treated with IFN alone, but can receive the normal IFN regimen when receiving GM-CSF.

1.7.6 Interleukin-12 (IL-12)

IL-12 is a heterodimeric cytokine synthesised by antigen presenting cells which promotes the activation of Th1 cells, maximising secretion of IFN-γ (Rossol *et al.*, 1997). This stimulates natural killer cells, the generation of a specific CTL response and production of opsonizing IgG antibodies. IL-12 has been shown to have therapeutic benefit in mouse models of various tumours and viral infections (Cavanaugh *et al.*, 1997). Because of the high species specificity of IL-12 (only the sequences of human and murine IL-12 are known), no trials have been performed on any of the hepadnavirus animal models. However, the importance of CTL in the resolution of chronic HBV is well known, and some evidence suggesting a role for IL-12 has been forthcoming. IL-12 has been shown to stimulate Kupffer cell activity and mononuclear cell infiltration in the livers of mice. The mononuclear infiltrates were shown to have enhanced natural killer activity and to secrete IFN-γ *in vitro* without any added stimuli.

Immunisation of mice transgenic for HBeAg with an HBe peptide led to a Th2-driven anti-HBe autoantibody response. This could be inhibited by IL-12 treatment, which switched the T-helper response to Th1. This suggests that IL-12 could be used in patients who have an ineffective immune response to allow them to develop protective CTL immunity.

Human trials have begun using IL-12. The relatively long serum half-life (2-5 hours) compared to other cytokines, and the low toxicity of IL-12, make such studies sensible.

1.7.7 Therapeutic vaccination

A new approach to dealing with infectious agents is that of therapeutic vaccination. Like conventional vaccination, therapeutic vaccination aims to trigger a protective immune response against a pathogen, though in the case of therapeutic vaccination the pathogen already resides in the patient. As chronic HBV infection may arise because of an ineffective immune response, or the patient becoming tolerised to HBV, IFN and other cytokines aim to boost the inherent immune response against HBV. Studies are underway to investigate whether vaccination with either HBV proteins or peptides corresponding to HBV CTL epitopes can give rise to protective immunity leading to clearance of HBV (Hourvitz *et al.*, 1996). Why should vaccination with proteins already present in the patient be successful? It

is likely that whilst the immune response may not recognise virally produced proteins generated endogenously, administration of these proteins with an adjuvant presumably enables the host to recognise these antigens. The route of administration could also enhance immunogenicity by delivering the antigens more directly to the lymph nodes.

Strains of mice which fail to respond to HBsAg as a result of H-2 type (the murine equivalent of HLA type) have been described. These mice can be induced to produce high levels of anti-HBs by administration of pre-S1 and pre-S2 epitopes. These regions should therefore possibly be included in a therapeutic vaccine. A recombinant vaccinia virus encoding the pre-S and S regions of duck HBsAg (DHBsAg) has been used to immunise ducks persistently infected with DHBV. This resulted in a significant, though transient, decrease in serum DHBsAg. Preliminary studies have shown infants chronically infected with vaccine escape mutants to respond favourably to administration of pre-S2 vaccines (Machida *et al.*, 1994, Noto *et al.*, 1997).

A peptide therapeutic vaccine based on HLA-A2-restricted HBcAg CTL epitopes has been developed. Peptides corresponding to CTL epitopes are poor immunogens, so to aid presentation these peptides are covalently attached to a T helper epitope peptide and to a pair of lipid moieties (Vitiello *et al.*, 1995). A peptide mapping to amino acids 18 to 27 of HBcAg was linked to a T helper epitope from the tetanus toxoid protein and two molecules of palmitic acid. This conjugate was shown to elicit a primary HBV-specific CTL response in normal subjects in a dose dependent fashion. Although early indications were promising, this approach as since been abandoned because of commercial considerations.

1.8 ENZYME INHIBITORS

Numerous agents have been studied to investigate their ability to inhibit the HBV polymerase. These are primarily nucleoside analogues, many of which were developed for treating other viral infections, primarily herpesviruses (figure 1.8). These have been used alone, in combination or in conjunction with immune modulators.

For a nucleoside analogue to become active, it must first be converted to a triphosphate form. The majority of compounds active against herpesviruses are only phosphorylated by the viral thymidine kinase, and not by host cell kinases. Therefore these cannot be used against HBV, which is not known to possess a nucleoside kinase activity. A limited number of nucleoside analogues are phosphorylated by cellular kinases, but these are more likely to have increased toxicity, or less specificity for the viral polymerase. In particular, mitochondrial DNA polymerase is sensitive to inhibition by some of these agents. The efficacy of a number of these agents against hepadnaviruses has been evaluated in animal models and clinical trials.

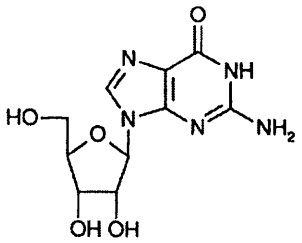

Guanosine

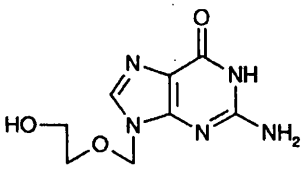

Acyclovir

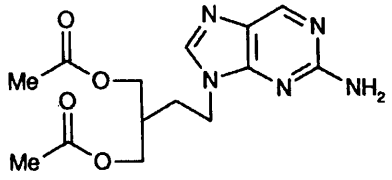

Famciclovir

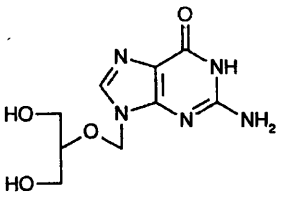

Ganciclovir

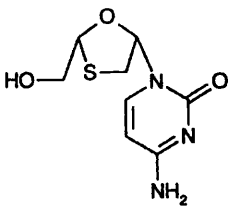

Lamivudine

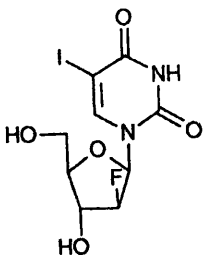

Fialuridine

Figure 1.8a. Guanosine plus nucleoside analogues which have been used in clinical trials against HBV. Acyclovir, famciclovir and ganciclovir where originally designed for use against herpesviruses. Lamivudine was originally designed as an anti-HIV agent, whilst fialuridine was designed specifically for use against HBV.

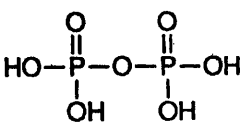

Pyrophosphate

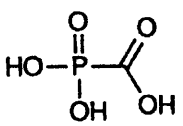

Foscarnet

Figure 1.8b. Pyrophosphate plus the pyrophosphate analogue foscarnet (phosphonoformic acid). Foscarnet is particularly effective when used in combination with nucleoside analogues, especially ganciclovir. Foscarnet is administered as sodium phosphonoformate.

1.8.1 Acyclovir

Acyclovir (9-(2-Hydroxyethoxymethyl) guanine), a guanosine analogue which is widely used to treat herpes infections, has been tried in chronic HBeAg positive infection (Weller *et al.*, 1982, Weller *et al.*, 1983). Preliminary studies showed that intravenous administration caused a reduction in DNA polymerase and HBV DNA levels (Trepo *et al.*, 1986). *In vitro* studies using the cell line HB611, which continuously replicates HBV DNA from a transfected genome, confirmed these findings. Administration of acyclovir to this cell line not only reduced HBV replication, it also removed the HBV-induced block on HLA

class-1 expression, which has important implications for immune recognition of infected cells (Takehara *et al.*, 1992).

However, acyclovir has poor bioavailability when administered orally, and can be nephrotoxic when delivered intravenously. *In vitro* studies using DHBV-infected primary hepatocytes showed acyclovir to be ineffectual against cells obtained from carrier ducks, though some reduction in DHBV DNA levels was seen if cells were treated immediately after infection.

Acyclovir is not considered to be a viable option as a single therapeutic agent. One study has looked at its use in conjugation with lymphoblastoid IFN-α, but acyclovir was not found to enhance the effects of interferon on serum HBeAg levels. An oral prodrug, 6-deoxyacyclovir, is completely absorbed through the gut. Despite 6-deoxyacyclovir's increased bioavailability, the single pilot study performed using it resulted in no seroconversions (Weller *et al.*, 1986).

1.8.2 Adenine arabinoside

A potent inhibitor of DNA polymerase activity, the purine analogue adenine arabinoside (ARA-A) has limited clinical use because of its low solubility in water (Watanabe *et al.*, 1982b). A highly soluble derivative, adenine arabinoside monophosphate (ARA-AMP), has been studied in various trials (Trepo *et al.*, 1983). Because of heterogeneity between the populations studied seroconversion rates vary widely between 5% and 80% (Watanabe *et al.*, 1982a, Perillo 1985, Trepo 1986). A more recent study (Buti 1993) showed in patients who seroconverted to anti-HBe following treatment with ARA-AMP that all patients who also lost HBsAg also became HBV DNA negative by PCR, whilst 81% of those who failed to lose HBsAg also became HBV DNA negative (Buti *et al.*, 1993).

Successful treatment with ARA-AMP does depend on low initial levels of HBV DNA (below 100pg/ml) (Marcellin *et al*, 1995). This could be due to the necessity of limiting the duration of treatment to under 28 days because of ARA-AMP's side effects. Many patients develop severe neuropathies and myalgias, which can sometimes lead to long-standing disability. This has lead to ARA-AMP being withdrawn from use in single agent treatments in chronic HBV infection. However, the development of ARA-AMP-lactosaminated albumin conjugates which can be specifically targeted to hepatocytes has enabled lower effective doses to be used . Although studies using these conjugates are in an early stage, it is hoped that the results will lead to the reintroduction of ARA-AMP as a therapeutic agent

1.8.3 Fialuridine

Although fialuridine (1-β-D-2'-deoxy-2'-fluoro-arabinofuranosyl-5-iodouracil) is a potent reverse transcriptase inhibitor, it has been withdrawn from use as an antiviral following the deaths of a number of patients in a clinical trial. Animal and cell culture

experiments have shown that fialuridine has an extremely high mitochondrial toxicity (Colacino, 1996).

1.8.4 Ganciclovir and foscarnet

Ganciclovir (9-(1,3-Dihydroxy-2-propoxymethyl) guanine) is an acyclic guanosine analogue which is used to treat CMV infection in immunocompromised patients. It was observed that ganciclovir significantly inhibited HBV DNA replication in patients coinfected with HIV (Locarnini *et al.*, 1989). It has since been shown to inhibit DHBV replication in persistently infected hepatocytes in cell culture and *in vivo* (Luscombe *et al.*, 1996), and to inhibit WHV replication in chronic carrier woodchucks.

Despite its efficacy against HBV, ganciclovir does have some drawbacks. It requires parenteral administration due to poor oral bioavailability. As ganciclovir is virustatic, rather than virucidal, withdrawal of treatment causes rebound of viral replication. This necessitates long term treatment, which frequently leads to myelosuppression.

These problems have lead to ganciclovir being used in combination with foscarnet (sodium phosphonoformate). Foscarnet is a pyrophosphate analogue which inhibits DNA polymerase (figure 1.8b). The inhibitory action of foscarnet differs from that of the nucleoside analogues, as a different part of the reverse transcriptase active site is targeted. A combination of ganciclovir and foscarnet has been shown to act synergistically against human herpesviruses and against DHBV *in vivo* (Civitico *et al.*, 1996). This combination therapy also reduces HBV replication in immunosuppressed patients, suggesting a role post liver transplant (Gish *et al.*, 1994).

1.8.5 Famciclovir

Famciclovir (9-(4-acetoxy-3-acetoxymethylbut-1-yl)-2-amino purine) is the oral prodrug of penciclovir, and was originally used as an anti-herpesvirus agent (Cirelli *et al.*, 1996). The conversion of famciclovir to penciclovir is mediated by an esterase and xanthine oxidase (figure 1.9). Penciclovir is efficiently phosphorylated in infected cells by herpesvirus specific thymidine kinase to generate an active triphosphate form with an intracellular half life of up to 20 hours. In treatment of varicella zoster virus infection, famciclovir has been shown to accelerate healing of cutaneous lesions and reduce the period of post-herpetic neuralgia.

HBV is not known to encode a thymidine kinase. Although penciclovir is poorly phosphorylated by cellular kinases, it is thought that hepadnaviral reverse transcriptase is particularly sensitive to penciclovir triphosphate inhibition (Dannaoui *et al.*, 1997) (Korba & Boyd, 1996) (Shaw *et al.*, 1996). The antiviral effect is prolonged by penciclovir triphosphate's long half life.

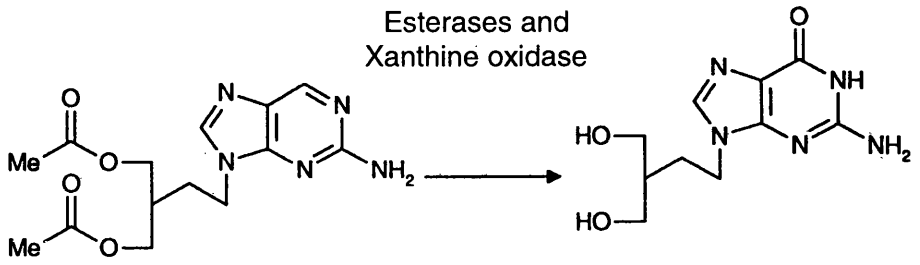

Figure 1.9. The conversion of the oral prodrug famciclovir to the active antiviral penciclovir by intracellular esterases and xanthine oxidase.

Famciclovir is unique amongst nucleoside analogues as short-term treatment has been shown to result in a sustained response, with undetectable HBV DNA and normalised ALT. Trepo *et al* (1997) showed in a phase II trial that patients who had received 500mg famciclovir thrice daily for 16 weeks still showed a sustained response 8 months after the end of treatment. There was also evidence for an increased rate of seroconversion to anti-HBe over the placebo group. In addition to these encouraging results, famciclovir is also well tolerated. Famciclovir also shows promise in the treatment of orthotopic liver transplant patients, being used either prophylactically pre-transplant (Singh *et al.*, 1997), or post-transplant to prevent reinfection (Prieto *et al.*, 1996).

1.8.6 Lamivudine

Lamivudine (β-L-2'3'dideoxy-3'thiacytidine), or 3TC, was originally designed for use against HIV. It was observed in patients coinfected with both HIV and HBV that lamivudine inhibited HBV replication as well as HIV (Benhamou *et al.*, 1995). Further studies confirmed this, paving the way for clinical trials in patients with chronic HBV. Lamivudine has good oral bioavailability and lacks long term toxicity (Honkoop *et al.*, 1996). This is a great benefit, as lamivudine treatment may have to be life-long because HBV can reappear even from undetectable levels on withdrawal of treatment. An important observation was that lamivudine can inhibit HBV replication in Oriental patients who fail to respond to interferon treatment (Lai *et al.*, 1994, Lai *et al.*, 1997) (see section 1.7.1d).

Despite lamivudine only having been used for a short period of time, resistant HBV mutants are already appearing (Bartholomew *et al.*, 1997). These viruses carry mutations in the YMDD motif of the reverse transcriptase active site (Tipples *et al.*, 1996, Schalm, 1997). Similar mutations have also been observed in lamivudine resistant strains of HIV. Lamivudine escape mutants occur in approximately 30% of patients per year who relapse. However, the viral load is often below pre-treatment levels, so the clinical importance of such mutants is not yet clear. Combination therapy may offer a solution to this problem.

Lamivudine and penciclovir have been shown to act synergistically in blocking HBV replication when administered together (Colledge *et al.*, 1997). It was also hypothesised that treatment with lamivudine to reduce viral replication may assist IFN treatment in patients who fail to respond to IFN alone. Unfortunately this was not the case, with no increase in IFN induced CTL response in patients treated with lamivudine and IFN compared to those patients treated with IFN alone (Kuhns *et al.*, 1995). However, it is generally considered that lamivudine is the best of the current enzyme inhibitors available.

1.8.7 Dideoxynucleosides

Dideoxynucleosides are potent inhibitors of HIV reverse transcriptase. Several studies *in vitro* and in ducks have shown that dideoxynucleosides can inhibit hepadnaviral reverse transcriptases. However they fail to show any appreciable effect on HBV replication in humans.

1.9 FUTURE DIRECTIONS FOR ANTI-HBV THERAPIES

It can be clearly seen that there is a desperate need for an anti-HBV agent which produces improved rates of HBe seroconversion and loss of HBV DNA compared to current therapies, but without any danger of side effects. Gene therapy is being considered as a possible treatment for chronic viral infections, including HBV and HIV. One approach is to use dominant negative mutants to interfere with the viral lifecycle (Scaglioni *et al.*, 1996). Fusion proteins containing the N-terminal region of HBc and the C-terminal region of HBs have been shown to inhibit the replication of HBV, DHBV and WHV in cell culture by over 95% (von Weizsacker *et al.*, 1996). These mutant proteins blocked encapsidation of the pgRNA and DNA synthesis, and prevent normal HBc from functioning correctly. RNAs corresponding to the *tat* and *rev* response elements have been used to block HIV replication *in vitro*. The *tat* and *rev* response elements are structured regions of the HIV transcripts which bind the *tat* and *rev* proteins as a necessary step in the regulation of viral translation. The RNAs used in this study titrate out the *tat* and *rev* proteins, thus blocking viral protein synthesis. It is feasible that similar RNAs corresponding to the HBV ε signal could be used to block the encapsidation of HBV pgRNA.

Another new approach which is being widely investigated with regards to the treatment of viral infections and cancers is the direct targeting of deleterious genes and their transcripts. These protocols utilise nucleic acids (NA) or their chemically modified derivatives as agents for silencing genes. Such treatments can take the form of gene therapy, in which the therapeutic molecule is an RNA transcribed from a gene which has been delivered to the diseased tissue, or more conventionally can involve the administration of exogenously synthesised DNA or modified NA. This area can be broadly divided into three sections; 1) triplex forming oligonucleotides (TFOs), 2) antisense oligonucleotides and 3)

ribozymes. Although a few of these agents have entered preliminary clinical trials, most work in this area is still at an experimental stage. These three different approaches will now be reviewed, and their applications with regards to chronic HBV infection will be discussed.

1.10 TRIPLEX FORMING OLIGONUCLEOTIDES (TFOs)

Since the late 1950s it has been known that some DNA sequences are able to assume a triple helix, or triplex, structure (Felsenfeld *et al.*, 1957). This was initially shown to occur between duplexes in which one strand consisted entirely of purines (R) and the other entirely of pyrimidines (Y), and a third strand consisting of either purines (R, giving a YR*R triplex) or pyrimidines (Y, giving a YR*Y triplex). The initial duplex is bound by conventional Crick-Watson base pairing, whilst the third strand binds by Hoogsteen base pairing into the major groove of the duplex (figure 1.10). The third strand always lies anti-parallel to its analogous strand in the duplex (i.e. if the third strand is a homopurine, it will lie anti-parallel to the homopurine strand of the duplex). A triplex can either be intra- or inter-molecular, with the third strand in the latter being either RNA, DNA or a modified NA (figure 1.11) (Reviewed in (Frank-Kamenetskii & Mirkin, 1995)). Kinetic studies have shown that triplex formation is two to three orders of magnitude slower than duplex formation. The rate limiting step is formation of the first three or four base triplets, after which the rest of the TFO rapidly zips into place (Plum *et al.*, 1995, Paes & Fox, 1997). This phenomenon was largely ignored until the mid-eighties when its potential as a gene silencing technique was first mooted.

Two major factors have to be addressed in considering TFOs as therapeutic agents: specificity and stringency. As TFOs are limited to targeting homopurine-homopyrimidine sequences, there have been extensive studies investigating alternative bases which can be incorporated into the TFO to enable recognition of thymines or cytosines in the otherwise homopurine duplex strand (Griffin & Dervan, 1989, Macaya *et al.*, 1991, Mergny *et al.*, 1991, Griffin *et al.*, 1992). Although single mismatches can be tolerated, each successive mismatch disfavours triplex formation, with energies of 3 to 6 kcal/mol being lost with each mismatch, though this does at least reduce the chances of non-specific binding. Attempts to replace bases in the third strand with non-canonical bases (e.g. GC*T rather than TA*T) have not been very successful, mainly due to the weaker binding of these pairs. Artificial DNA bases may provide the solution. Several studies utilising non-natural bases, including 2'-deoxynebularine (Stilz & Dervan, 1993) and 2'-deoxyformycin A (Rao *et al.*, 1994), suggest that these bases form stable triads with cytosine and thymines interrupting the homopurine strand, though it is as yet unclear whether they provide the required specificity and stringency.

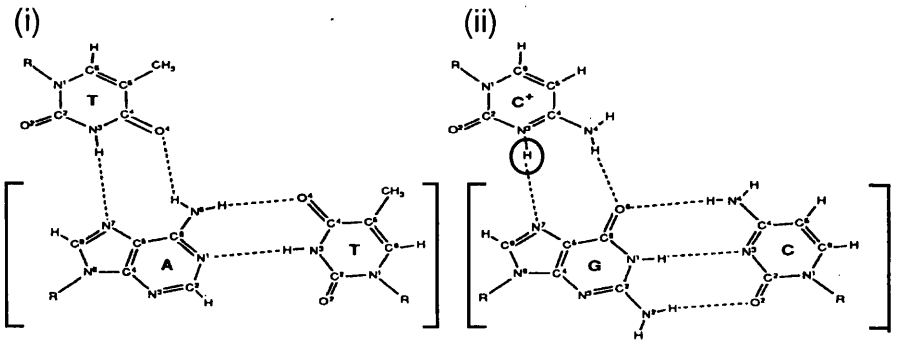

Figure 1.10a. Base triads of YR*Y triplexes: TA*T (i) and CG*C$^+$ (ii). Note that the triplex cytosine is protonated (encircled) on N1. Crick-Watson duplex base pairs are within brackets. Taken from Frank-Kamenetskii and Mirkin, (1995)

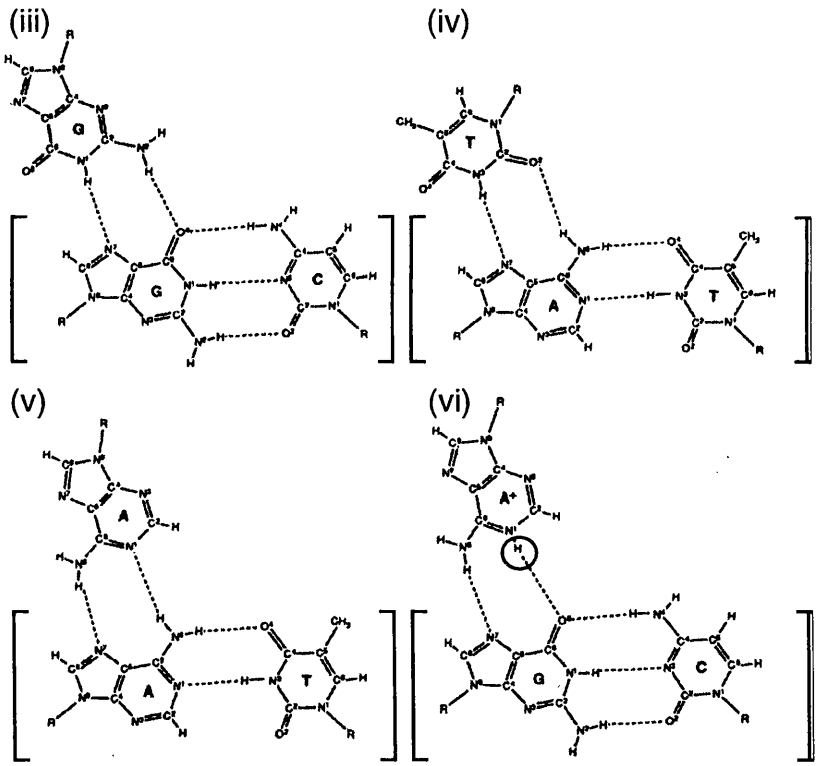

Figure 1.10b. Base triads of YR*R triplexes. In addition to the canonical triads CG*G (iii) and TA*A (v), YR*R triplexes can also accommodate TA*T (iv) and CG*A$^+$ (vi) triads, often resulting in greater stability. Crick-Watson duplex base pairs are within brackets. Taken from Frank-Kamenetskii and Mirkin, (1995).

Can triplexes be stabilised *in vivo* without any loss of specificity? Stable triplex formation *in vitro* requires non-physiological conditions, with YR*Y triplexes requiring a pH below 4 (as cytosine residues must be protonated) and YR*R triplexes requiring

millimolar quantities of bivalent cations. YR*Y triplexes can be stabilised by polyamines, which are found at millimolar quantities in the nucleus (Hampel *et al.*, 1991, Barawkar *et al.*, 1996), and by basic oligopeptides (Potaman & Sinden, 1995). The requirement for cytosine protonation can be overcome slightly by substituting it with 5-methylcytosine in the TFO (Barawkar *et al.*, 1994, Rajeev *et al.*, 1997). A range of artificial bases are also being investigated for this role, with extended aromatic bases to allow intercalation into the target duplex (Lehmann *et al.*, 1997).

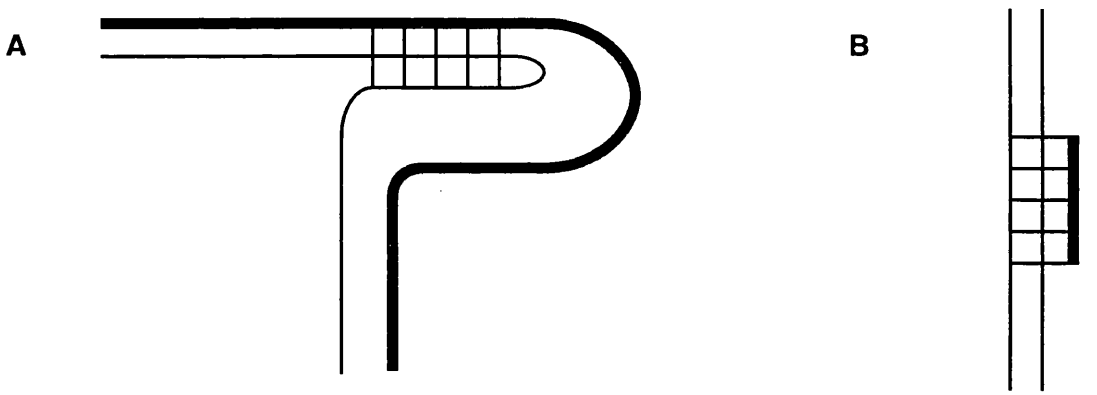

Figure 1.11. Formation of triplex DNA. Triplex can arise either from one strand of a region of duplex DNA doubling-back on itself **(A)**, or from the binding of an oligonucleotide into the major groove of duplex DNA **(B)**.

Addition of an intercalator can also stabilise TFO binding. Moieties such as acridine (Miller *et al.*, 1991) and psoralen (Bates *et al.*, 1995) slot between the two strands of the target duplex, anchoring the TFO into its binding site. UV-irradiation can irreversibly cross-link psoralen TFOs with DNA, allowing permanent gene suppression. This is more effective if the intercalator is bound to the 5' end of the TFO, though it is not known why. Agents which preferentially intercalate into triplex DNA, such as benzo[e]pyridoindole (Escude *et al.*, 1995) and coralyne (Lee *et al.*, 1993), have also been shown to stabilise TFO binding. TFOs can also be modified to mediate cleavage of the target DNA duplex by conjugation with organometallic complexes (Joshi & Ganesh, 1994, Kane *et al.*, 1994), or inclusion of a radioactive atom (McShan & Kinsey, 1993).

A new class of agent which could be used as a TFO is peptide nucleic acid (PNA). This forms strong triplex complexes with duplex DNA by forming a P-loop structure (figure 1.12). The strength of interaction is thought to be due to PNA's protein-like uncharged backbone (Knudsen & Nielsen, 1996). However, P-loop formation is kinetically unfavourable, as it depends on duplex DNA 'breathing' and opening up homopurine-homopyrimidine tracts, and is also sensitive to ionic conditions. Despite this, PNA activity

has been shown in transient transfections in cell culture (Vickers *et al.*, 1995). PNA has been used to inhibit HIV-1, though this may be by a non-triplex mechanism, as PNA has been shown to stimulate IFN-γ production (Hirschman & Chen, 1996).

The use of TFOs *in vivo* could be limited by competition for binding sites from DNA-binding proteins (Espinas *et al.*, 1996). The promoters of many genes contain homopurine-homopyrimidine regions which could be targeted by TFOs. However, these regions are usually binding sites for transcription factors. Therefore TFOs must bind with greater affinity than these proteins in order to silence genes. It is perhaps more important to consider inhibition by histones (Giovannangeli *et al.*, 1997). These are basic proteins which form the nucleosomes which package DNA into chromatin. *In vitro* studies have shown that nucleosomes can block TFO binding and *vice versa* (this would appear to be down to whether the nucleosome or the TFO binds to the DNA first). Fortunately, active genes are located in areas of decondensed chromatin and therefore should be accessible to TFOs. TFOs have been shown to alter the patterning of nucleosome binding in the mouse mammary tumour virus long terminal repeat (MMTV LTR) (Westin *et al.*, 1995). The organization of nucleosomes in the MMTV LTR is very important for viral gene expression. This work has implications for using TFOs not only to silence genes, but also to lock genes into a state of permanent expression by manipulating chromatin structure and recruiting transcription factors (Svinarchuk *et al.*, 1997).

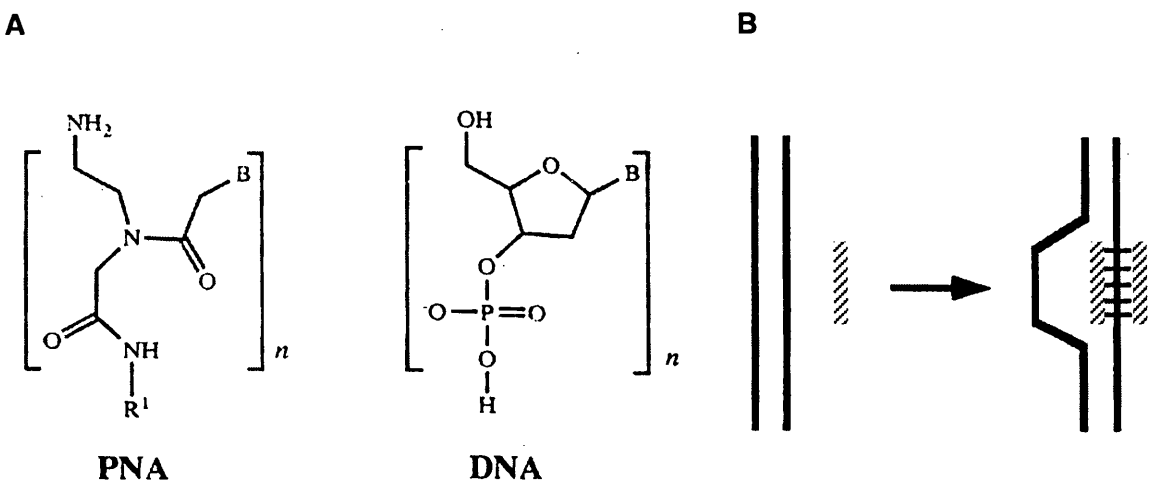

Figure 1.12. (A) The chemical structures of peptide nucleic acid (PNA) and DNA. **(B)** P-loop formation. A PNA oligo (dashed line) displaces one of the strands of the DNA duplex (bold lines). Binding of the PNA to the DNA is stabilized by a second PNA oligo slotting into the major groove of the PNA-DNA hybrid duplex. Taken from Frank-Kamenetskii and Mirkin, (1995).

1.9.1 Therapeutic applications for TFOs

Following the successful demonstration of TFOs selectively binding their targets and inhibiting transcription *in vitro* and in transient transfections, the next stage was to investigate whether TFOs could specifically inhibit expression of clinically relevant endogenous genes. Two major areas of research have looked at the *c-myc* oncogene and the HIV-1 provirus.

Mutations in the *c-myc* proto-oncogene are implicated as playing a key role in the development of many malignancies. Two studies have demonstrated a downregulation of *c-myc* mRNA following treatment with TFOs. The first study used a 27-base TFO targeted against the P1 promoter of *c-myc* in HeLa cells. The TFO was shown to protect the P1 region from DNase I digestion, and to reduce *c-myc* mRNA relative to total cellular RNA, β-actin mRNA and *c-myc* mRNA produced from the *c-myc* P2 promoter (Postel *et al.*, 1991). More recently a 37-base TFO, again targeted against the *c-myc* promoter, was shown not to bind to, or inhibit transcription from, the *c-myc* promoter in MCF-7 breast carcinoma cells (Thomas *et al.*, 1995). However, addition of the synthetic polyamine, 1,3-diaminopropane (DAP), in conjunction with 10μM TFO, led to a 65% reduction in *c-myc* mRNA. This was not observed with DAP alone. Addition of synthetic polyamines can sometimes disrupt the tightly controlled balance of endogenous polyamines, such as spermine and spermidine, in the nucleus. The endogenous polyamines are important in regulating cell proliferation and differentiation. Fortunately in this study, addition of DAP to concentrations of 2mM caused no disruption.

Studies investigating TFO inhibition of the HIV-1 provirus have used the U937 cell-line, which contains two stably integrated copies of the viral DNA (Giovannangeli *et al.*, 1996, Giovannangeli *et al.*, 1997). Targeting of the polypurine tracts in the transcription initiation site and the SP-1 binding site have been shown to reduce p24 antigen production, viral titre and levels of intact 9.2kb viral mRNA. Circular dichroism indicated the presence of triplex DNA, though the specificity was not unambiguously proven. The accessibility of these sequences by TFOs has since been demonstrated using TFO-psoralen conjugates crosslinked to the target site by UV-irradiation. These were shown to specifically block a *Dra*I cleavage site in the target from restriction digestion. Efficiency can be increased using the polyaromatic antibiotic chromomycin (Bianchi *et al.*, 1997).

Targeting the cccDNA of HBV in chronic carriers is a particularly attractive proposition. It is the repository of cccDNA in infected hepatocytes which allows the virus to rebound on the removal of antiviral therapy. A TFO targeted against a 21 base-pair purine rich region of the core promoter has been shown to function in HuH7 cells. A luciferase reporter gene was cloned downstream of the core promoter. 24 hour treatment with 1mM TFO reduced luciferase activity by 60% (Ito *et al.*, 1997). No work has yet been done targeting TFOs against wild-type HBV.

1.11 ANTISENSE OLIGONUCLEOTIDES

Whilst TFOs target the gene of interest itself, antisense oligonucleotides are targeted against RNA (Wagner & Flanagan, 1997). A number of targets are available: the small nuclear RNAs, which are involved in splicing; the pre-mRNA, where antisense can interfere with splicing and polyadenylation; and tRNA, which is involved in translation. Probably the most important target is the mRNA, which is the template for translation. The sequence-specific mechanism of inhibition depends on the type of oligonucleotide used. Indeed, there has also been controversy in recent years as to whether the antisense effect *in vivo* is real, or whether it is a result of non-sequence specific effects (see section 1.10.4). However, antisense inhibition has been observed in natural systems such as the nematode, *Dictyostelium* and in prokaryotes (Thomas, 1992). It has also recently been proposed that the highly conserved 5' and 3' UTR (untranslated regions) of many eukaryotic genes are targets for endogenous antisense binding, as part of a control mechanism for regulating mRNA stability.

Therapeutic antisense oligonucleotides can be divided into two groups: RNA antisense (which is expressed endogenously and can therefore be considered as a form of gene therapy); and DNA antisense and its chemically modified derivatives. Both of the latter forms of antisense must be synthesised outside the body and delivered to their targets like conventional drugs.

1.11.1 Antisense RNA

The principle of antisense RNA is simply to introduce RNA into the cell which is complementary to the mRNA of interest (reviewed in (Takayama & Inouye, 1990)). This leads to the formation of dsRNA which either blocks the passage of the ribosome down the mRNA during translation, or triggers host cell responses to dsRNA (see section 1.7.1b). As these responses are in part mediated by IFN, there is a strong case for using antisense RNA and IFN in combination therapy. In cell culture, antisense RNA can be easily delivered to target cells by standard transfection techniques or by microinjection. These are not practical in a therapeutic situation, so genes encoding the antisense RNA must be delivered to the target cells within the organism. However, this requires the development of a safe, efficient vector, which is a problem facing all gene therapy strategies. Vectors under development include cationic liposomes, which can be conjugated with membrane proteins in order to improve targeting efficiency, and a range of viral vectors, including retroviruses, adenoviruses, herpesviruses and adeno-associated virus. Although many groups are working on designing such vectors, with some entering clinical trials, none are yet licensed for use *in vivo* in humans. Problems include an immune response against the vector, recombination with wild-type (or in the case of retroviruses, endogenous) virus, or the development of disease. In light of these problems all antisense strategies currently in the

final stages of clinical trials are oligodeoxyribonucleotide derivatives, which are synthesised *ex vivo* and delivered as conventional drugs.

1.11.2 Antisense DNA

Antisense oligodeoxyribonucleotides are short, single-stranded DNA fragments synthesised *in vitro*. Their mechanism of action has been the subject of some debate (see section 1.10.3), though it is considered that sequence-specific antisense effects are mediated either by the DNA-RNA complex blocking progress of the ribosome during translation or by cleavage of the RNA strand of the hybrid duplex by RNase H (reviewed in (Toulme & Helene, 1988)).

Antisense DNA has been studied since the 1970s (Stephenson & Zamecnik, 1978) but it soon became apparent that unmodified DNA would be unsuitable for therapeutic applications. There are three problems. The first is that DNA is a strongly charged polyanion and is therefore unable to cross through the lipid cell membrane. In addition, this strong charge can cause the oligonucleotides to bind to cationic proteins and be repelled away from other nucleic acids. This problem can be reduced to an extent by using shorter oligonucleotides. However, there is a limit to how short an antisense molecule can be. It has been calculated, taking into account the non-random distribution of nucleotides in human genomic DNA (which is 40% GC), that an antisense oligonucleotide must be at least 11 to 15 bases long to ensure that its target site is unique. Another disadvantage of longer oligonucleotides is that their specificity is reduced, as mismatches are tolerated better the longer the oligonucleotide is.

Perhaps more importantly, single-stranded DNA is very susceptible to nuclease degradation, especially in serum. Degradation is not quite as severe for the small fraction of oligonucleotides which enter cells, and which manage to avoid destruction in the endosome. Degradation can be partially blocked by incorporating hairpins at the ends of the antisense oligonucleotide, thus preventing cleavage from the ends by exonucleases, though the central portion of the oligonucleotide is still exposed to endonucleases (Zhang *et al.*, 1995). Another problem is that the affinity of the antisense DNA for its target site may be low. This can be influenced by the mRNA secondary structure and competition with RNA binding proteins. These problems mean that an effective therapeutic dose may be unfeasibly high, and has led to the development of chemically modified oligonucleotides.

1.11.3 Chemically modified oligonucleotides

As described in the previous section, chemical modifications need to deal with a number of problems: nuclease degradation, cellular uptake and binding affinity. Any modifications made must still allow RNase H degradation of the mRNA strand of an antisense:mRNA complex, as well as not make the oligonucleotide toxic (Miller, 1996).

Nucleases function by cleaving the phosphodiester bonds between adjacent nucleotides in a stretch of nucleic acid. The phosphodiester bond has been the subject of a number of modifications, some of the most common of which are shown in figure 1.13.

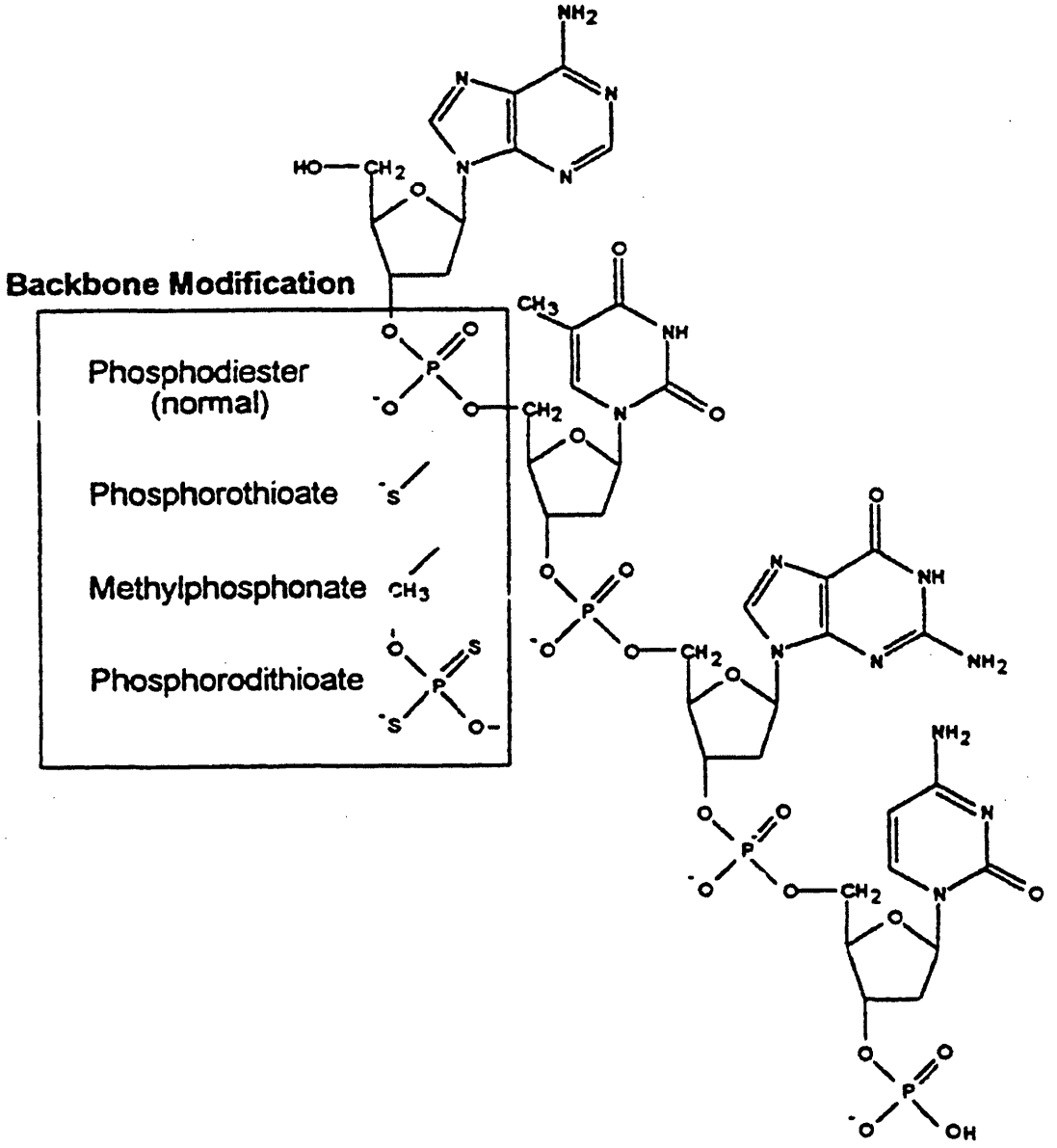

Figure 1.13. The structure of single-stranded DNA, showing the naturally occurring phosphodiester bond, plus three modifications commonly used in the construction of antisense oligonucleotides; phosphorothioate, methylphosphonate and phosphorodithioate. Taken from Arnold (1996).

The most widely used modification is the phosphorothioate (Crooke *et al.*, 1995), which has been characterised in detail, can be produced on an industrial scale, and which is now entering clinical trials. Initial trials have focused on haematological malignancies (Bayever & Iversen, 1994, Bishop *et al.*, 1996), where mutant forms of the tumour

suppressor gene p53 have been targeted. Initial results have reported no side effects, and no degradation of the oligonucleotide, with intact molecules being recovered in patients' urine.

Despite the substitution of a sulphur for an oxygen, phosphorothioate oligonucleotides can still direct RNase H cleavage of mRNA, though some oligonucleotide sequences do appear to inhibit RNase H activity (Gao *et al.*, 1992). However, phosphorothioates are still charged, and can have some non-sequence specific effects (see section 1.11.4). Concerns have also been raised regarding possible toxicity, though this is dependent on dose, length of the oligonucleotide and the method of delivery. Side effects include prolongation of blood coagulation (Nicklin *et al.*, 1997), activation of complement (Shaw *et al.*, 1997) and B-cell stimulation (Monteith *et al.*, 1997).

Methylphosphonates do not carry a charge, and are therefore less likely to interact non-specifically and to have increased lipid solubility, thus aiding passage across the cell membrane (Miller, 1991). However, they do have a centre of chirality at the phosphorus atom, and one of the enantiomers is sterically hindered in binding its target by the 3'-H sugar proton (figure 1.14). Removal of this enantiomer gives an oligonucleotide preparation that has a much tighter binding affinity than the racemic mixture. Methylphosphonates also have increased stability (table 1.2). The chirality of the phosphorothioate modification has also been investigated. The chiral centre can be lost if a second sulphur-for-oxygen substitution is made to give a phosphorodithioate (Ghosh *et al.*, 1993). This extra modification did not increase antisense activity compared to the phosphorothioate.

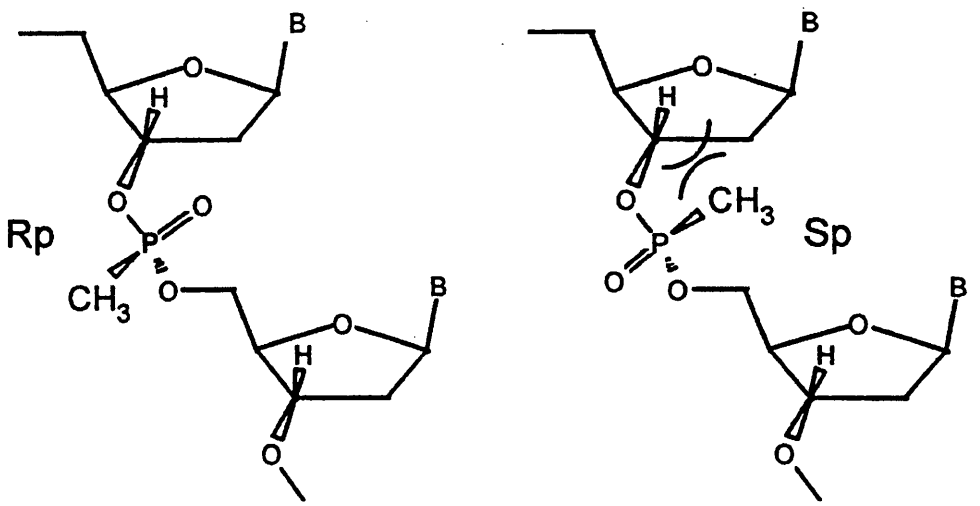

Figure 1.14. The Rp and Sp enantiomers of the methylphosphonate linkage. In the Sp enantiomer the methyl group sterically interacts with the 3' proton on the sugar. This interaction weakens the oligonucleotide's binding affinity for its target. In the Rp enantiomer the methyl group points out from the major groove and has no interactions with the sugar. Taken from Arnold (1996).

Further modifications can be made to the sugar component of the backbone. Alkylation of the 2' position, particularly addition of an O-methyl group, has been shown to increase binding affinity and protect against nucleases (Fisher *et al.*, 1993) (figure 1.15). Addition of the O-methyl group induces the oligonucleotide to assume A-form helical geometry. This is the same form assumed by RNA, which presumably favours the binding of the modified oligonucleotide to mRNA. The benefits of this modification are synergistically increased by including it in methylphosphonate oligonucleotides (table 1.2).

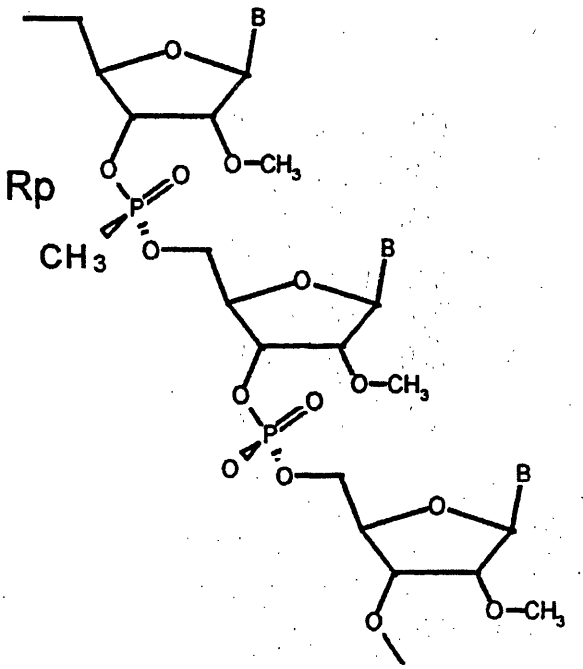

Figure 1.15. Oligonucleotide phosphate-sugar backbone with both the Rp methylphosphonate and 2'-O-methyl modifications. Incorporation of both modifications greatly enhances stability and binding affinity. Taken from Arnold (1996).

As well as changing or adding chemical groups, modifications can take the form of changes in the backbone linkages. Normal DNA and RNA is formed of nucleotides polymerized via 3'-5' phosphodiester bonds. In some situations, such as IFN stimulation (see section 1.7.1b) and during intron splicing, 2'-5' phosphodiester bonds can form. These cannot be cleaved by the majority of cellular nucleases. 2'-5' phosphorothioate oligonucleotides show preferential binding to RNA compared to DNA, and *in vitro* studies suggest they also have less side effects (Kandimalla *et al.*, 1997). One drawback is that 2'-5' oligonucleotides cannot recruit RNase H to the antisense:mRNA complex. It is therefore necessary to produce mixed backbone oligonucleotides, composed of 2'-5' linkages at the ends, and a central portion with 3'-5' linkages.

HALF-LIFE OF BACKBONE ANALOGUE

ENZYMATIC CONDITION	Normal phospho-diester	2'-O-Methyl RNA	Rp-MP/DE	2'-O-Methyl Rp-MP/DE
10% Foetal calf serum, pH 8.0	12 minutes	40 minutes	5 hours	>300 hours
Green monkey kidney cell lysate, pH 6.0	< 10 minutes	~ 5 hours	~ 25 hours	Stable*
Green monkey kidney cell lysate, pH 7.4	< 5 minutes	~ 5 hours	~ 20 hours	Stable*
E.coli lysate	1-3 minutes	1.2 hours	~ 65 hours	Stable*
S.aureus lysate	13 minutes	~ 20 hours	~ 75 hours	Stable*
Snake venom phosphodiesterase	15 minutes	2.5 minutes	167 minutes	Stable*

Table 1.2. Half-lives of normal DNA oligonucleotides and three modified DNA analogues in a range of conditions. The modifications include the 2'-O-methyl addition to the ribose group, the methylphosphonate diester backbone (Rp-MP/DE) and a combination of the two modifications (see figure 1.15). Although both single modifications give some degree of nuclease protection, incorporation of both modifications yields stable oligonucleotides. (*, no detectable degradation after 24 hours incubation.) Taken from Arnold (1996).

1.10.4 2'-5'A-antisense

In section 1.7.1b it was described how IFN stimulates the production of oligoadenylate with the generalised structure ppp(A2'p)$_n$A, known as 2'-5'A. This stimulates RNase L activity, which cleaves double-stranded RNA. This can be taken advantage of by conjugating 2'-5'A to antisense RNA. If unconjugated 2'-5'A is applied to cells there is a general degradation of mRNA and rRNA. However, if 2'-5'A is conjugated to the 3' end of a specific antisense molecule, then only the RNA to which the antisense is complementary is degraded, with cleavage occurring at the 3' end of the chimaera. Recruitment of RNase L is dependent on the terminal 2' phosphate. Removal of this phosphate from the 2'-5'A-antisense chimaera prevents degradation of the target RNA. This approach has been used successfully to suppress replication of respiratory syncitial virus in human tracheal epithelium cells. Unconjugated 2'-5'A and antisense alone showed minimal inhibitory effects.

1.10.5 Is the antisense effect real?

As already described, the most commonly used antisense molecule at present is the phosphorothioate. Despite the successful use of this class of antisense in cell culture and *in vivo*, it has been questioned whether or not the inhibitory effects observed are really due to sequence-specific binding to mRNA.

Phosphorothioates are polyanionic, and therefore bind strongly to proteins (Bock *et al.*, 1992, Gao *et al.*, 1992, Yakubov *et al.*, 1993). As the oligonucleotide's positive charge resides in the backbone of the molecule, this binding is not sequence dependent, and increases in affinity with the length of the oligonucleotide. It has been shown that phosphorothioate oligonucleotides can bind to soluble CD4 near the HIV-1 binding site, and also to the V3 loop of the HIV-1 envelope glycoprotein gp120. In cell culture these oligonucleotides can inhibit HIV-1 infection (Lederman *et al.*, 1996, Lederman *et al.*, 1997).

This non-sequence dependent effect quite clearly could have a therapeutic benefit. Unfortunately this probably will not be the case *in vivo*. Phosphorothioate oligonucleotides can bind to a wide range of proteins. This affinity for binding proteins can be increased by the presence of a guanosine tetrad, or G4, motif (Agrawal *et al.*, 1997). This tertiary structure is formed by non-Crick-Watson base pairing, and the mechanism by which it enhances oligonucleotide-protein binding is unclear. This observation is particularly of concern for studies where the G4 motif has been included in specific antisense oligonucleotides to protect against nuclease degradation.

Misinterpretation of results caused by the presence of the G4 motif can best be seen in the study of the rat carotid model of restenosis after balloon angioplasty (Simons *et al.*, 1992, Morishita *et al.*, 1993, Abe *et al.*, 1994, Bennett *et al.*, 1994, Morishita *et al.*, 1994, Simons *et al.*, 1994). Much work has been done to try and inhibit restenosis by using *c-myc* and *c-myb* antisense with apparent success. The inhibition was believed to be sequence specific as a random sequence control oligonucleotide did not block restenosis. However, the phosphorothioate oligonucleotides used in this study all contained the G4 motif, except for the control oligonucleotide. Such oligonucleotides have been shown to block the binding of a variety of vascular growth factors to their receptors, including fibroblast growth factor, platelet-derived growth factor and vascular epithelium growth factor. It is thought that inhibition of these growth factors was the mechanism by which the oligonucleotides mediated their anti-restenosis effect. This later study also failed to find any antisense oligonucleotides outside the endosome, suggesting that the oligonucleotides failed to cross the cell membrane and reach the mRNA targets anyway. Many other studies have also utilised oligonucleotides containing G4 motifs, all of which will have to be re-evaluated. It is not enough to simply include a random sequence control oligonucleotide containing a G4 motif, as the activity of the G4 motif is dependent on both the surrounding sequence and the length of the oligonucleotide.

Is it sufficient to simply exclude G4 motifs from antisense oligonucleotides in order to ensure a sequence-specific antisense effect? Unfortunately not, as oligonucleotides containing unmethylated CpG motifs can be strongly immunogenic (Krieg *et al.*, 1996). Vertebrate DNA is methylated at virtually all CpG motifs as part of the controls of gene expression. Bacterial and viral DNA is not, and therefore appears to be recognised as being foreign by the immune system. CpG containing DNA has been shown to elicit strong B and T-cell responses, and has been suggested as a possible adjuvant for vaccines. However, these observations call into question the results of studies in mouse tumour models where antisense oligonucleotides have been implicated in causing tumour regression.

What can be done to ensure that any changes following treatment with oligonucleotides is due to an antisense effect, other than eliminating G4 and CpG motifs unless really necessary? In future it will be important to monitor the levels of target protein and target mRNA relative to a constant marker such as a housekeeping gene. This need for confirming specificity will become more important as the first generation of antisense drugs starts to enter the clinic.

1.10.6 Oligonucleotide aptamers

Although the interaction between oligonucleotides and proteins can be a problem with antisense strategies, oligonucleotides are being specifically designed to bind to protein targets. Single-stranded nucleic acids can form an immense variety of structures depending on sequence. By using selection techniques and '*in vitro* evolution' it is possible to screen libraries of randomly generated nucleic acids for enzyme- or receptor binding inhibitors (figure 1.16). These oligonucleotide ligands are known as aptamers (Chapman & Szostak, 1994).

Although this technology has yet to be applied to HBV, a number of studies have looked at aptamer applications for anti-HIV agents. Most notable among these are the *tat* and *rev* response element decoys (see section 1.8.8), though these were based on the native sequence rather than being derived from *in vitro* selection. However, *in vitro* selection has been used to identify an RNA aptamer capable of inhibiting the NS3 protease of hepatitis C virus (Kumar *et al.*, 1997, Urvil *et al.*, 1997).

1.10.7 Antisense inhibition of HBV

As HBV replicates via an RNA genomic intermediate, the pgRNA, it is an ideal target for an antiviral strategy, such as antisense inhibition, which targets RNA. Initial studies looked at hepatoma cell lines either transiently or stably transfected with HBV genomes. Blum *et al*, (1991) showed that a 40-mer oligodeoxyribonucleotide antisense molecule could inhibit HBsAg and HBeAg production when applied to HuH7 cells transiently transfected with HBV genomes. Inhibition was not observed with the corresponding sense

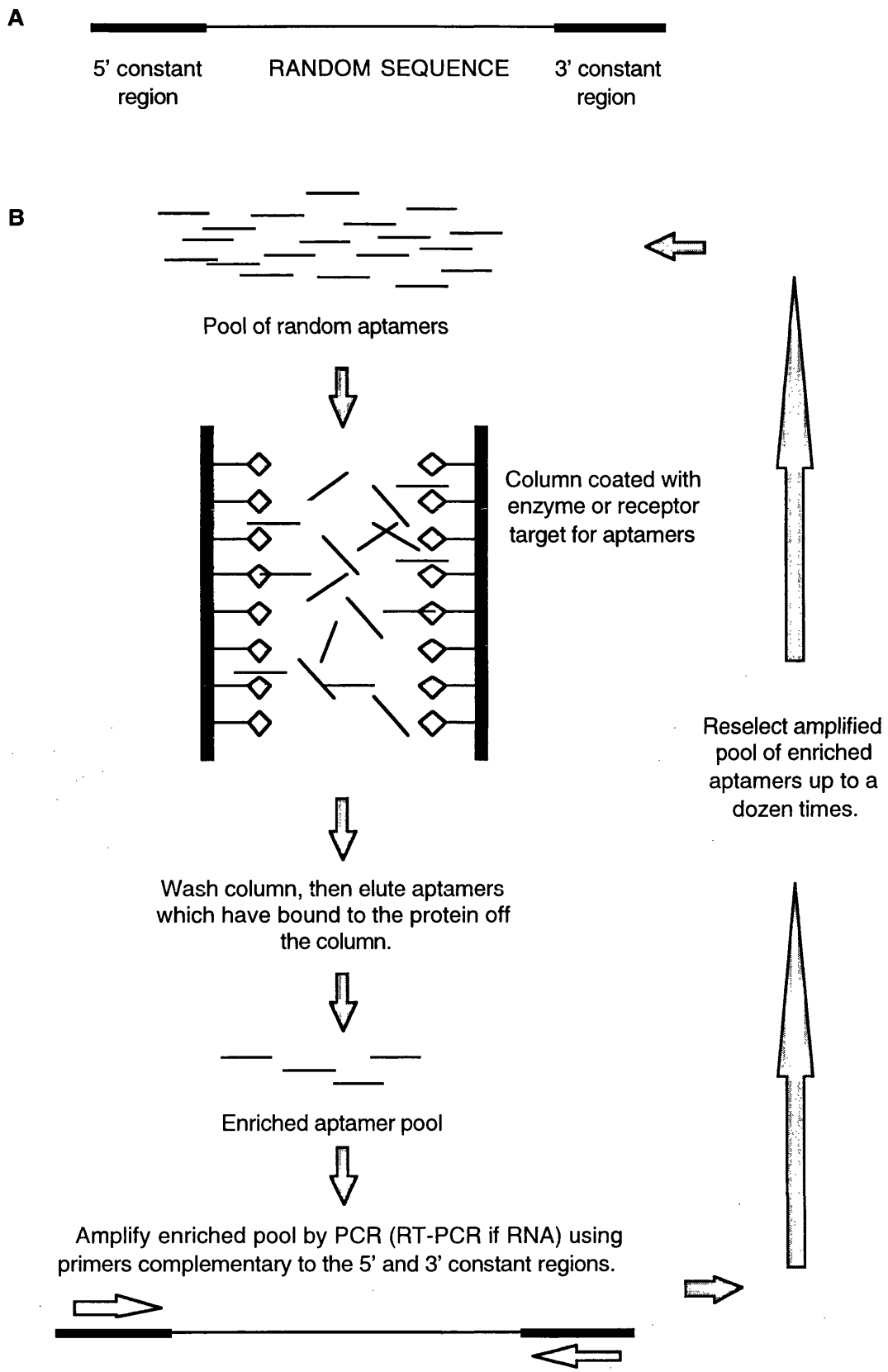
A
5' constant region
RANDOM SEQUENCE
3' constant region
B
Pool of random aptamers
Column coated with enzyme or receptor target for aptamers
Reselect amplified pool of enriched aptamers up to a dozen times.
Wash column, then elute aptamers which have bound to the protein off the column.
Enriched aptamer pool
Amplify enriched pool by PCR (RT-PCR if RNA) using primers complementary to the 5' and 3' constant regions.

Figure 1.16. *In vitro* selection of oligonucleotide ligands, or aptamers. A pool of oligonucleotides with the structure show in panel A are produced, with 5' and 3' regions with constant sequence flanking a region with random sequence. Depending on the length of this region, up to 10^{10} to 10^{12} different oligonucleotides can be generated. These oligonucleotides can either be used directly (as DNA aptamers) or be made double stranded and cloned into plasmids for use as *in vitro* transcription templates for generating RNA aptamers.

The selection procedure is shown in panel B. A column is coated with the protein of interest. The pool of random aptamers is passed through the column, allowing any possible binding interactions to occur. After washing away any unbound aptamers, those aptamers which have bound to the column are eluted off. This enriched pool is then amplified by PCR (or RT-PCR if the aptamers are RNA) using primers complementary to the 5' and 3' constant regions. The amplified products are then used to repeat the process, enriching the pool even further. The selection pressure can be increased in further rounds of screening by increasing the stringency of the binding and washing steps. Use of a DNA polymerase lacking proof-reading capabilities in the PCR step can introduce mutations in the enriched pool, which are then selected in subsequent rounds of screening by a process of *in vitro* evolution.

oligonucleotide. Goodarzi *et al.*, (1990) targeted antisense 15-mers to the cap site and translation initiation site of SP-II mRNA in stably transfected PLC/PRF/5 cells, which secrete HBsAg. The antisense oligonucleotides achieved 90% inhibition of HBsAg production when administered at 17.4μM. Phosphorothioate derivatives of these oligonucleotides also produced 90% inhibition, but at a lower concentration (5.8μM). 15-mer phosphorothioate oligodeoxynucleotides have been shown to have no toxicity towards cultured hepatoma cell-lines at concentrations up to 20mM (Yao *et al.*, 1996b). In this study, phosphorothioate antisense oligonucleotides were shown to inhibit HBsAg production in transfected HepG2 cells in a dose dependent fashion. Maximum inhibition occurred between 3 and 5 days after treatment, but inhibition was completely lost after 15 days. This work has been successfully followed up with delivery of phosphorothioate oligonucleotides to human hepatoma cells implanted in athymic nude mice (Yao *et al.*, 1996a).

In all these studies the 5' ends of mRNAs were targeted, due to the belief that these regions are not locked in secondary structure which could not only block antisense binding, but also impair capping and translation initiation. Korba and Gerin (1995) showed that for antisense to be most effective, it should be targeted at functionally important regions of mRNA (Korba, 1996). They screened over 50 antisense oligonucleotides between 14 and 23 bases long targeted against various regions of the HBV genome in the 2.2.15 cell line. Antisense oligonucleotides targeted directly to key regions such as capping, translation initiation and polyadenylation signals all were far more efficient at inhibiting protein synthesis and viral DNA levels. Interestingly levels of viral transcripts did not fluctuate significantly from the controls, suggesting that RNase H mediated destruction of transcripts was not occurring. HBV replication was most inhibited by antisense targeted against the encapsidation signal. This is surprising, as the encapsidation signal is highly structured (figure 1.4) with very little single-stranded RNA to which antisense oligonucleotides could feasibly bind. There is some controversy over how significant a factor substrate secondary structure is in choosing target sites for antisense and ribozymes (see section 1.15.4), though this is probably due in part to an incomplete understanding of RNA tertiary structure.

How can antisense be efficiently delivered into HBV infected cells? A number of methods have been studied *in vitro*. Nucleic acids can be targeted to liver cells using poly-L-lysine-asialoglycoprotein conjugates. Poly-L-lysine is a strong polycation, which enables nucleic acids to bind strongly, but non-covalently. Asialoglycoprotein is a serum protein which binds specifically to receptors on hepatocytes. Wu and Wu (1991) showed that a 21-mer antisense oligonucleotide complexed with the poly-L-lysine-asialoglycoprotein carrier targeted to the HBV polyadenylation signal could be specifically delivered to cultured 2.2.15 cells and result in an 80% reduction in viral DNA and HBsAg in the culture medium after 24 hours exposure. This inhibition was maintained for 6 days. No significant inhibition could

be seen with uncomplexed antisense or with complexed random control oligonucleotides. The inhibition could be competitively blocked with free asialoglycoprotein.

Although this approach clearly works, the use of oligodeoxyribonucleotides and their derivatives requires frequent administration in order to maintain inhibition. Delivery of genes encoding antisense RNA would provide prolonged inhibition with only a single administration of therapy. Vectors based on the Moloney murine leukaemia retrovirus have been used to deliver antisense *in vitro* (Ji & Si, 1997). A 2.3kb antisense RNA to preS/S and a 1.5kb antisense RNA to preC/C were delivered to 2.2.15 cells. The 2.3kb antisense produced a 71% inhibition of HBsAg and a 23% inhibition of HBeAg, whilst the 1.5kb antisense produced a 23% inhibition of HBsAg and a 59% inhibition of HBeAg. Inhibition started 3 days after transduction with the retroviruses and was still maintained 11 days later. It is possible that inhibition was not complete because the antisense RNAs were so long that they adopted secondary structures which prevented them from hybridising with their targets. It is unlikely that antisense constructs this long would be used as therapeutic agents because of the potential decrease in specificity. There are also problems in using retroviral vectors. Retroviruses can only infect cells in mitosis and only a small proportion of hepatocytes will be dividing at a given time. Although murine viruses, such as the one used in this study, are used in experimental human gene therapy protocols to avoid the risk of recombination with endogenous human retroviruses, they do elicit a strong immune response. This results from complement activation by the lipids in the retroviral envelope, which are derived from murine cells. Vectors derived from human lentiviruses such as HIV may provide the answer to these problems, as they are capable of infecting non-dividing cells and do not contain immunogenic lipids.

A more successful technique has utilised episomal vectors, which form stable, replicating units in the nucleus (Wu & Gerber, 1997). Three constructs, encoding 1.4kb, 1.0kb and 0.58kb antisense RNA to the 5' end of SPII mRNA were transfected into Hep3B cells, a cell line which secretes HBsAg. All three constructs caused a total block of HBsAg production which was maintained for 10 months.

Initial *in vivo* studies have focused on phosphorothioate oligonucleotides targeted against the pre-S region of DHBV . Following initial *in vitro* studies, a 15-mer targeted against the pre-S region of DHBV was administered to chronically infected ducks at a dose rate of 20μg/g body weight daily. After 10 days treatment, DHBsAg had been lost from serum and DHBcAg had been lost from the liver, with no detectable side effects. This closely matched the *in vitro* results, suggesting that the inhibition was due to an antisense effect. An identical regime was used in athymic nude mice into which 2.2.15 cells had been injected in order to establish tumours which secrete HBsAg and HBeAg. Administration of phosphorothioate oligonucleotides targeted to the translation initiation point on the SP-II RNA led to an 81% reduction in HBsAg and a 60% reduction in HBeAg. Delivery of anti-

DHBV antisense can be enhanced by trapping the oligonucleotides in liposomes (Soni *et al.*, 1995, Soni *et al.*, 1996, Soni *et al.*, 1997).

The poly-L-lysine-asialoglycoprotein carrier has been used in woodchucks to deliver antisense oligonucleotides targeted against the polyadenylation signal of WHV in neonately infected animals (Bartholomew *et al.*, 1995). The antisense-carrier complex was administered at 0.1mg/kg body weight per day for 5 days. Although there was no significant decrease in WHBsAg, there was a five to ten fold decrease in viraemia, as measured by serum viral DNA levels, 25 days post treatment. The decline in viraemia lasted for two weeks, after which viral DNA levels in serum began to rise. This decrease in vireamia was not seen when antisense DNA alone, or carrier complexed with a random oligonucleotide, were used.

Although antisense technology does appear to offer a promising alternative to current anti-HBV therapies, there are still a number of problems that need to be addressed. Most important is the need to decide whether antisense RNA or DNA should be used, and how these constructs could be delivered safely. As the cccDNA is not targeted by antisense therapy, it will be necessary to maintain treatment for a long time, which raises concerns about possible side effects. Although current studies have only looked at antisense in isolation, it will eventually become necessary to see how antisense performs in combination with immune modulators and enzyme inhibitors.

1.12 RIBOZYMES

In 1982 Thomas Cech and co-workers made the surprising discovery that some RNA molecules possessed the ability to undergo chemical reactions without the aid of any protein enzymes (Kruger *et al.*, 1982). These initial studies focused on the group I self-splicing introns from the protozoan *Tetrahymena*, which are not truly catalytic as the mechanism is intramolecular, with only a single turnover in which the molecule is changed. A true catalyst can process multiple substrates without becoming chemically altered itself. The term 'ribozyme' was coined for these pseudo-catalytic RNAs. The group of ribozymes known has since expanded to include the group II self-splicing introns, the RNA moiety from RNase P and a variety of motifs from RNA viroids and satellite DNA transcripts. The term 'ribozyme' is generally restricted to these motifs, all of which possess a sequence-specific endoribonuclease, and in some cases RNA ligase, activity. *In vitro* evolution experiments, similar to those described in section 1.11.5, have produced catalytic RNAs with a variety of other functions, such as kinase (Lorsch & Szostak, 1995), amino-acyl transferase (Lohse & Szostak, 1996) and C-C bond formation activities (Hager & Szostak, 1997). These experiments have important implications for the 'RNA world' hypothesis of the origins of life. This theory states that the earliest self-replicating organic molecules were likely to have been ribozymes, as RNA possesses both an informational storage capacity (in the genetic

code) and catalytic activity. DNA could also have had an early role, as recent experiments have also discovered catalytic DNA.

This thesis is concerned solely with the classical phosphodiesterase ribozymes. These all produce fragments containing a 5'-hydroxyl and 2',3'-cyclic phosphate and have a requirement for divalent cations, usually Mg^{2+}. Ribozymes are potentially more powerful gene silencing tools than antisense oligonucleotides (Altman, 1993). The catalytic domain of ribozymes can cleave a targeted mRNA, thus irreversibly blocking translation, whereas antisense oligonucleotides can fall off or be displaced from their targets.

1.12.1 SELF-SPLICING INTRONS

This group includes the first catalytic RNA discovered, the group I self-splicing intron from the nuclear pre-rRNA of the protozoan *Tetrahymena thermophila* (Zaug *et al.*, 1986). It has since expanded to include group II introns. Examples have been found in the nuclei of protists and fungi, fungal mitochondria, the chloroplasts of algae and higher plants and in bacteriophages (Durrenberger & Rochaix, 1991, Ferat & Michel, 1993). Group I and group II introns differ in their mechanisms (figure 1.17). Although both can function *in vitro* on their own, there is evidence that proteins are required for successful splicing *in vivo.*

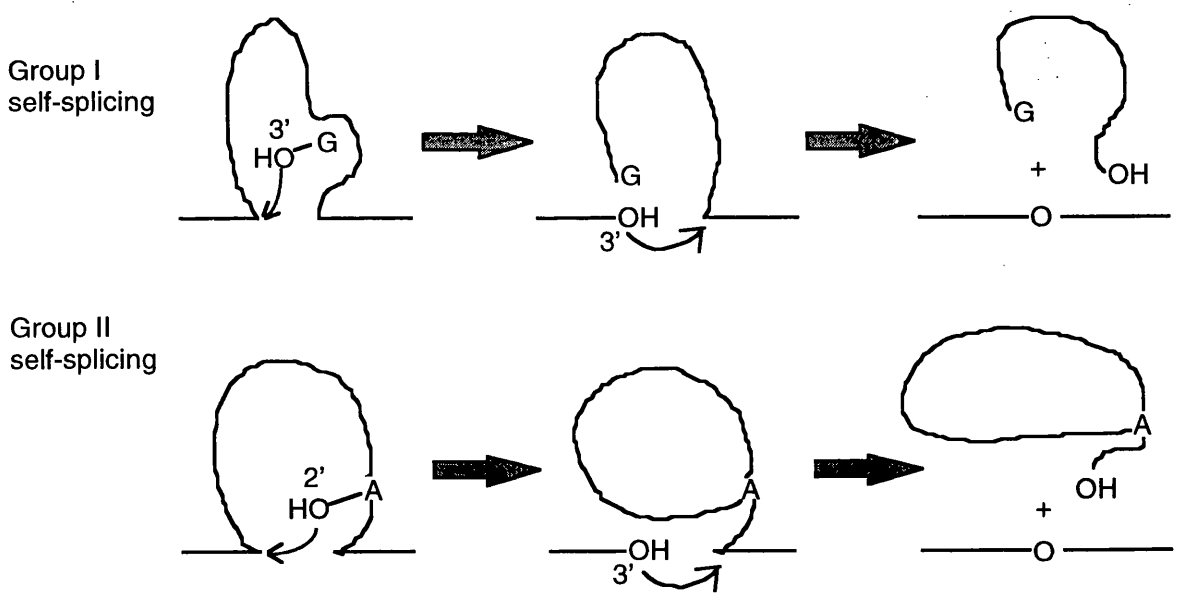

Figure 1.17. Simplified view of the cleavage mechanisms of group I and II self-splicing introns. The attacking group in group I introns is the ribose 2'-hydroxyl of a guanosine cofactor. In group II introns the attacking group is the ribose 2'-hydroxyl of an adenosine residue within the intron sequence itself.

Computer modelling has suggested that although the tertiary structure of the intron is important to self-splicing (Inoue, 1990), the actual sequence of folding which the intron passes through as it assumes its active structure is also important (Emerick & Woodson, 1993, Jaeger *et al.*, 1993, Franzen *et al.*, 1994,). This is thought to allow the recruitment of co-factors to the correct places within the structure (Bass & Cech, 1984). It is believed that divalent cations play a direct role in the cleavage reaction (Christian & Yarus, 1993). Substitution of the bridging 3'-oxygen at the cleavage point with a sulphur reduces cleavage by a thousand-fold when Mg^{2+} is used as the cation (Suh & Waring, 1992). However, when Mn^{2+} or Zn^{2+} are used, there was little inhibition of cleavage. This is because the two transition metal ions co-ordinate sulphur more strongly than Mg^{2+} does, implying that the metal ion plays a direct role in catalysis by co-ordination to the 3'-oxygen in the transition state (Suh & Waring, 1992).

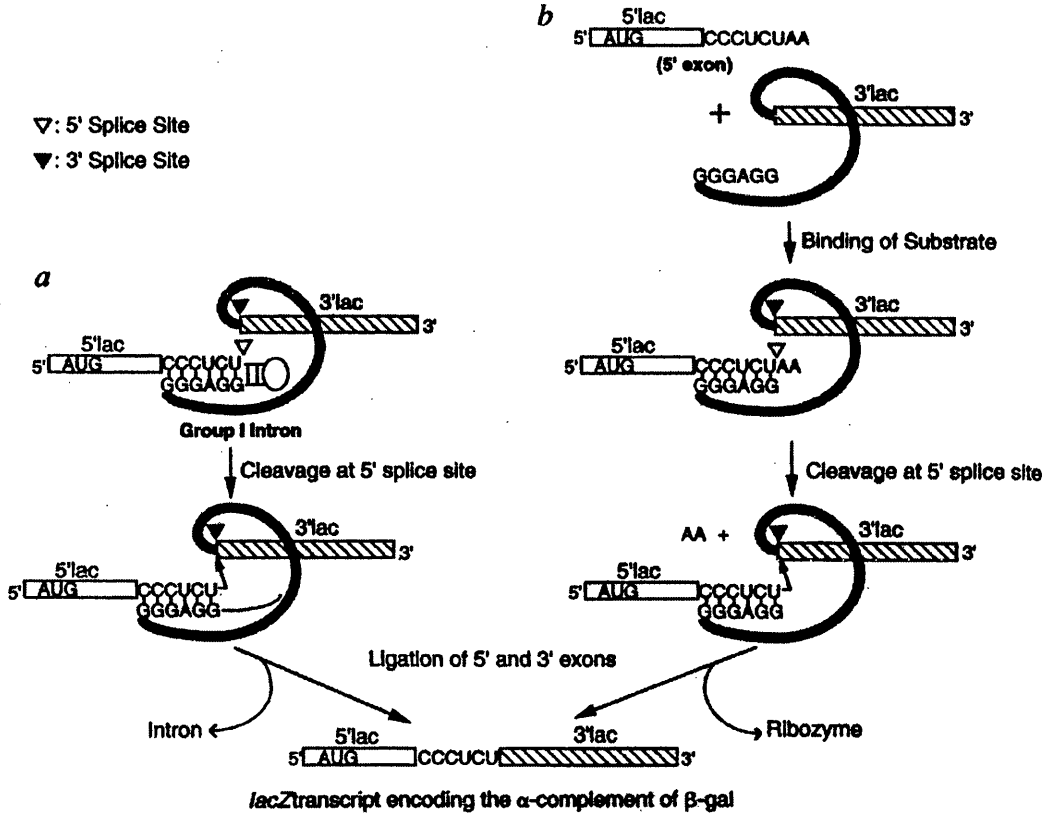

Figure 1.18. *Cis*- and *trans*-splicing of *lacZ* transcripts. ***(a)*** The *lacZ* mRNA containing a group I self-splicing intron. The intron excises itself from the pre-mRNA, and ligates the two exons together. The specificity of the splicing reaction comes from the hybridization of the CCCUCU sequence at the 3' end of the 5' exon with its complementary sequence within the intron. ***(b)*** A truncated *lacZ* mRNA, with the group I self-splicing intron recognition sequence, CCCUCU, at the 3' end. A free group I intron, carrying the 3' end of the *lacZ* gene, hybridizes with the recognition sequence at the 3' end of the 5'-truncated portion of the *lacZ* mRNA. Despite operating in *trans* the group I intron can splice together the ends of the 5' and 3' portions of the *lacZ* mRNA. Taken from Sullenger & Cech, (1994b).

Group I self-splicing introns catalyse both a phosphodiesterase activity (in excising themselves from the pre-mRNA) as well as an RNA ligase activity which joins together the exons on either side of the excised intron (Zaug & Cech, 1986). The reaction's specificity arises from internal guide sequences which direct cleavage and religation to specific splice sites. This specificity has been used to direct self-splicing introns to cut mRNA and replace the 3' end of the RNA with RNA from the 3' end of the intron itself (figure 1.18) (Been *et al.*, 1987). This could have potential applications in gene therapy for inherited disorders, enabling the mRNA of a defective gene to be repaired without having to replace the faulty gene at the DNA level. Modified *trans*-splicing introns have been used in *E. coli* to regenerate the coding capacity of truncated *lacZ* transcripts, allowing protein synthesis (Sullenger & Cech, 1994b).

1.12.2 RNASE P

RNase P is a ubiquitous enzyme which processes the 5' ends of tRNA precursors (Altman *et al.*, 1981). RNase P is a ribonucleoprotein, the best characterised of which is from *E. coli*. The *E. coli* enzyme consists of a 13.8kD basic protein and a 377 nucleotide RNA known as M1 (Altman & Guerrier-Takada, 1986). The sequence of the RNA is poorly conserved between bacterial species, though all share remarkably similar secondary structures. The protein and M1 RNA segments from different bacterial RNase P holoenzymes can be reconstituted to form functional hybrid enzymes (Altman *et al.*, 1987). Under certain conditions *in vitro*, the M1 RNA can function catalytically in the absence of the protein subunit, though this has only been shown for bacterial RNase P (Guerrier-Takada *et al.*, 1983, Altman *et al.*, 1989). These isolated RNAs have similar catalytic efficiencies to the native holoenzyme. Unlike the self-splicing introns and the small catalytic RNAs, the RNase P ribozyme is a true catalyst, as it cleaves other RNA molecules rather than itself, and processes multiple substrates.

How does one enzyme manage to recognise and process the several dozen pre-tRNAs which are produced in all cells? All tRNAs have a CCA triplet at their 3' end, in the acceptor arm which binds amino acids. The M1 RNA contains a conserved GGU triplet which forms Watson-Crick base-pairs with the CC doublet in the CCA motif, whilst the U residue interacts with the so called 'discriminator' base (figure 1.19). This discriminator base can either be an A residue, allowing a third, tight Watson-Crick base-pair, or a 'wobble' residue which produces a weaker interaction, and slows down cleavage (Guerrier-Takada *et al.*, 1989). In addition to this tight binding, a number of weaker non-Watson-Crick interactions have also been found by cross-linking experiments. Once the pre-tRNA is bound by the M1 RNA, the 5' end of the pre-tRNA is cleaved.

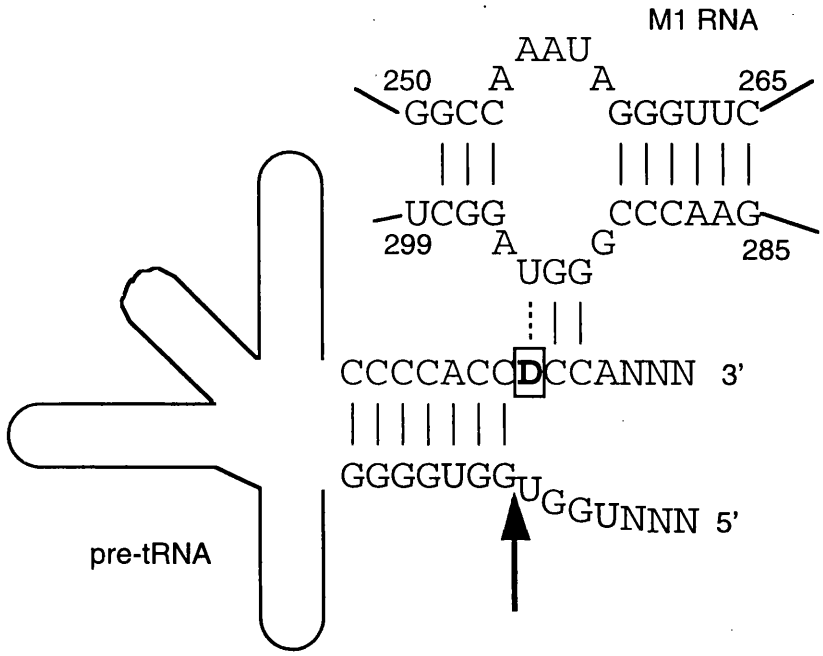

Figure 1.19. Binding of RNase P M1 RNA to the 3' acceptor arm of pre-tRNA. The discriminator base (**D**) is highlighted, with the cleavage point indicated by an arrow. The key recognition step is the hybridization of the CC residues in the pre-tRNA acceptor arm with residues 292 and 293 of the M1 RNA. Cleavage is particularly favoured if the discriminator base is an A, though non-Crick-Watson recognitions are made between the two RNAs (not shown). Taken from Tallsjo (1996).

1.12.2a External Guide Sequences (EGS)

Cleavage of the 5' end of pre-tRNA by RNase P is directed by the M1 RNA recognising the CCA motif in the 3' acceptor arm of the pre-tRNA. As this recognition domain is not within the substrate (the 5' end of the pre-tRNA) itself, this has become termed the external guide sequence (EGS). Forster and Altman proposed that short RNAs containing the CCA motif could be targeted to any RNA and direct the cleavage of that RNA by RNase P (figure 1.20) (Forster & Altman, 1990). This has been successfully demonstrated using the *E. coli* enzyme *in vitro* and *in vivo* to reverse an antibiotic resistance phenotype (Yuan & Altman, 1994).

EGSs are being extensively studied as potential agents for use against HBV (Bockman *et al.*, 1993). Activity has been demonstrated in HeLa cell extracts against an 837 nt RNA fragment corresponding to parts of pre-S2 and S (George *et al.*, 1993). It was shown that phosphorothioate RNA EGSs had increased stability in cell extracts compared to their RNA counterparts, and could still mediate cleavage by M1 RNA and RNase P (Narayan *et al.*, 1993). EGSs made from DNA could not mediate cleavage (Kahle *et al.*, 1993). This work is rapidly moving towards initial clinical trials.

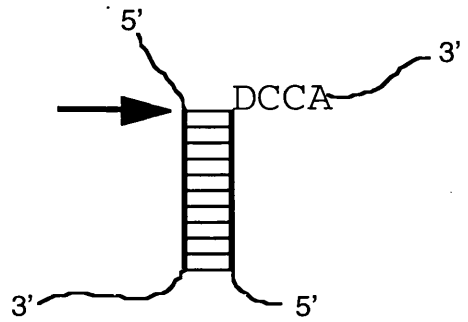

Figure 1.20. An RNase P substrate bound to an EGS. The discriminator base (D) and the CCA triplet are shown within the EGS, with the cleavage site indicated by an arrow. Cleavage is not dependent on the substrate sequence, allowing EGSs to be used to target any RNA.

1.12.3 SMALL CATALYTIC RNAS

This group of ribozymes consists of several motifs found in a number of viroids, as well as in the RNA transcripts of Neurospora mitochondrial DNA and a newt satellite DNA. All these motifs participate in single turnover, intramolecular reactions and are therefore pseudo-catalytic. However, these ribozymes can be manipulated to function in *trans*, thus offering potential as extensions of antisense RNA for gene silencing.

1.12.3a Plant viroid ribozymes

Viroids are infectious agents which require coinfection with a virus which provides helper functions to assist with the viroid's replication (Symons *et al.*, 1987). A number of RNA viroids have been characterised in plants which replicate by a rolling circle mechanism (figure 1.21). This generates a string of viroid genomes joined head-to-tail which must be separated to allow viroid maturation. This is achieved by small regions of secondary structure at the junction of adjacent genomes. Two such motifs have been described. The

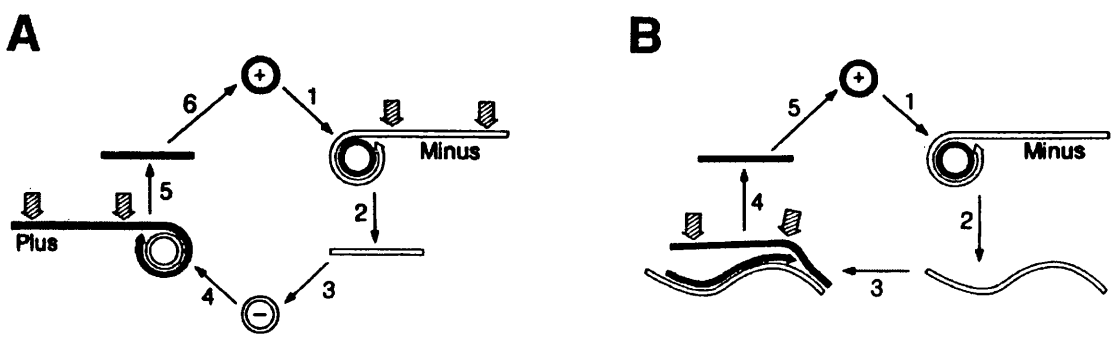

Figure 1.21. Two alternative forms of rolling circle replication employed by viroid RNAs. **A** Both plus and minus strands are self-cleaved. **B** Only the plus strand self-cleaves. Sites of self cleavage are indicated by arrows. Taken from Forster & Symons, (1987).

first to be discovered was the hammerhead motif, which is discussed in detail in section 1.12.4. The second motif is the hairpin ribozyme (figure 1.22).

The hairpin was originally found in the 359 nt linear satellite RNA of tobacco ringspot virus (Haseloff & Gerlach, 1989). The (+) strand RNA is cleaved by a hammerhead domain, whilst the (-) is cleaved by the hairpin. The hairpin differs from the hammerhead by catalysing the reverse, re-ligation, reaction as well as the phosphodiesterase cleavage. Essential residues have been investigated by *in vitro* selection of a pool of variants containing point mutations at all sites in a 50 nt hairpin catalytic RNA (Joseph & Burke, 1993). This allowed the precise base-pairing requirements of helices III and IV to be shown, and to identify eight essential nucleotides (G8, A9, A10, G21, A22, A23, A24, and C25). The importance of the ribose 2'-hydroxyl groups was determined by making single substitutions with deoxyribonucleotides. This identified residues A10, G11, A24 and C25 as providing hydroxyl residues vital for ribozyme function (Chowrira *et al.*, 1993). These results are supported by data showing that 2'-O-methyl substitutions at G11 and A24 also inhibit ribozyme activity. The hydroxyl moieties are thought to provide either important tertiary structure contacts or co-ordination sites for Mg^{2+} (Berzalherranz *et al.*, 1993). Although Mg^{2+} is required for hairpin activity it is unclear whether it provides a structural or catalytic function (Hampel & Cowan, 1997). The helix IV stem has been extended to allow RNA binding proteins to associate, such as *rev* from HIV. This does not seem to affect ribozyme activity, and offers intriguing possibilities for modulating ribozyme expression and intracellular localisation.

The hairpin ribozyme can be manipulated to function in *trans*. Modified hairpins have been used to cleave HBV substrates *in vitro* (Welch *et al.*, 1997). However, most progress in the therapeutic application of hairpin ribozymes has come in the targeting of HIV, where studies have progressed to human clinical trials.

1.12.3b Therapeutic uses of the hairpin ribozyme

Work leading to the first human clinical trials of a ribozyme has been performed by Wong-Staal's group. Initially they designed a hairpin ribozyme under the control of a β-actin promoter, which was shown *in vitro* to cleave HIV-1 RNA in the U5 leader region, leading to a reduction in *tat* activity and p24 production (Rappaport *et al.*, 1993). For this work to be extended to a cell culture system it was deemed necessary to increase the expression of the ribozyme. This was done by cloning the ribozyme into a murine retroviral vector under the control of a polymerase III promoter. Retroviral vectors insert into the transduced cell's DNA, giving long-term stable expression of any cloned genes. Genes with polymerase III promoters (in this case from human $tRNA^{Val}$ and adenovirus *VA1* genes) are

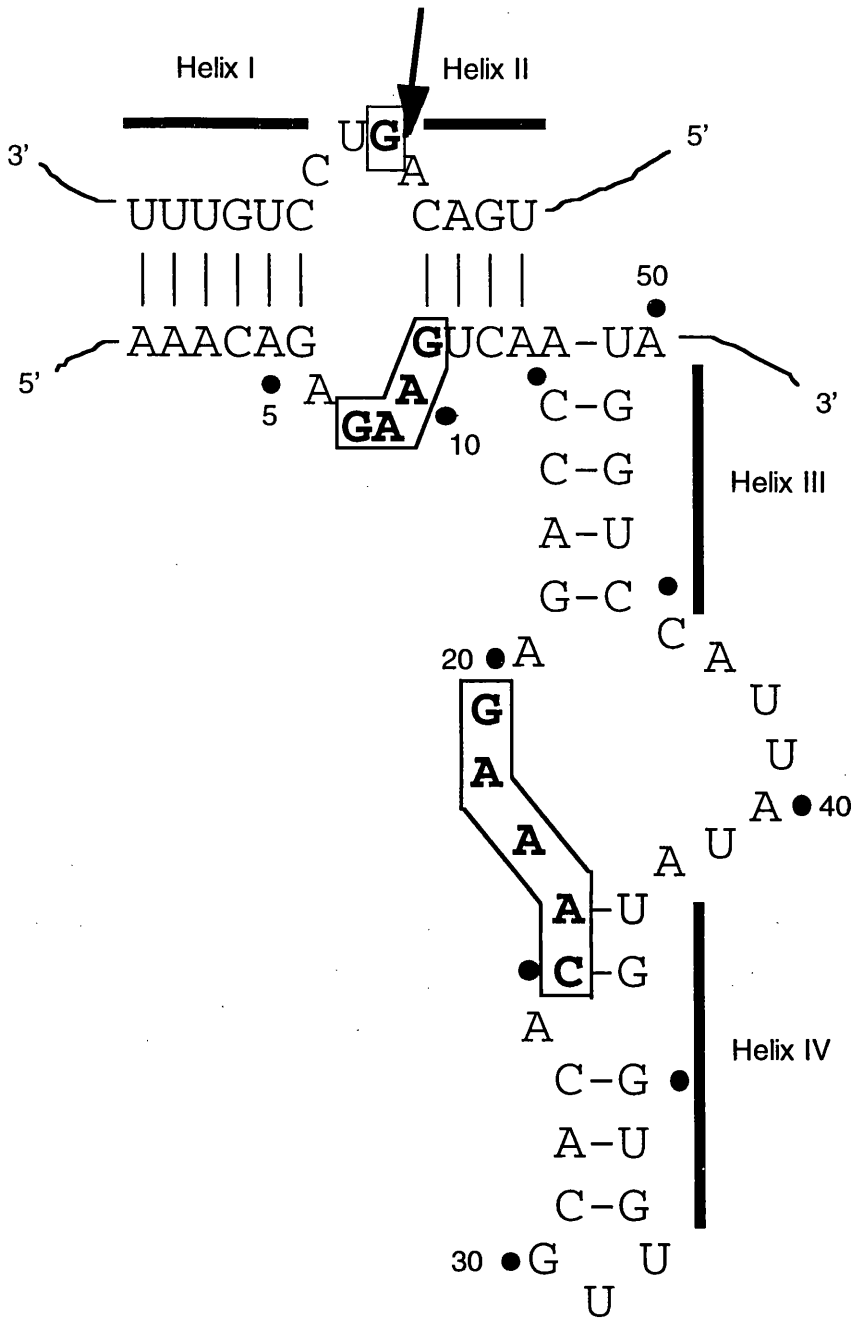

Figure 1.22. Secondary structure model of the hairpin ribozyme from the negative strand of the tobacco ringspot virus satellite RNA. The ribozyme sequence is numbered from 1 to 50, with essential residues marked in bold and boxed. The cleavage site on the substrate strand is to the 5' side of an essential G residue, and is indicated by an arrow. Taken from Berzalherranz *et al.*, (1993).

expressed in all cell types at a much higher level than those with polymerase II promoters, which drive protein-encoding genes. In transient transfections of HeLa cells, these constructs were shown to reduce p24 expression by 95%. An inactive ribozyme mutant was shown to inhibit p24 production by only 10%, thus showing the bulk of the inhibitory activity is due to ribozyme, rather than antisense, activity (Ojwang *et al.*, 1992).

The long-term goal of this work is to create a population of lymphoid cells which are resistant to HIV infection. The human lymphoid cell line CEM/174 was transduced with a retroviral vector encoding a hairpin, under the control of a polymerase III promoter, targeted to the 3' LTR of SIV (Heusch *et al.*, 1996). This treatment provided long-term resistance to infection by SIV, reducing the burden of proviral DNA. This was achieved by presumably cleaving viral RNA as it entered the cells. This has paved the way to human stem cell therapy.

Human haematopoeitic stem cells can be identified by the CD34 marker. This has enabled stem cells to be enriched from the umbilical cord blood of healthy and HIV-positive donors. Transduction of these cells with retroviral vectors encoding the U5 ribozyme yielded stable ribozyme expression with no changes in phenotype or proliferation. The macrophage progeny of these cells were resistant to HIV infection (Yamada *et al.*, 1994a, Yamada *et al.*, 1994b). However, to reduce the risk of escape mutants appearing, cells will be transduced with a second ribozyme targeted to the pol region. The importance of this was demonstrated by targeting a hairpin to the rev/env region at a point where the infectious clone SF2 has a single nucleotide substitution compared to the HXB2 prototype virus (N*GUC mutated to N*UUC). The ribozyme could inhibit HXB2 replication in Molt 4 cells, but could not block SF2 replication (Yu *et al.*, 1993). A phase I clinical trial has been undertaken using these vectors to transduce peripheral blood lymphocytes *ex vivo*, which will then be used for autologous reinfusion. The possibility of using modified CD34 cells from cord blood for autologous reinfusion of neonates born to HIV-positive mothers is also being investigated (Ho *et al.*, 1994, Rosenzweig *et al.*, 1997).

1.12.3c Hepatitis delta ribozyme

Hepatitis delta virus (HDV) is similar to the plant viroids. It has a circular RNA genome of 1.7kb, and is only able infect persons already infected with HBV, or to coinfect along with HBV (Rizzetto, 1990). HDV encodes a single nucleocapsid protein, the delta antigen. The HDV particle also includes HBsAg provided by HBV. HDV replicates via a rolling circle mechanism, and processes its genomes using a unique ribozyme motif (Perrotta & Been, 1990). The HDV ribozyme structure consists of four helices (figure 1.23a) and is thought to contain a pseudoknot four base-pair sequence, which corresponds to helix III. Mutational data from different laboratories do differ, leading some to suggest that the ribozyme has an axehead, rather than a pseudoknot, structure (figure 1.23b) (Kumar *et al.*, 1992, Wu *et al.*, 1992). The pseudoknot structure is supported by the observation that most of the sequence which forms helix IV in this model can be deleted without a loss of activity. The hepatitis delta ribozyme does have a requirement for Mg^{2+} ions, though they appear to play a structural rather than a catalytic role.

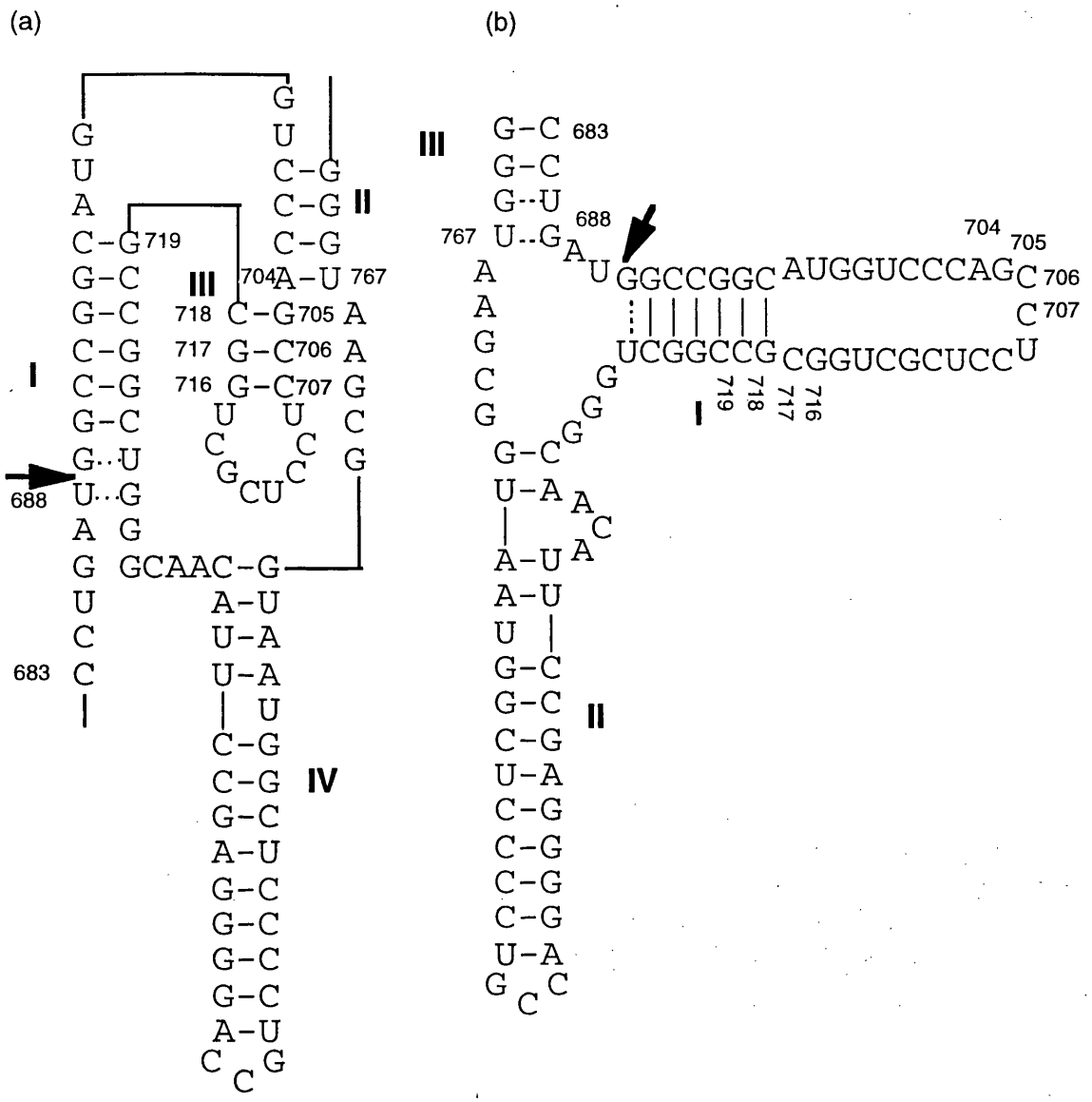

Figure 1.23. Two alternative structures for the hepatitis delta ribozyme. (a) pseudoknot structure formed by helices II and III. (Perrotta & Been, 1990). (b) 'axehead' structure. (Branch & Robertson, 1991). The cleavage point is indicated by an arrow. Base positions within the HDV genome are also shown.

The hepatitis delta ribozyme has been used to generate precise 3' ends of *in vitro* transcribed RNAs for use in *in vitro* assembly of negative-stranded RNA viruses (Bridgen & Elliott, 1996). This was acheived by blunt-end cloning the ribozyme domain onto the 3'-end of the gene of interest. The ribozyme can also be modified to function in *trans* by allowing the formation of helix I between two separate RNA molecules, one of which carries the ribozyme catalytic domain (Perrotta & Been, 1992, Shih *et al.*, 1993, Fauzi *et al.*, 1997). This offers the possibility of infecting chronic HBV carriers with a modified HDV which carries a ribozyme which not only allows HDV to replicate, but which also cleaves HBV

RNA. However, coinfection with wild-type HDV can lead to more severe disease, which may prevent the use of modified HDV as a therapeutic agent.

1.12.3d Other motifs

The genomes of the newts *Notophthalamus* and *Triturus* contain a highly repetitive family of satellite DNAs which are distributed in clusters throughout the genome and which are transcribed to produce stable, strand-specific RNAs (Luzi *et al.*, 1995). This differs from other satellite DNAs which are usually transcriptionally inert and restricted to the heterochromatin. The RNAs exist as monomers or multimers of the 330 base repeat of the satellite sequences, and contain a motif similar to the hammerhead ribozyme (see section 1.15). Although these ribozymes do cleave at a specific site in the same fashion as the plant viroid hammerheads, cleavage has also been observed about 50 nt upstream of the expected cleavage site, suggesting some other mechanism. It has been shown that for the newt ribozyme to function *in vivo* it must be associated in a ribonucleoprotein complex of approximate size 12S (Luzi *et al.*, 1997).

The 881 nt transcript of the circular *Neurospora* VS mitochondrial DNA plasmid contains a ribozyme motif which is thought to be similar to the hairpin motif (Saville & Collins, 1991). This is purely on the basis of computer modelling, as there is too little variation between VS RNA isolates to allow the identification of essential residues. The cleavage activity has been localised to a 154 nt region, with only one residue required 5' to the cleavage site (Rastogi *et al.*, 1996). The functions of both the newt and the *Neurospora* motifs are unknown (Crisell *et al.*, 1993).

1.12.4 HAMMERHEAD RIBOZYMES

The hammerhead motif was the first of the small catalytic RNAs to be discovered (Tritz & Hampel, 1988). It has since been found in a number of plant viroids, either in both the positive and negative strands (*e.g.* avocado sunblotch viroid, ASBV (Daros *et al.*, 1994)) or just in the positive strand (*e.g.* tobacco ringspot encapsidated linear satellite RNA (Feldstein & Bruening, 1993)). The hammerhead is the best characterised of all the catalytic RNAs, with detailed studies of its structure and mechanism being facilitated by its small size. There have also been many studies focused on trying to manipulate the hammerhead ribozyme for use as a gene silencing and therapeutic agent.

1.12.4a Key elements

The hammerhead ribozyme consists of three helices surrounding a central region containing 13 conserved residues (figure 1.24) (Haseloff & Gerlach, 1989). Cleavage occurs on the 3' side of a triplet with the consensus sequence NUX, where N can be any base and X can be any base other than guanosine. In wild-type hammerheads this triplet is always GUC, with the exception of the Lucerne transient streak viroid in which the triplet is

CUC. Despite the flexibility of the NUX triplet sequence, the rate of cleavage at different triplets is variable (Zoumadakis & Tabler, 1995). The greatest rates are seen at GUC and CUC triplets. The sequences of the three helices are not important provided that base-pairing is maintained. The lengths of these helices can effect ribozyme activity (see section 1.12.4d).

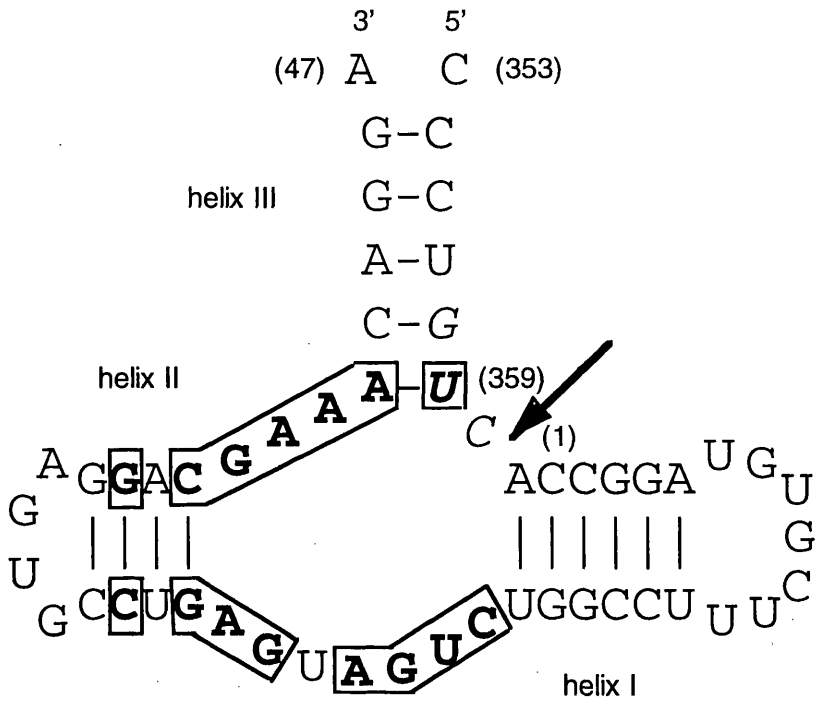

Figure 1.24. The hammerhead domain from the positive strand of the tobacco ringspot virus satellite RNA. Conserved bases are boxed and in bold type. The NUX triplet (in this case GUC) is in italics. The cleavage point is indicated by the arrow, and helices I, II and III are marked. The numbers in brackets refer to the base positions in the satellite RNA's genome, with the first base immediately following the cleavage point (Haseloff & Gerlach, 1989).

There is evidence in ASBV for a double-hammerhead structure consisting of the plus strand motif and the complement of the negative strand motif (Daros *et al.*, 1994). This has been shown to have greater cleavage efficiency than just the positive strand motif alone. This is probably due to the increased stability gained by having both structures next to each other. The ASBV hammerhead is particularly likely to benefit from increased stability as helix II only has two or three base-pairs.

1.12.4b *Cis*- and *trans*-cleaving hammerheads

Wild-type hammerhead ribozymes all operate in a *cis* conformation, with the whole structure being formed by RNA from the same small segment of the molecule. However, helices I and III of the ASBV positive and negative strand hammerheads are formed between sequences from opposite sides of the genome (figure 1.25a). This suggested that

Figure 1.25a

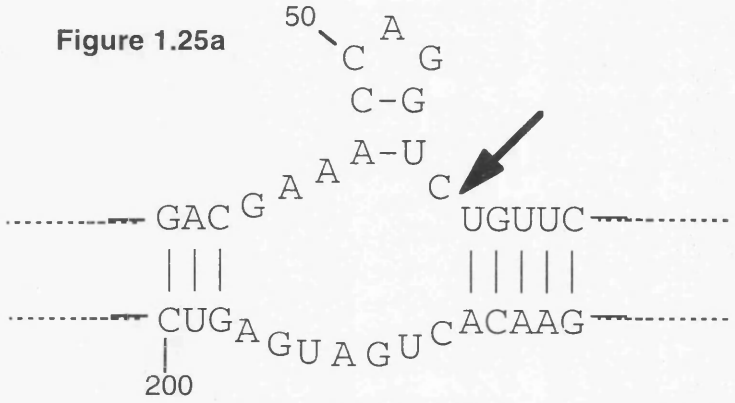

Figure 1.25b

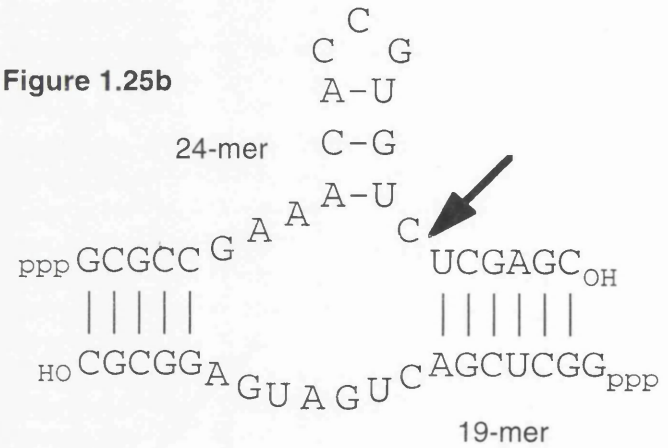

Figure 1.25c

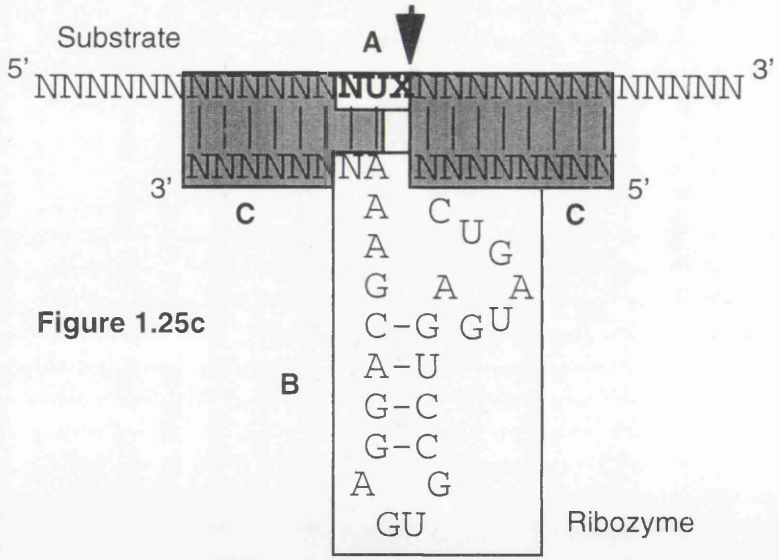

Figure 1.25a. Detail of the ASBV positive strand hammerhead ribozyme. *The numbers in brackets refer* to the base position in the 247 base genome. The hammerhead structure is produced by the hybridization of sequences from opposite sides of the circular genome. **1.25b.** The first synthetic hammerhead ribozyme, produced by the hybridization of a 19-mer and a 24-mer, both produced by *in vitro* transcription. The intermolecular contacts are made within helices I and II. The cleavage point is indicated by an arrow. Taken from Uhlenbeck, (1987). **1.25c.** A model for the design of *trans*-cleaving hammerhead ribozymes. The cleavage point is indicated by an arrow. Variable bases are indicated as 'N'. Three structural domains are boxed. (A) the NUX triplet, which lies to the 5' side of the cleavage point. (B) The catalytic core domain and (C) the variable flanking sequences, which hybridize with their complementary sequences in the target RNA to form helices I and III. Taken from Haseloff and Gerlach, (1988).

hammerheads had the potential for *trans*-cleavage. Uhlenbeck demonstrated this using a 24-mer generated by *in vitro* transcription which contained helix III, the cleavage site and sequences which would allow it to hybridise with a 19-mer to form helices I and II (figure 1.25b) (Uhlenbeck, 1987). The sequences of these constructs matched that of the ASBV hammerhead. The 24-mer substrate was cleaved and, as the 19-mer was not consumed in the reaction, the 19-mer was able to dissociate from the products and mediate subsequent reactions.

Could the specificity of a *trans*-cleaving hammerhead be altered? This was shown by Haseloff and Gerlach who designed a hammerhead to cleave the mRNA of the chloramphenicol acetyl transferase gene (Haseloff & Gerlach, 1988). This ribozyme differed from Uhlenbeck's in that the ribozyme strand contained helix II and the central loop, and hybridised with the substrate strand to form helices I and III. This lead to a generalised model for the design of hammerhead ribozymes (figure 1.25c). This model does not demand any structural constraints in the choice of substrate, merely that an NUX triplet is present.

1.12.4c Structure and mechanism

The determination of RNA tertiary structures by X-ray diffraction crystallography has lagged considerably behind that of proteins. This is mainly due to the difficulty in obtaining crystals of sufficient quality for analysis. The first RNA structure to be determined was that of yeast $tRNA^{Phe}$ (Brown *et al.*, 1983, Brown *et al.*, 1985). The RNA was treated with Pb(II) prior to crystallisation, with the unexpected result that the tRNA was specifically cleaved between residues 17 and 18. This cleavage was at its most efficient at neutral pH, producing a 5' hydroxyl and 2'3'-cyclic phosphate, products which are also produced by ribozymes. By altering the pH and freeze-trapping, it was possible to obtain a structure of the $tRNA^{Phe}$-Pb(II) complex. The Pb^{2+} ion was shown to be bound covalently in the TψC loop next to the cleaved bond. It was proposed that the Pb^{2+} ion acts as a source of metal-bound hydroxyl ions (which would only be present at neutral pH) which could abstract a proton from the ribose 2'-hydroxyl group of residue 17, thus cleaving the phosphodiester bond. This gives clues as to the hammerhead mechanism, as the hammerhead also requires divalent cations and a neutral pH for cleavage.

The first hammerhead structure was obtained by Pley *et al*, (1994, 1995). To prevent the substrate being cleaved, an all-RNA ribozyme/ all-DNA substrate complex was crystallised (Pley *et al.*, 1993). Intermolecular contact was made within helices I and III, as in Haseloff and Gerlach's model. It was believed that the structure would not be radically different from that formed with an all-RNA substrate, as the ribozyme was shown to cleave a substrate which was entirely DNA apart from the residue to the 5' side of the cleavage site. The high salt concentration (1.6M LiCl) in which the crystals were grown was also cause for

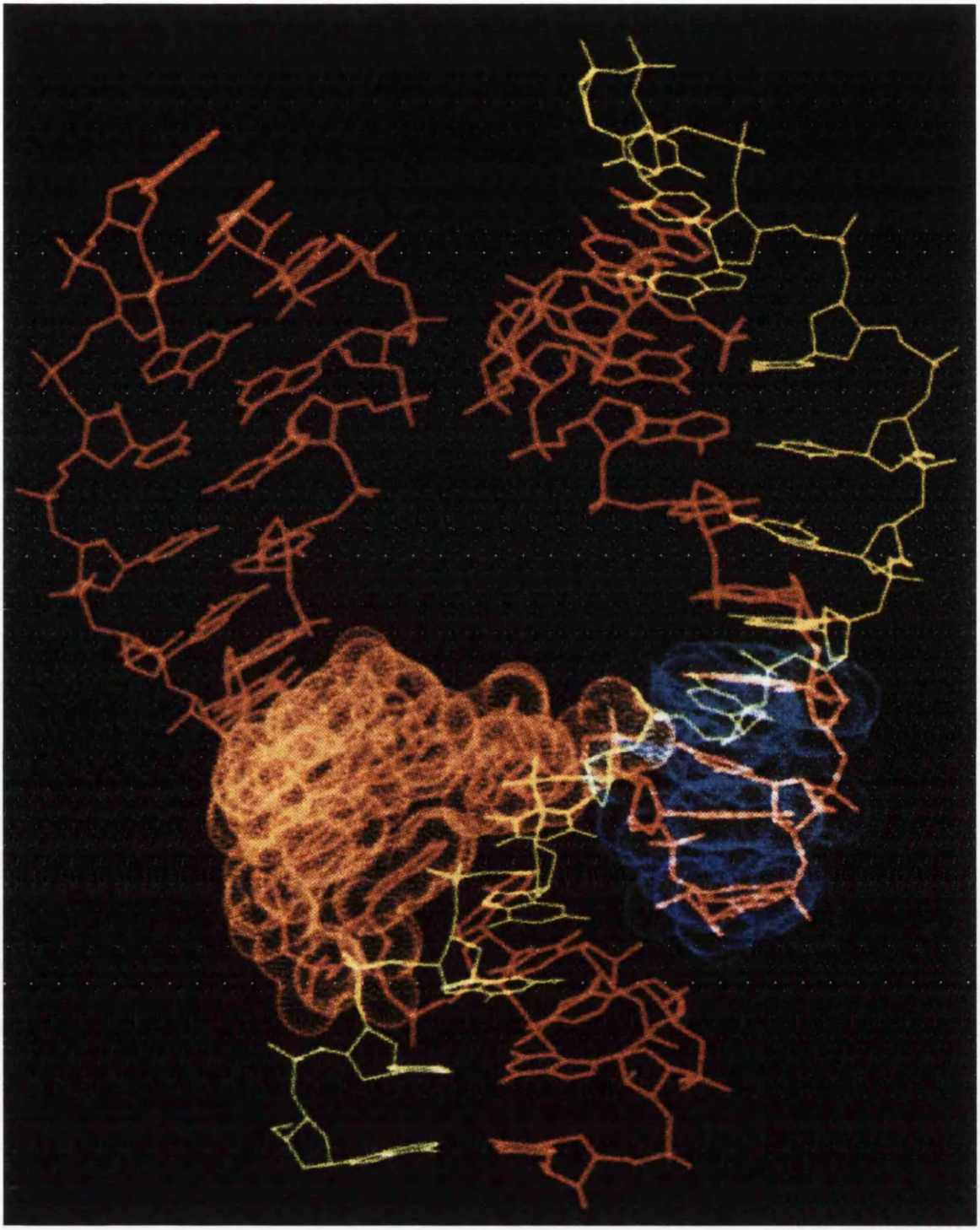

Figure 1.26a. Crystal structure of hammerhead ribozyme (red) bound to an all-DNA substrate (yellow). Bases in domain I (the uridine loop) are shown as blue dot-surfaces. Domain II (the non-Watson-Crick base-pairing) is shown as gold dot-surfacing. Intermolecular contacts are made within helices I and III. Helix I is at the top right, helix II at the top left and helix III at the bottom. Taken from Pley *et al.*, (1994).

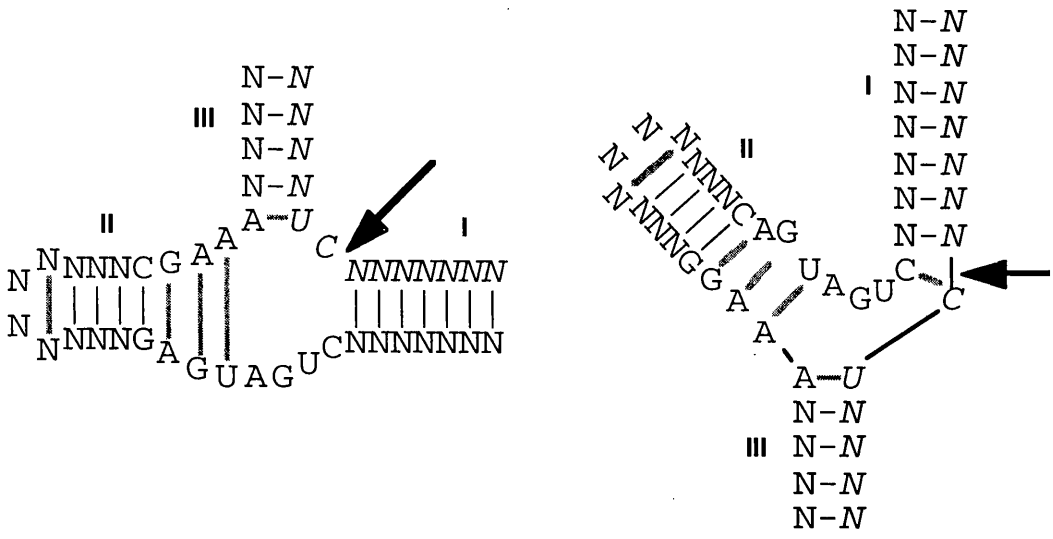

Figure 1.26b. The original proposed secondary structure of the hammerhead ribozyme (left) and the secondary structure suggested by the three-dimensional structure determined by Pley et al. The substrate strand is shown in italics, Watson-Crick base-pairs as thin black lines, and novel base-pairs as thick grey lines. The cleavage site is indicated by an arrow.

concern. However, the ribozyme was shown to cleave an RNA substrate in these conditions. The final structure (figure 1.26) was very different from the predicted secondary structure, which was based purely on Watson-Crick base-pairing (figure 1.24). The three helices all showed an A-form structure typical of double-stranded RNA. The core was shown to have two domains. The first, following helix I with the sequence 5'CUGA, forms a sharp turn identical to the uridine turn of the anticodon loop from tRNA (Schweisguth & Moore, 1997). This is followed by the second domain, a 3 base-pair duplex of non-Watson-Crick base-pairing stabilised by base-stacking which has the potential to bind divalent cations. The structure suggested that the ribozyme twists the substrate in such a way as to bring the ribose 2'-hydroxyl group on the cytosine to the 5' side of the cleavage site into position to attack the phosphate in the scissile bond. There was no indication as to whether a divalent cation is situated at the cleavage site, though some evidence suggesting this is the case has been gleaned from the use of modified substrates (Kuimelis & McLaughlin, 1997). If the Rp oxygen of the scissile bond phosphate is replaced with sulphur, cleavage in the presence of Mg^{2+} is substantially reduced, though cleavage with Mn^{2+} is unaffected (see section 1.12) (Herschlag *et al.*, 1991). This is not observed if the Sp oxygen is substituted, suggesting a direct interaction between the Rp oxygen and a divalent cation. However, a conformational change would be required in the RNA-DNA crystal structure for a divalent cation at this position to be brought into the correct position for cleavage to occur.

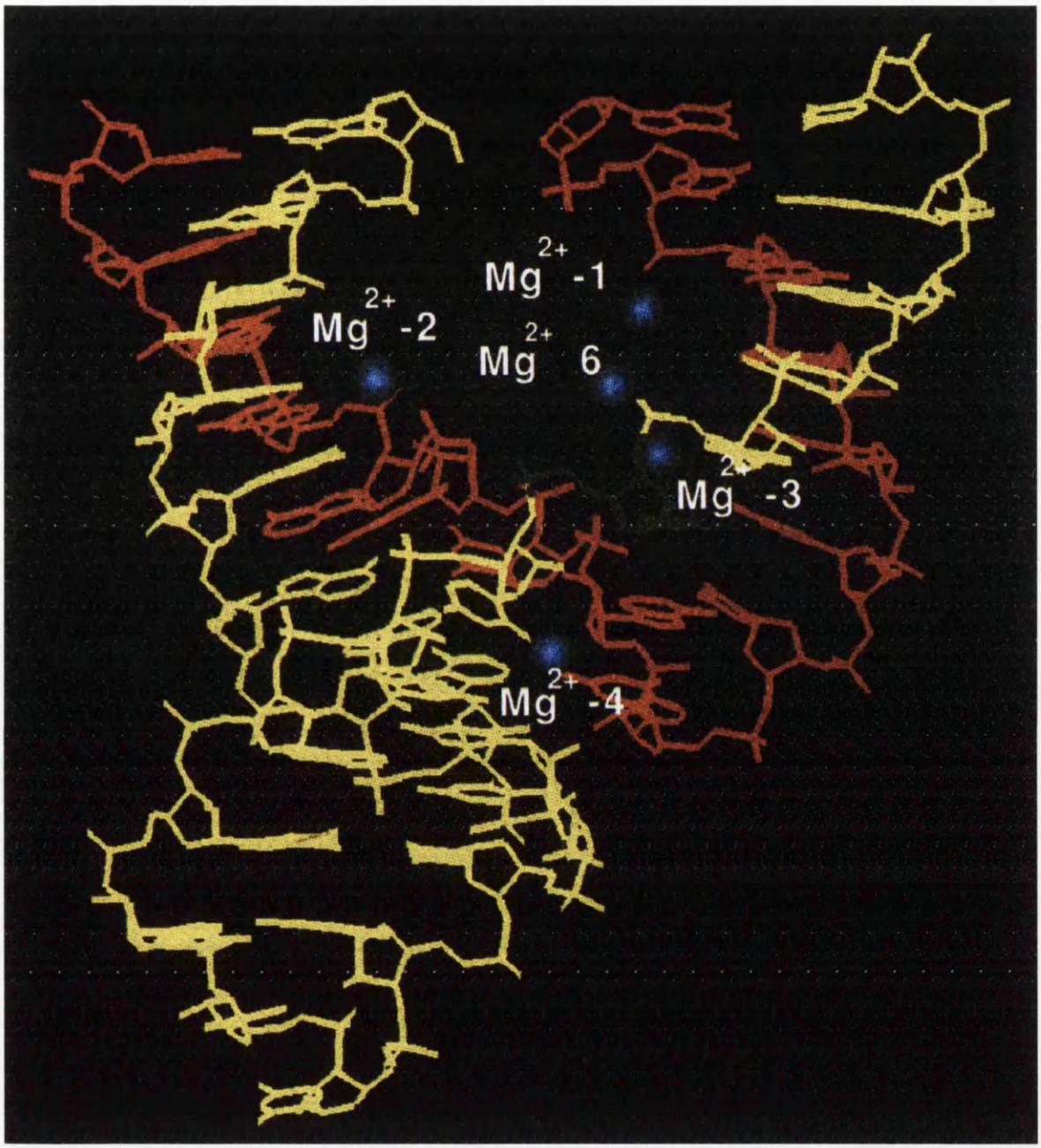

Figure 1.27. Structure of a hammerhead ribozyme (red) bound to an all-RNA substrate (yellow). The key cytosine residue, whose ribose 2'-hydroxyl group is involved in the cleavage reaction, is shown in green. Five of the six potential Mg^{2+} binding sites are shown in blue (site 5, though it binds Mn^{2+}, does not bind Mg^{2+} as tightly as the other sites). This intermediate was captured by freeze-trapping. The Mg^{2+} at site 6 is deemed to be important in the base-catalysed step of the cleavage reaction. Taken from Scott *et al.*, (1996).

Scott *et al* (1995) produced the structure of a hammerhead attached to an all RNA substrate. Cleavage was blocked by substituting the ribose 2'-hydroxyl on the 5' side of the scissile bond with a 2'-O-methyl group. The backbone connectivity differed from that of Pley *et al*'s (1994) ribozyme, with the intermolecular contacts being made within helices I and II, as in Uhlenbeck's ribozyme (Uhlenbeck, 1987). The crystals of the ribozyme-RNA substrate were grown in a much lower salt concentration, and were packed differently from the ribozyme-DNA substrate complex, with two complexes per unit cell rather than three. Despite these differences, the two structures are both very similar, the only difference being a few extra stabilising hydrogen bonds in the all-RNA structure. Five potential binding sites for divalent cations were also located, including one near the catalytic pocket (figure 1.27) which had the potential to approach the cleavage site through conformational change. Subsequent work using an unmodified RNA substrate has produced crystals in which substrate cleavage can occur when the crystals are soaked in a solution of divalent cations. Modulating conditions by varying pH and freeze-trapping has enabled two intermediates to be trapped (Scott *et al.*, 1996). The first shows metal binding prior to cleavage, and has revealed a sixth divalent cation binding site on the Rp oxygen of the phosphate in the scissile bond, as previously predicted. This binding site is only occupied at neutral to alkaline pH. This, rather than the binding site revealed in the previous structure, is likely to be the critical point in the cleavage mechanism. Binding of Mg^{2+} at this point is believed to induce the conformational change needed for in-line attack at the cleavage site ribose 2'-hydroxyl, as

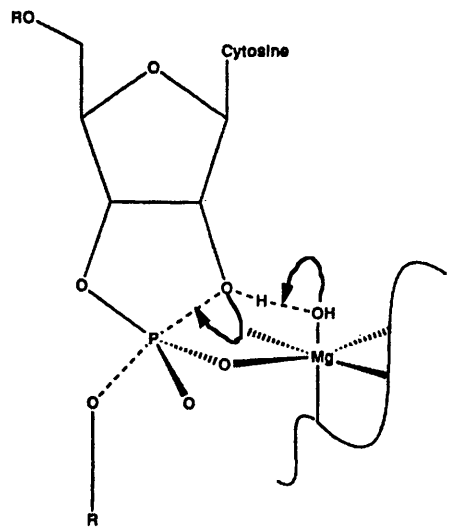

Figure 1.28. The metal hydroxide transitional state, with arrows indicating electron movements. A lone-pair of electrons on the oxygen of the metal hydroxide attacks the proton of the ribose 2'-hydroxyl (nucleophilic attack). This results in the proton being removed to produce H_2O and a free Mg^{2+}. This then makes it thermodynamically favourable for the lone-pair of electrons on the ribose 2'-oxygen (formed by the removal of the proton) to attack the phosphorus to form a 2'3'-cyclic phosphate.

well as providing a metal hydroxide to initiate the base-catalysed step of the cleavage reaction (figure 1.28). The second intermediate accumulates just before cleavage occurs. The restrictions of the crystal lattice are believed to trap this intermediate. This shows an increase in hydrogen bonding within the core produced by base stacking interactions, thus stabilising the transition-state.

Although the hammerhead mechanism is becoming clearer, more work needs to be done. Generation of 'kinetic bottleneck' mutants will enable the cleavage reaction to be stalled at different points, extending the lifespans of intermediates enabling structural analysis. This approach has proved fruitful with protein enzymes.

1.12.4d Factors affecting activity

Although it has been demonstrated that the hammerhead ribozyme can be manipulated to target any RNA, there are a number of factors which must be considered. The lengths of the flanking sequences on either side of the conserved catalytic core, which hybridise with the substrate to form helices I and III, are very important. Like antisense oligonucleotides, it is important that the flanking sequences are sufficiently long (at least 11 to 15 bases) to give the required degree of specificity. However, there is a limit to how long the flanks can be. If they are too long, then the cleavage products will fail to dissociate from the ribozyme, preventing multiple turnover. Goodchild and Kohli (1991) demonstrated that by reducing the total flanking sequences of a hammerhead targeted against HIV mRNA from 20 to 12 bases increased the rate of cleavage 10-fold. In addition, only the shorter ribozymes showed multiple turnover. The sequence of the target can also affect the optimum flanking sequence length. If helices I and III are GC-rich, then they will be more stable than AU-rich helices of the same length. Not only does this slow down the rate of product dissociation, but it also makes the ribozyme more tolerant of mismatches in the target site (Werner & Uhlenbeck, 1995). U-rich flanking sequences are to be avoided if possible, as G-U wobble base-pairs can form, further reducing target specificity (Herschlag, 1991).

Whether ribozymes are generated by *in vitro* transcription or intracellularly, they always carry exogenous sequence outside of the catalytic core and complementary flanking sequences. This sequence is derived from the promoter and the transcription termination signal. This excess sequence can sometimes assume secondary structures with the ribozyme sequences which prevent the ribozyme from binding its target. An example of this can be found in the barley yellow dwarf viroid where, under certain conditions, a sequence adjacent to the ribozyme can interact with the bulge of helix II and form a pseudoknot structure (Miller & Silver, 1991). This is believed to operate as a form of control over viroid replication. The incorporation of *cis*-cleaving hammerheads into transcripts which can excise the *trans*-cleaving hammerhead from the surrounding sequence has been successfully demonstrated. Such constructs have allowed hammerheads which were otherwise inactive to bind to and cleave their substrates.

Excess sequences have been specifically chosen to exert allosteric control over ribozyme activity. Allostery is a well-characterised phenomenon of protein enzymes, where the binding of a factor to an enzyme somewhere other than the active site varies the enzyme's activity. Addition of an ATP-binding RNA aptamer (selected by *in vitro* screening) to a hammerhead ribozyme transcript blocked ribozyme activity when ATP was present (Tang & Breaker, 1997). This offers the potential of tightly controlling ribozyme activity with small ligands, which could be used to restrict activity to particular cell types.

Substrate secondary structure can also prevent ribozyme binding. mRNAs are dynamic structures which constantly switch between a number of different conformations all of similar free energy. If any of these structures include regions of duplex within the ribozyme target site, then ribozyme-substrate binding may be blocked. Fedor and Uhlenbeck (1990) designed four hammerheads of 34 bases each targeted against four different 13 base substrates. These showed a 70-fold variation in cleavage rates. However, k_{cat} remained virtually the same, whilst K_m varied, indicating the variation arose from ribozyme-substrate binding, though this had no effect on the cleavage reaction itself. The four substrates each migrated differently when run on a non-denaturing electrophoresis gel, indicating they all assumed different secondary structures. In all cases approximately 10% of the substrate was resistant to further cleavage, suggesting that some of the substrate had become trapped in a stable, but ribozyme-insensitive, structure. As substrates become larger (many mRNAs have lengths in the range of kilobases) this problem becomes more significant. The presence of single-stranded bulges has been shown to favour the hybridisation of sense-antisense RNA (Homann *et al.*, 1993), whilst the elimination of any single-stranded RNA from the target site can completely block ribozyme cleavage (Xing *et al.*, 1992). If such regions are unavailable in the desired target, lengthening the flanking sequences can allow hybridisation to occur. This was demonstrated by Beck and Nassal, who showed that a hammerhead with total flanking sequences of 10 bases could not cleave the highly structured HBV encapsidation signal, whereas a hammerhead with flanks of 38 bases could (Beck & Nassal, 1995). In general it has been found that longer flanking sequences are needed for hybridisation to full-length mRNA substrates, presumably because of the problems of secondary structure. Although, as discussed, this could reduce the rate of product dissociation, this problem can be partially bypassed by designing ribozymes with asymmetric flanks. Such ribozymes have one long flank, which binds tightly to the substrate, and one short flank, which can be as short as three bases, from which the product can rapidly dissociate.

One fact that has become clear from all this work is that there is no set of general rules which can be applied to the design of all hammerhead ribozymes. At present, the only route to the optimum structure of a ribozyme targeted against a particular point is by trial and error. The design of any hammerhead ribozyme for *in vivo* use will have to be based on a compromise of all these factors.

1.12.4e How can activity be increased?

Although hammerhead ribozymes are promising therapeutic agents, is there any way in which their activity can be increased, perhaps circumventing some of the limitations described in the previous section?

It has been demonstrated that up to nine hammerhead motifs targeted against different sites can be included in a single transcript, resulting in greater cleavage activity than any one of the single ribozymes alone (Chen *et al.*, 1992). This construct was targeted against the *env* region of HIV, with sequence comparisons indicating potential activity against all sequenced HIV isolates then known. Although this approach is important for dealing with escape mutants, this construct did not exhibit a nine-fold increase in activity compared to the single ribozymes, suggesting that the hammerhead motifs were not functioning at maximal catalytic efficiency. Incorporation of *cis*-cleaving ribozymes between multiple *trans*-cleaving ribozymes targeted against different sites has been shown to result in greater cleavage efficiency than if the *trans*-cleaving ribozymes remained joined in the same transcript (figure 1.29) (Ohkawa *et al.*, 1993, Ventura *et al.*, 1993, Xing *et al.*, 1995). This is known as the 'shotgun' approach. Increasing the number of tandemly linked ribozymes in a single transcript did increase cleavage efficiency until n=3, when activity reached a plateau. However, when a *cis*-cleaving ribozyme was included to release the *trans* cleaving ribozymes, activity continued to increase as the number of units grew.

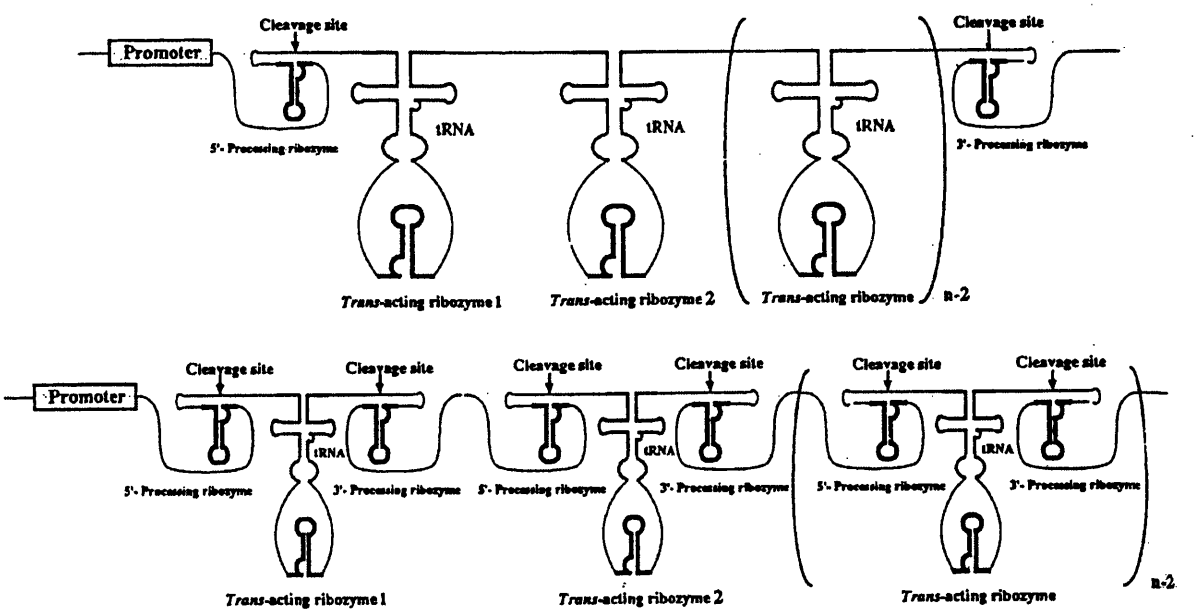

Figure 1.29. Simple tandem-repeat ribozyme expression vector (top), with ribozymes exposed in the tRNA anticodon loop. Exogenous sequence is trimmed by *cis*-acting ribozymes at each end. 'Shotgun' expression vector (bottom). Each individual ribozyme-tRNA unit is liberated from the whole transcript by *cis*-acting ribozymes. Taken from Ohkawa *et al.*, (1993).

Optimising flanking sequence length is a problem when full-length mRNAs are the target. Although ribozymes with longer flanking sequences have been shown to hybridise more effectively to long substrates than their counterparts with shorter sequences, they do not operate at maximum efficiency, with the ribozyme having to be many hundreds-fold in excess of the substrate. This probably arises from the failure of products to dissociate. One answer to this problem is the utilisation of 'facilitator' oligonucleotides (Jankowsky & Schwenzer, 1996a). These are antisense molecules which bind to the substrate immediately next to the ends of the ribozyme flanking sequences (figure 1.30). Facilitators can increase the stability of ribozyme-substrate binding. It is assumed that this is acheived by base-stacking interactions between the terminal residues of the facilitator and the ribozyme. These interactions have the energetic equivalent of an extra base-pair in the ribozyme-substrate helix, which means that facilitators have greatest benefit when used with ribozymes with short flanking sequences (Nesbitt & Goodchild, 1994). However, the greatest benefit may come from facilitators opening up any inhibitory secondary structure in the ribozyme target by binding to nearby regions of the substrate (Denman, 1996).

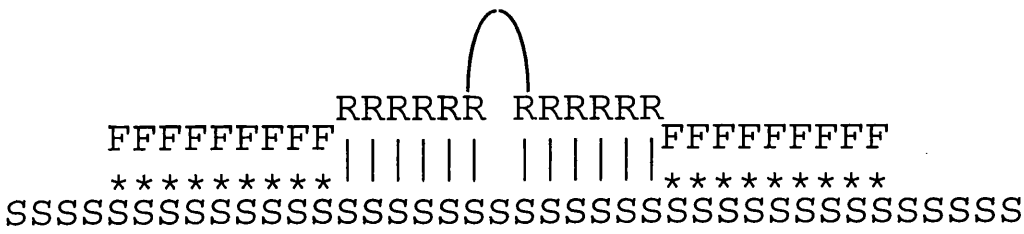

Figure 1.30. Schematic representation of the binding of facilitator oligonucleotides. The facilitators (F) bind to the substrate (S) immediately next to the 5' and 3' ends of the ribozyme (R).

The use of facilitators will probably be dictated by the system under development. Facilitators have been shown to reduce k_{cat}, though not in all cases. Facilitators can also stabilise the ribozyme-product complex, blocking ribozyme cycling. Janowsky and coworkers showed that a facilitator binding at the 3' end of their ribozyme enhanced ribozyme activity, whilst a facilitator binding at the 5' end reduced activity (Jankowsky & Schwenzer, 1996b). The binding energy of the 5' flank of the ribozyme was higher than that of the 3' flank, leading to the assumption that the 5' flank was stabilised to such a degree by the facilitator that it could not dissociate from the product. The optimum length of the facilitators, and whether they are made of RNA or DNA is again dependent on the system, in particular the substrate sequence and the concentrations of the ribozyme and substrate.

If hammerhead ribozymes are to be used *in vivo* they will have to be able to function in an environment which contains a number of proteins which can bind non-specifically to

RNA. Some of these proteins have been shown to enhance hammerhead ribozyme activity (Tsuchihashi *et al.*, 1993, Herschlag *et al.*, 1994). The HIV nucleocapsid protein NCp7 has been shown to enhance the *in vitro* activity of a hammerhead with total flanks of 14 bases against a long substrate, though the activity of hammerheads with longer and shorter flanks was inhibited (Bertrand & Rossi, 1994). Further work has shown that k_{cat} is not varied by addition of NCp7; enhancement comes from increasing the rate of ribozyme-substrate hybridisation and dissociation of products. A peptide from the C-terminal of NCp7 can also enhance hammerhead activity in this way. It is believed that NCp7 promotes the destabilisation of intramolecular helices, such as inhibitory substrate secondary structure, allowing the formation of intermolecular helices between ribozyme and substrate. This chaperone property also enables NCp7 to restore a misfolded ribozyme-substrate complex to an active conformation. Without addition of NCp7 approximately 20 to 30% of substrate was resistant to cleavage, but addition of NCp7 allowed this remainder to be cleaved. As this is an HIV nucleocapsid protein which has this ability, it raises possibilities of using hammerhead ribozymes as anti-HIV agents. *In vitro* studies have shown that the tumour suppressor protein p53 can enhance the formation of RNA duplexes, which could enable p53 to enhance ribozyme-substrate hybridisation (Nedbal *et al.*, 1997). Although this activity has been shown to be independent of sequence, the mechanism is unknown, and is inhibited by Mg^{2+}.

1.12.4f Cell culture and *in vivo* applications

The intracellular environment is very different from that found in the *in vitro* assays used to assess hammerhead activity. Ribozymes will have to be able to find their target amidst an excess of other cellular RNAs and proteins. *In vitro* studies have shown that addition of total cellular RNA can reduce hammerhead activity (Denman *et al.*, 1992), though it is unclear whether this observation can be extended to all ribozymes. A major problem is the susceptibility of ribozymes to nuclease degradation. The lifespan of cellular mRNAs is regulated by the 5' and 3' untranslated regions and by polyadenylation. Though addition of such sequences may stabilise ribozymes expressed intracellularly, care must be taken to ensure that they will not include inhibitory secondary structures. Addition of palindromic sequences at the 3' end of an anti-tumour necrosis factor-α hammerhead resulting in the formation of a hairpin has been shown to increase stability by protecting against 3'-exonuclease degradation. However, inclusion of double-stranded regions may produce sites for RNA-binding proteins which could possibly inhibit cleavage (Sioud, 1994).

Investigations of intracellular hammerhead activity have usually been based on ribozymes proven to have worked *in vitro*. Such ribozymes do not always work in cells, though there are cases of a ribozyme not working *in vitro* which did work once expressed in cells, suggesting the presence of a protein cofactor (see section 1.12.4e) (Crisell *et al.*, 1993). Initial studies claimed to have detected specific ribozyme-mediated inhibition of gene

expression or RNA degradation in cells (Cotten & Birnstiel, 1989, Cameron & Jennings, 1994). Although controls were unaffected by the presence of the ribozyme, cleavage products were not detected. Intracellular cleavage was first demonstrated by Saxena and Ackermann, who microinjected ribozymes targeted against the α-sarcin sensitive site of 28S rRNA into *Xenopus* oocytes. Not only were cleavage products detected, but cleavage of the 28S rRNA lead to a total block of oocyte protein synthesis.

One problem with trying to detect cleavage products is that the target RNA may be at such low abundance that it, and any ribozyme cleavage products, may be undetectable by Northern blotting or RNase protection assays. Therefore it is important to use an inactive ribozyme mutant as a control. Such a mutant behaves as an antisense oligonucleotide, binding to the target sequence, but not mediating cleavage. This enables the relative contributions of ribozyme cleavage and the antisense effect to gene silencing to be determined. In some cases both mechanisms play a role (Steinecke *et al.*, 1994), whilst in other cases inclusion of an active ribozyme domain does not increase gene-silencing ability.

Once a ribozyme has been demonstrated to function intracellularly, how can it be delivered to its target? Ribozyme expression has been demonstrated *in vivo* in transgenic mice, though the development of a vector system is required for therapeutic use. Exogenously synthesised ribozymes have been delivered in cell culture using liposomes, though this is hampered by degradation by serum nucleases and by the poor transfection efficiency of untargeted liposomes. There has been some success in stabilising exogenously synthesised ribozymes by incorporating phosphorothioate linkages into the flanking sequences (Koizumi & Ohtsuka, 1991, Shimayama *et al.*, 1993, Heidenreich *et al.*, 1994). However, these have the same drawbacks as modified antisense oligonucleotides (see section 1.10.5). Retroviral vectors have been used to stably transfect CD4+ cell lines with anti-HIV hammerheads, rendering the cells resistant to HIV infection in a manner similar to that being used in the clinical trials of the hairpin ribozyme (see section 1.12.3f) (Rossi *et al.*, 1993). Anti-HCV ribozymes have been successfully delivered to cultured human hepatocytes using an adenoviral vector (Lieber *et al.*, 1996a). E1-deleted replication-incompetent adenovirus has been used to deliver an anti-human growth hormone (hGH) ribozyme to the livers of hGH transgenic mice. This led to a 96% reduction in hepatic hGH (Lieber *et al.*, 1996b). Though this is encouraging for the potential gene therapy of chronic hepatitis, there have been problems with E1-deleted adenoviruses eliciting inflammatory responses in human clinical trials.

Is there any way in which intracellular hammerhead activity can be increased? It has been proposed that the reason why so many promising ribozymes fail to function intracellularly is because they fail to enter the same compartments of the cell as their target. Addition of polyadenylation and splicing signals could forseeably allow a ribozyme transcript to pass through the same processing pathways as mRNA. Some viral targets have

the additional advantage of packaging elements, which target viral transcripts to regions of the cell where virion formation occurs. Sullenger demonstrated that a hammerhead targeted against a *lacZ* reporter in a murine leukaemia retrovirus was inactive in cells. However, if the retroviral packaging signal was included in the ribozyme transcript, then expression of the *lacZ* reporter was reduced (Sullenger & Cech, 1994a).

1.12.4g Hammerheads and HBV

Initial *in vitro* studies demonstrated cleavage of a fragment of HBcAg mRNA by a single transcript containing three hammerhead motifs (von Weizsacker *et al*, 1992). All three active sites were simultaneously active, with cleavage occurring at a 1:1 molar ratio of ribozyme to substrate. The data suggest that the cleavage products dissociate independently from the ribozyme. This is probably why the long total flanking regions (45 bases) do not impair activity. The shotgun approach (see section 1.12.4e) has been used *in vitro* to cleave up to 80% of substrate (derived from the core region), with the substrate in excess of the ribozyme constructs (Ruiz *et al.*, 1997).

Beck and Nassal designed a series of hammerheads targeted against the encapsidation signal (see section 1.12.4d). They showed that highly structured substrates could be targeted by lengthening the flanking sequences of the hammerhead. Although their ribozymes functioned *in vitro*, they failed to work when transfected into HepG2 cells. Cleavage could be detected in cell lysates, but only if the lysates were supplemented with extra Mg^{2+} (Beck & Nassal, 1995).

Luber *et al.*, (1997) have successfully targeted the X region with a hammerhead with asymmetric flanks up to a kilobase in length. This was shown to cleave the target efficiently *in vitro*. The hammerhead construct was cotransfected into HepG2 cells with HBV DNA, and was shown to reduce viral replication, as determined by measuring pgRNA, HBsAg in the supernatant and HBcAg. However, an inactive ribozyme mutant was shown to have the same inhibitory potential, suggesting that this construct operates purely by the antisense mechanism .

Despite the potential of ribozymes as antiviral agents having been demonstrated, work with anti-HBV ribozymes has not progressed as far as with anti-HIV constructs. In part this is due to the lack of an effective *in vitro* model for viral replication. The main problem is the safe, efficient targeting of gene therapy constructs to the liver. The development of hepatocyte-specific vectors is progressing, but as yet there is nothing approaching the rigorous safety specifications required for a vector for use *in vivo* in humans.

CHAPTER 2 MATERIALS AND METHODS

2.1 MATERIALS

a) Plasmids

pGEM-3z	Promega, Madison, WI
pRK5	Prof. H. Will, Hamburg
pRZ60, pY98	Dr. G. Sczakiel, Heidelberg
pZeo-5D	Dr. A. Patel, Institute of Virology

b) Bacterial Strain and growth media

DH5α	*Escherichia coli.* Genotype: ϕ80d*lacZ*ΔM15, *recA*1, *endA*1, *gyrA*96, *thi*-1, *hsdR*17(r_K^-,m_K^-), *supE*44, *relA*1, *deoR*, Δ(*lacZYA-argF*)U169.
L-broth	10g bacto-tryptone, 5g bacto-yeast extract, 5g NaCl in 1l water

c) Radioisotopes

All radiolabelled compounds were obtained from Dupont-NEN.

Radiolabelled compound	*Activity (Ci/mmol)*
α^{35}S-dATP	1250
α^{32}P-UTP	800
α^{32}P-dCTP	3000
γ^{32}P-ATP	6000
^{35}S-L-methionine	1175

Radiolabelled nucleic acids and proteins were visualized on electrophoretic gels using Kodak X-OMAT film.

d) Enzymes

Restriction enzymes and buffers and calf intestinal alkaline phosphatase were purchased from Boehringer Mannheim; RNA polymerases, recombinant RNase inhibitor (RNasin) and ribonucleotides were obtained from Promega and Ambion; RNase A was purchased from Sigma Chemicals; T4 polynucleotide kinase, T4 DNA ligase and T4 RNA ligase were purchased from New England Biolabs; *Taq* DNA polymerase and deoxyribonucleotides for PCR were purchased from Gibco; terminal deoxynucleotidyl transferase was obtained from Promega.

e) Labels and antibodies for ELISA

Biotin-16-ddUTP, biotin-16-dUTP, digoxigenin-16-ddUTP, digoxigenin-16-UTP, all purchased from Boehringer Mannheim/ Enzo Diagnostics.

Peroxidase-anti peroxidase and donkey anti-sheep IgG- peroxidase conjugate secondary antibodies were both purchased from Sigma Chemical Co.

f) Common Reagents

Manufacturer	*Chemicals*
Beecham Research	Ampicillin
Biorad	TEMED, Ammonium persulphate
Boehringer Mannheim	Agarose, Tris base
Fluka	Formaldehyde
National Diagnostics	Sequagel 6 and Protogel pre-prepared acrylamide solutions.
Oncor	Deionized formamide
Prolabo	Boric acid, chloroform, ethanol, glacial acetic acid, glycerol, isopropanol, methanol

All other reagents and chemicals were purchased from Sigma-Aldrich Co.,Poole, UK or BDH Chemicals, Poole, UK.

g) Reagents and buffers for PCR, DNA sequencing and cloning

Acrylamide gel elution buffer	500mM CH_3COONH_4, 10mM $MgCl_2$, 0.1% SDS, 1mM EDTA
10X PCR buffer	200mM Tris-HCl (pH 8.4), 500mM KCl
10X agarose gel loading buffer	1X TBE, 1% SDS, 50% glycerol, 0.025% bromo-phenol blue.
10X dNTPs	100 mM each of dATP, dTTP, dCTP, dGTP
10X TBE,	89mM Tris-HCl (pH 8.0), 89mM H_3BO_3, 1mM EDTA
10X TE	0.1M Tris-HCl (pH 4.5 or pH 8.0), 10mM EDTA
10X ligase buffer	250mM Tris-HCl (pH 7.6), 50mM $MgCl_2$, 5mM DTT, 5mM ATP, 25% PEG 8000

h) Reagents and solutions for small scale plasmid preparation

Solution I	25mM Tris-HCl (pH 8.0), 10mM EDTA, 50mM glucose
Solution II	0.2M NaOH, 1% (w/v) SDS

Solution III	3M CH_3COOK, 5M CH_3COOH

i) Reagents and solutions for large scale plasmid preparation

These were purchased as part of a kit from QIAGEN, Crawley, UK.

Buffer P1	50mM Tris-HCl (pH 8.0), 10mM EDTA, 100µg/ml RNAse A
Buffer P2	0.2M NaOH, 1% (w/v) SDS
Buffer P3	3M CH_3COOK, pH 5.5
Buffer QBT	750mM NaCl, 50mM MOPS (pH 7.0), 15% EtOH, 0.15% triton X-100
Buffer QC	1M NaCl, 50mM MOPS (pH 7.0), 15% EtOH
Buffer QF	1.25M NaCl, 50mM Tris-HCl (pH 8.5), 15% EtOH

j) Reagents and solutions for *in vitro* transcription, RNA gel shifts and ribozyme cleavage reactions

a) Small scale RNA synthesis

5X Transcription buffer	200mM Tris-HCl (pH 7.5), 30mM $MgCl_2$, 10mM spermidine, 50mM NaCl.
Nucleotide solutions	10mM ATP in H_2O, (pH 7.0), 10mM CTP in H_2O, (pH 7.0), 10mM GTP in H_2O, (pH 7.0), 10mM GTP in H_2O, (pH 7.0)

b) RiboMAX system (Promega) for large scale RNA synthesis

5X Transcription buffer	400mM HEPES-KOH (pH 7.5), 120mM $MgCl_2$, 200mM DTT
Nucleotide mix	25mM each of ATP, CTP, GTP, TTP (pH 7.0)

c) Ribozyme analysis

10X Ribozyme hybridization buffer	200mM Tris-HCl (pH 7.5), 1M NaCl
RNA gel shift stop solution	50mM Tris-HCl (pH 8.0), 50mM EDTA, 0.5% SDS, 0.5M urea, 0.025% bromophenol blue
Formamide gel loading buffer	90% formamide, 1X TBE

k) Reagents and solutions for ELISA

Cacodylate buffer	500mM cacodylate (pH 6.8), 5mM $CoCl_2$, 0.5mM DTT

All other buffers were all provided with Boehringer Mannheim's PCR detection ELISA kit.

l) *In vitro* translation

In vitro translation was performed using Promega's TNT rabbit reticulocyte lysate coupled transcription-translation system. All reagents were provided with the kit.

Final concentrations of reaction components

10mM creatine phosphate, 50μg/ml creatine phospho-kinase, 2mM DTT, 50μg/ml calf liver tRNA, 79mM CH_3COOK, 0.5mM $(CH_3COO)_2Mg$, 0.02mM haemin

m) Reagents and buffers for immunoprecipitation

Protein-A sepharose beads	Purchased from Sigma. Resuspended in H_2O.
Wash buffer	0.5M LiCl, 0.1M Tris-HCl (pH 8.0)
Rabbit anti-HBcAg polyclonal antiserum	Purchased from Dako Corporation.

n) Reagents and buffers for SDS-PAGE and western blotting

4X stacking gel buffer	0.5M Tris base, 0.4% SDS, adjusted to pH 6.8
4X separating gel buffer	1.5M Tris base, 0.4% SDS, adjusted to pH 8.8
10X SDS polyacrylamide gel running buffer	0.25M Tris base, 1.9M glycine, 1% SDS
SDS sample buffer	20% glycerol,, 2% SDS, 1X stacking gel buffer, 5% β-mercaptoethanol, 0.25mg bromophenol blue
Towbin buffer	25mM Tris-HCl (pH 8.3), 192mM glycine, 20% CH_3OH
5X TBS	100mM Tris-HCl (pH 7.5), 2.5M NaCl.
TTBS	1X TBS, 0.05% Tween 20.

Rabbit anti-HBcAg polyclonal antisera was purchased from Zymed Laboratories or Dako Corporation. These were used at dilutions of 1:2 and 1:1000 respectively. Goat anti-rabbit IgG whole molecule peroxidase conjugate was purchased from Sigma.

Hybond-N nylon membrane (also used for northern blotting) was purchased from Amersham.

o) Firefly luciferase reporter assay

The firefly luciferase reporter assay was performed using Promega's Luciferase Assay System.

Assay reagent	20mM tricine, 1.07mM $(MgCO_3)_4Mg(OH)_25H_2O$, 2.67mM $MgSO_4$, 0.1mM EDTA, 33.3mM DTT, 270μM coenzyme A, 470μM luciferin, 530μM ATP, (pH 7.8)

p) Reagents and solutions for northern blotting

10X MOPS buffer	0.4M MOPS, 0.1M CH_3COONa, 10mM EDTA
RNA sample buffer	720μl deionized formamide, 160μl 10X MOPS buffer, 260μl 37% formaldehyde. (Store -20°C, renew every 2 weeks.)
Denhardt's Reagent, 50X	5g Ficoll, type 400, 5g polyvinyl-pyrrolidone, 5g bovine serum albumin dissolved in DEPC treated water to give final volume of 500ml.
20X SSC	3M NaCl, 0.3M $Na_3C_6H_5O_7$ (pH 7.2)
Hybridization solution	5X SSC, 50% deionized formamide, 1% SDS, 5X Denhardt's reagent, 20μg/ml sonicated salmon sperm DNA.

q) Buffer for primer extension analysis

Promega's MMLV-RT H⁻ primer extension system was used.

MMLV-RT 2X buffer	100mM Tris-HCl, (pH 8.3), 150mM KCl, 6mM $MgCl_2$, 20mM DTT, 1mM dATP, 1mM dCTP, 1mM dGTP, 1mM dTTP

r) Buffers for radiolabelling nucleic acids

10X nick translation buffer	0.5M Tris-HCl, (pH 7.5), 0.1M $MgSO_4$, 1mM DTT, 500μg/ml bovine serum albumin
10X polynucleotide kinase buffer	500mM Tris-HCl (pH 7.6), 100mM $MgCl_2$, 50mM DTT, 1mM spermidine.
10X calf intestinal alkaline phophatase buffer	500mM Tris-HCl (pH 9.3), 10mM $MgCl_2$, 1mM $ZnCl_2$, 10mM spermidine

s) Synthetic oligodeoxyribonucleotides

Table 2.1 Primers used for PCR construction of ribozymes. Restriction sites are underlined.

Primer	Sequence	Restriction sites
RZ1	CTCACAGAATTCATGCTCAGCTGATGAGTCCGTGAGGACG AAAGACTCTATGTTTATTGCAGCTTATAATGGTT	*Eco*RI
RZ2	CTCACAGAATTCAGTATGGTCTGATGAGTCCGTGAGGACG AAAGGTGAACTGTTTATTGCAGCTTATAATGGTT	*Eco*RI
RZ534	CTCACAGAATTCCGTCGTCTCTGATGAGTCCGTGAGGACG AAACAACAGTTGTTTATTGCAGCTTATAATGGTT	*Eco*RI
RZ551	CTCACAGAATTCTTCTAGGGCTGATGAGTCCGTGAGGACG AAACCTGCCTTGTTTATTGCAGCTTATAATGGTT	*Eco*RI
RZ556	CTCACAGAATTCTCTTCTTCCTGATGAGTCCGTGAGGACG AAAGGGGACCTGTTTATTGCAGCTTATAATGGTT	*Eco*RI
RZ568	CTCACAGAATTCAGGCGAGGCTGATGAGTCCGTGAGGACG AAAGTTCTTCTGTTTATTGCAGCTTATAATGGTT	*Eco*RI
RZ572	CTCACAGAATTCTGCGAGGCCTGATGAGTCCGTGAGGACG AAAGGGAGTTTGTTTATTGCAGCTTATAATGGTT	*Eco*RI
CP1	GTCACGACGTAAGCTTGTAAAACGACGGC	*Hin*dIII

Table 2.2 Oligonucleotides used as run-off transcription templates.

Oligonucleotide	Sequence
T7P	AATTTAATACGACTCACTATAG
RZSUB	TCGTCTGCGAGGCGAGGGAGTTCTTCTTCTAGGGGACCTGCCTCGT CGTCTAACAACAGTAGCCCTATAGTGAGTCGTATTAAATT
RZ534T	ACTGTTGTTTCGTCCTCACGGACTCATCAGAGACGACGAACCCTAT AGTGAGTCGTATTAAATT
RZ551T	AGGCAGGTTTCGTCCTCACGGACTCATCAGCCCTAGAAAACCCTAT AGTGAGTCGTATTAAATT
RZ556T	GGTCCCCTTTCGTCCTCACGGACTCATCAGGAAGAAGAAACCCTAT AGTGAGTCGTATTAAATT
RZ568T	GAAGAACTTTCGTCCTCACGGACTCATCAGCCTCGCCTAACCCTAT AGTGAGTCGTATTAAATT
RZ572T	AACTCCCTTTCGTCCTCACGGACTCATCAGGCCTCGCAAACCCTAT AGTGAGTCGTATTAAATT
RZ572BT	ACTGTTGTTAGACGACGAGGCAGGTCCCCTAGAAGAAGAACTCCCT TTCGTCCTCACGGACTCATCAGGCTCGCAGACGACCCTATAGTGAG TCGTATTAAATT

2.2 METHODS

2.2.1 PCR, sequencing and cloning

a) Preparation of oligodeoxyribonucleotides

Oligodeoxyribonucleotides were synthesized in house using a Cruachem PS250 oligonucleotide synthesizer. Oligodeoxyribonucleotides were eluted from the synthesis columns with 1.5ml concentrated ammonia, and deprotected by incubation at 55°C for 5 hours. The oligos were recovered as lyophilized pellets by spinning the ammoniacal solution under vacuum overnight. The pellets were resuspended in 200µl H_2O. Oligos over 45 bases in length were further purified by polyacrylamide gel electrophoresis. 50µl of resuspended oligo were mixed with 50µl deionized formamide and run on a 15% polyacrylamide gel (30ml 30% Protogel (National Diagnostics), 6ml 10X TBE buffer, 0.6ml 10% (w/v) ammonium persulphate, 40µl TEMED, 23.4ml H_2O). Bands were visualized by ultraviolet shadow-casting. The bands were cut out of the gel, placed in 1ml acrylamide gel elution buffer and incubated overnight at 37°C. The elution buffer was removed, phenol/chloroform extracted, and the oligo recovered by precipitation with 2 volumes EtOH at -20°C for 30 minutes. The oligo was pelleted by spinning at 13,000rpm for 30 minutes in a Scotlab microfuge. The pellet was washed with 70% EtOH, dried under vacuum, then resuspended in 50µl H_2O. The oligo's concentration was determined by measuring the optical density (OD) at 260nm of a 1:100 dilution, where 1 OD unit equals 50µg/ml DNA.

b) Polymerase chain reaction (PCR)

PCR was used to generate ribozyme cassettes to clone into pGEM-3z and pRK5 plasmids. Each reaction contained 5µl 10X PCR reaction buffer, 2µl 100mM $MgCl_2$, 1µl of each primer to give a final concentration of 50pmol/µl of each primer, 1µl dNTP mix (each dNTP at 125µM final concentration), 2 units *Thermophilus aquaticus* (*Taq*) DNA polymerase (Gibco), 10ng target DNA and H_2O to a final volume of 50µl. The reaction mix was overlaid with 50µl mineral oil to prevent evaporation. The reactions were performed on a Biometra TRIO Thermoblock using the following program; 95°C for 4 minutes followed by 5 cycles of

95°C for 1 minute
55°C for 1 minute
72°C for 1 minute, 30 seconds followed by 35 cycles of
90°C for 1 minute
55°C for 1 minute
72°C for 1 minute, 30 seconds followed by a final 4 minutes at 72°C. Products were detected by agarose gel electrophoresis (see section 2.2.1.iv).

c) Restriction digests

Cloning was confirmed by restriction digestion of miniprep plasmid DNA with appropriate restriction enzymes followed by agarose gel electrophoresis. A standard restriction digest typically consisted of 1.5µl 10X restriction buffer (Boehringer Mannheim), 0.2 µl (2 units) of each appropriate restriction enzyme, 5µl miniprep plasmid DNA and H_2O to a final volume of 15µl. Digests were incubated for 3 hours at 37°C. The same protocol was also used to prepare PCR products and plasmids for ligation and for generating templates for run-off *in vitro* transcription reactions.

d) Agarose gel electrophoresis

Agarose gel electrophoresis was used to analyse restriction digests of miniprep DNA, and also to prepare linearized plasmids for *in vitro* transcription reactions. Gels were prepared by boiling 1g agarose (Boehringer Mannheim) in 100ml 1X TBE buffer. The solution was allowed to cool, and 50µl ethidium bromide (1mg/ml) was added prior to casting the gel. Samples were prepared by adding 1 volume of agarose gel loading buffer, and run at 80V in 1X TBE buffer. On completion of running, the bands were visualized on an ultra-violet transilluminator.

e) Gene-cleaning

PCR products, restriction digest products and linearized plasmids were isolated from agarose gels using the Geneclean kit (BIO 101 Inc.). Bands were located by visualizing the gel on an ultraviolet transilluminator. The correct bands were cut out and placed in 1.5ml eppendorf tubes with 4.5 volumes sodium iodide and 0.5 volumes TBE gel modifier and incubated at 55°C until the gel slice had melted. 6µl glassmilk was added to each tube. The tubes were vortexed and left on ice for 5 minutes. The tubes were spun briefly at 13,000rpm in a Scotlab microfuge, and the resulting glassmilk pellet washed three times with 1ml ice cold NEW wash. (NEW wash was prepared by adding 14ml concentrate provided with the Geneclean kit to 280ml distilled water and 310ml 100% ethanol.) Following the final wash the glassmilk pellet was airdried. The DNA was eluted from the glassmilk by resuspending the glassmilk pellet in 50µl H_2O, and incubating at 55°C for 5 minutes. The glassmilk suspension was spun at 13,000rpm for 5 minutes and the supernatant containing the eluted DNA was removed.

f) DNA ligations

Concentrations of vector and insert DNA were estimated by agarose gel electrophoresis with molecular weight markers of known concentration. Ligations were optimized by trying vector:insert ratios of 3:1, 1:1 and 1:3. Vector-insert DNA mixes were added to 2µl 5X T4 ligase buffer (BRL), 1 unit T4 ligase and H_2O to a final volume of 10µl.

Ligation reactions were incubated at room temperature for 3 hours and then transformed into competent bacteria.

g) Preparation of competent *Escherichia coli* cells

10µl of DH5α glycerol stock was placed in 10ml L-broth, and incubated at 37°C overnight. 500µl of overnight culture was transferred to 50ml L-broth and incubated for a further 2 to 2.5 hours, until the OD_{600} of the culture was between 0.2 and 0.4. Cells were then placed into chilled 50ml Falcon tubes on ice for 10 minutes, and then spun at 2800rpm for 10 minutes at 4°C. The supernatant was decanted and the tube inverted to dry the pellet. The pellet was resuspended in 15ml ice cold 100mM $CaCl_2$ by vortexing and then left on ice for at least 30 minutes. The cells were respun, then carefully resuspended in 2.5ml 100mM $CaCl_2$. Competence was enhanced by leaving cells overnight at 4°C. Alternatively, cells were stored in 15% glycerol (v/v) at -70°C for up to 3 weeks.

h) Transformation of competent cells

10µl of ligation reaction was added to 100µl of competent *E. coli* and then placed on ice for 30 minutes. Transformation efficiency was enhanced with a 90 second heatshock at 42°C, followed by chilling bacteria on ice for a further 5 minutes. The bacteria were incubated with 1ml L-broth at 37°C for 1 hour. Cells were spun for 5 seconds at 13,000rpm. The supernatant was removed and the pellet resuspended in 100µl L-broth. The resuspended cells were spread on L-agar/ ampicillin (100µg/ml) plates. The plates were inverted and incubated overnight at 37°C.

i) Small Scale Plasmid Preparations

Colonies were picked from L-agar/ ampicillin plates into 2ml L-broth and incubated at 37°C for 6 hours. 1ml of this bacterial culture was decanted to a 1.5ml eppendorf tube and spun at 13,000rpm for 30 seconds, the supernatant removed and the tube inverted to dry the pellet. The pellet was resuspended by vortexing in 100µl ice cold Solution I. 200µl freshly prepared Solution II was added, and mixed by inverting the tube several times. The tube was left on ice for 3 minutes. 150µl Solution III and 50µl phenol/chloroform were added and mixed in by gentle vortexing. The tubes were then spun at 13,000 rpm for 5 minutes. The aqueous phase was transferred to a fresh tube, and contaminating RNA removed by adding 1µl RNase A (10mg/ml) and incubating at 37°C for 30 minutes, followed by a phenol/chloroform extraction. Plasmid DNA was precipitated with 2 volumes 100% EtOH at -20°C for 15 minutes and recovered by centrifugation at 13,000rpm for 10 minutes. The supernatant was removed and the pellet washed with 500µl 70% EtOH. The pellet was air dried and resuspended in 50µl H_2O.

j) Large Scale Plasmid Preparations

Large scale plasmid preparations were performed using the QIAGEN Plasmid Midi Kit. 100µl of overnight bacterial culture was added to 50ml L-broth supplemented with 100µg/ml ampicillin and incubated at 37°C overnight. This culture was spun at 3000rpm for 10 minutes at 4°C. The supernatant was removed, and the pellet resuspended in 4ml buffer P1. 4ml buffer P2 was added and mixed gently by inverting the tube several times. Following a five minute incubation of the bacterial lysate at room temperature, 4ml buffer P3 was added and mixed by inverting the tube. The bacterial lysate was then poured into a QIAfilter syringe and allowed to stand for 10 minutes. During this time a QIAGEN-tip 100 was equilibrated with 4ml buffer QBT. The lysate was filtered through the QIAfilter syringe into the QIAGEN tip, and allowed to enter the tip resin by gravity flow. After all the lysate had passed through the QIAGEN tip, the tip was washed twice with 10ml wash buffer QC. The plasmid DNA was eluted from the resin with 5ml elution buffer QF, and precipitated with 0.7 volumes isopropanol. The precipitate was spun at 15,000rpm for 30 minutes at 4°C. The supernatant was removed, the pellet washed with 70% EtOH, air-dried for 5 minutes and resuspended in 100µl H_2O. DNA yield was determined by UV absorption.

k) Bacterial glycerol stocks

Glycerol was added to overnight bacterial cultures to a final concentration of 40%. Glycerol stocks were then snap-frozen in liquid nitrogen and stored at -70°C.

l) DNA sequencing

DNA sequencing was performed using the Sequenase version 2.0 DNA sequencing kit or the Sequenase PCR product sequencing kit (Amersham).

i) Template Preparation

Double stranded plasmid DNA was prepared using the QIAGEN Plasmid Midi Kit (see section 2.2.1.x). 5µg of plasmid DNA in 20µl H_2O was denatured by adding 0.1 volumes of 2M NaOH, 2mM EDTA and incubating for 15 minutes at 65°C. The mixture was neutralized by adding 0.1 volumes 3M sodium acetate and the DNA precipitated with 3 volumes of ethanol (30 minutes at -70°C). The DNA was pelleted by spinning at 13,000rpm for 30 minutes. The DNA pellet was washed with 70% ethanol, dried under vacuum and resuspended in 7µl H_2O.

PCR products were purified by adding 1µl shrimp alkaline phosphatase (to remove unincorporated nucleotide triphosphates) and 1µl exonuclease I (to remove primers) (both enzymes were supplied with the kit) to 5µl PCR reaction, and incubating for 15 minutes at 37°C. The enzymes were then inactivated by incubating for 15 minutes at 80°C.

Between 0.5-1.0 pmol of primer was used per sequencing reaction. 1µl primer and 2µl 5X Sequenase buffer were added to 7µl template DNA, incubated for 10 minutes at 65°C and then cooled to room temperature.

ii) Sequencing Reactions

To each primed template in a volume of 10µl was added 2µl 1:5 dilution of labelling mix, 1µl 0.1M dithiothreitol, 5µCi [α-^{35}S]dATP (Dupont-NEN) and 2µl 1:8 dilution Sequenase version 2.0 T7 DNA polymerase. The mixture was incubated at 20°C for 2 minutes. 3.5µl of labelling reaction was added to each of four termination tubes containing 2.5µl of one dideoxynucleotide (ddA, ddC, ddG or ddT) and incubated for a further 5 minutes at 37°C. The termination reactions were ended by adding 4µl formamide stop solution. The completed reactions were incubated at 72°C for 2 minutes and then loaded onto a 6% polyacrylamide sequencing gel. Following electrophoresis the gel was fixed in 10% methanol, 10% glacial acetic acid, then dried and exposed to autoradiography film.

2.2.2 RNA preparation

a) Preparation of nuclease-free water

Diethylpyrocarbonate (DEPC) (Sigma) was added to deionized water to a final concentration of 0.1%. Following incubation at 37°C for 30 minutes the DEPC treated water was autoclaved.

b) *In vitro* transcription

i) Template preparation

Plasmids containing templates to be transcribed were linearized with an appropriate restriction enzyme with a cleavage site at the 3' end of the insert. 5µg of plasmid was incubated with 10 units of restriction enzyme for 3 hours at 37°C. Digests were then run against uncut plasmid on a 1% agarose gel to confirm cutting had occurred. The linearized plasmid band was excised from the gel and gene-cleaned.

Short RNAs (less than 80 bases) were generated from partially single-stranded oligodeoxyribonucleotide templates (Milligan *et al*, 1987). An oligonucleotide encoding the T7 phage promoter and the template was annealed to a second oligonucleotide complementary to only the promoter region. Both oligonucleotides were incubated together in water at a final concentration of 50µM at 95°C for 2 minutes, and then allowed to slowly cool to room temperature.

ii)Transcription reactions

Large scale transcription reactions were performed using Promega's RiboMAX kit. Briefly, reactions were set up with 4µl 5X transcription buffer, 6µl rNTP mix, 2µl T7

enzyme mix, 1μg DNA template and nuclease free water to a final volume of 20μl. The reactions were incubated at 37°C for 3 hours, after which 1μl RQ1 RNAse free DNAse was added (supplied with kit), followed by a further 15 minute incubation at 37°C. RNA was extracted with TE-saturated phenol (pH 4.5) and precipitated with 0.1 volumes 3M ammonium acetate (supplied with kit) and 2.5 volumes EtOH at -70°C for at least 30 minutes. The precipitate was spun down at 13,000rpm at 4°C for 30 minutes, the pellet washed with 70% EtOH, vacuum dried and resuspended in 50μl nuclease free water. RNA concentration was determined by measuring the OD_{260} of a 1:100 dilution of the purified RNA in nuclease free water, where 1 OD unit equals 40μg/ml RNA.

High specific activity radiolabelled RNA was generated using Promega's T7 RNA polymerase. 30μl reactions were set up containing 6μl 5X transcription buffer, 1.5μl each of 10mM rATP, rCTP, and rGTP (final concentration 0.5mM), 3μl 100μM UTP (final concentration 10μM), 5μl α^{32}P-UTP (Dupont-NEN) (final concentration 2.1μM), 1μl recombinant RNAse inhibitor (Promega), 1μl T7 RNA polymerase (Promega) and nuclease free water to final volume 30μl. Following incubation at 37°C for 1 hour, 0.5 volumes 90% w/v formamide gel loading buffer was added to the RNA, which was denatured at 95°C, 2 minutes. The labelled RNA was run on a 10% acrylamide, 4M urea gel at 50mA for 1 hour in 1X TBE buffer. The band corresponding to the labelled RNA was located by autoradiography and cut out. The RNA was eluted from the gel slice in acrylamide gel elution buffer overnight at room temperature. The elution buffer was removed, extracted with TE-saturated phenol (pH 4.5), and precipitated with 2.5 volumes EtOH at -70°C for at least 30 minutes. The RNA was then treated as for the large scale preparations as described above.

All RNA was stored in water at -70°C following purification.

2.2.3 *In vitro* ribozyme studies

a) RNA gel shifts

Labelled ribozyme RNA was incubated with an excess of unlabelled substrate RNA in 1X ribozyme hybridization buffer at 37°C in a volume of 20μl, with 20 units RNAsin (Promega). 2μl aliquots were taken at time zero and subsequent points and quenched in 20μl stop solution. RNA complexes were analysed by polyacrylamide gel electrophoresis. The percentage of acrylamide and urea concentration in the gel varied depending on the extent of base pairing expected in the complex under study. Following electrophoresis, the dried gels were exposed to X-ray film (Kodak) for autoradiography, or alternatively to a phosphoroimager plate, and the resulting image analysed using the IMAGEQUANT package (Molecular Dynamics).

b) *In vitro* ribozyme cleavage

Unlabelled ribozyme RNA and radioactively labelled substrate RNA were pre-annealed by incubating at 95°C for 5 minutes, then cooling to 37°C in 1X ribozyme hybridization buffer. The cleavage reaction was started by adding $MgCl_2$ to varying final concentrations in a final volume of 20µl. 2µl aliquots were taken at time zero and subsequent points and quenched in 20µl stop solution. Cleavage products were separated by denaturing polyacrylamide gel electrophoresis. Following electrophoresis the dried gels were exposed to a phosphoroimager plate, and the resulting image analysed using the IMAGEQUANT package (Molecular Dynamics).

Cleavage reactions were also performed in which the ribozyme and substrate were not pre-annealed, although the remainder of the procedure was identical to that described above.

2.2.4 RNA ELISA

a) RNA endlabelling

RNA endlabelling was attempted using both T4 RNA ligase (Boehringer-Mannheim or New England Biolabs) and terminal deoxynucleotidyl transferase (TdT) (Promega).

T4 RNA ligase was used to ligate the BIO-1 biotinylated oligonucleotide (sequence dA_{18}-BIO) to the 3'-end of Y98 RNA. Prior to ligation the BIO-1 oligonucleotide was 5'-phosphorylated with T4 polynucleotide kinase (New England Biolabs) and cold ATP, and the Y98 RNA was 5'-dephosphorylated using calf intestinal alkaline phosphatase (Boehringer-Mannheim). The ligation reactions were performed using 1X T4 RNA ligase buffer (50mM Tris-HCl, 10mM $MgCl_2$, 10mM DTT, 1mM ATP, pH 7.8). 10nM internally radiolabelled, alkaline phosphatase treated Y98 was incubated with varying concentrations of BIO-1 oligonucleotide and T4 RNA ligase at 37°C for 30 minutes. Ligation reactions were repeated using New England Biolabs RNA ligase with 10nM Y98 and 1mM BIO-1 with varying concentrations of DMSO, in accordance with recommendations included in the protocol supplied with the enzyme.

RNA was 3' endlabelled using TdT for the ELISA hybridization experiments with either biotin-11-ddUTP, digoxigenin-16-ddUTP or digoxigenin-16-UTP (Boehringer-Mannheim/ Enzo Diagnostics). 1 nmol RNA was end-labelled with either 1 nmole labelled ddUTP or 10 nmoles digoxigenin-16-UTP in a total reaction volume of 50µl containing 10µl 5X cacodylate buffer (Promega) and 10 units TdT. Reactions were incubated at 37°C for 60 minutes, then at 70°C for 10 minutes to inactivate the enzyme. The labelled RNA was purified by precipitation with 0.1 volumes ammonium acetate, 20µg/ml glycogen (Boehringer-Mannheim) and 2.5 volumes EtOH (BDH) for at least 30 minutes at -70°C. The RNA was recovered as described in section 2.2.2.b.

b) RNA-RNA hybridization ELISA

Components from Boehringer-Mannheim's PCR-ELISA kit were used. RNA 3' end-labelled with biotin-11-ddUTP was fixed to streptavidin wells in 200µl 1X ribozyme hybridization buffer or the hybridization buffer supplied with the kit at 4°C overnight. Unbound RNA was removed by washing five times with wash buffer. RNA 3' end-labelled with digoxigenin-16-UTP was added to the wells in 200µl 1X ribozyme hybridization buffer, and incubated at 37°C for varying times. Unbound RNA was again removed by washing five times with wash buffer.

The signal was detected using a 1:100 dilution of anti-digoxigenin sheep Fab fragments conjugated with horseradish peroxidase. Following a 30 minute, 37°C incubation excess antibody was removed by washing five times with wash buffer. The ELISA was then either immediately developed using the chromogenic peroxidase substrate ABTS (2,2'-azinobis(3-ethylbenzthiazoline-6-sulfonic acid)), or probed again with a secondary antibody. Peroxidase-anti-peroxidase conjugate (Sigma) and donkey anti-sheep IgG-horseradish peroxidase conjugate (Sigma) were both investigated as potential secondary antibodies.

The ELISA was developed by adding 200µl ABTS per well, and incubating for 1 hour at 37°C. The colour change was measured using a Titertek Multiwell plate scanner at 405nm.

c) Ribozyme cleavage ELISA

Equimolar amounts of biotin-11-ddUTP 3' end-labelled substrate and digoxigenin-16-UTP 3' end-labelled ribozyme were incubated at 37°C for 3 hours in 1X ELISA hybridization buffer. The resulting complex was added to streptavidin coated wells, with 20pmoles of complex in 200µl 1X ELISA hybridization buffer per well. The streptavidin coated wells were incubated overnight at 4°C to allow the ribozyme-substrate complex to bind to the well surface. Unbound ribozyme-substrate complex was removed from the wells by rinsing five times with wash buffer. 1X ribozyme hybridization buffer supplemented with varying concentrations of $MgCl_2$ was added to the wells, which were then incubated for varying periods of time. Cleavage products and unbound ribozyme was removed at the end of the incubations by rinsing five times with wash buffer. The ELISA was probed and developed as described in the previous section. The extent of cleavage was determined by comparing the reduction in the ABTS signal in wells where the ribozyme-substrate complex had been incubated in $MgCl_2$ supplemented 1X ribozyme hybridization buffer with the ABTS signal in wells where no $MgCl_2$ had been added.

2.2.5 *In vitro* translation

a) Rabbit reticulocyte lysate system

In vitro translation was performed using Promega's TNT T7 coupled transcription-translation rabbit reticulocyte lysate system. Kit components were stored at -70°C, with the

lysate being thawed rapidly by hand warming prior to use. Reactions in which proteins were either radiolabelled with ^{35}S-methionine or left unlabelled were performed. For radiolabelling, 25µl TNT rabbit reticulocyte lysate was added to 2µl TNT reaction buffer, 1µl TNT T7 RNA polymerase, 1µl 1mM amino acid mixture minus methionine, 4µl ^{35}S-L-methionine (Dupont-NEN), 40 units RNAse inhibitor (Promega), 1µg DNA template and nuclease-free water to a final volume of 50µl. For unlabelled protein synthesis, the ^{35}S-L-methionine was omitted from the reaction and replaced with 1µl 1mM complete amino acid mixture. Reactions were incubated at 30°C for 90 minutes. Alternatively, Promega's TNTQUICK T7 coupled transcription-translation rabbit reticulocyte lysate systemwas used. To 20µl TNTQUICK lysate mix was added 1µl ^{35}S-L-methionine (Dupont-NEN), 0.5µg template DNA and nuclease-free water and/ or ribozyme RNA to final volume 25µl. Lysates were analysed by acrylamide gel electrophoresis, western and northern blotting, immunoprecipitation and primer extension analysis.

b) Denaturing Gel Analysis of Translation Products

A 5µl aliquot of the translation reaction was added to 20µl SDS sample buffer, and heated to 100°C for 2 minutes. 10µl of the denatured sample was then loaded onto a 17.5% SDS-acrylamide gel.

17.5% separating gels were prepared using 1.12ml water, 4.38ml Protogel 30% stock acrylamide solution (National Diagnostics), 1.9ml separating gel buffer, 112µl 10% ammonium persulphate and 5µl TEMED (Biorad). 5% Stacking gels were prepared using 1.0ml water, 444µl stacking gel buffer, 300µl Protogel 30% stock acrylamide solution, 28µl ammonium persulphate and 5µl TEMED. Electrophoresis was carried out at a constant current of 15mA in the stacking gel and 30mA in the separating gel. Gels were run in Tris-glycine buffer. Proteins were visualized either by autoradiography or by western blotting. Prior to autoradiography gels were fixed by soaking in 10% glacial acetic acid, 10% methanol, for 30 minutes. Fixed gels were soaked in Enhance (National Diagnostics) for 30 minutes, then washed in water for 30 minutes. Gels were then vacuum dried and exposed for autoradiography.

c) Western blotting

Acrylamide gels were blotted onto Hybond-N nylon membrane (Amersham) using a Biorad Electroblotter running at 250mA for 3 hours in Towbin buffer. Icepacks were used to prevent the apparatus overheating. Following blotting, the membrane was blocked by incubating in 3% gelatin (Biorad) in TBS buffer overnight at 37°C. The blocked membrane was washed twice for five minutes in TTBS, and then incubated for 3 hours at room temperature with neat rabbit anti-HBc polyclonal antibody (Zymed). Following two 10 minute washes in TTBS the membrane was incubated for 2 hours at room temperature with

the secondary antibody, mouse anti-rabbit IgG-horseradish peroxidase conjugate (Dako). This secondary antibody was used at a 1:1000 dilution in 1% gelatin, TTBS. After four final washes of 15 minutes each in TTBS the blot was developed using ECL chemiluminescent peroxidase substrate (Amersham). The substrate was prepared by mixing 1ml of both solutions provided, and then placing this mixture directly onto the membrane. Following a 1 minute incubation at room temperature the membrane was exposed to photographic film for 15 seconds.

d) Firefly luciferase reporter assay

50µl room temperature luciferase assay reagent was dispensed into the required number of luminometer tubes. The luminometer was pre-programmed to perform a two second pre-measurement delay followed by a ten second measurement period. 2.5µl of rabbit reticulocyte lysate reaction was transferred to a luminometer tube containing assay reagent. The tube was mixed briefly, and placed in the luminometer to initiate a reading.

e) Northern blotting

Samples were run on 2% agarose gels. 3g agarose was boiled in 127.5ml water, and then allowed to cool for 10 minutes. 15ml 10X MOPS buffer, and 7.5ml 37% formaldehyde (Fluka) was added and the gel was cast. RNA samples were added to RNA gel loading buffer in the ratio 5 volumes RNA to 11 volumes buffer and heated to 95°C for 2 minutes prior to loading on the gel. Gels were run in 1X MOPS buffer at 40mA for 3 hours. Duplicate samples were loaded on each half of the gel.

Following electrophoresis the gel was washed twice for 10 minutes in DEPC treated water. The gel was then cut in half, with one half of the gel being used for blotting and the other half being stained with ethidium bromide. For ethidium bromide staining the gel was soaked in DEPC treated water containg 1µg/ml ethidium bromide for 15 minutes. The gel was then rinsed and destained for 10 minutes in DEPC treated water. Bands were then visualized by ultra-violet transillumination.

The other half of the gel was capillary blotted overnight using 10X SSC onto Hybond-N nylon membrane (Amersham), which was presoaked with 10X SSC. On completion of blotting the membrane was rinsed in 2X SSC, air dried and then baked at 80°C for 2 hours. The baked membrane was blocked by incubation at 42°C for 3 hours in 50ml hybridization buffer. Following blocking the denatured probe was added directly to the hybridization buffer. Probes were prepared either by nick translating PCR products or by end-labelling synthetic oligonucleotides. The probe was allowed to hybridize to the blot overnight at 42°C.

Following hybridization, the probe was poured off, and the membrane washed for 30 minutes in 300ml 2X SSC at room temperature, then for one hour at 65°C in 2X SSC + 1%

SDS, and finally for 10 minutes at room temperature in 0.1X SSC. The membrane was wrapped in cling film and exposed for autoradiography at -70°C with an intensifying screen.

If the blot required reprobing, it was stripped of the original probe by placing the membrane in boiling 0.1% SDS and allowing to return slowly to room temperature. The stripped blot was then blocked and probed as before.

f) Immunoprecipitation

25µl of rabbit reticulocyte lysate *in vitro* translation reaction was diluted with H_2O to give a final volume of 200µl. To this was added 25µl 5M LiCl and 25µl protein-A sepharose beads (Sigma). The tubes were incubated whilst spinning end-over-end at 4°C for 2 hours. This incubation cleared any proteins from the lysate which bound non-specifically to the beads. The tubes were spun at 13,000rpm for 1 minute, and the supernatant removed to a fresh tube. 5µl of rabbit anti-HBcAg polyclonal antiserum (Dako) was added to the supernatant. The tubes were incubated whilst spinning end-over-end at 4°C for 3 hours. 25µl of protein-A sepharose beads were added to each sample, which were then incubated at 4°C for a further 1 hour. The tubes were spun briefly to pellet the protein-A sepharose beads. The pellet was resuspended in 500µl wash buffer (0.5M LiCl, 0.1M Tris-HCl, pH 8.0), then repelleted. This washing procedure was repeated three times. The final pellet was resuspended in 30µl gel-loading buffer. The sample was boiled for 2 minutes, then loaded onto a SDS-polyacrylamide gel. The resulting gel was visualized by autoradiography.

g) Primer extension analysis

Primer extension analysis was used to detect ribozyme cleavage products in RNA extracted from rabbit reticulocyte lysate coupled transcription-translation reactions. Promega's MMLV-RT H$^-$ primer extension system was used. RNA was extracted with TE-saturated phenol (pH 4.5) and precipitated with 0.1 volumes 3M ammonium acetate and 2.5 volumes EtOH at -70°C for at least 30 minutes. The precipitate was spun down at 13,000rpm at 4°C for 30 minutes, the pellet washed with 70% EtOH, vacuum dried and resuspended in 25µl nuclease free water.

A primer was chosen from laboratory stocks which bound at the 3'-end of the core ORF (primer C2, sequence GAGATTTCTCAAGGGATACTAACATTCA). The primer was 5' endlabelled as described (section 2.2.5.viii). 100fmol (1µl) of labelled primer was added to 5µl MMLV-RT 2X buffer and 5µl RNA sample. The RNA and primer were annealled by heating the tubes at 95°C for 2 minutes, then allowing them to cool to room temperature. A master reverse transcriptase (RT) mix was prepared, containing 5µl MMLV-RT 2X buffer, 2 units MMLV-RT H$^-$ and nuclease-free water to a final volume of 9µl per reaction. 9µl of the RT mix was immediately added to each reaction tube containing annealed primer and RNA. Reactions were incubated at 42°C for 30 minutes. 20µl formamide gel loading buffer was

added to each tube. 20µl of each sample was loaded on a 10% denaturing polyacrylamide gel and run in 1X TBE buffer.

h) Nick translation

0.5µg of the double-stranded DNA to be labelled was mixed with 2.5µl 10X nick-translation buffer, 20nmoles each of unlabelled dATP, dTTP and dGTP, 16pmoles [α^{32}P]-dCTP (Dupont-NEN) and water to 21.5µl. The reaction mixture was chilled to 0°C. 2.5µl of DNase I (10ng/ml) (Boehringer-Mannheim) and 2.5 units DNA polymerase I were added. The reaction was incubated at 16°C for 60 minutes, after which it was stopped by adding 1µl 0.5M EDTA (pH 8.0). Labelled DNA was separated from unincorporated nucleotides by ethanol precipitation.

i) End-labelling nucleic acids

Prior to labelling, it is necessary to remove the 5' phosphate group from RNA with calf intestinal alkaline phosphatase (CIAP) (Boehringer Mannheim). The RNA to be labelled was incubated in 1X CIAP reaction buffer with 2 units CIAP for 1 hour at 37°C. The reaction was stopped by adding 2mM EDTA. The RNA was recovered by extraction with TE-saturated phenol (pH 4.5) and ethanol precipitation.

Synthetic oligonucleotides (synthesized without a 5' phosphate group) or CIAP-treated RNA was mixed with 3µl 10X kinase buffer, 5µl [γ^{32}P]-ATP (Dupont-NEN), 10 units T4 polynucleotide kinase and water to 50µl and incubated at 37°C for 60 minutes. Labelled DNA or RNA was purified by phenol-chloroform extraction and ethanol precipitation.

CHAPTER 3 RESULTS

The aim of this study was to investigate the effects of substrate secondary structure on hammerhead ribozyme activity and how this could influence the design of anti-HBV ribozymes. The study can be divided into three sections: I) measuring ribozyme-substrate hybridisation rates, II) determining ribozyme cleavage rates under single-turnover conditions and III) assessing the ability of ribozymes to block protein synthesis in an *in vitro* translation system. However, before this work could begin, ribozyme target sites in the HBV RNAs had to be determined, and constructs made for the expression of the ribozyme and substrate RNAs *in vitro*.

3.1 DOES SUBSTRATE SECONDARY STRUCTURE AFFECT RIBOZYME-SUBSTRATE HYBRIDISATION RATES?

3.1.1 Choice of target site

As described in section 1.3.3, the entire HBV genome encodes RNA. Therefore any NUX triplet within the genome could theoretically be targeted with a hammerhead ribozyme resulting in the destruction of an RNA. It was decided to target the pre-core/ core open reading frame (ORF). HBcAg is translated from the pgRNA (Yaginuma *et al.*, 1987). Cleavage within this region will not only destroy the pgRNA, a vital intermediate in genome replication, but will also block HBcAg production, which is important for capsid formation and minus-strand DNA synthesis. Figure 3.1 shows the sequence of the core region, with hammerhead ribozyme NUX target sites indicated (note that the NUX triplets do not have to be in frame with the HBcAg sequence). The pre-core/ core ORF has been targeted by hammerhead ribozymes in a previous study. von Weizsacker *et al.*, (1993) demonstrated that a set of three ribozymes could cleave core mRNA either singly, or if all three ribozymes were in the same transcript. It was decided to use two of the three ribozymes from this study in our system as controls, cleaving after bases 220 (designated ribozyme RZ1) and 238 (designated ribozyme RZ2) in the pre-core/ core ORF. The third ribozyme could not be used as its target site was mutated away from an NUX consensus triplet in the core sequence used as a transcription template in the current study.

It was important for the purposes of this study to know the secondary structure of the ribozyme substrate. The MFOLD computer program was used to determine the optimum and sub-optimum secondary structures of the HBcAg mRNA sequence 5D (figure 3.2). This program utilises the minimum energy algorithm developed by Jaeger *et al.*, (1989) to predict the most stable conformations assumed by an inputted RNA sequence. There was some variation between the optimum and sub-optimum structures, though one stem loop was conserved between all the structures generated. This lay between residues 525 and 585

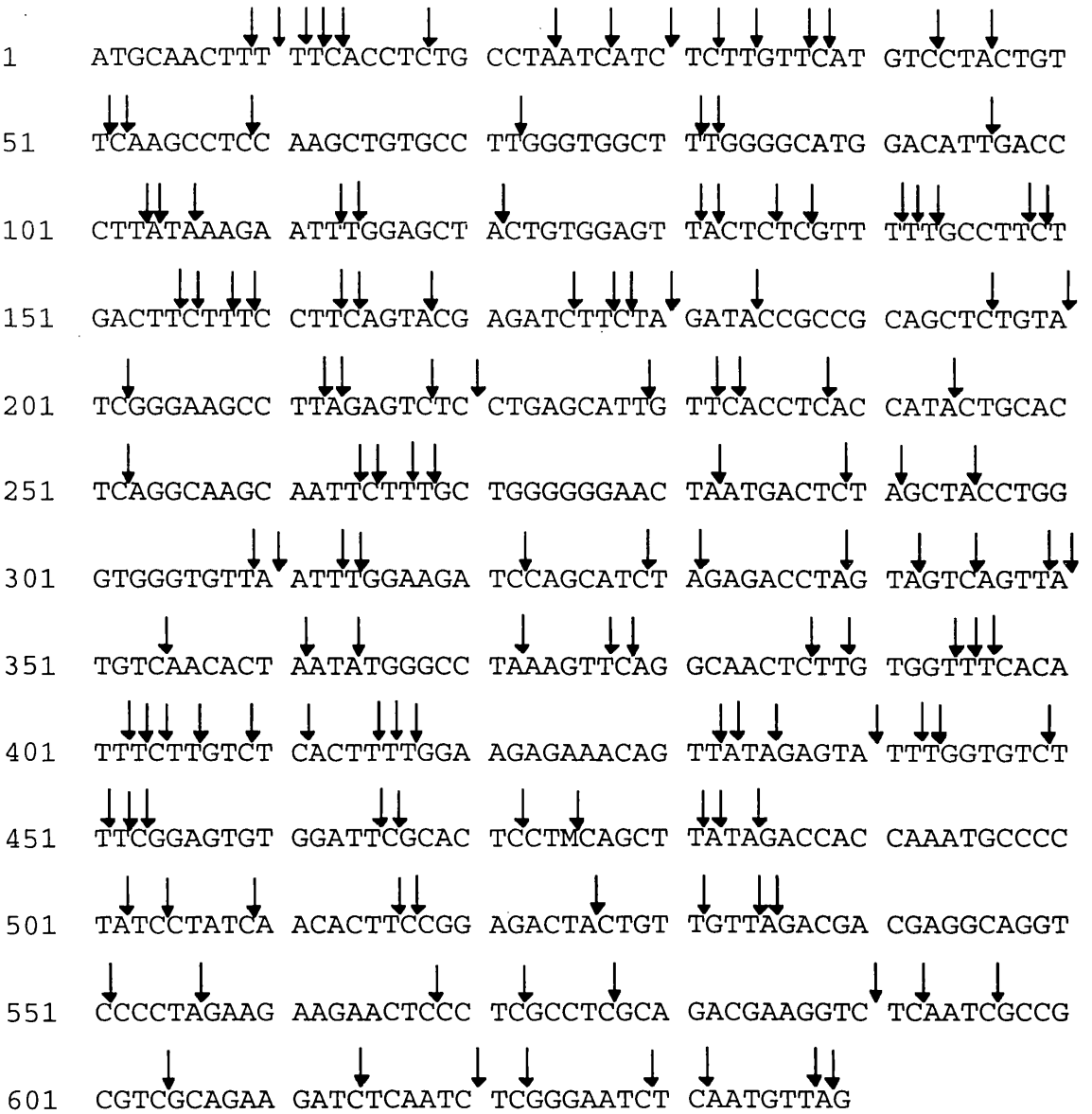

Figure 3.1. Sequence of the 639 base pre-core/core open reading frame, Italian isolate 5D. All 143 potential hammerhead ribozyme cleavage sites are indicated by arrows (NTX consensus). Base number 1 in this sequence corresponds to base 1814 in the HBV genome (numbered from the unique *Eco*RI restriction site in pre-S2). This sequence was kindly provided by E. Dornan, Institute of Virology.

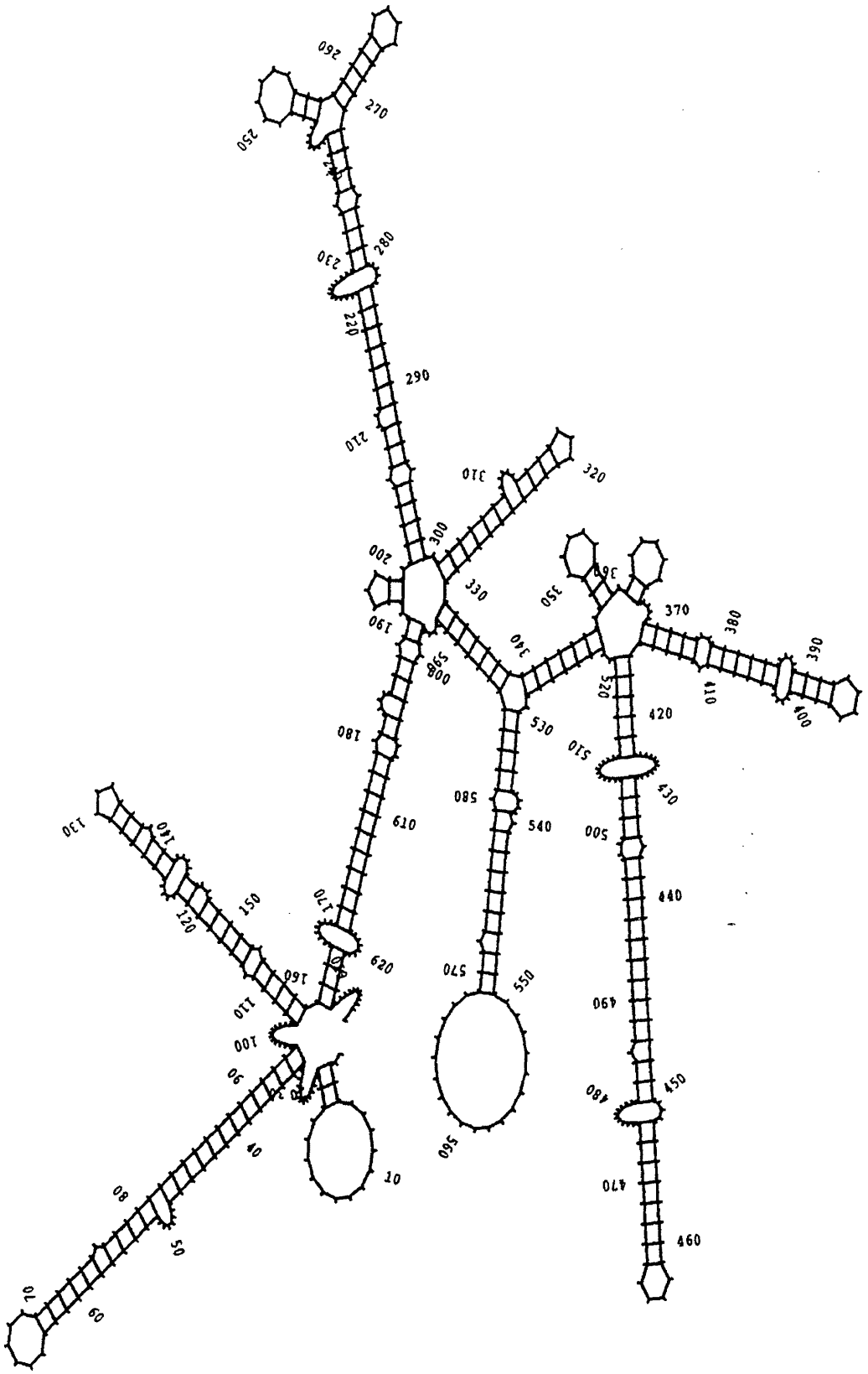

Figure 3.2. Optimum secondary structure for 5D mRNA, corresponding to the pre-core/ core ORF, as predicted by the MFOLD computer program. The structure has an energy of -134.5kJ/mol. Base numbers are indicated, with base number 1 corresponding to position 1814 in the HBV genome.

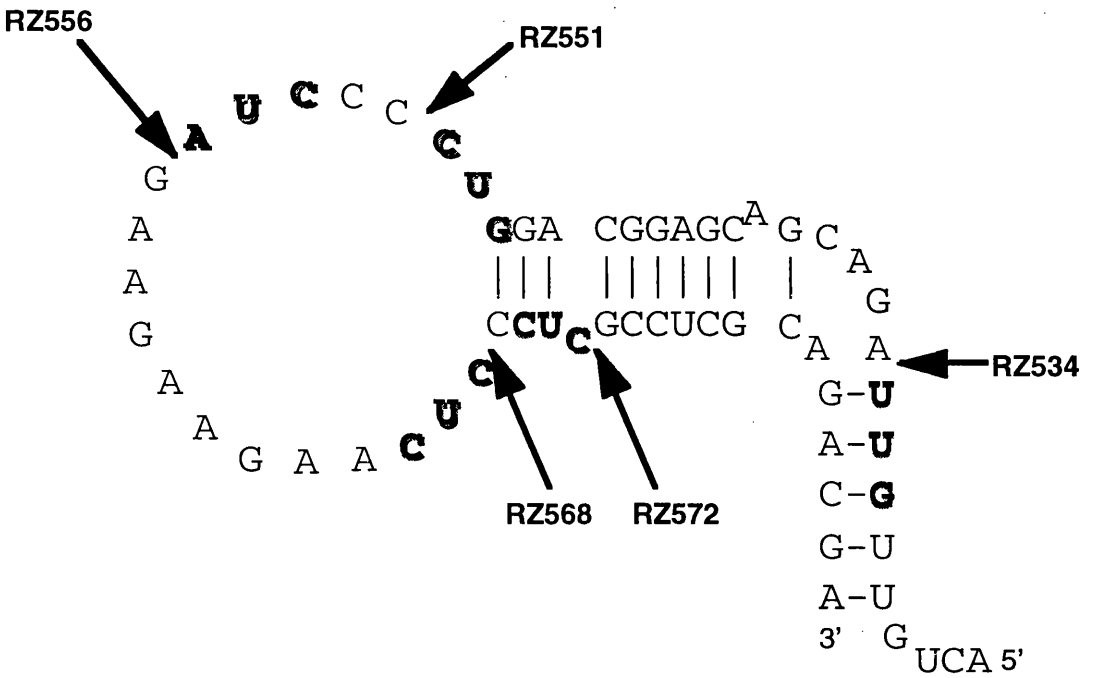

Figure 3.3. Detail of bases 526 to 585 from the pre-core/ core ORF. The predicted structure shown here was generated using the MFOLD computer program using just the sequence between bases 526 and 585 as the input sequence. Cleavage sites are indicated by arrows, with the target triplets highlighted in bold type. The ribozymes are named for the base after which they are designed to cleave.

RZ534
gacaacaa cugcugcu
RZ551
uccgucca gggaucuu
RZ556
ccagggga cuucuucu
RZ568
cuucuuga ggagcgga
RZ572
uugaggga cggagcgu
HBcAg mRNA sequence
acuguuguuagacgacgaggcaggucccc uagaagaagaacucccucgccucgcagacgu
* *
526 **585**

Figure 3.4. The sequence of HBcAg mRNA between bases 526 and 585, corresponding to the stem loop shown in figure 3.3, and the flanking sequences of ribozymes RZ534, 551, 556, 568 and 572. The ribozyme sequences are aligned with their complementary target sequences in the HBcAg mRNA. For clarity the conserved catalytic cores have been omitted. The sequence between bases 526 and 585 of 5D RNA corresponds to the sequence of the truncated ribozyme substrate, RZSUB.

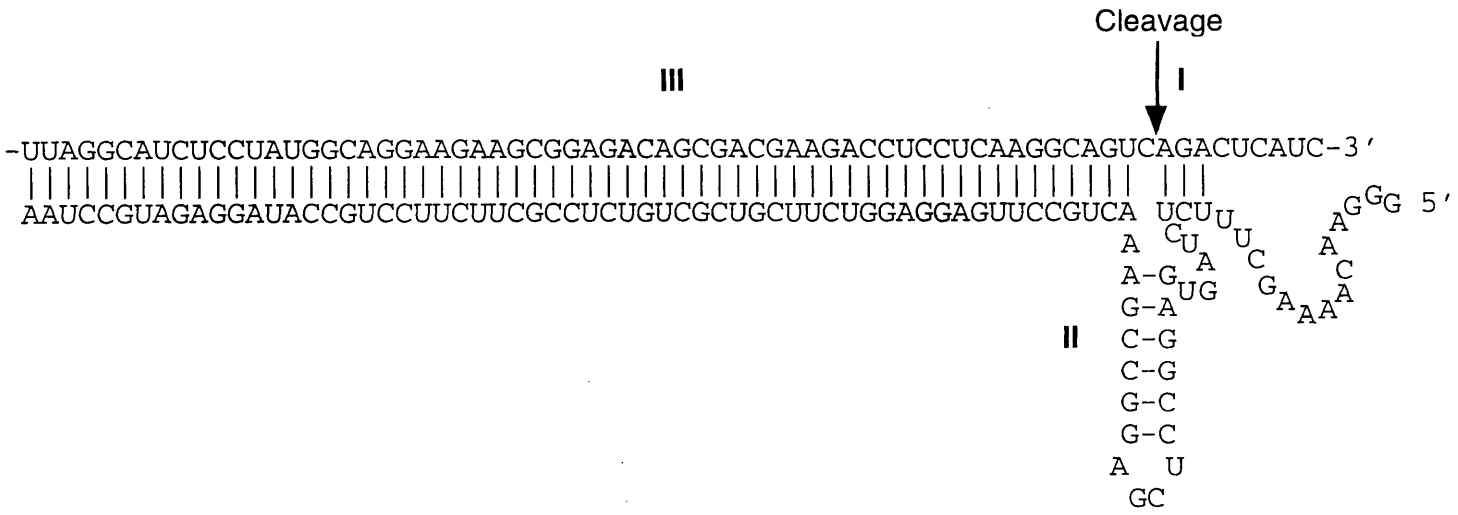

Figure 3.5. Positive control ribozyme RZ60, obtained from G. Sczakiel, Deutscheskrebsforschungcentrum, Heidelberg. Note the assymmetric design, with helix III (length 57 base-pairs) being considerably longer than helix I (length 3 base-pairs). This ribozyme is targeted against a region of HIV-1 *tat*, with cleavage occuring after base 5597 (numbered from the start of the HIV-1 genome). The substrate used, Y98, is a fragment of the *tat* gene of length 100 bases. Both constructs were cloned under the control of the bacteriophage T7 promoter. Figure taken from Hormes *et al.*, (1997).

(figure 3.3). Five NUX triplets within this region were identified, and hammerhead ribozymes were designed to be targeted against them. Each ribozyme had a total of 16 bases in the flanking sequences, with 8 bases in each flank (figure 3.4). In addition to these ribozymes a positive control ribozyme, RZ60, and substrate, Y98, were obtained from Dr. G. Sczakiel, Heidelberg (figure 3.5).

3.1.2 Ribozyme-substrate hybridisation (I)

3.1.2a Construction of ribozymes

It was initially decided to produce ribozyme constructs by PCR (figure 3.6). The primers used for this are shown in table 2.1. The pRK5 mammalian expression plasmid was used as the substrate, allowing the SV40 polyadenylation signal to be incorporated into the PCR product. At this stage of the project it was hoped that the ribozyme constructs could have been used in cell culture experiments. It was decided to incorporate the poly-adenylation signal into the ribozyme construct to limit the amount of exogenous vector sequence in the transcripts generated from the expression of the cloned PCR product.

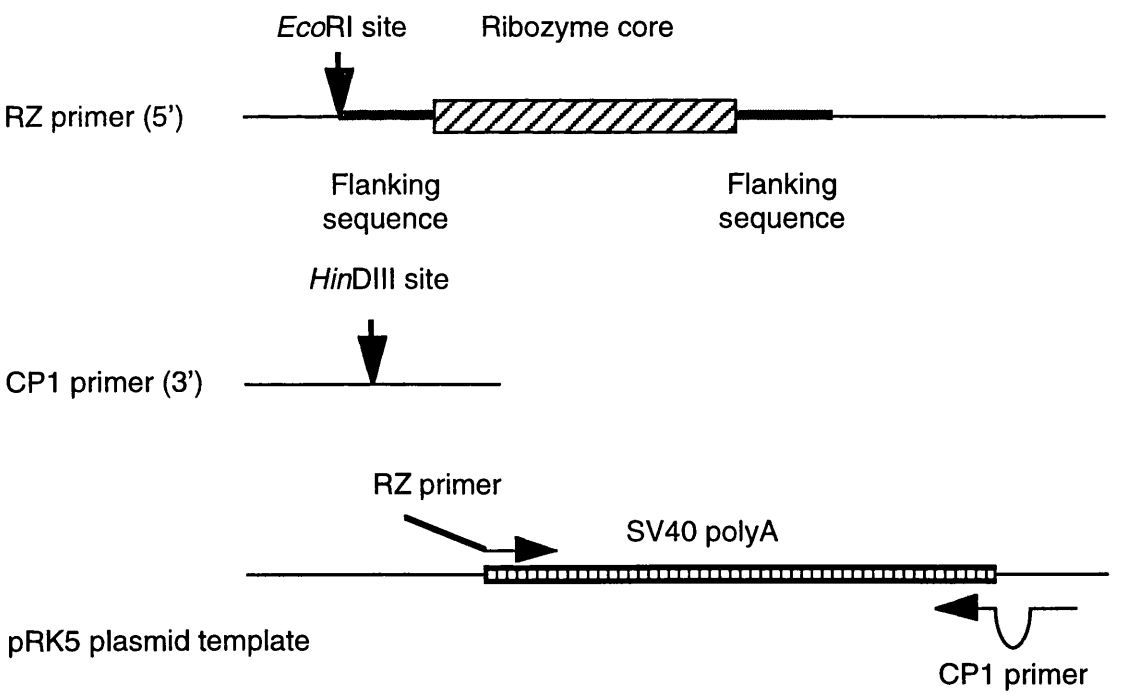

Figure 3.6. Generation of ribozyme expression cassettes by PCR. The primers used are described in detail in table 2.1. The 5'-RZ primer contains the complete ribozyme sequence plus an *Eco*RI restriction site. The 3'-CP1 primer contains a *Hin*DIII restriction site. Incorporation of these restriction sites at the 5' and 3' ends of the PCR product allowed it to be cloned into the pGEM-3z plasmid. The resulting construct contains a complete hammerhead ribozyme domain at the 5' end and the SV40 polyadenylation signal at the 3' end. The total length is 450 bases.

The PCR product was cloned into the bacterial plasmid pGEM-3z. This plasmid has two bacteriophage promoters, T7 and SP6. The promoters were situated at opposite ends of the polylinker, with both promoters aligned to initiate transcription through the polylinker region. The ribozyme construct was under the control of the T7 promoter. Linearizing the plasmid at the *Hin*dIII site enabled run-off transcripts of the ribozyme-polyadenylation signal construct to be generated (figure 3.7).

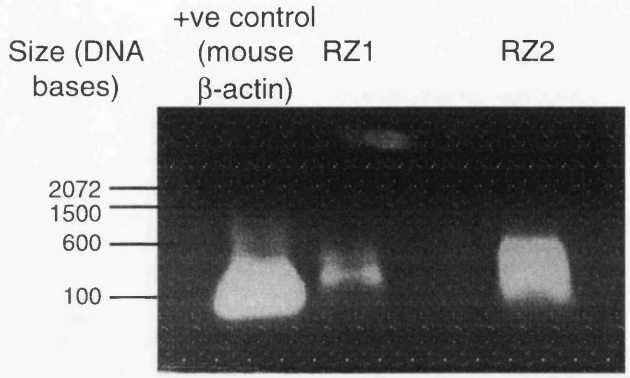

Figure 3.7. Run-off *in vitro* transcripts obtained from PCR cassettes cloned into pGEM-3z plasmid. Transcripts were generated using T7 bacteriophage RNA polymerase. The resulting RNA was acid phenol/ chloroform extracted, ethanol precipitated and pelleted. The pellet was resuspended in 50µl H_2O. 5µl of the dissolved RNA was added to 5µl agarose gel loading buffer. The resulting sample was run on a 1% agarose gel in 1X TBE buffer.

3.1.2b Gel shift assays

The interaction between ribozyme and substrate was studied by gel shift assay. Initially RZ1 and RZ2, constructs based on von Weizsacker's study, were used. Both ribozyme and substrate were generated by *in vitro* transcription, with the ribozyme being internally labelled with α-^{32}P-UTP. The ribozyme and substrate were incubated together at 37°C, with aliquots being taken at various time-points and placed in gel loading buffer. The gel loading buffer contained urea in order to remove any intramolecular structure from the ribozyme-substrate complex, whilst maintaining base-pairing between the ribozyme and substrate. This is to prevent the occurrence of any structural isoforms which could migrate different distances to give multiple bands, making analysis of the gel difficult. Therefore the concentration of the urea is critical. Too little and the final gel will have multiple bands, making it difficult to distinguish the ribozyme-substrate complex and the unbound ribozyme. Too much and the ribozyme-substrate complex will be broken apart. Concentrations of 1M urea or less should not denature RNA duplexes of 8 base-pairs in length (G. Sczakiel, personal communication).

complex could be observed (figure 3.9). Using both gel loading buffer and acrylamide gels containing no urea did not change this result.

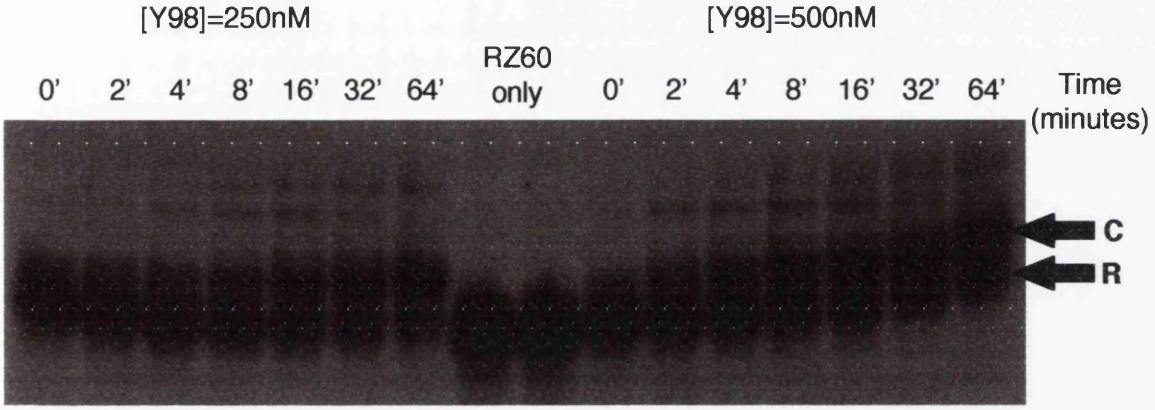

Figure 3.8. Gel shift performed with radiolabelled RZ60 positive control ribozyme and an excess of unlabelled Y98 positive control substrate. Both RNAs were incubated together in 1X ribozyme hybridisation buffer at 37°C. Aliquots were taken at the times indicated and placed in gel loading buffer containing 1.0M urea. Samples were run on an 8% acrylamide, 1.0M urea gel. Ribozyme-substrate complex (**C**) and unbound ribozyme (**R**) are indicated.

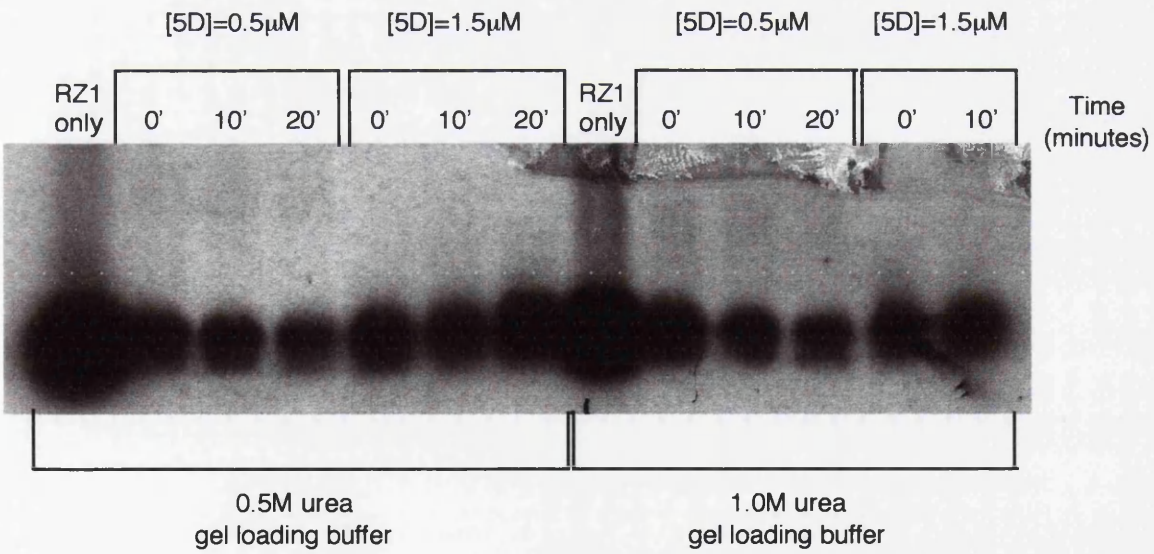

Figure 3.9. Gel shift performed with radiolabelled RZ1-SV40 polyadenylation signal and an excess of unlabelled 5D RNA substrate (at a concentration of 0.5μM or 1.5μM). Both RNAs were incubated together in 1X ribozyme hybridisation buffer at 37°C. Aliquots were taken at the times indicated and placed in gel loading buffer containing either 0.5M or 1.0M urea as indicated. Samples were run in a 1% agarose gel at 4°C. Even though this is the gentlest method for separating RNA species, no ribozyme-substrate complex is observed.

It was considered that the extra sequence in the ribozyme construct derived from the SV40 polyadenylation signal may have been obscuring the ribozyme flanking sequences. The MFOLD program was used to generate predictions for the secondary structure of the RZ1-SV40 polyadenylation signal RNA (figure 3.10). Only a single predicted structure was generated, which showed that the ribozyme domain was trapped within a double-stranded region of the RNA.

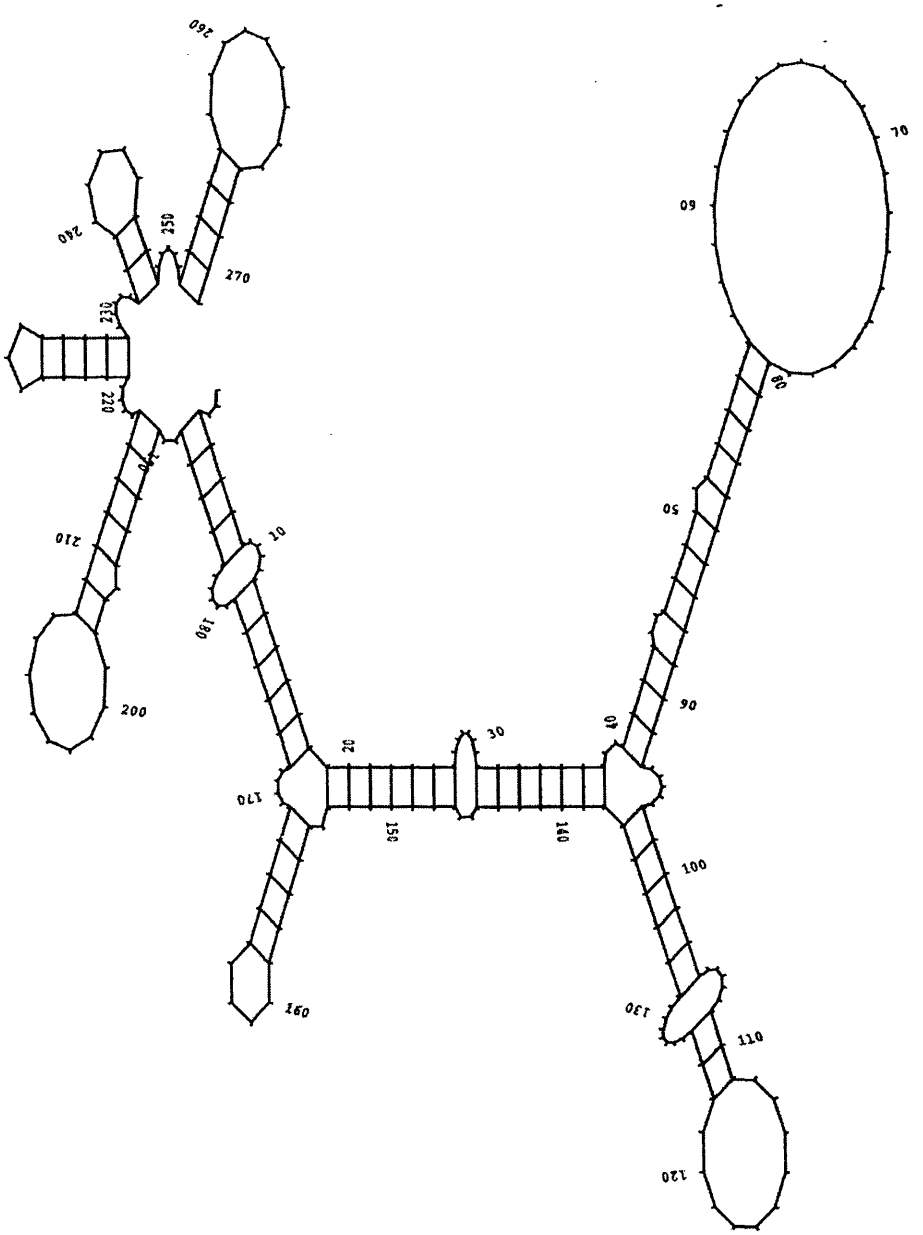

Figure 3.10. Prediction of RZ1-SV40 polyadenylation signal RNA secondary structure, generated by MFOLD program. The ribozyme domain lies between bases 1 and 40, which forms part of an almost entirely double-stranded region of the RNA. For clarity only bases 1 to 271 are shown. The transcript's full length is 450 bases.

Nucleic acid secondary structure which inhibits the binding of two complementary nucleic acid molecules can be removed by heating the nucleic acids to 95°C, which melts the secondary structure, and then snap-cooling the nucleic acids on ice. This snap-cooling step brings the nucleic acids back down to a temperature at which intermolecular hybridisation can occur before intramolecular secondary structure can form. Although it can be seen from figure 3.2 that the 5D RNA has long stretches of intramolecular helices, formation of these regions of extended secondary structure is slower than the formation of short helices, such as those formed between ribozyme and substrate. Therefore, denaturation followed by snap-cooling provides a window in which ribozyme-substrate hybridisation, if such a thing is possible, can occur.

A truncated version of RZ1 was produced, lacking the SV40 polyadenylation signal, by linearizing the RZ1-SV40 polyadenylation signal plasmid with a restriction enzyme cutting just after the ribozyme domain. This was then used as a template for radiolabelled *in vitro* transcription (figure 3.11). This truncated RZ1 was used in a denaturation-snap-cooling experiment. Figure 3.12 shows that this process allowed the formation of a complex between the positive controls RZ60 and Y98, but not between RZ1 (truncated) and 5D.

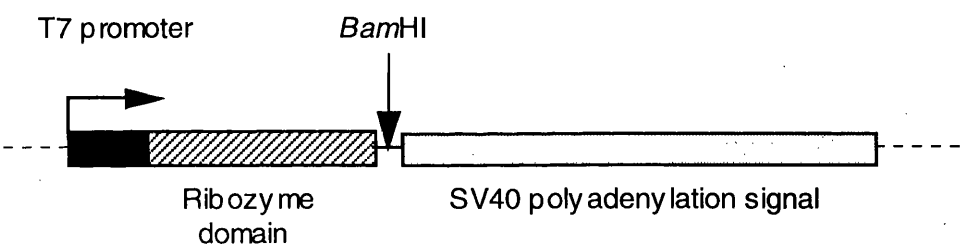

Figure 3.11. Generation of truncated RZ1. The RZ1-SV40 polyadenylation signal cassette contains a *Bam*HI site immediately after the ribozyme domain. The plasmid was linearized at this *Bam*HI site and used as a template for run-off *in vitro* transcription, producing a 40-mer RNA.

3.1.2c Discussion

These initial results were a cause for concern. Although sequencing of the cloned PCR product showed that the complete ribozyme sequence was present, the RZ1 RNA did not appear to be binding to its complementary sequence in the substrate. Why should this be? The first possibility to consider is that the conditions in which the gel shift assay samples are analysed are too harsh. Whilst the RZ60-Y98 complex can withstand 0.5M urea, this is not a fair comparison with RZ1-5D. The RZ60-Y98 complex contains a total of 60 intermolecular base-pairs compared to 16 in the predicted RZ1-5D complex. However, in other people's experience RNA duplexes of at least 8 base-pairs should be able to withstand 0.5M urea (G. Sczakiel, personal communication). Both acrylamide and agarose gels were

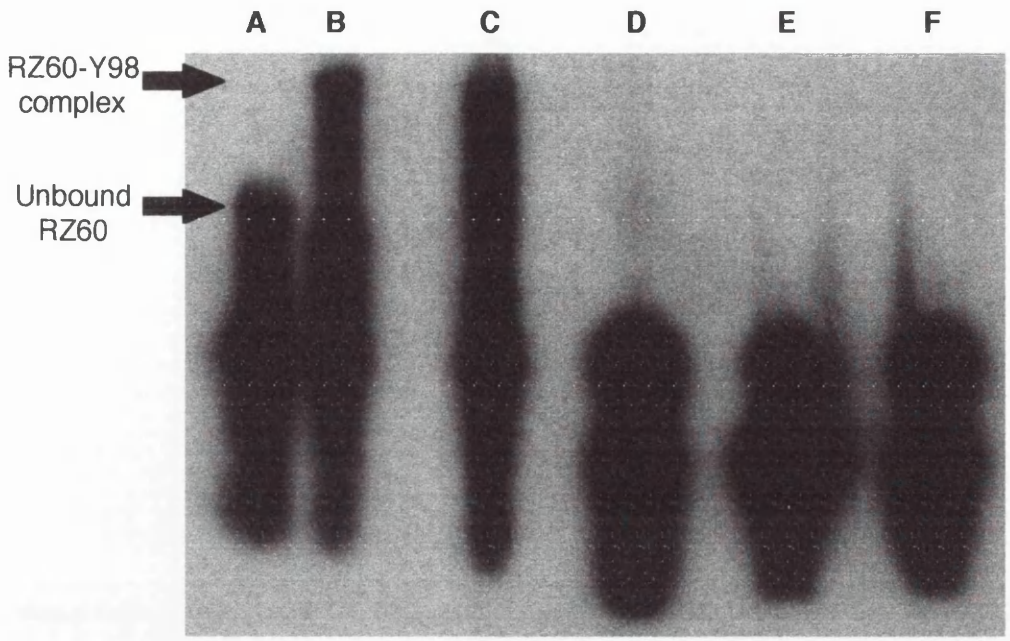

Figure 3.12. Formation of ribozyme-substrate complexes after denaturation at 95°C followed by snap-cooling on ice in 1X ribozyme hybridisation buffer. Key to lanes: (A) RZ60 only; (B) RZ60 + Y98, 95°C 2', snap-cooling; (C) RZ60 + Y98, 95°C 2', slow cooling to room temperature; (D) RZ1 (truncated) only; (E) RZ1 (truncated) + 5D, 95°C 2', snap-cooling; (F) RZ1 (truncated), 95°C 2', slow cooling to room temperature. Despite degradation of the radiolabelled RNA by RNases (resulting in the smearing of the bands on the gel), RZ60-Y98 complex can be observed in lanes B and C.

used to try to separate RZ1-5D complex from unbound RZ1, though this made no difference.

Another possibility lies within the sequence of the constructs used. Secondary structure in the ribozyme and/or substrate RNAs could block hybridisation between the two RNAs. Although the secondary structure predictions do suggest this to be the case (figure 3.10), the denaturation-snap-cooling experiment utilising the truncated RZ1 RNA does not support this hypothesis (figure 3.12). von Weizsacker *et al.* did not use the entire pre-core/core ORF as a transcription template. It is possible that their RNA substrate had a very different secondary structure from the 5D RNA used in the current study. However, the region containing the cleavage sites for RZ1 and RZ2 does not appear to interact with any sequence from distant parts of the 5D RNA which were omitted from von Weizsacker's substrate (figure 3.2).

3.1.3 Ribozyme-substrate hybridisation (II)

It was decided to abandon trying to duplicate von Weizsacker's work, and to focus on targeting ribozymes against the stem loop between bases 525 and 585 of the 5D RNA. This region has been shown to be accessible to large antisense molecules, thanks to the large loop between bases 550 and 570 (Patzel *et al.*, 1997), but is the same region accessible to small hammerhead ribozymes with total flanking regions of 16 bases?

3.1.3a Construction of ribozymes

For this work it was decided to use, in addition to the full length 5D RNA substrate (length 639 bases), a shorter substrate, 60 bases in length, corresponding to the region between bases 526 and 585 of 5D RNA (RZSUB, figure 3.3). Ribozymes would also be produced with the minimum of exogenous sequence. These ribozyme transcripts would have a total length of 40 bases.

When producing short RNAs by *in vitro* transcription, the rate limiting step is the association of the RNA polymerase with the promoter. To get adequate yields of RNA from the transcription reaction it is necessary to use a high concentration of DNA template. The amount of DNA which can be added to a transcription reaction cannot be so high that the reaction buffer becomes saturated with DNA. If the transcription template is contained within a plasmid, then most of the DNA will be non-coding vector sequence. Therefore it is better to limit the amount of non-coding sequence to increase the concentration of promoters in the reaction. It was decided to use partially double-stranded oligonucleotides as transcription templates (figure 3.13). This method allowed the generation of large amounts of small RNA (figure 3.14).

3.1.3b Gel shift assays

Initial experiments were discouraging. No binding was observed between labelled ribozymes and unlabelled 5D RNA, or between unlabelled ribozymes and labelled RZSUB. When RZSUB was examined by non-denaturing PAGE, two bands were visible. When RZSUB was incubated with an excess of ribozyme at 95°C for two minutes and then cooled rapidly to 37°C, a band was visible between the two RZSUB bands (figure 3.15). It was assumed that this band was the ribozyme-RZSUB complex, but what was the slow-migrating RZSUB band which lay above this proposed complex on the gel? There are two possible explanations. The first is that RZSUB preferentially formed homodimers during renaturation rather than binding ribozyme. Unfortunately no molecular weight markers were available to confirm whether the top RZSUB band had a molecular mass twice that of the lower band. When separating small RNAs by non-denaturing PAGE, the structures of the RNAs play a significant part in determining migration distance, making it impossible to make accurate estimation of molecular mass. The second possibility is contamination from DNA template left over from the transcription reaction, though RNA produced by *in vitro*

T7P oligonucleotide

AATTTAATACGACTCACTATAG

RZSUBT oligonucleotide

ACGTCTGCGAGGCGAGGGAGTTCCTCCTCTAGGGGACCTGCCTCGTCGTCTAACAACAGTCCCTATAGTGAGTCGTATTAAATT

Template

T7 Promoter

*

AATTTAATACGACTCACTATAG

TTAAATTATGCTGAGTGATATCCCTGACAACAATCTGCTGCTCCGTCCAGGGGATCTCCTCCTTGAGGGAGCGGAGCGTCTGCA

Resulting transcript gggacuguuguuagacgacgaggcaggucccctagaggaggaacucccucgccucgcagacgu

Figure 3.13. Partially single-stranded templates for run-off *in vitro* transcription. The T7P oligonucleotide, which is complementary only to the promoter region of the template oligonucleotide (in this example the template oligonucleotide, RZSUBT, encodes the RZSUB RNA), is annealed to the template oligonucleotide. T7 bacteriophage RNA polymerase only requires that the basal promoter (the region marked in the figure) and the transcription initiation site (indicated by an asterix) are double-stranded. Therefore only one new oligonucleotide needs to be synthesized for each RNA. The length of transcript obtained from this type of template is limited to approximately 80 to 90 bases, as synthetic oligonucleotides longer than 110 bases cannot be reliably synthesized. It should be noted that the template region begins with a CCC triplet. This is necessary for maximal activity of the T7 RNA polymerase. (Milligan *et al.*, 1987).

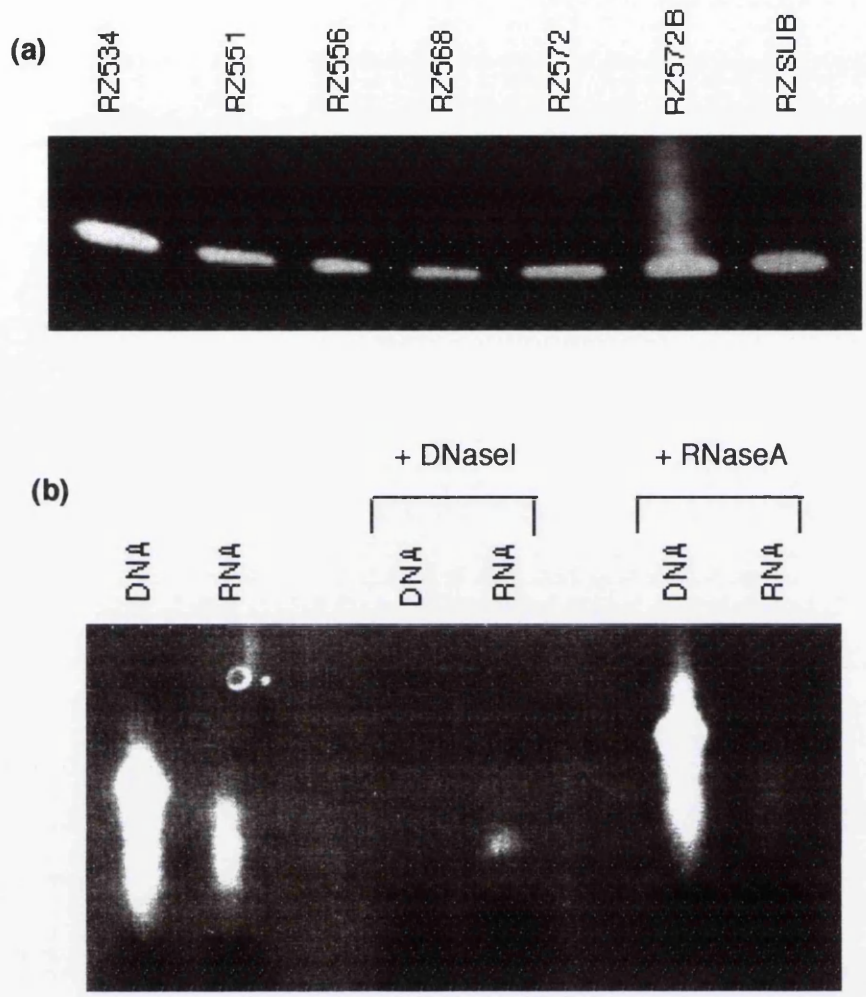

Figure 3.14. **(a)** Run-off transcripts generated from partially single-stranded *in vitro* transcription templates. RNA from a 20μl transcription reaction was treated with 10 units DNase I for 15 minutes at 37°C. Following acid phenol/ chloroform extraction the RNA was ethanol precipitated and pelleted. The resulting pellet was resuspended in 50μl H_2O. 5μl was removed from each transcription reaction, added to 5μl agarose gel-loading buffer, and run on a 1% agarose gel in 1X TBE, which allows the bands to be visualised, but cannot resolve the small differences in length of such short RNAs. **(b)** Treatment of RZSUB partially single-stranded DNA transcription template and RZSUB with DNase I or RNase A. DNA or RNA was incubated for 1 hour at 37°C in 1X transcription buffer with either 10 units DNase I, 10 units RNase A, or no addition. Reactions were then run on a 1% agarose gel in 1X TBE. It can be seen that whilst RNase A clearly degrades RZSUB RNA and DNase I degrades RZSUB DNA, treatment of RZSUB RNA with DNase I causes a reduction in band intensity. This could be due to contaminating RNase in the DNase I preparation, or some RZSUB DNA transcription template remaining after the initial DNase/ acid phenol treatment immediately after transcription.

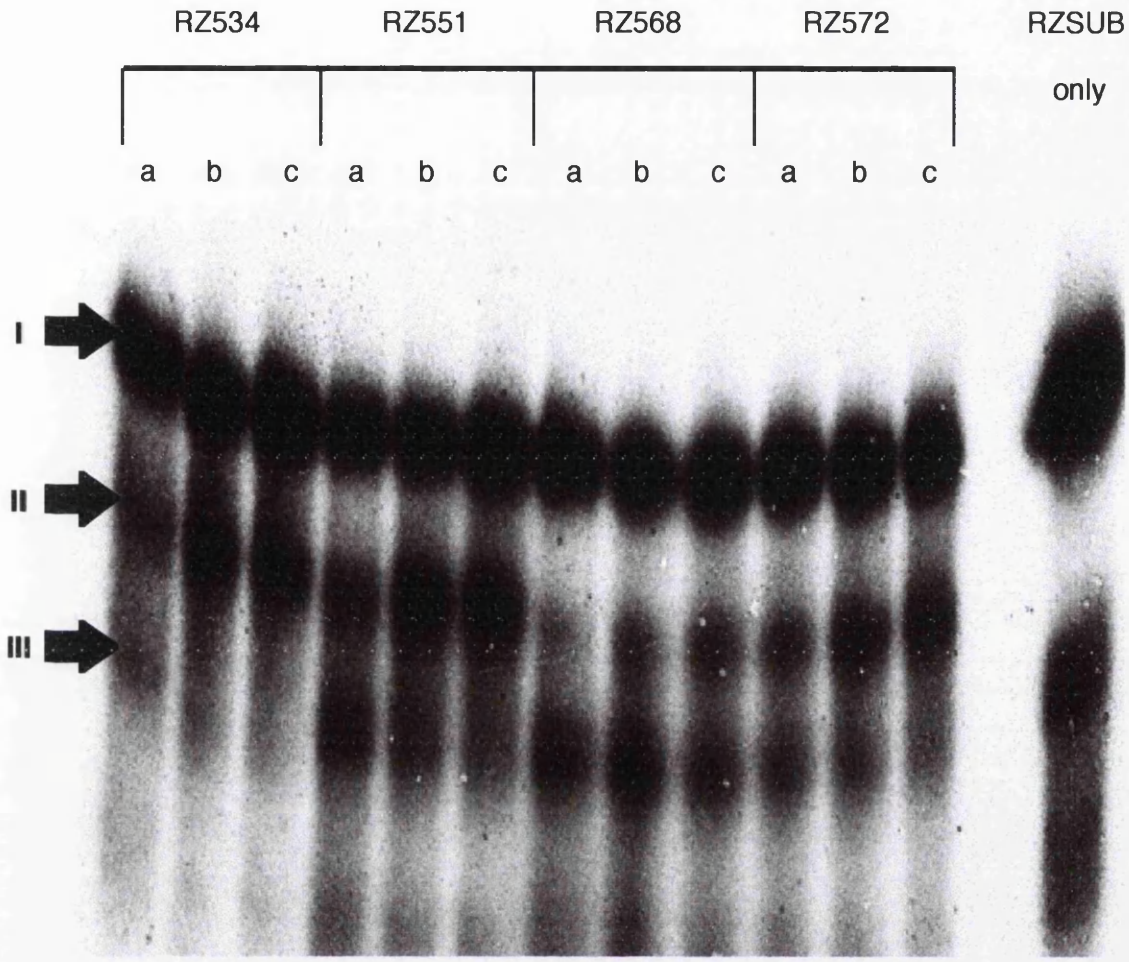

Figure 3.15. Initial gel-shift experiments performed with radiolabelled RZSUB and an excess of unlabelled RZ534, RZ551, RZ568 or RZ572. Unlabelled ribozymes were added in either (a) 100, (b) 300 or (c) 500-fold excess over radiolabelled RZSUB. Reactions were incubated at 95°C for 2 minutes, then rapidly cooled to 37°C in 1X ribozyme hybridisation buffer. Reactions were incubated at 37°C for 30 minutes before being added to 0.5M urea gel-loading buffer. Samples were run on an 8% non-denaturing polyacrylamide gel in 1X TBE. Two bands (labelled **I** and **III**) are visible when RZSUB is incubated alone (far right-hand-side). However, when an excess of ribozyme is added to the reaction, an intermediate band, labelled **II**, is seen.

transcription was treated with DNase and acid-phenol extracted (which should remove all DNA). 2 units DNase was added to gel-shift reactions. Analysis of these reactions showed a single RZSUB band, and formation over time of ribozyme-RZSUB complex. Addition of DNase also permitted the formation of complexes between labelled ribozymes and unlabelled 5D RNA.

Whilst this work was proceeding, it was considered that perhaps the flanking sequences of the ribozymes (totalling 16 bases) were too short to allow rapid binding to the substrate. A new ribozyme, RZ572B, was designed, with total flanking sequences of 59

bases (13 bases in the 5' flank, 46 bases in the 3' flank) (figure 3.16). This ribozyme was designed to bind to the entire length of RZSUB, and cleave RZSUB after base 572. Preliminary gel-shift experiments using dilution series of unlabelled RZSUB with radiolabelled RZ572B showed ribozyme-substrate complex formation at 37°C after 2 hours incubation (figure 3.17).

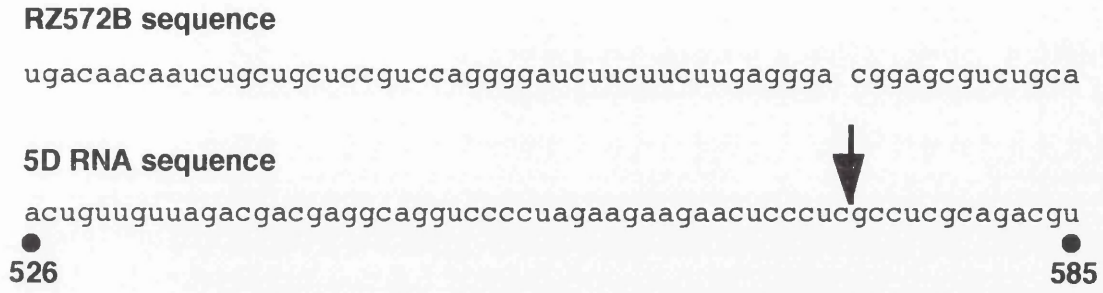

Figure 3.16. RZ572B flanking sequences lined up with their complementary sequences in 5D RNA. The region of 5D RNA shown corresponds to the whole sequence of RZSUB. For clarity the catalytic domain of RZ572B has been omitted. The cleavage point is indicated by an arrow.

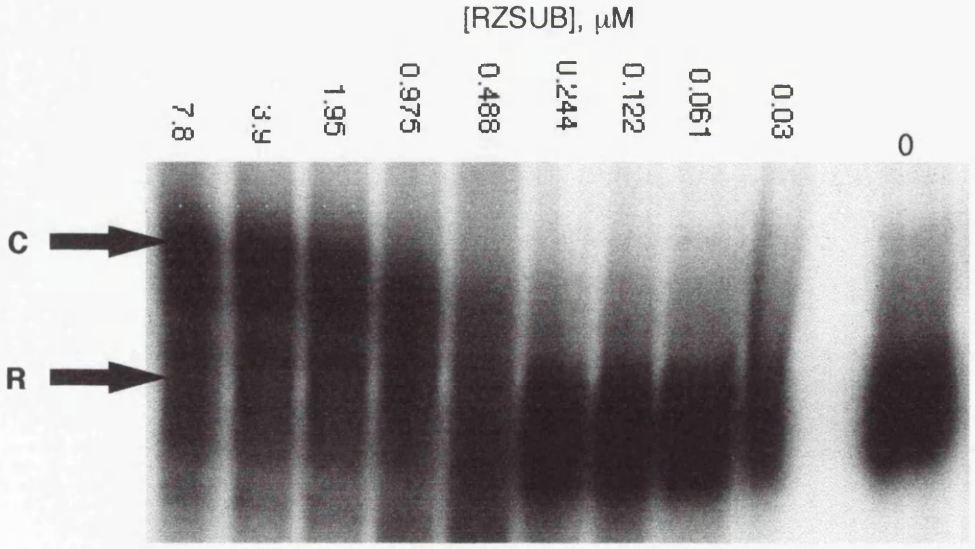

Figure 3.17. Gel-shift experiment with radiolabelled RZ572B and an excess of unlabelled RZSUB (concentrations indicated), incubated for 2 hours in 1X ribozyme hybridisation buffer. Reactions were stopped in 0.5M urea gel-loading buffer. Samples were run on an 8% non-denaturing polyacrylamide gel in 1X TBE. Ribozyme-substrate complex (**C**) and unbound radiolabelled ribozyme (**R**) are indicated.

Gel-shifts were analysed by scanning the dried gels with a phosphorimager. The bands to be measured were boxed using the IMAGEQUANT package (see figures 3.18 and 3.22). The boxes for all bands plus the background were all of the same size. The band intensity was determined as the volume of the box, the volume being defined as the sum of the signal intensities of each pixel within the box. Band intensities quantified in this way were used to determine the rate of formation of ribozyme-substrate complex. The amount of ribozyme-substrate complex was determined as a percentage of the total labelled RNA:

$$\% \text{ binding} = \frac{\text{(ribozyme-substrate complex)}}{\text{(ribozyme-substrate complex) + (labelled RNA)}} \text{ X } 100 \quad (i)$$

Percentage binding was plotted against time, and a best-fit linear curve was determined. This curve was used to calculate the $t^1/_2$ for the ribozyme-substrate hybridisation reaction.

The binding of two molecules is a second-order reaction, with the initial rate of complex formation being dependent on the concentrations of both molecules. The initial rate can be represented by:

$$v_i = k_2 \text{ X } [\text{Ribozyme}] \text{ X } [\text{Substrate}] \quad (ii)$$

where k_2 is the second-order binding rate constant. In the gel-shift experiments in the current study, the unlabelled RNA is always in excess of the radiolabelled RNA. Therefore the concentration of the unlabelled RNA effectively does not change during the course of the experiment. This gives the binding reaction pseudo-first-order kinetics (hence the linear best-fit on the graphs) (Tomizawa & Som, 1984, Persson *et al.*, 1990). The best-fit curve was used to determine the pseudo-first-order rate constant, k'_1:

$$k'_1 = \frac{\ln 2}{t_{1/2}} \quad (iii)$$

The constant k'_1 is related to the second-order rate constant, k_2, as follows:

$$k_2 = \frac{k'_1}{[S]} \quad (iv)$$

where S is the unlabelled component in excess. Therefore only the concentration of the component in excess needs to be known, as k_2 is independent of the molar ratio between the labelled and unlabelled components of the reaction. The rate constant k_2 is an indication of the affinity the two molecules have for each other. The higher the value of k_2, the stronger the binding.

Results of gel-shifts performed with both RZSUB and 5D RNA substrates are shown in figures 3.18 to 3.27. In both groups of experiments, the ribozymes were radiolabelled, whilst RZSUB and 5D RNA were unlabelled. The results from all these experiments are summarised in table 3.1. In all cases experiments were repeated in triplicate; the data plotted on the graphs are the means of these experiments, with error bars showing

the standard deviations. In some cases the experiments were repeated at different concentrations of the unlabelled RNA.

As the gel-shift reactions were subject to pseudo-first order kinetics, it was expected that the data plotted would lie approximately on a straight line. However, in many cases the data appeared to follow an exponential curve. This suggests that in certain cases there are two phases to ribozyme-substrate association; an initial burst of rapid hybridisation followed by a period of slower hybridisation. In these cases, linear best-fits were made for just the initial phase of hybridisation.

RIBOZYME	% GC	RZSUB	5D RNA
RZ534	50	-	$(9.8\pm3.2)\ X10^3 s^{-1}M^{-1}$
RZ551	56.3	$17 s^{-1}M^{-1}$	$(10\pm4)\ X10^3 s^{-1}M^{-1}$
RZ556	50	$(4.1\pm1.4) s^{-1}M^{-1}$	$(8.2\pm1.8)\ X10^3 s^{-1}M^{-1}$
RZ568	50	-	$0.72\ X10^3 s^{-1}M^{-1}$
RZ572	62.5	$3.3 s^{-1}M^{-1}$	$1.6\ X10^3 s^{-1}M^{-1}$
RZ572B	-	$(24\pm9) s^{-1}M^{-1}$	$0.76X10^3 s^{-1}M^{-1}$

Table 3.1. Pseudo-first-order rate constants of association between ribozymes RZ534, RZ551, RZ556, RZ568, RZ572 and RZ572B and substrates RZSUB and 5D RNA. All rates shown are for the initial rapid phase of ribozyme-substrate complex formation. Gel-shift experiments performed using radiolabelled ribozymes, with the unlabelled substrate in excess. The derivation of these data is shown in figures 3.18 to 3.27. All rate constants are approximated to two significant figures. The percentage of GC residues in helices I and III of the ribozyme-substrate complex is also shown.

Figure 3.18. Gel-shift experiment using radiolabelled RZ572 and an excess of unlabelled RZSUB. **(a)** Gel, with unbound RZ572 (**R**) and RZ572-RZSUB complex (**C**) indicated. The boxes indicate the regions in which the signal volume was determined. Note that all the boxes are of the same size. This process was repeated for all other gels (figures 3.19 to 3.21), though only the full gel is shown here. The background was determined in a region of the gel away from the sample lanes, in this case above the wells. **(b)** Rate of formation of ribozyme-substrate complex with 38.4μM RZSUB, with linear best-fit to initial rate shown (dashed lines). **(c)** best-fit line formula, $t^1/_2$, k'_1 and k_2 for initial rate.

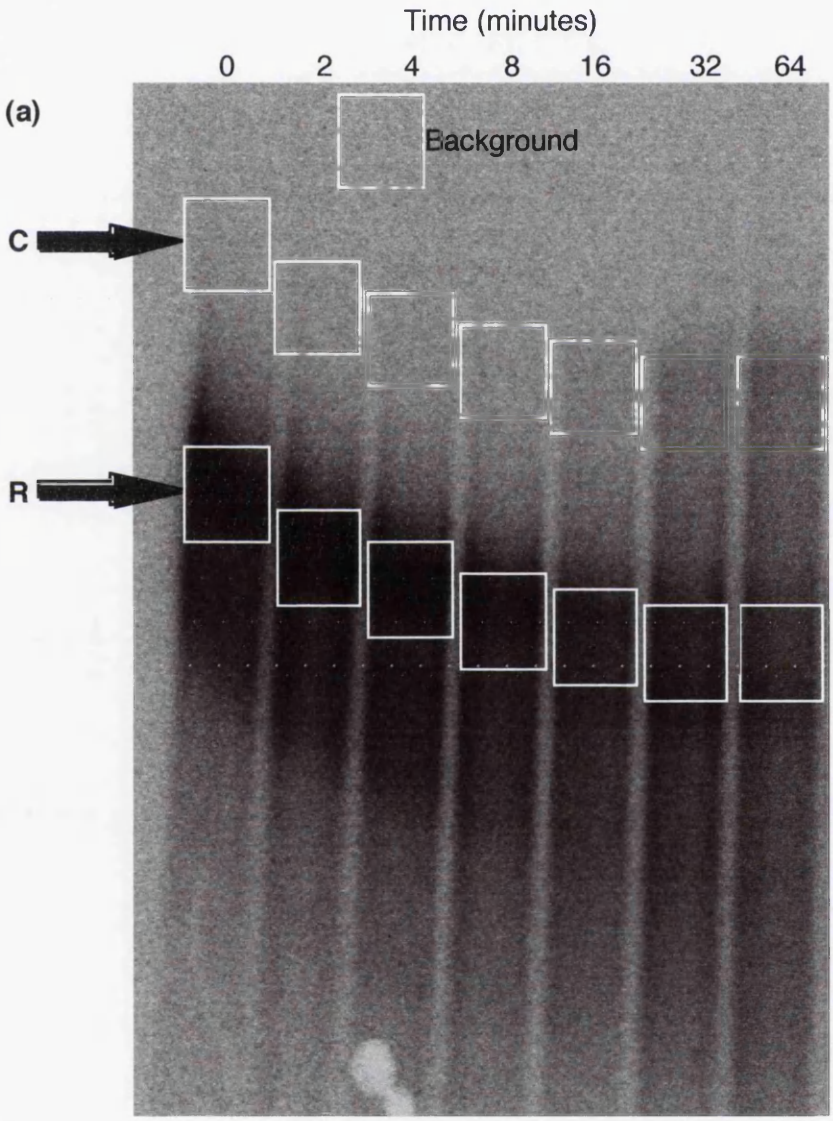

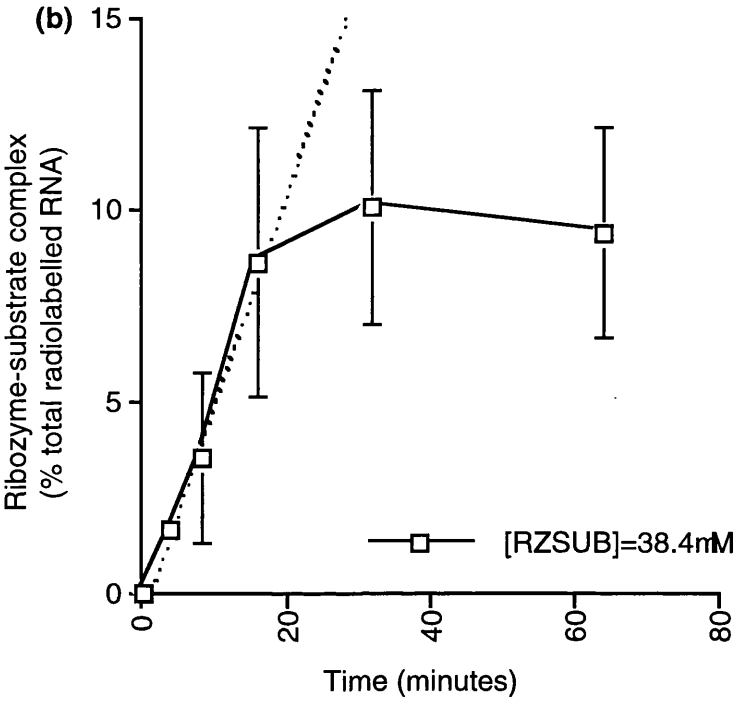

(c)

[RZSUB]	38.4μM
Best-fit line	y=0.54x-0.38
$t^1/_2$ (seconds)	5500
k'_1 (s^{-1})	0.0001
k_2 ($s^{-1}M^{-1}$)	3.3

Figure 3.19. Gel-shift experiments using radiolabelled RZ572B and an excess of unlabelled RZSUB. **(a)** Gel, with unbound RZ572B (**R**) and RZ572B-RZSUB complex (**C**) indicated. **(b)** Rate of formation of ribozyme-substrate complex with 5.675μM, 16.875μM or 33.75μM RZSUB, with linear best-fit to initial rates shown (dashed lines). **(c)** best-fit line formula, $t^1/_2$, k'_1 and k_2 for initial rates in each set of experiments.

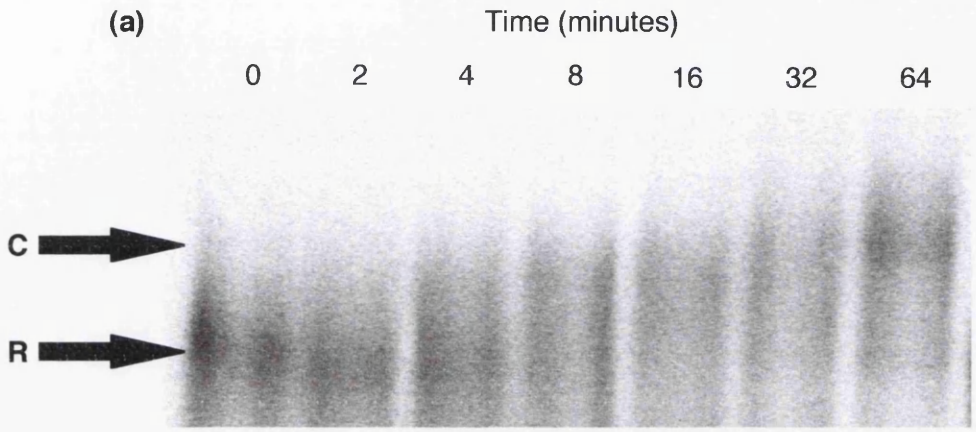

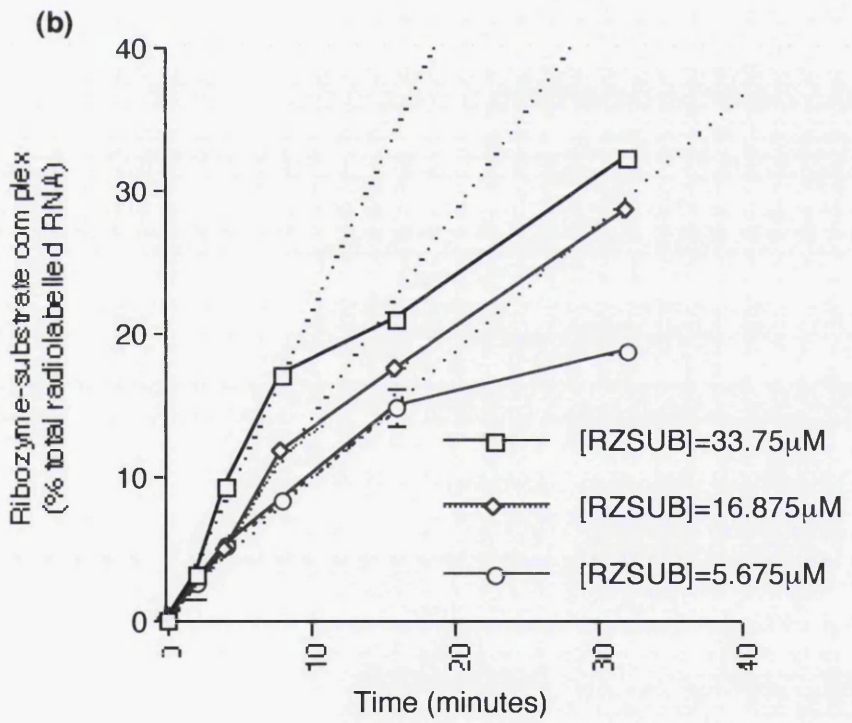

(c)

[RZSUB]	5.675μM	16.875μM	33.75μM
Best-fit line	y=0.9x+0.74	y=1.5x-0.3	y=2.2x-0.34
$t^1/_2$ (seconds)	3350	2020	1370
k'_1 (s^{-1})	0.0005	0.0003	0.002
k_2 ($s^{-1}M^{-1}$)	15	20	37

Figure 3.20. Gel-shift experiment using radiolabelled RZ551 and an excess of unlabelled RZSUB. **(a)** Gel, with unbound RZ551 (**R**) and RZ551-RZSUB complex (**C**) indicated. **(b)** Rate of formation of ribozyme-substrate complex with 14.8μM RZSUB, with linear best-fit to initial rate shown (dashed lines). **(c)** best-fit line formula, $t^1/_2$, k'_1 and k_2 for initial rate.

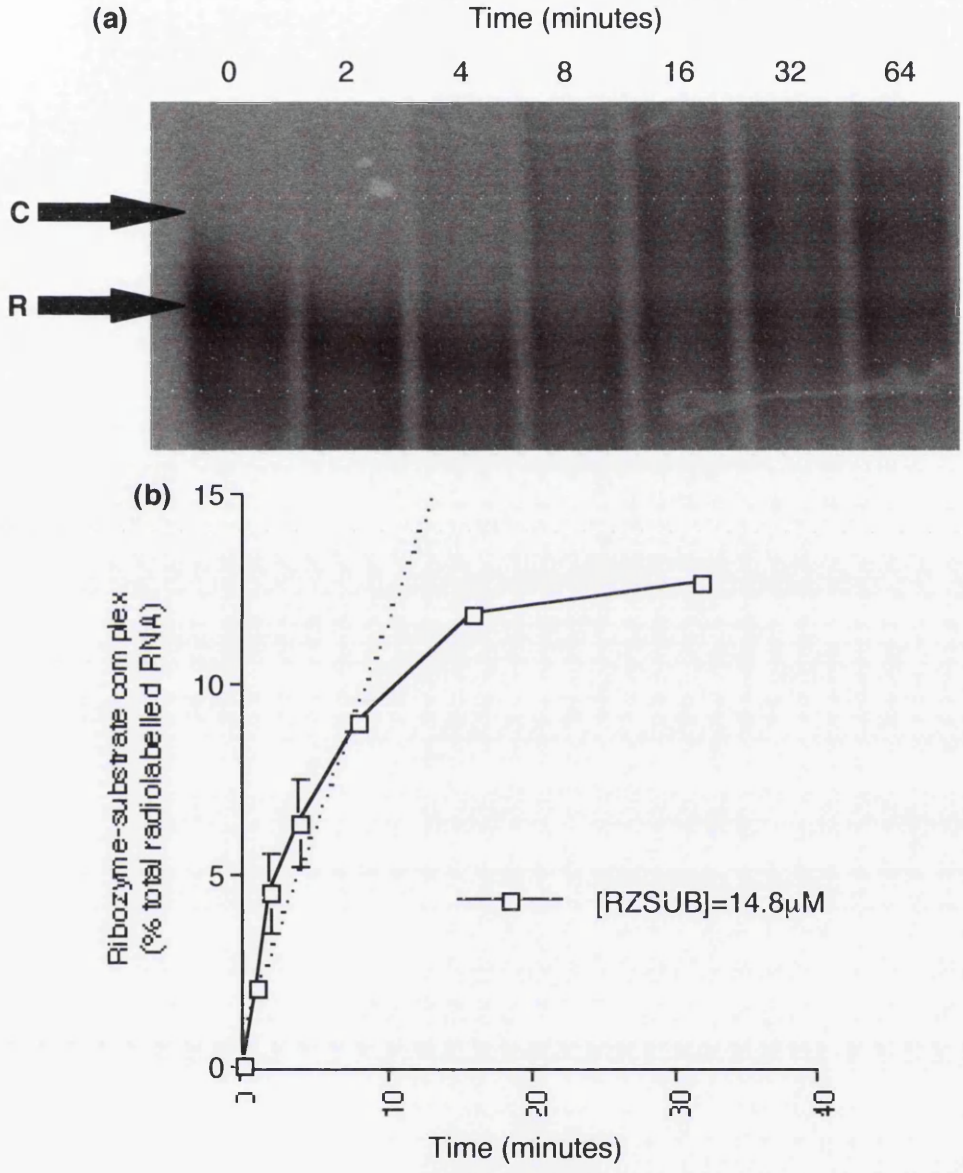

(c)

[RZSUB]	14.8μM
Best-fit line	y=1.1x+1.2
$t^1/_2$ (seconds)	2830
k'_1 (s^{-1})	0.00025
k_2 ($s^{-1}M^{-1}$)	17

Figure 3.21. Gel-shift experiments using radiolabelled RZ556 and an excess of unlabelled RZSUB. **(a)** Gel, with unbound RZ556 (**R**) and RZ556-RZSUB complex (**C**) indicated. **(b)** Rate of formation of ribozyme-substrate complex with 13.2μM or 39.6μM RZSUB, with linear best-fit to initial rates shown (dashed lines). **(c)** best-fit line formula, $t^1/_2$, k'_1 and k_2 for initial rates in each set of experiments.

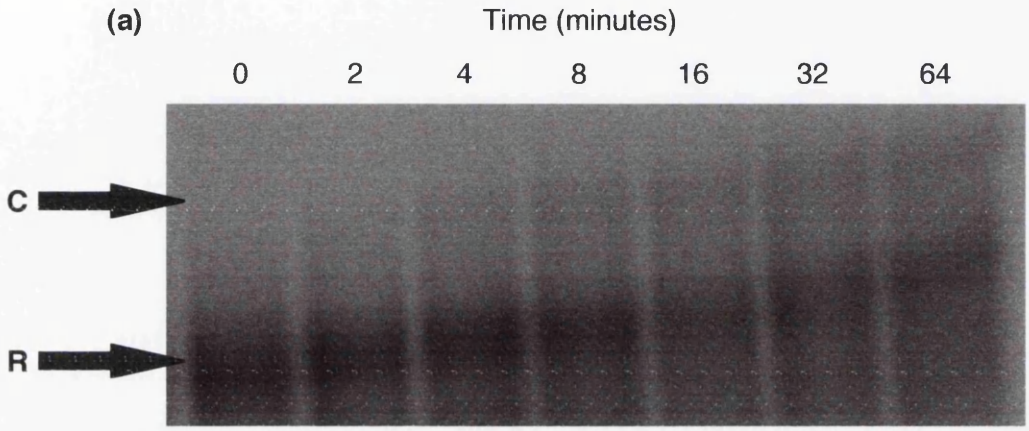

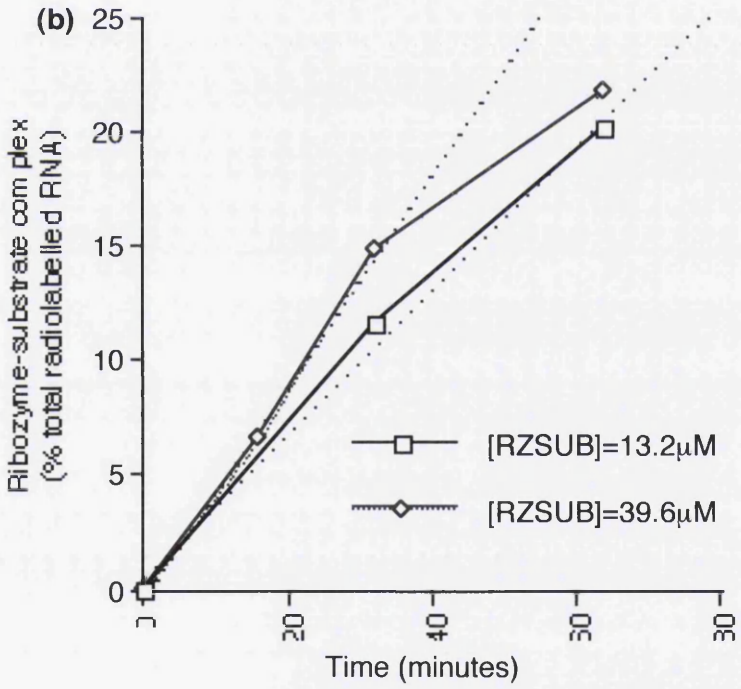

(c)

[RZSUB]	13.2μM	39.6μM
Best-fit line	y=0.3x+0.5	y=0.46x-0.3
$t^1/_2$ (seconds)	9550	6480
k'_1 (s^{-1})	0.000073	0.00011
k_2 ($s^{-1}M^{-1}$)	5.5	2.7

Figure 3.22. Gel-shift experiment using radiolabelled RZ572B and an excess of unlabelled 5D RNA. **(a)** Gel, with unbound RZ572B (**R**) and RZ572B-5D RNA complex (**C**) indicated. The boxes indicate the regions in which the signal volume was determined. Note that all the boxes are of the same size. This process was repeated for all other gels (figures 3.23 to 3.27), though only the full gel is shown here. The background was determined in a region of gel away from the sample lanes (not shown). **(b)** Rate of formation of ribozyme-substrate complex with 263.5nM 5D RNA, with linear best-fit to initial rate shown (dashed lines). **(c)** best-fit line formula, $t^1/_2$, k'_1 and k_2 for initial rate.

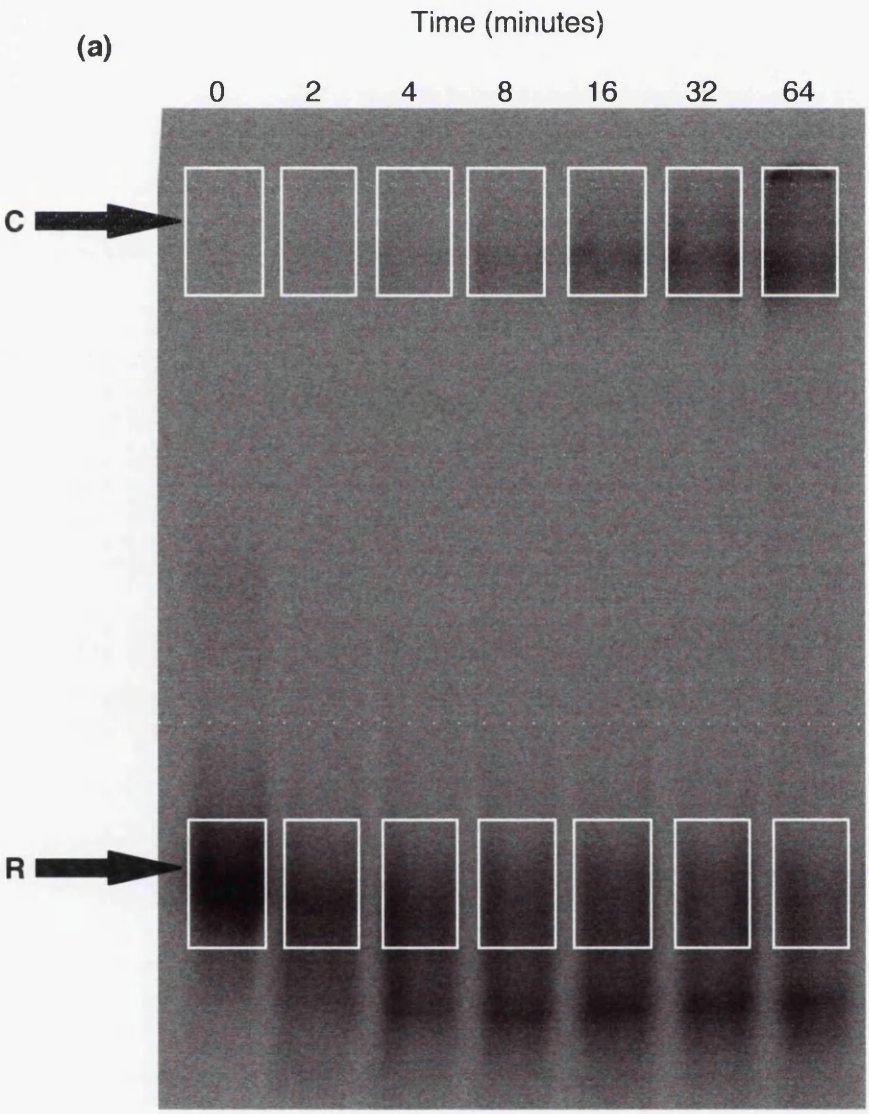

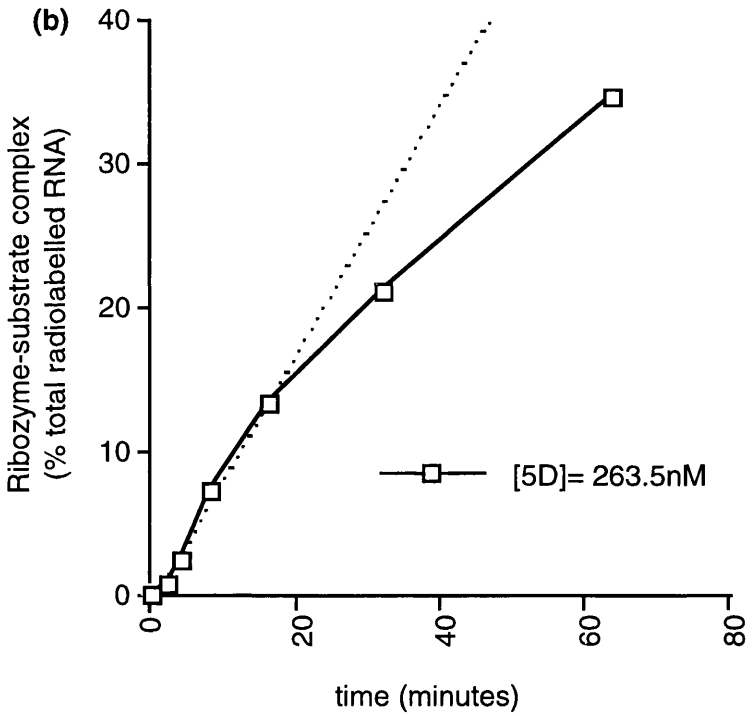

(c)

[5D RNA]	263.5nM
Best-fit line	y=0.87x-0.4
$t^1/_2$ (seconds)	3450
k'_1 (s^{-1})	0.0002
k_2 ($s^{-1}M^{-1}$)	760

Figure 3.23. Gel-shift experiments using radiolabelled RZ534 and an excess of unlabelled 5D RNA. **(a)** Gel, with unbound RZ534 (**R**) and RZ534-5D RNA complex (**C**) indicated. **(b)** Rate of formation of ribozyme-substrate complex with 125nM or 375nM 5D RNA, with linear best-fit to initial rates shown (dashed lines). **(c)** best-fit line formula, $t^1/_2$, k'_1 and k_2 for initial rates in each set of experiments.

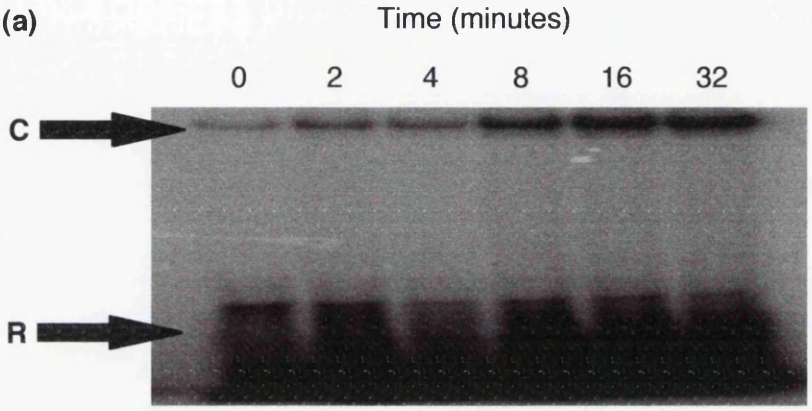

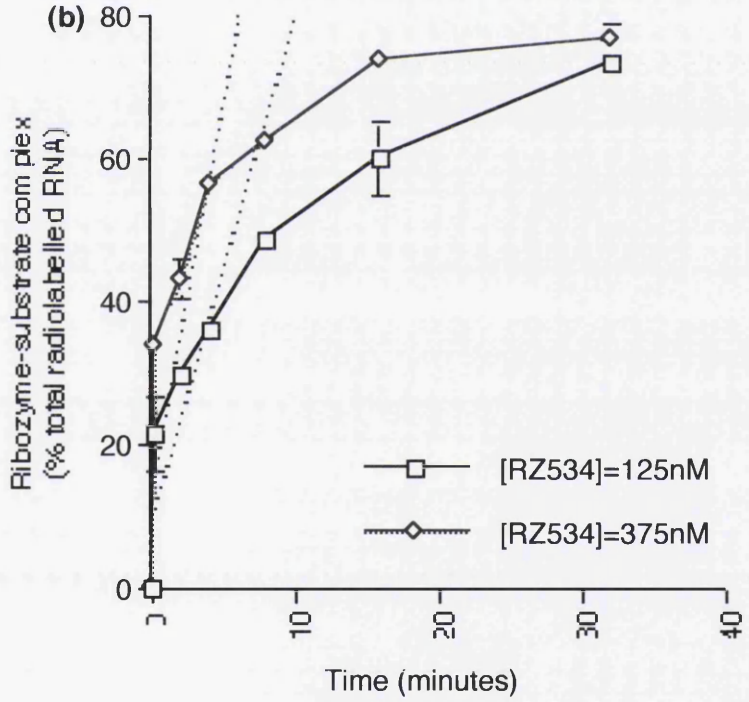

(c)

[5D RNA]	125nM	375nM
Best-fit line	y=7. x+10.6	y=10.9x+16
$t^1/_2$ (seconds)	430	280
k'_1 (s^{-1})	0.0016	0.0027
k_2 ($s^{-1}M^{-1}$)	13000	6700

Figure 3.24. Gel-shift experiments using radiolabelled RZ551 and an excess of unlabelled 5D RNA. **(a)** Gel, with unbound RZ551 (**R**) and RZ551-5D RNA complex (**C**) indicated. **(b)** Rate of formation of ribozyme-substrate complex with 125nM or 375nM 5D RNA, with linear best-fit to initial rates shown (dashed lines). **(c)** best-fit line formula, $t^1/_2$, k'_1 and k_2 for initial rates in each set of experiments.

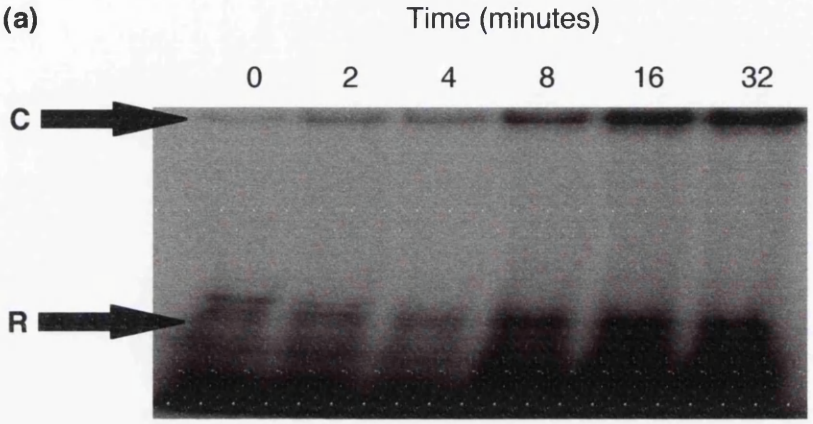

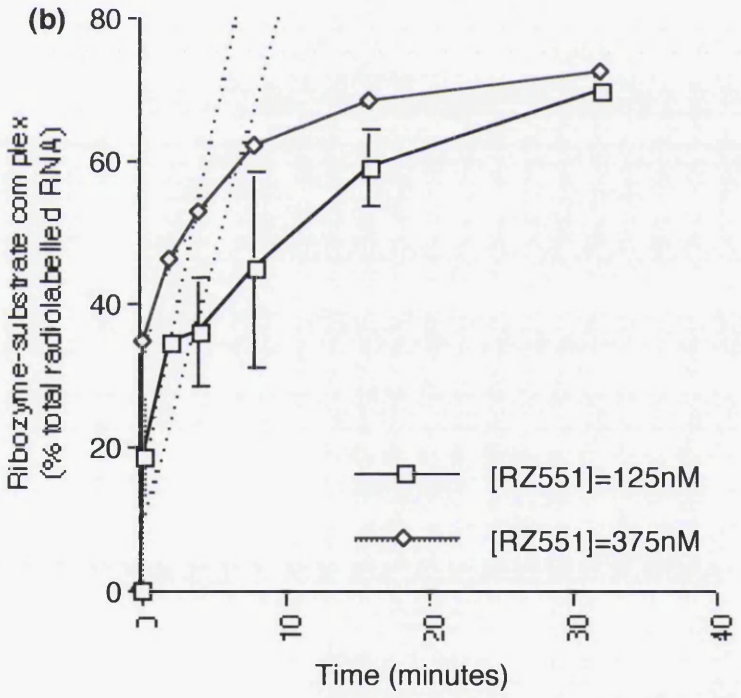

(c)

[5D RNA]	125nM	375nM
Best-fit line	y=7.6x+10.3	y=10x+17.5
$t^1/_2$ (seconds)	400	300
k'_1 (s^{-1})	0.0018	0.0023
k_2 ($s^{-1}M^{-1}$)	14000	6100

Figure 3.25. Gel-shift experiments using radiolabelled RZ556 and an excess of unlabelled 5D RNA. **(a)** Gel, with unbound RZ556 (**R**) and RZ556-5D RNA complex (**C**) indicated. **(b)** Rate of formation of ribozyme-substrate complex with 125nM or 375nM 5D RNA, with linear best-fit to initial rates shown (dashed lines). **(c)** best-fit line formula, $t^1/_2$, k'_1 and k_2 for initial rates in each set of experiments.

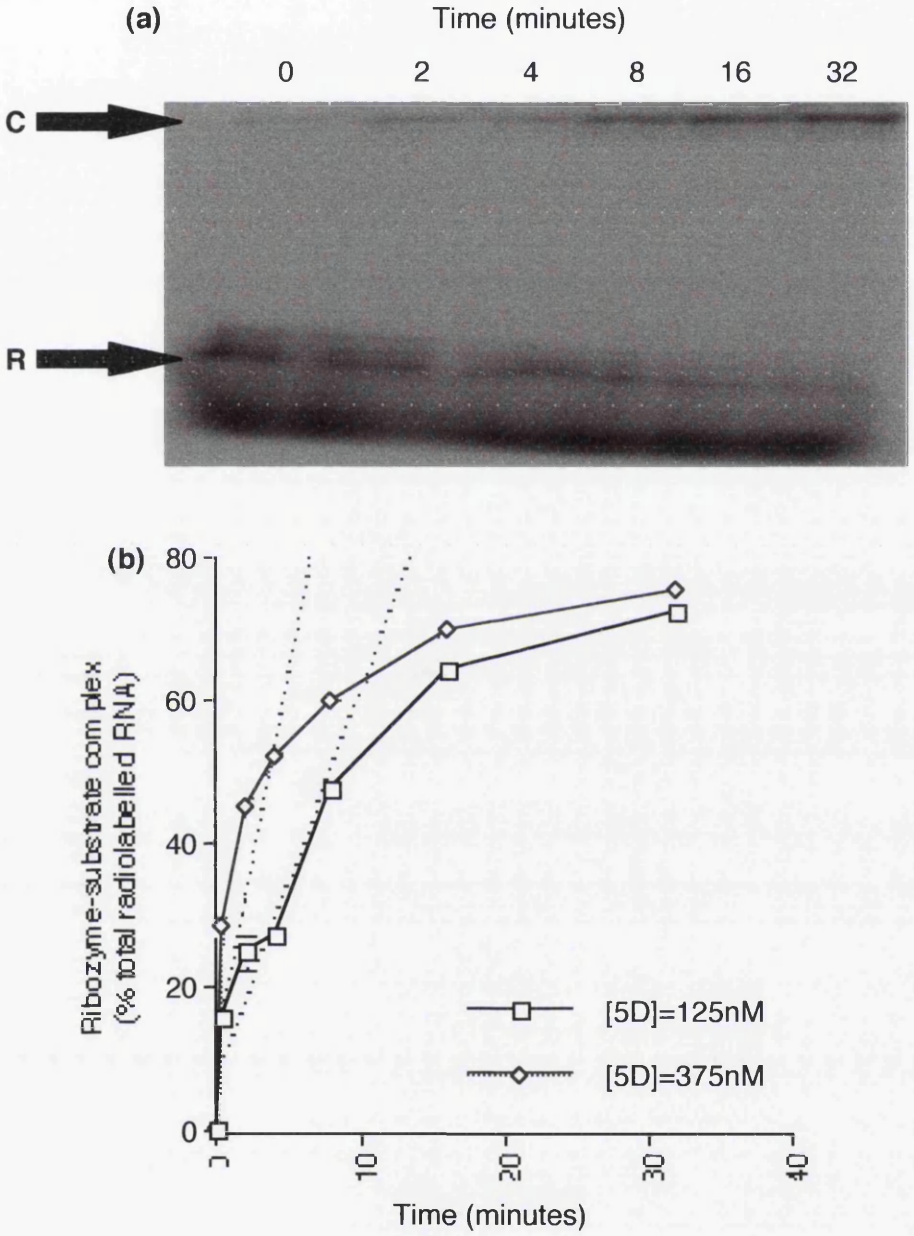

(c)

[5D RNA]	125nM	375nM
Best-fit line	y=5.4x+8.2	y=10.5x+14.5
$t^1/_2$ (seconds)	555	290
k'_1 (s^{-1})	0.00125	0.0024
k_2 ($s^{-1}M^{-1}$)	10000	6500

Figure 3.26. Gel-shift experiment using radiolabelled RZ568 and an excess of unlabelled 5D RNA. **(a)** Gel, with unbound RZ568 (**R**) and RZ568-5D RNA complex (**C**) indicated. **(b)** Rate of formation of ribozyme-substrate complex with 156nM 5D RNA, with linear best-fit to initial rate shown (dashed lines). **(c)** best-fit line formula, $t^1/_2$, k'_1 and k_2 for initial rate.

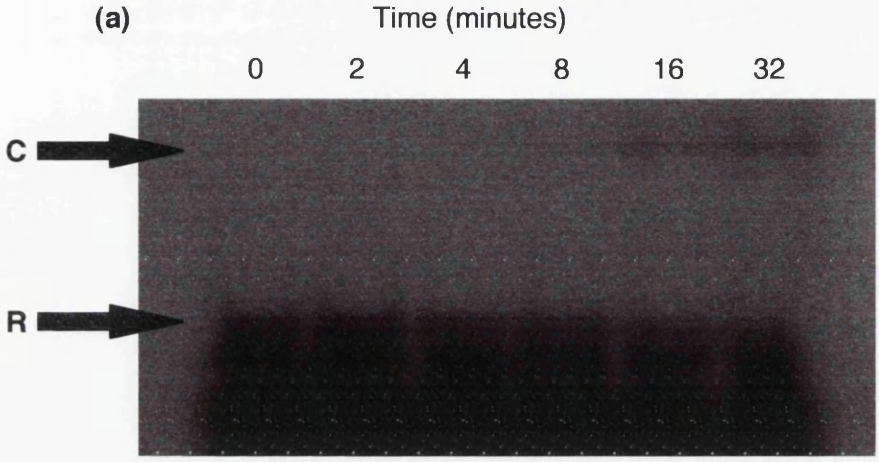

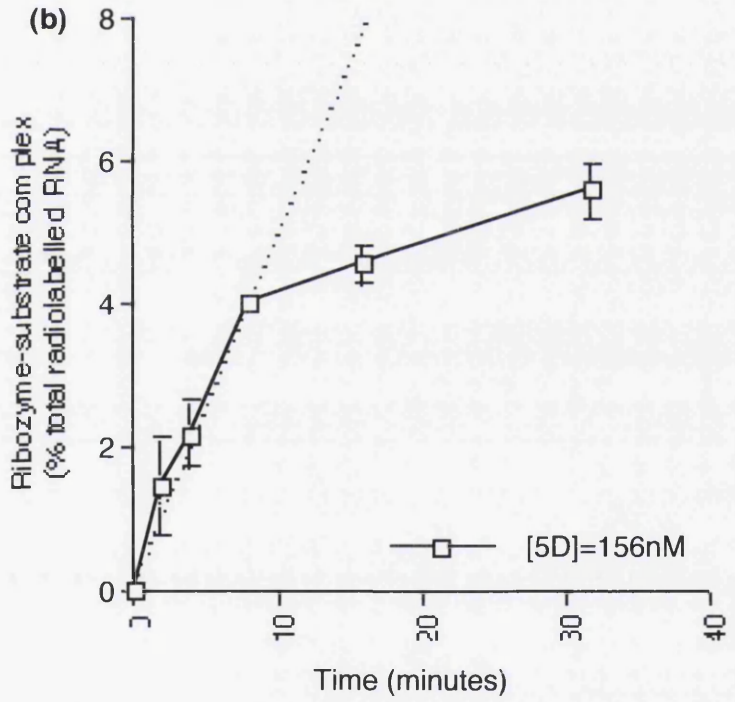

(c)

[5D RNA]	156nM
Best-fit line	y=0.5x+0.2
$t^1/_2$ (seconds)	6200
k'_1 (s^{-1})	0.0001
k_2 ($s^{-1}M^{-1}$)	720

Figure 3.27. Gel-shift experiment using radiolabelled RZ572 and an excess of unlabelled 5D RNA. **(a)** Gel, with unbound RZ572 (**R**) and RZ572-5D RNA complex (**C**) indicated. **(b)** Rate of formation of ribozyme-substrate complex with 312nM 5D RNA, with linear best-fit to initial rate shown (dashed lines). **(c)** best-fit line formula, $t^1/_2$, k'_1 and k_2 for initial rate.

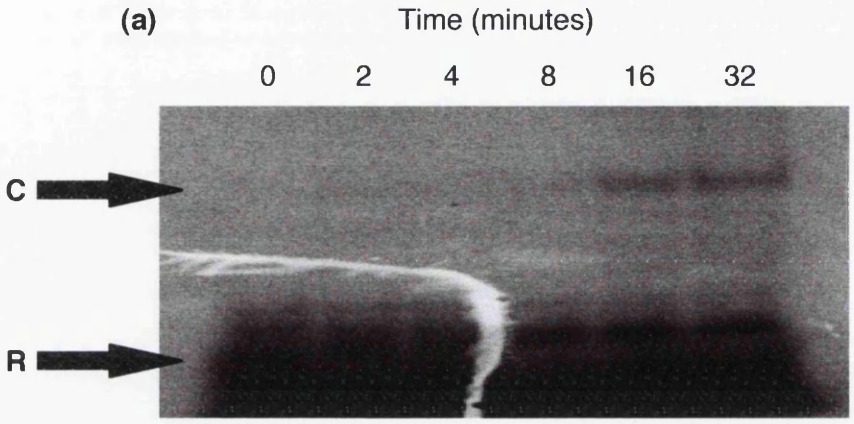

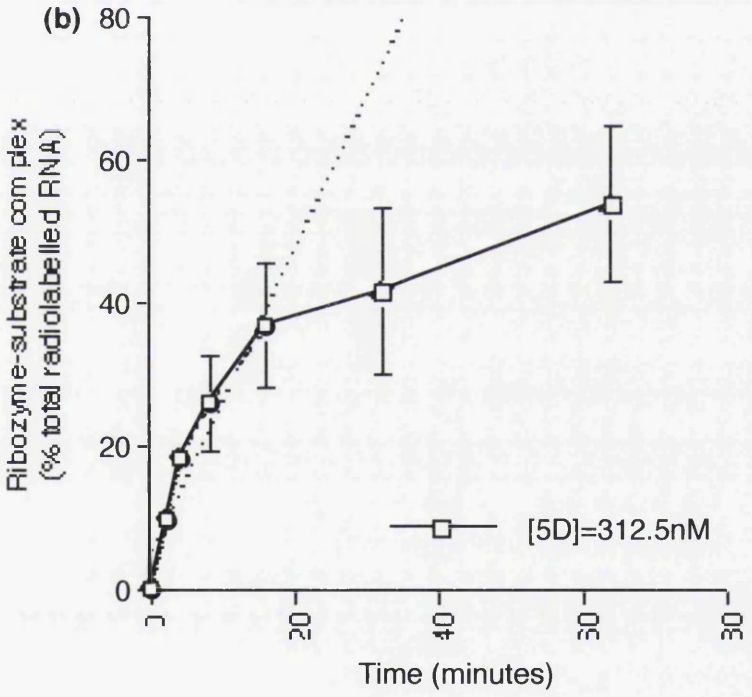

(c)

[5D RNA]	312.5nM
Best-fit line	y=2.15x+5
$t^1/_2$ (seconds)	1400
k'_1 (s^{-1})	0.0005
k_2 ($s^{-1}M^{-1}$)	1600

3.1.3c Discussion

Before considering the data obtained from this set of experiments it is important to discuss the accuracy of the results. The determination of the location of the bands was very difficult, as a result of low band intensity in the set of experiments using RZSUB (figures 3.18 to 3.21) and degradation of the labelled RNA in all the experiments shown (figures 3.18 to 3.27). The location of the unbound ribozyme was taken to be level with the most intense band in the zero time-point lane. However, this was complicated in many cases by the gel 'smiling'. In figure 3.18 it can be seen that in cases of gels 'smiling' an estimate of the position of the unbound ribozyme had to be made, taking into account the curvature of the gel. In the experiments using 5D RNA as the unlabelled substrate degradation of the labelled ribozyme was a problem, as can be seen from the smearing at the bottom of figures 3.22 to 3.28. In these cases the top band in this region was taken as being the complete unbound ribozyme (figure 3.22). In the experiments using RZSUB, the signal intensity of the ribozyme-substrate complex was very low, with the complex only being seen in the later timepoints. Therefore the positions of the complex in earlier timepoints had to be estimated by placing the quantification box at the same height above the unbound ribozyme band in all lanes. It must be stressed though that location of the bands was easier than may be first imagined from seeing the figures presented here. This is because a computer monitor has better contrast than the output of an inkjet printer. Even so, the accuracy of these gel-shift experiments, especially those performed with RZSUB as the unlabelled substrate, is very low.

It was initially hypothesised that ribozymes targeted against regions of the substrate containing a high percentage of single-stranded sequence would bind more readily to their target sites than ribozymes targeted against double-stranded regions of the substrate. Therefore it was predicted that RZ551, RZ556 and RZ568 would bind more readily to both substrates than RZ534 and RZ572, whilst RZ572B, with its long flanking sequences, was predicted to bind most rapidly. These predictions were found to be partially true when RZSUB was used as a substrate. RZ572B was found to have the greatest rate of association (k_2=24±9$s^{-1}M^{-1}$), with RZ551 having the greatest rate of association of the small ribozymes (k_2=17$s^{-1}M^{-1}$). There was no significant difference between RZ556 (k_2=4.1±1.4$s^{-1}M^{-1}$) and RZ572 (k_2=3.3$s^{-1}M^{-1}$), whilst no ribozyme-RZSUB complex was detected when RZ534 and RZ568 were used. These results did not correlate with those obtained when 5D RNA was used as the substrate. The greatest rates of association were seen with RZ534 (k_2=[9.8±3.2]X$10^3s^{-1}M^{-1}$), RZ551 (k_2=[10±4]X$10^3s^{-1}M^{-1}$) and RZ556 (k_2=[8.2±1.8]X$10^3s^{-1}M^{-1}$), whilst the remaining ribozymes showed significantly reduced rates of association. However, given the lack of accuracy using this technique, it is impossible to draw any real conclusions from this data. The lack of correlation between the results obtained with the two different substrates, RZSUB and 5D RNA also supports the queries as to the validity of these experiments. The apparent greater affinity of the ribozymes for the larger 5D RNA

compared to the shorter RZSUB RNA contradicts observations made in previous studies which have shown that ribozymes are up to a thousand-fold more active against short substrates than against full-length mRNAs (Campbell *et al.*, 1997). This is assumed to be because of the presence of more inhibitory secondary structure in the larger RNA. The current data shows the converse (table 3.1). It is impossible to say whether this huge discrepancy is entirely due to the inaccuracies of the technique, given that the study by Campbell *et al* (1997) looked at the ribozyme reaction as a whole, rather than just focusing on the ribozyme-substrate hybridization step as this current study does.

Although the primary concern regarding these experiments is the accuracy of the gel retardation technique, it is also important to consider the validity of the MFOLD predictions. It is likely that the secondary structure predictions for both substrates produced by the MFOLD program are incorrect. The algorithm used to produce these predictions only takes into account Watson-Crick and Hoogsteen base-pairing. It does not take into account non-base-pair hydrogen bonding, which can influence RNA tertiary structure, base-stacking in single-stranded regions, or allow for structures such as pseudoknots. Such variations between the structures of RZSUB and 5D RNA could contribute in part for the differences in hybridisation rates, though this would probably only become significant if the gel-shift technique could be refined to increase accuracy. In such circumstances it would be necessary to confirm the structures of RZSUB and 5D RNA by RNase probing. Different RNases have different target specificities; some cleave double-stranded RNA, whilst others cleave single-stranded RNA. Substrate sequence can also affect RNase activity. Knowledge of the different activities of RNases can allow the pattern of cleavage of a given RNA with different RNases to be interpreted to give a structural prediction. However, it is possible that the substrate RNAs used in the current investigation can assume several different structures with similar energies. This hypothesis is supported by the observation that the graphs produced with the data obtained from the gel-shift experiments are non-linear, even though the reactions have been set up to follow pseudo-first order kinetics. This is probably due to there being two phases of hybridisation; an initial rapid phase, followed by a period of slower association. This could arise from the presence of two isomers of either the ribozyme or the substrate RNA, with each isomer having different binding affinity for the complementary RNA. Although the non-linearity of the graphs could also be attributed to inaccuracies in the technique, this is unlikely given that this phenomenon appeared again and again in many different experiments.

Another serious problem encountered in this study was the lack of reproducibility between experiments, resulting in the large errors obtained when experiments were repeated with different concentrations of unlabelled RNA (i.e. RZ556 and RZ572B plus RZSUB and RZ534, RZ551 and RZ556 plus 5D RNA). This is not solely a result of the inaccuracies of the technique as these differences arose when different batches of RNA were used. Although all RNA was prepared in the same way, it is possible that some salt could have

remained in the RNA preparations following the ethanol precipitation step: Monovalent cations have been shown to influence nucleic acid hybridisation and structure (Wang *et al.*, 1995). This problem was reduced as the study progressed as an increased number of 70% ethanol washes were used to clean the RNA pellet after precipitation. Dialysis would offer a solution to this problem. However, this would require the RNA to be dissolved in a large volume, making the RNA too dilute to be used in the gel-shift experiments. In some instances no ribozyme-substrate complex was seen to form. It must be stressed though that in the cases where no rate of association was determined (RZ534 and RZ568, both with RZSUB), the experiment was repeated many times but no complex was seen to form.

In light of these difficulties arising from using gel-shift analysis, it was decided to develop an ELISA-based protocol for analysing ribozyme-substrate binding.

3.1.4 RNA-RNA ELISA

3.1.4a Introduction

ELISA (enzyme-linked immunosorbant assay) is a well-established technique for detecting an interaction between two biological molecules. One molecule is fixed to a matrix (for example the bottom of a well on a microtitre plate), whilst the second molecule is added in solution into the well. After incubating for a period of time, any of the second molecule which has not bound to the first molecule is washed from the well. An antibody to the second molecule is used to detect if any of the second molecule has become bound to the first. This antibody is conjugated to an enzyme, such as horseradish peroxidase. Enzymes are chosen which have chromogenic substrates, thus producing a colour change which is which can be measured by spectrophotometry (figure 3.28). The intensity of the colour change is proportional to the amount of enzyme present.

Microtitre plates coated with streptavidin are commonly used in ELISAs. Streptavidin binds biotin very strongly. Biotin can be easily incorporated into proteins and nucleic acids by a number of methods, enabling these macromolecules to be firmly anchored in streptavidin-coated microtitre plates. It was decided to biotinylate the positive control substrate, Y98. The positive control ribozyme, RZ60, was to be labelled with digoxigenin. Digoxigenin is a commonly used ligand in ELISAs, and there is a wide range of antibody-enzyme conjugates targeted to digoxigenin available. It was decided to endlabel both the ribozyme and substrate. Internal labelling with biotin or digoxigenin could interfere with ribozyme-substrate binding. Microtitre plates, buffers and detection reagents were taken from a commercial PCR product detection ELISA kit (Boehringer-Mannheim).

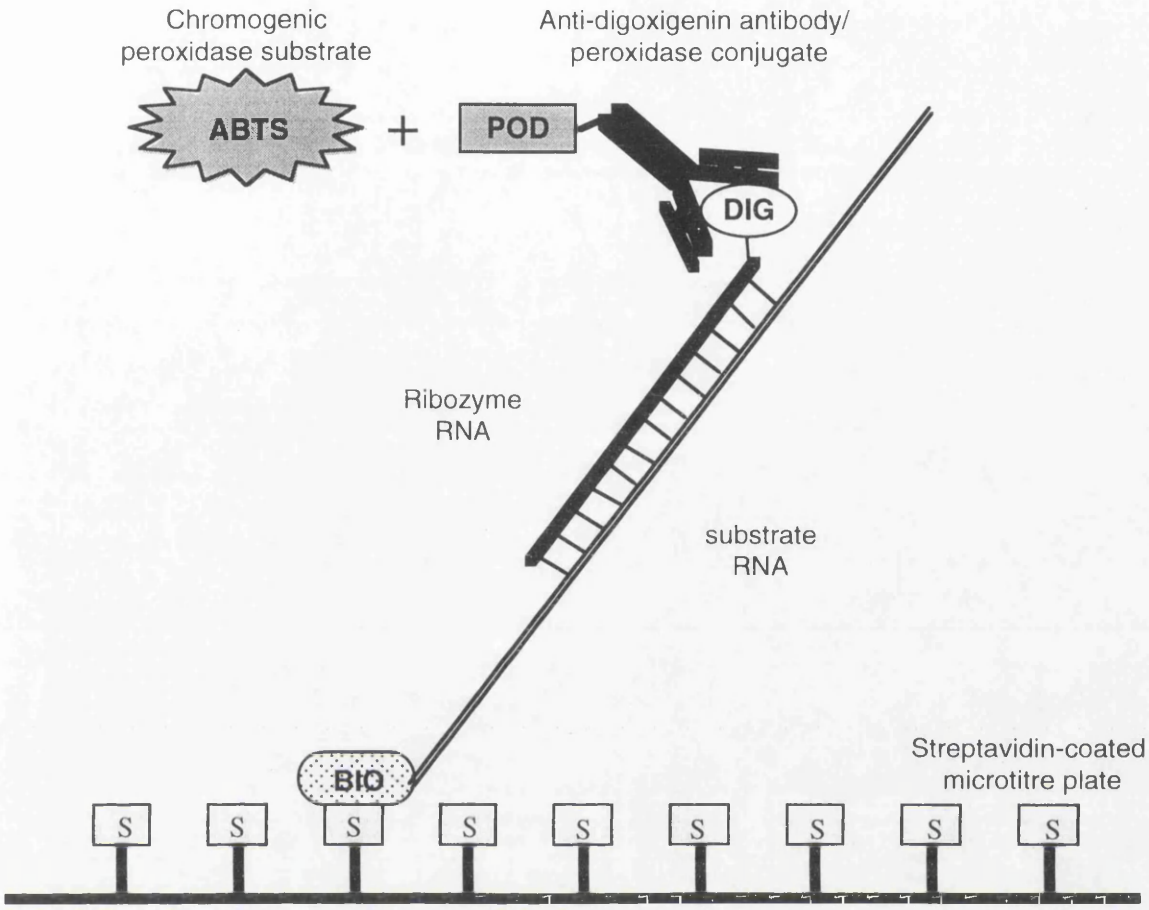

Figure 3.28. The principle behind the ribozyme-substrate hybridisation enzyme-linked immunosorbant assay (ELISA). Substrate RNA is 3'-endlabelled with biotinylated nucleotide derivatives (BIO). The biotinylated substrate RNA is anchored in streptavidin-coated microtitre well plates by the strong interaction between biotin and streptavidin (S). Ribozymes 3'-endlabelled with digoxigenin-labelled nucleotide derivatives (DIG) hybridise with the anchored substrate in microtitre plate wells. Unbound ribozyme is washed away, leaving ribozyme-substrate complex bound to the microtitre plate well. The ribozyme-substrate complex is detected with an anti-digoxigenin antibody/ peroxidase enzyme conjugate. Any unbound antibody/ enzyme conjugate is removed by washing. The remaining antibody/ enzyme conjugate is bound to the ribozyme-substrate complex, and can be detected using a chromogenic peroxidase substrate, such as ABTS. The change in colour of ABTS, from colourless to green, produced by peroxidase activity can be quantified by spectrophotometry, and is proportional to the amount of ribozyme-substrate complex.

3.1.4b RNA labelling

It was initially decided to endlabel the substrate RNA by using RNA ligase to ligate a biotinylated oligonucleotide, BIO-1, to the 3'-end of the substrate RNA (figure 3.29). RNA ligase requires a 5'-phosphate group in one substrate and a 3'-hydroxyl group in the other substrate to function (Uhlenbeck & Gumport, 1982). If a single-stranded nucleic acid has both a 5'-phosphate and a 3'-hydroxyl group it will be circularised by RNA ligase. Therefore it was necessary to use polynucleotide kinase to phosphorylate the 5'-end of the BIO-1 oligonucleotide and to use alkaline phosphatase to remove the 5'-phosphate from the substrate RNA. The ligation reactions were performed using 1X T4 RNA ligase buffer (50mM Tris-HCl, 10mM $MgCl_2$, 10mM DTT, 1mM ATP, pH 7.8). 10nM internally radiolabelled, alkaline phosphatase treated Y98 was incubated with varying concentrations of BIO-1 oligonucleotide and RNA ligase purchased from either Boehringer-Mannheim or New England Biolabs at 37°C for 30 minutes (figure 3.30a). Under these conditions no ligation was acheived. The ligation reactions were repeated using New England Biolabs RNA ligase with 10nM Y98 and 1mM BIO-1 with varying concentrations of DMSO, in accordance with recommendations included in the protocol supplied with the enzyme. Even with this modification no ligation was detected (figure 3.30b).

An alternative method of adding modified nucleotides to the 3'-end of single-stranded RNA utilises terminal deoxynucleotidyl transferase (TdT). This enzyme can be used to add homopolymer tails when NTPs or dNTPs are used, or can be used to add a single nucleotide when a ddNTP is used (Roychoudhury *et al.*, 1976). The efficiency of TdT was examined by using it to endlabel radiolabelled RZ572 RNA. The biotinylated or digoxigen-labelled radiolabelled RZ572 RNA was resolved by electrophoresis (figure 3.31). Despite background degradation, it can be seen that TdT can be used to endlabel single-stranded RNA.

Could biotinylated nucleic acid bind to streptavidin-coated microtitre plates? This was investigated by incubating the BIO-1 oligonucleotide , which has the sequence $(dA)_{18}$, overnight at 4°C in 1X ribozyme hybridisation buffer in streptavidin-coated microtitre plates. Following incubation, unbound BIO-1 was removed by rinsing the wells with wash buffer. The oligonucleotide primer CP1 was end-labelled with α^{32}P-dTTP using TdT. This gave CP1 a radiolabelled oligo-dT tail that was complementary to the BIO-1 oligonucleotide bound to the streptavidin wells. The end-labelled CP1 was added to the BIO-1-streptavidin wells in 1X ribozyme hybridisation buffer and incubated at 37°C for 3 hours. Unbound CP1 was removed at the end of the incubation and quantified by liquid scintillation counting (figure 3.32). These results show that the BIO-1 oligonucleotide was bound to the streptavidin wells, and was able to capture a complementary single-stranded nucleic acid.

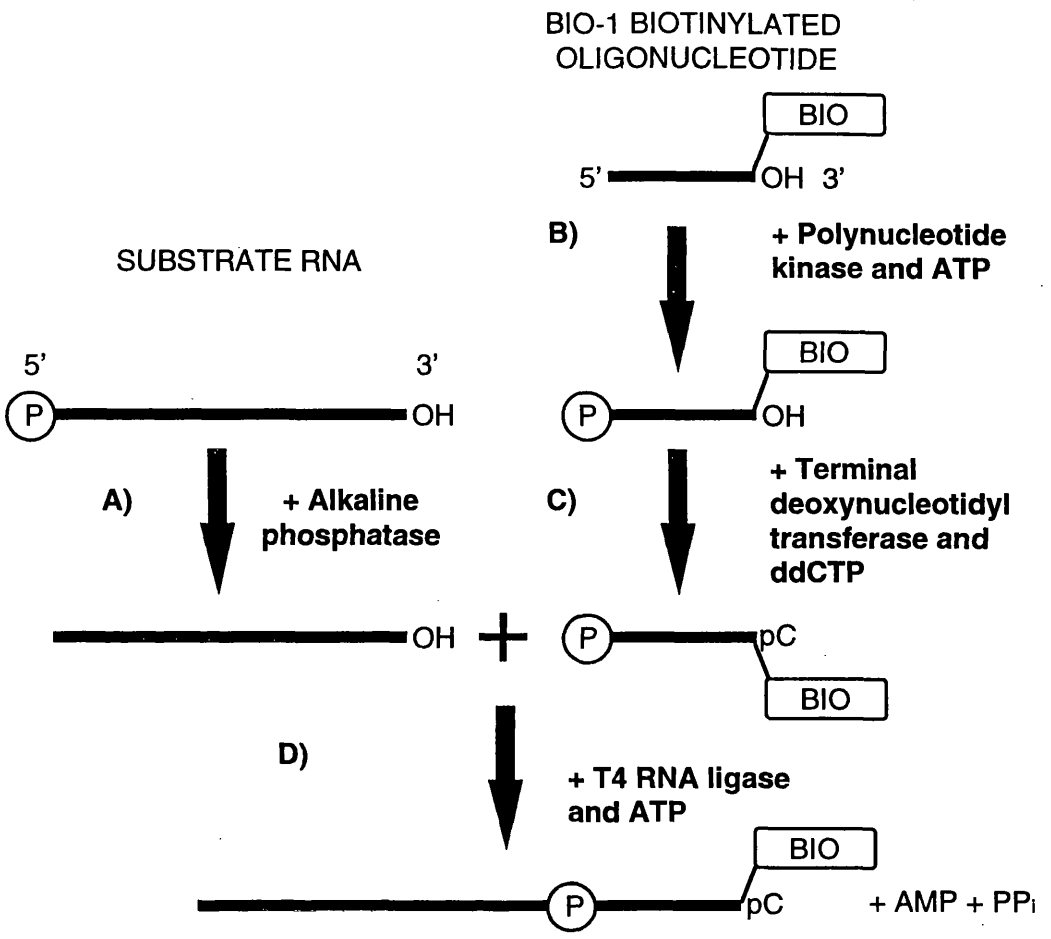

Figure 3.29. Reaction scheme for ligation of substrate RNA and BIO-1 biotinylated oligonucleotide using T4 RNA ligase. T4 RNA ligase catalyses the ATP-dependent joining of 5'-phosphoryl-terminated nucleic acid donor to a 3'-hydroxyl-terminated nucleic acid acceptor. In this case the BIO-1 oligonucleotide is the donor and the substrate RNA is the acceptor. Before ligation both nucleic acids need modifying. The substrate RNA must have its 5'-phosphate RNA removed with alkaline phosphatase to prevent T4 RNA ligase circularising it, by ligating the 5'-phosphate and 3'-hydroxyl group from the same molecule, and to prevent head-to-tail multimerization **(A)**. The synthetic oligonucleotide BIO-1 requires the addition of a 5'-phosphate group. This is done using polynucleotide kinase and ATP **(B)**. The 3'-hydroxyl group of the BIO-1 oligonucleotide must be blocked, again to prevent circularisation or multimerization. This is done by adding ddCTP, which itself lacks a 3'-hydroxyl group, to the 3'-end of BIO-1 with terminal deoxynucleotidyl transferase **(C)**. The modified substrates can then be joined by T4 RNA ligase **(D)**. This reaction requires ATP, and generates, in addition to the ligated product, AMP and pyrophosphate (PP_i).

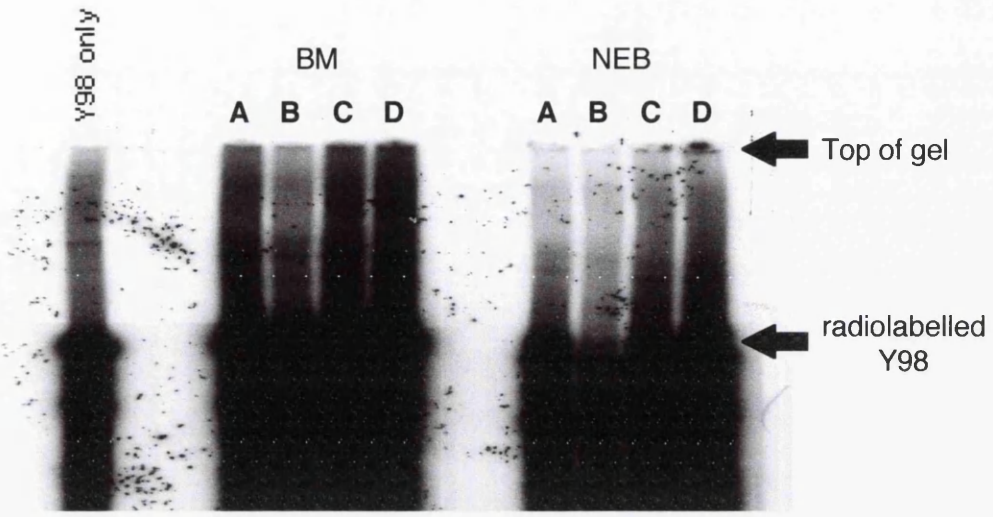

Figure 3.30a. Testing efficacy of RNA ligase purchased from Boehringer-Mannheim (BM) and New England Biolabs (NEB). Y98, internally labelled with α^{32}P-UTP, was incubated with varying concentrations of oligonucleotide BIO-1 (A, 10μM, B, 1μM, C, 100nM, D, 10nM) at 37°C overnight. Samples were separated on a 10% denaturing polyacrylamide gel in 1X TBE buffer. No increase in size of the radiolabelled band is visible following incubation of Y98 with RNA ligase and BIO-1. Both Y98 and BIO-1 were treated as described in figure 3.29 prior to the ligation reaction.

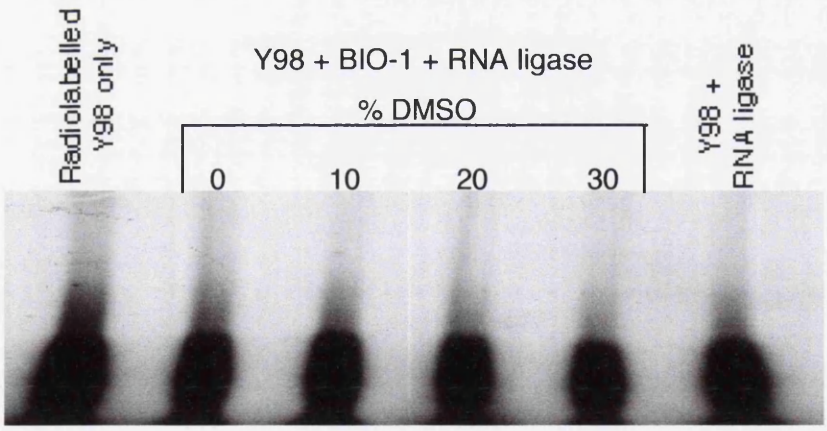

Figure 3.30b. Investigating the effects of dimethylsulphoxide (DMSO) on RNA ligase activity. DMSO has been widely reported to enhance RNA ligase activity. Varying dilutions of DMSO were used in ligation reactions with BIO-1 oligonucleotide and internally radiolabelled Y98. Reactions were incubated overnight at 37°C, with the products being separated on a 10% denaturing polyacrylamide gel in 1X TBE buffer. No increase in the size of the radiolabelled band is visible following incubation of Y98 with BIO-1 and RNA ligase.

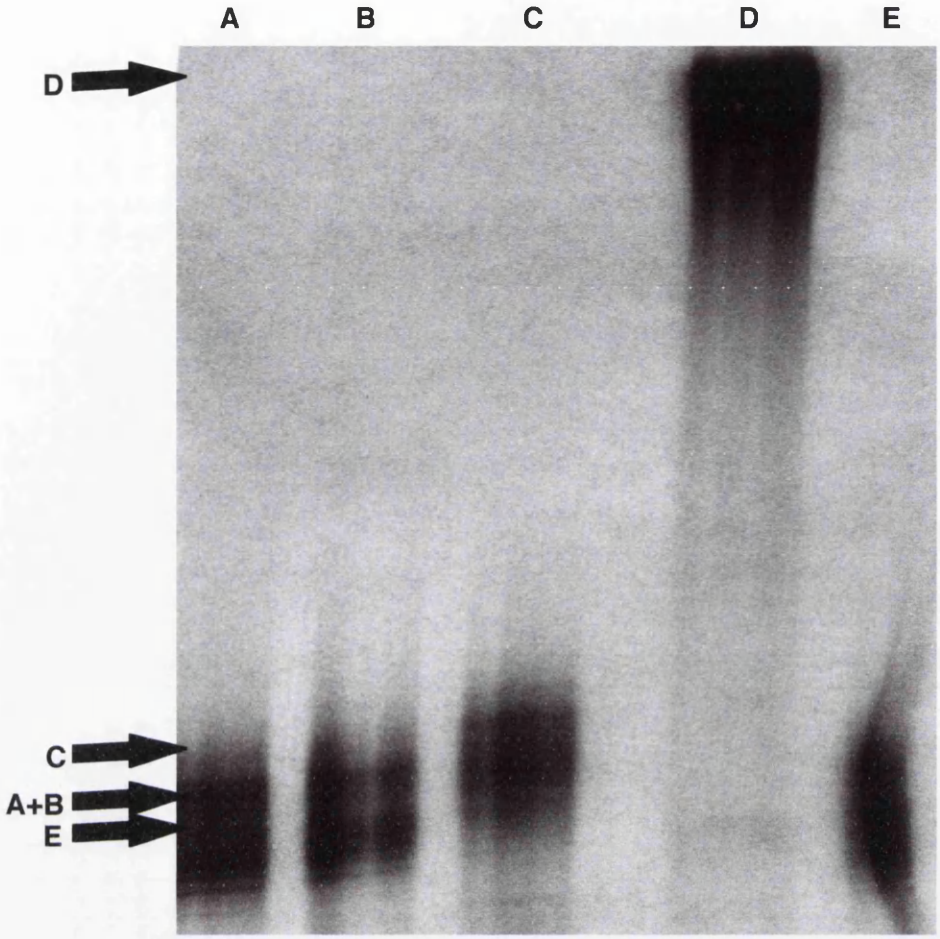

Figure 3.31. Radiolabelled RZ572 RNA was incubated with terminal deoxynucleotidyl transferase (TdT) at 37°C for 1 hour with a variety of modified nucleotides. Reactions were terminated in formamide gel-loading buffer, and samples were run on 7M urea, 12% polyacrylamide gel in 1X TBE buffer. All reactions contained 0.4 pmoles radiolabelled RZ572 plus the following additions; (**A**) 10 pmoles biotin-11-ddUTP, (**B**) 10 pmoles digoxigenin-16-ddUTP, (**C**) 50 pmoles digoxigenin-16-UTP, (**D**) 50 pmoles digoxigenin-16-UTP + 450 pmoles dCTP, (**E**) no additions. Despite the curving of the gel it is possible to see that the addition of the modified nucleotides by TdT has resulted in an increase in the size of RZ572 RNA, as indicated by the arrows. This is particularly apparent in lane C, where the use of digoxigenin-16-UTP has permitted the addition of multiple modified nucleotides to RZ572, and in lane D, where inclusion of dCTP in nine-fold excess over digoxigenin-16-UTP has resulted in a large increase in the size of RZ572. The ability to include multiple digoxigenin moieties at the 3'-end of the ribozyme RNA is very important, as this could allow an increase in the signal-to-noise ratio. It has been reported previously that inclusion of a non-labelled dNTP, as in lane D, can further increase the signal-to-noise ratio by spreading out the digoxigenin-modified residues in the 3'-tail, thus reducing steric hindrance between antibody/ enzyme conjugates attempting to bind neighbouring digoxigenin moieties.

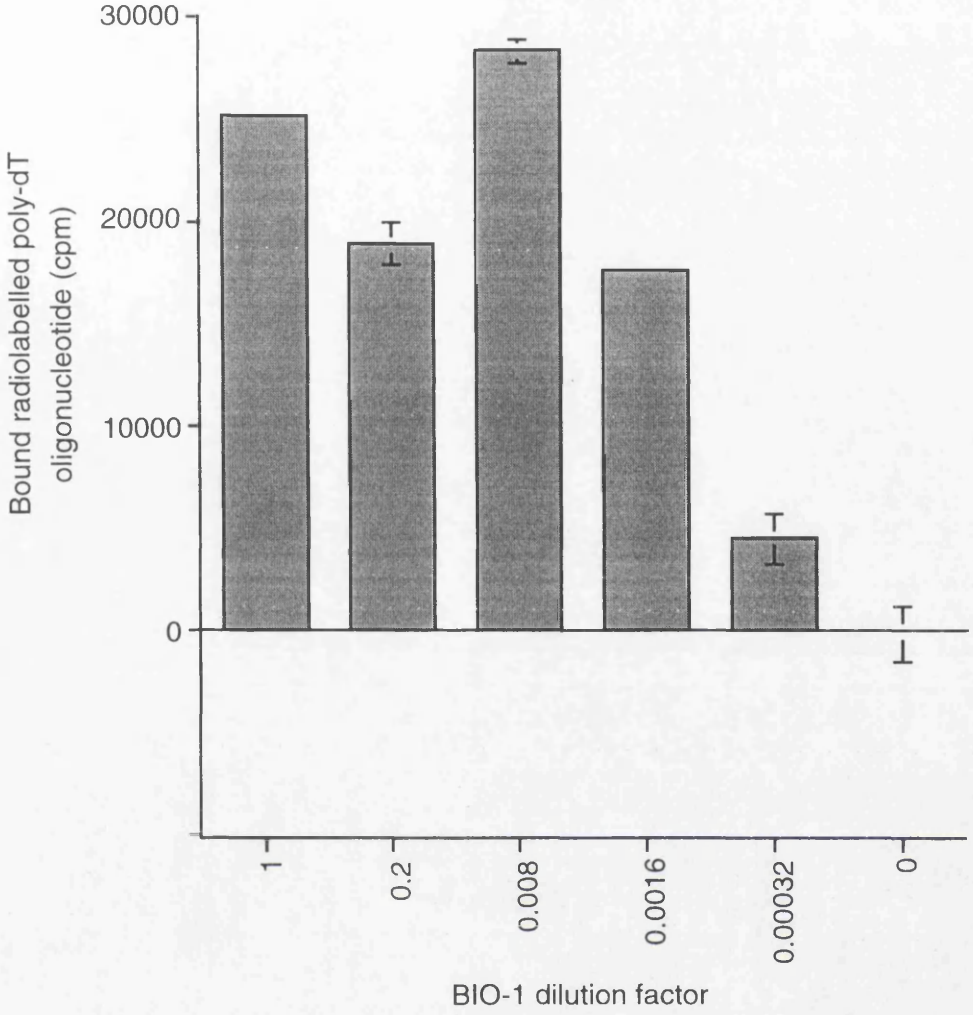

Figure 3.32. Binding of radiolabelled poly-dT oligonucleotide to BIO-1 biotinylated oligonucleotide in streptavidin-coated microtitre wells. Varying dilutions of BIO-1 oligonucleotide, stock concentration 1μM, were fixed in streptavidin-coated microtitre wells by incubation in 1X ribozyme hybridisation buffer at 4°C overnight. Unbound BIO-1 was removed by rinsing the wells with wash buffer. Oligonucleotide CP1 was 3'-endlabelled using TdT and α^{32}P-dTTP, to give the oligonucleotide a 3'-poly-dT tail. Equal amounts of the α^{32}P-dTTP-labelled oligonucleotide were added to each well in 1X ribozyme hybridisation buffer, and incubated for 3 hours at 37°C, allowing the oligonucleotide's poly-dT tail to hybridise with BIO-1 (sequence dA_{18}). Following the incubation the wells were rinsed with wash buffer, with the washes being saved, and the radioactivity they contained being quantified by scintillation counting. These counts were subtracted from those obtained from the washes from wells containing no BIO-1 to give an estimate of how much α^{32}P-dTTP-labelled oligonucleotide remained bound in the wells.

3.1.4c Detection of ribozyme-substrate complex

Following confirmation that RNA could be end-labelled using TdT and that biotinylated nucleic acids could bind to streptavidin-coated microtitre plates and be detected by hybridisation with a radiolabelled probe, the next step was to try and detect binding of the positive-control ribozyme, RZ60, and substrate, Y98, in the ELISA system. The binding of the positive controls RZ60 and Y98 had already been confirmed by gel-shift assay (figure 3.5). Although ELISAs are sensitive to pH and ion concentrations, it was considered to be important to keep conditions as close to a physiological environment as possible. Therefore 1X ribozyme hybridisation buffer was used as in the gel-shift assays. It should be noted that this buffer was Mg^{2+}-free, to prevent substrate cleavage, and the collapse of the ribozyme-substrate complex. A checkerboard was set up using varying dilutions of biotinylated Y98 and digoxigenin-labelled RZ60 (figure 3.33). The results of this initial experiment are shown in figure 3.34.

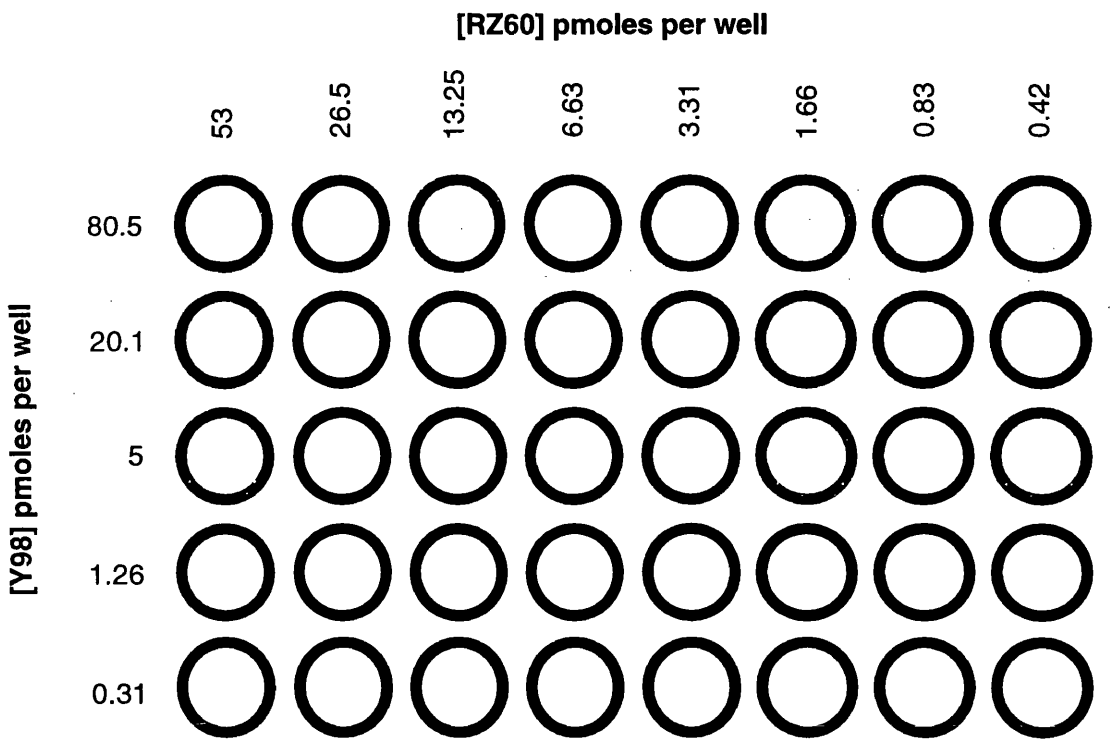

Figure 3.33. Layout of ELISA checkerboard experiment. Biotinylated Y98 (Y98-BIO) positive control substrate was fixed to streptavidin-coated microtitre plate wells in 1X ribozyme hybridisation buffer, incubated overnight at 4°C. Following removal of unbound Y98-BIO by rinsing the wells with wash buffer, varying dilutions of digoxigenin-labelled RZ60 positive control ribozyme were added. The plates were then incubated at 37°C for 3 hours. Results are shown in figure 3.34.

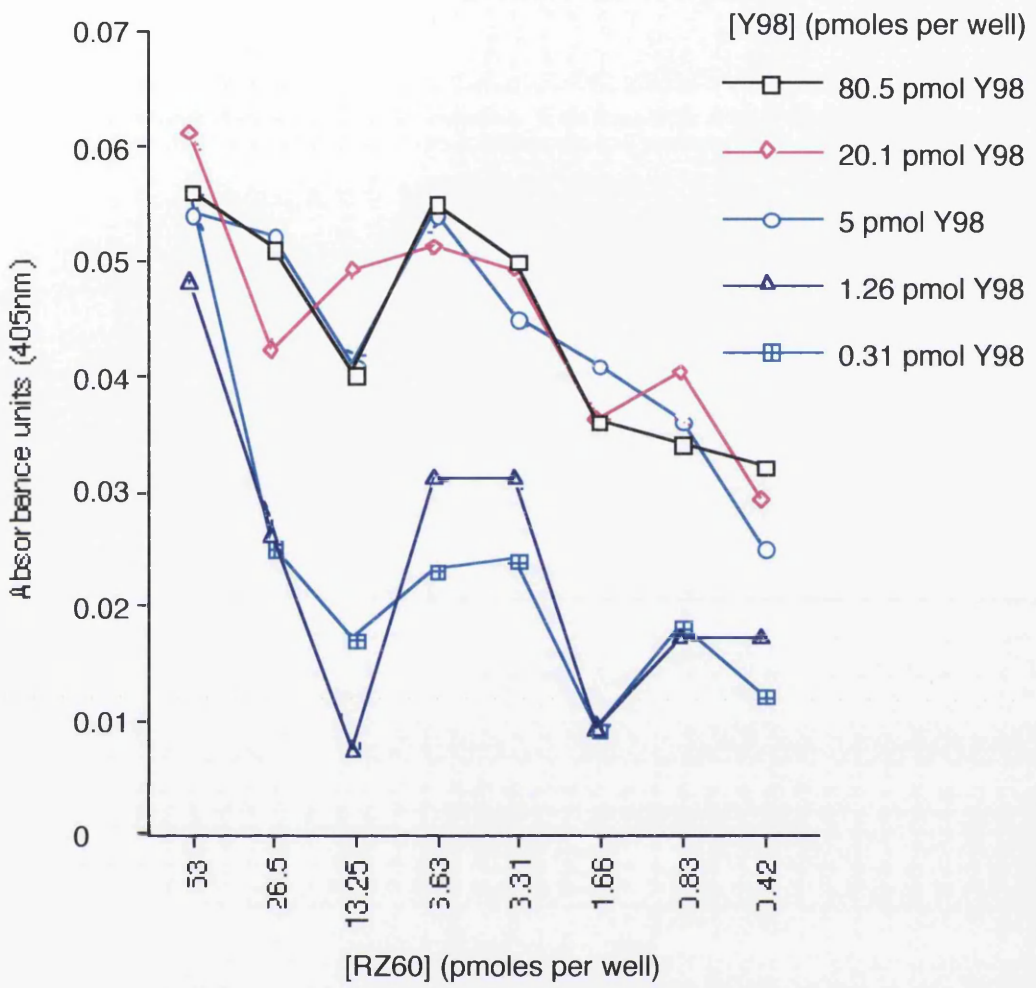

Figure 3.34. Results of ELISA checkerboard experiment. Varying concentrations of Y98 positive control substrate, end-labelled with biotin-11-ddUTP, was fixed to streptavidin-coated microtitre plates in 1X ribozyme hybridisation buffer. Following removal of unbound Y98 by washing, varying concentrations of RZ60, end-labelled with digoxigenin-16-UTP, were added to the wells in the pattern shown in figure 3.34. The microtitre plates were incubated on a rotary shaker at 37°C for 3 hours. Following incubation, unbound RZ60 was removed by washing. The ELISA plates were developed using an anti-digoxigenin antibody/ peroxidase conjugate and ABTS chromogenic substrate. The developed ELISA plates were quantified using a multiwell plate-scanner at 405nM. The absorbance values shown are measured from the background reading. The background was determined by incubating 53pmoles RZ60 in duplicate wells containing no Y98, and then developing as all the other wells.

Although a dose dependent response was seen, the readings taken by the microtitre plate scanner are all below 0.1 absorbance units (at 405nm). This is much too low for accurate information regarding intermolecular interactions to be obtained. Why should these readings be so low? When the positive control digoxigenin-labelled PCR product and biotinylated capture oligonucleotide supplied with the commercial kit were used, readings greater than 2 absorbance units (at 405nm) were routinely obtained. Could the labelled RNA be degrading? Samples of both Y98 and RZ60, endlabelled using TdT, were run on a 1% agarose gel (figure 3.35). No degradation was observed.

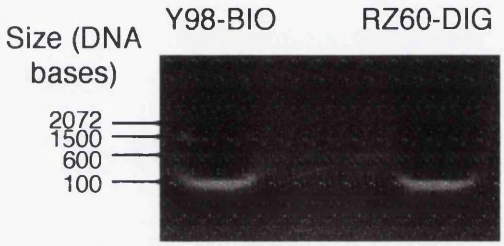

Figure 3.35. Y98 positive control substrate RNA, end-labelled with biotin-16-ddUTP (Y98-BIO), and RZ60 positive control ribozyme, end-labelled with digoxigenin-11-UTP (RZ60-DIG), run on a 1% agarose gel in 1X TBE. Both RNAs were end-labelled using TdT. No degradation is apparent.

Is it possible that the ribozyme RZ60 is unable to bind its substrate Y98 when Y98 is anchored to the streptavidin-coated wells? This could be due to steric hindrance. This hypothesis was tested by preincubating RZ60 and Y98 together at 37°C for 4 hours, and then fixing the resulting complex to streptavidin-coated microtitre wells (figure 3.36). This also did not increase the signal. An alternative possibility was that the streptavidin-coated wells were not saturated with biotinylated substrate RNA. In the initial experiment, a maximum of 80.1 pmoles of biotinylated Y98 was added per well. The manufacturers claim that each well can bind a maximum of 20 pmoles of biotin. It is possible that not all the available biotin is binding streptavidin. However, increasing the amount of biotinylated Y98 up to 800 pmoles per well did not increase the signal (figure 3.36).

Therefore it became apparent that the detection system was insufficiently sensitive enough to detect the small number of digoxigenin residues in the ribozyme-substrate complex. The positive control PCR product supplied with the kit was labelled throughout its length with digoxigenin. As described earlier, this was not possible with the ribozyme RNAs. It was decided to try using a secondary antibody to increase the ELISAs sensitivity.

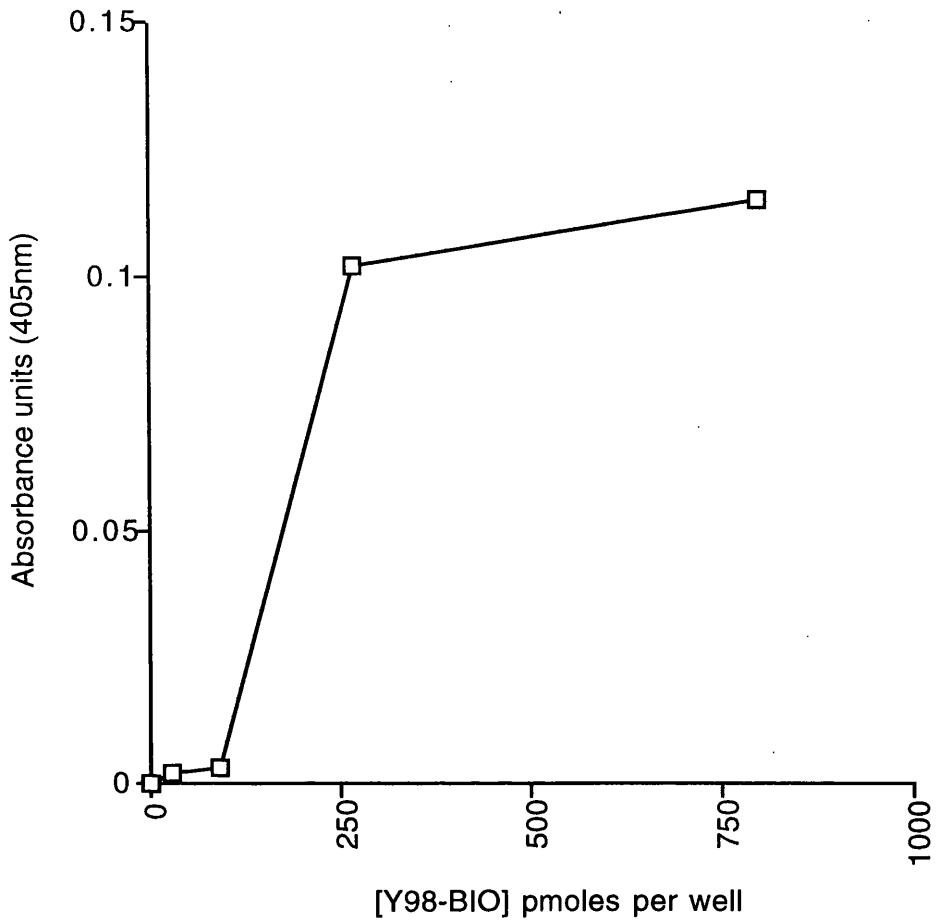

Figure 3.36. Increased [Y98-BIO] in ELISA. Even increasing [Y98-BIO] to 800 pmoles per well does not significantly increase the final signal. Equimolar amounts of Y98-BIO and RZ60-DIG were prehybridised overnight at 37°C, prior to addition to the streptavidin-coated microtitre plates. The ribozyme-substrate complex was allowed to bind to the plates for 3 hours at 37°C. After washing to remove unbound complex the ELISA was developed as previously described.

3.1.4d RNA-RNA ELISA using secondary antibodies

The sensitivity of any antibody-based detection system can be enhanced by utilising a secondary antibody chosen to bind to the primary antibody which itself binds directly to the ligand of interest. The digoxigenin detection system provided with the PCR product detection ELISA kit utilised anti-digoxigenin F_{ab} fragments generated in sheep conjugated to horseradish peroxidase. Two secondary antibodies were tried: an anti-sheep antibody-peroxidase conjugate (developed in donkey) and a peroxidase-anti-peroxidase (P-AP) conjugate.

Using a secondary antibody increases the likelihood of high background readings. Therefore trial experiments utilising combinations of blocking agents and washes were performed in order to limit this problem. An initial experiment was performed using Y98-BIO and RZ60-DIG with P-AP conjugate being used as a secondary antibody. 1% BSA in

1X ribozyme hybridisation buffer was used as a blocking agent (figure 3.37). It can be seen from this data that although P-AP does increase the signal, there is considerable background. Although addition of 1% BSA does reduce the background, the signal-to-noise ratio is still too low to enable this system to be used.

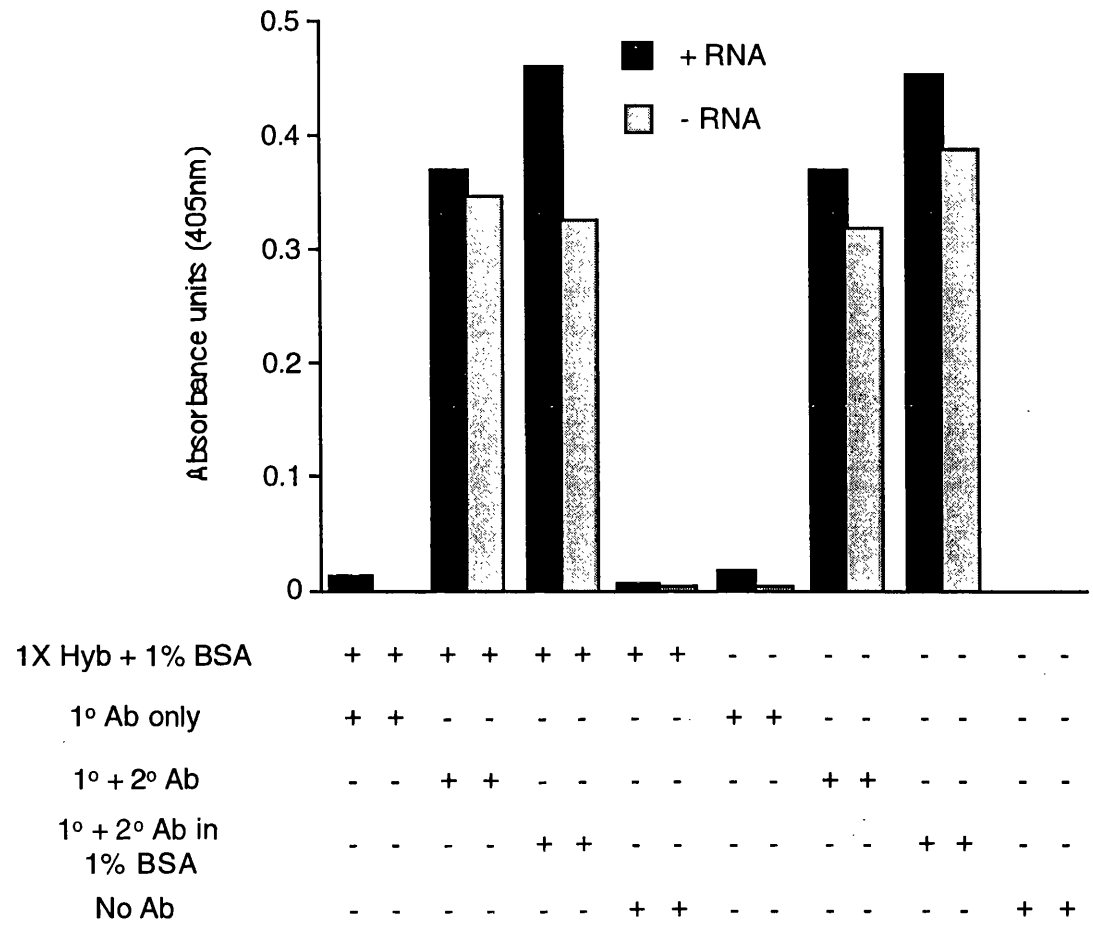

Figure 3.37. Results of ELISA performed using Y98-BIO and RZ60-DIG. Fixing of RNA complex to the streptavidin wells was performed in 1X ribozyme hybridisation buffer (1X Hyb) either with or without 1% BSA at 4°C overnight. The ELISA was probed using either just a primary antibody (1° Ab; sheep anti-digoxigenin F_{ab} fragments conjugated to horseradish peroxidase, 1:100 dilution), primary and secondary antibodies (2° Ab; peroxidase anti-peroxidase conjugate, 1:200 dilution), primary and secondary antibodies plus 1% BSA and with no antibody. Although use of the peroxidase anti-peroxidase conjugate as a secondary antibody clearly increases signal strength, there is considerable background even when 1% BSA is used as a blocking agent. All antibody incubations were at 37°C for 3 hours. Wells were rinsed five times for at least 30 seconds with wash buffer after each incubation. The ELISA was developed using ABTS, with absorbance being measured at 405nm.

Further experiments were performed using 5D-BIO and RZ572B-DIG RNAs. These experiments utilised both P-AP and donkey anti-sheep IgG secondary antibodies. 1% gelatine and a 1:100 dilution of mouse IgG-FITC conjugate were used as blocking agents. The absorbances obtained from these experiments are shown in table 3.2 and in figure 3.38. The absorbances are again far too low to be of any use. Neither blocking agent increases the signal to noise ratio, with considerable peroxidase activity being seen even when no RZ572B-DIG has been added to the wells, suggesting that a significant proportion of the background is coming from non-specific binding of the anti-digoxigenin primary antibody.

	Blocking agent	no 2° Ab	P-AP	anti-sheep IgG
5D-BIO + 1° Ab	no block	0.118	0.374	0.283
	1% gelatine	0.12	0.277	0.198
	1:100 mouse IgG	0.144	0.799	0.311
5D-BIO - 1° Ab	no block	0.092	0.252	0.199
	1% gelatine	0.099	0.23	0.145
	1:100 mouse IgG	0.093	0.678	0.199
5D-BIO + RZ572B-DIG + 1° Ab	no block	0.11	0.302	0.214
	1% gelatine	0.098	0.174	0.176
	1:100 mouse IgG	0.117	0.62	0.214
5D-BIO + RZ572B-DIG - 1° Ab	no block	0.098	0.264	0.195
	1% gelatine	0.099	0.194	0.14
	1:100 mouse IgG	0.094	0.63	0.195

Table 3.2. Results of ELISA performed using 5D-BIO and RZ572B-DIG RNAs to assess efficacy of secondary antibodies, peroxidase anti-peroxidase conjugate and donkey anti-sheep IgG-peroxidase conjugate. 5D-BIO was fixed to streptavidin plates in 1X ribozyme hybridisation buffer at 4°C overnight. 1X ribozyme hybridisation buffer was supplemented with either 1% gelatine, 1:100 dilution of mouse IgG-FITC conjugate (both being used as blocking agents) or had no addition. Half the wells containing 5D-BIO had RZ572B-DIG added in 1X ribozyme hybridisation buffer with the addition of blocking agents in wells where they had been used previously. Following addition of RZ572B-DIG the wells were incubated for 3 hours at 37°C. Following this incubation the wells were rinsed with wash buffer, after which half the wells were incubated with the primary antibody (1° Ab), sheep anti-digoxigenin F_{ab} fragment-peroxidase conjugate for 3 hours at 37°C. Following this incubation the wells were rinsed with wash buffer, and incubated with a secondary antibody for 3 hours at 37°C, as shown in the table. Following this incubation the wells were again rinsed with wash buffer, and the ELISA was developed using ABTS. The table shows the absorbance of the contents of the wells at 405nm.

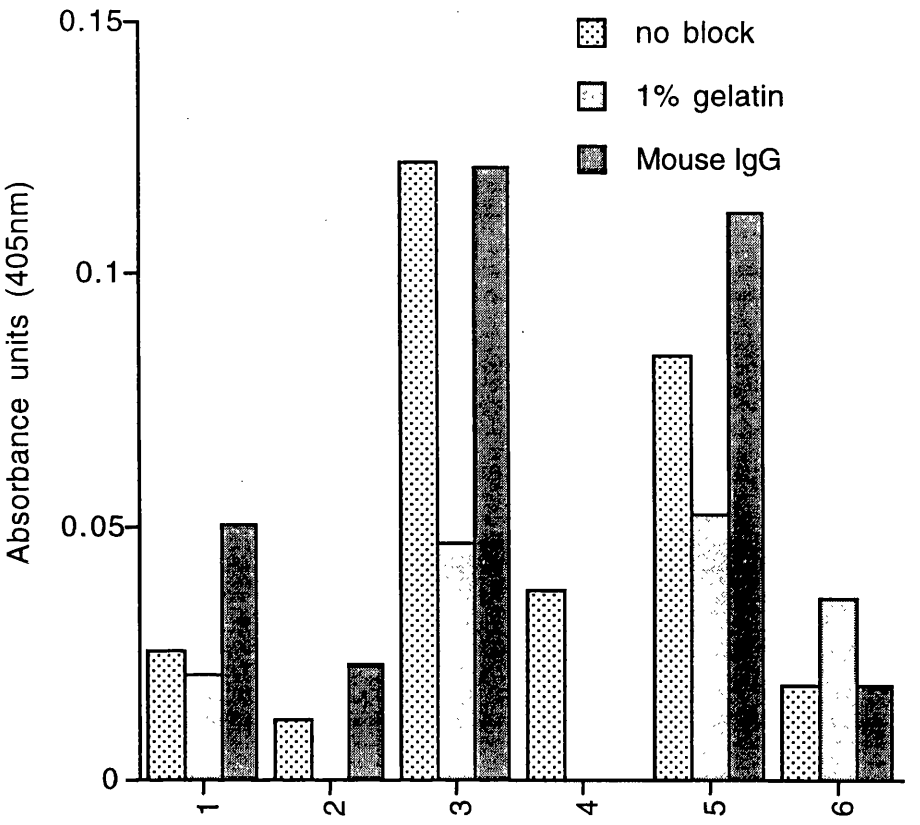

Figure 3.38. Results of ELISA performed using 5D-BIO and RZ572B-DIG RNAs to assess efficacy of various secondary antibodies and blocking agents. The data for this graph was obtained from table 3.2 by subtracting the absorbances obtained in incubations performed with no primary antibody from the absorbances obtained in incubations identical accept for the use of the primary antibody. Key to columns: (1) 5D-BIO plus 1° Ab, no 2° Ab, (2) 5D-BIO plus RZ572B-DIG and 1° Ab, no 2° Ab, (3) 5D-BIO plus 1° Ab and P-AP, (4) 5D-BIO plus RZ572B-DIG, 1° Ab and P-AP, (5) 5D-BIO plus 1° Ab and donkey anti-sheep IgG, (6) 5D-BIO plus RZ572B-DIG, 1° Ab and donkey anti-sheep IgG. Incubations were performed using either no blocking agent, 1% gelatine or 1:100 dilution of mouse-IgG-FITC conjugate.

3.1.5. Discussion

Although ELISA could provide a rapid, efficient method of screening many ribozymes for binding activity simultaneously, it has been shown that the system tried in the current study was not sensitive enough to allow accurate determination of ribozyme-substrate binding kinetics. Despite demonstrating that nucleic acid binding could be detected by radioactive labelling in microtitre wells (figure 3.32), and that the digoxigenin detection system could follow ribozyme-substrate hybridisation in a dose-dependent fashion (figure

3.34), it was clear that using end-labelled RNA would not provide enough binding sites for the anti-digoxigenin antibody.

This conclusion was reached after examining a number of other possibilities that could have explained the low readings. The RNA was clearly being endlabelled by TdT (figure 3.31), and was not degrading through the labelling process (figure 3.35). However, it was not demonstrated whether the RNA was degraded in the microtitre wells during the ELISA process. Increasing the quantity of RNA did not increase the signal, suggesting that the wells were saturated (figure 3.36). The ribozyme binding site in the substrate was not occluded by binding the biotinylated substrate to the streptavidin -coated wells, as binding pre-formed ribozyme-substrate complexes into the streptavidin-coated wells did not increase the signal (figure 3.36).

Two different secondary antibodies, P-AP and donkey-anti-sheep IgG, were used in an attempt to increase the signal. Although both of these antibodies did increase the signal, the signal to noise ratio was very low. Three different blocking agents were used to try and increase the signal to noise ratio; 1% BSA, 1% gelatine and 1:100 dilution of mouse IgG-FITC conjugate. None of these blocking agents appreciably increased the signal to noise ratio. In conclusion the ELISA based system did not prove to be an effective method for assessing ribozyme-substrate hybridisation. As stated earlier, ELISAs are sensitive to pH and ionic concentrations. Altering these parameters may allow the RNA-RNA ELISA to work. However, it was considered important to use the same conditions as have been used previously in *in vitro* ribozyme studies which have been shown to allow ribozyme-substrate binding and ribozyme-mediated substrate cleavage in non-ELISA systems.

3.2 DOES THE CHOICE OF TARGET SITE AFFECT CLEAVAGE EFFICIENCY?

3.2.1 What factors affect ribozyme cleavage?

Section 3.1 detailed how ribozymes directed to different parts of a stem-loop of pre-core/ core RNA hybridise with their target sequences at different rates. Is binding the rate determining step of a cleavage reaction, with cleavage happening at the same rate irrespective of the target sequence? It is often assumed that cleavage fails because of substrate binding failure. However, in cell culture, ribozyme constructs can block gene expression even when no cleavage products can be detected (or when the ribozyme domain is inactivated by mutation). This implies that 'inactive' ribozymes are able to bind to their target sequences and block gene expression by an antisense mechanism.

Why should these ribozymes be able to bind to their target sites but be unable to cleave their substrate? Here, the ribozymes targeted against the stem-loop between bases 526 and 585 of the pre-core/ core ORF RNA were studied under single-turnover conditions *in vitro* to determine whether the rate of substrate cleavage differed between ribozymes. By splitting the ribozyme reaction into two parts, ribozyme-substrate hybridisation and substrate cleavage, it should be possible to determine whether hybridisation guarantees substrate cleavage.

3.2.2 Choice of substrate

Initial cleavage experiments were performed using 5D RNA. However, as these experiments consisted of incubations lasting up to 24 hours, the bulk of the 5D RNA degraded due to RNase activity, making it impossible to detect any ribozyme-generated cleavage products. Therefore it was decided to use the 60 base substrate RZSUB for all cleavage experiments.

3.2.3 Initial experiments

To determine whether any substrate cleavage could be detected, radiolabelled RZSUB was incubated with either a 100-fold excess, a 10-fold excess, or an equimolar amount of RZ534, RZ551, RZ556, RZ568, RZ572 or RZ572B. The ribozyme and substrate RNAs were incubated in 1X ribozyme hybridisation buffer supplemented with 25mM $MgCl_2$ (final concentration) at 37°C for 5 hours (figure 3.39). Under these conditions, RZ556 cleaved 69% RZSUB when RZ556 was in a 100-fold excess over RZSUB. Both RZ572 and RZ572B cleaved approximately 60% RZSUB when both ribozymes were in a 100-fold excess over RZSUB (table 3.3).

A longer incubation at a lower $MgCl_2$ concentration was performed to investigate whether these ribozymes would still be active under physiological conditions. Ribozyme and substrate RNAs were incubated in 1X ribozyme hybridisation buffer supplemented with 5mM $MgCl_2$ (final concentration), and incubated at 37°C for 24 hours (figure 3.40).

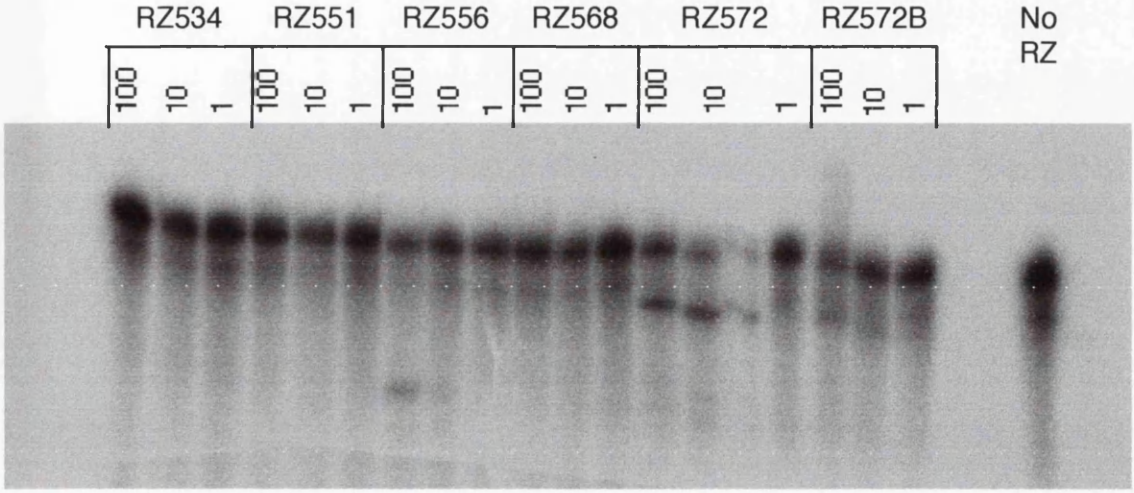

Figure 3.39. 5 hour ribozyme incubation with 25mM $MgCl_2$. Radiolabelled RZSUB was incubated with either a 100-fold or a 10-fold excess of each individual ribozyme, or with an equimolar amount of each individual ribozyme, in 1X ribozyme hybridisation buffer supplemented with 25mM $MgCl_2$ (final concentration). RZSUB was also incubated in 1X ribozyme hybridisation buffer supplemented with 25mM $MgCl_2$ (final concentration) in the absence of any ribozymes. Reactions were incubated for 5 hours at 37°C. Following incubations, an equal volume of formamide gel loading buffer was added to each reaction, which were then boiled for 2 minutes. Samples were run on a 10% denaturing polyacrylamide gel in 1X TBE buffer. Cleavage products are visible in the 100-fold excess lanes with RZ556 and RZ572B, and in both the 100-fold and 10-fold excess lanes with RZ572.

Ribozyme	RZ556			RZ572			RZ572B		
RZ:RZSUB	100:1	10:1	1:1	100:1	10:1	1:1	100:1	10:1	1:1
% Cleavage	**69**	**-**	**-**	**57**	**49**	**-**	**59**	**-**	**-**

Table 3.3. Extent of cleavage of RZSUB by RZ556, RZ572 and RZ572B after 5 hours incubation in 1X ribozyme hybridisation buffer supplemented with 25mM $MgCl_2$ (final concentration). These data were derived by quantifying the gel shown in figure 3.39 with the phosphorimager.

RZ551, RZ556, RZ572 and RZ572B all showed cleavage activity when incubated with RZSUB. RZ534 and RZ568 failed to generate any cleavage products. These observations tie in with the gel-shift experiments described in section 3.1.3b, in which RZ534 and RZ568 failed to hybridise with RZSUB. RZ551 and RZ556 both exhibited similar activities (table 3.4). The greatest amount of cleavage was seen with RZ572 which, when in 100-fold excess, cleaved 90% of RZSUB and, when in 10-fold excess, cleaved 83% of RZSUB.

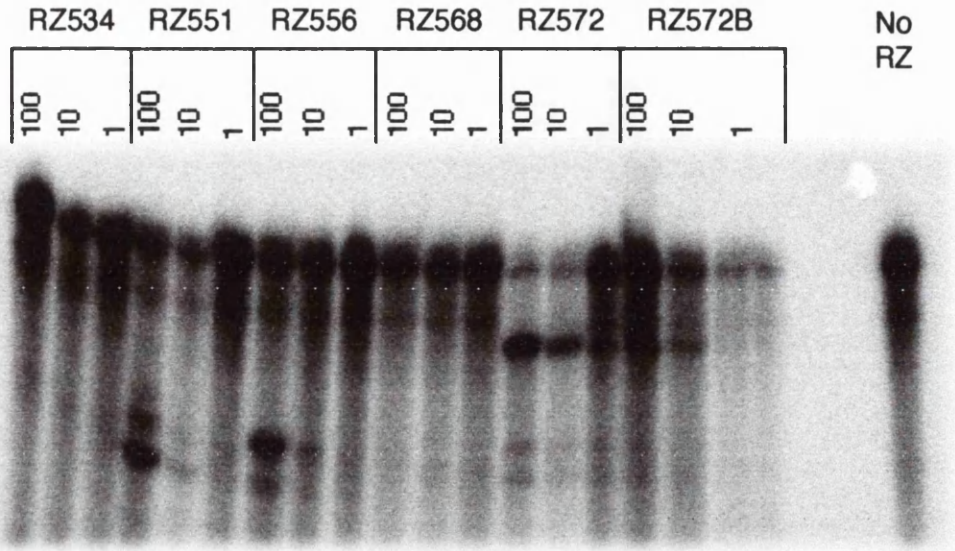

Figure 3.40. 24 hour ribozyme incubation with 5mM $MgCl_2$. Radiolabelled RZSUB was incubated with either a 100-fold or a 10-fold excess of each individual ribozyme, or with an equimolar amount of each individual ribozyme, in 1X ribozyme hybridisation buffer supplemented with 5mM $MgCl_2$ (final concentration). RZSUB was also incubated in 1X ribozyme hybridisation buffer supplemented with 5mM $MgCl_2$ (final concentration) in the absence of any ribozymes. Reactions were incubated for 24 hours at 37°C. Following incubations, an equal volume of formamide gel loading buffer was added to each reaction, which were then boiled for 2 minutes. Samples were run on a 10% denaturing polyacrylamide gel in 1X TBE buffer. Cleavage products are visible in the 100-fold excess lanes with RZ551 and RZ556, and in all three lanes with RZ572 and RZ572B.

Ribozyme	RZ551			RZ556			RZ572			RZ572B		
RZ:RZSUB	100:1	10:1	1:1	100:1	10:1	1:1	100:1	10:1	1:1	100:1	10:1	1:1
% Cleavage	**69**	**23**	**-**	**55**	**21**	**-**	**90**	**83**	**31**	**38**	**35**	**17**

Table 3.4. Extent of cleavage of RZSUB by RZ551, RZ556, RZ572 and RZ572B after 24 hour incubation in 1X ribozyme hybridisation buffer supplemented with 5mM $MgCl_2$ (final concentration). These data were derived by quantifying the gel shown in figure 3.40 with the phosphorimager.

This suggests that approximately 10% of RZSUB is resistant to cleavage. This resistance could be due to substrate secondary structure, or the formation of inactive ribozyme-substrate complexes. In contrast, an excess of RZ572B, which cleaves RZSUB at the same point as RZ572, only cleaved 35% of RZSUB. This is despite RZ572B having a 13-fold greater affinity for RZSUB than RZ572. In multiple turnover experiments, ribozymes with high substrate affinities have low cleavage rates due to the slow release of cleavage products.

Here, large excesses of ribozymes are being used which should ensure single turnover conditions where the rate of product dissociation is irrelevant.

Duplicating this experiment with 10mM EDTA added to the 1X ribozyme hybridisation buffer resulted in no cleavage products being detectable, confirming that the cleavage products seen in the previous two experiments were the result of the addition of $MgCl_2$ (figure 3.41).

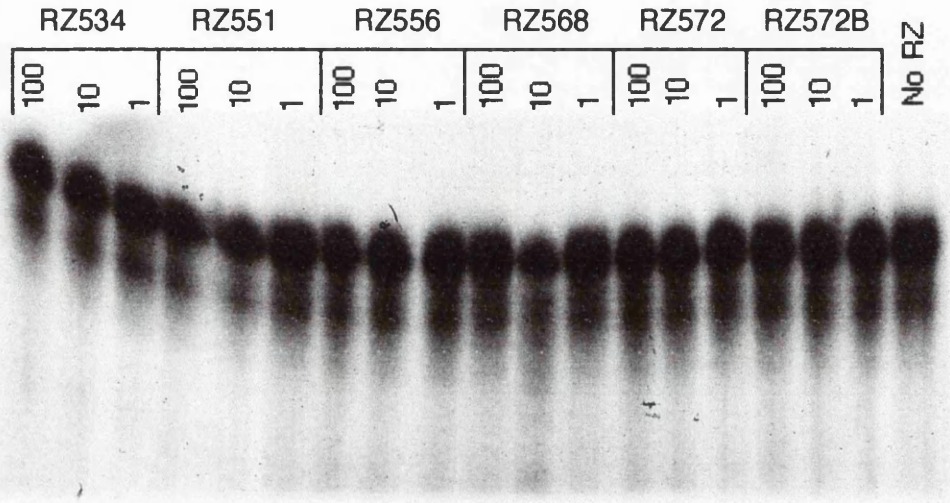

Figure 3.41. 24 hour ribozyme incubation with 10mM EDTA. Radiolabelled RZSUB was incubated with either a 100-fold or a 10-fold excess of each individual ribozyme, or with an equimolar amount of each individual ribozyme, in 1X ribozyme hybridisation buffer supplemented with 10mM EDTA (final concentration). RZSUB was also incubated with no ribozyme added. Reactions were incubated for 24 hours at 37°C. Following incubations, an equal volume of formamide gel loading buffer was added to each reaction, which were then boiled for 2 minutes. Samples were run on a 10% denaturing polyacrylamide gel in 1X TBE buffer. After 24 hours incubation in the presence of the Mg^{2+} chelator, EDTA, no cleavage products are seen, thus demonstrating that the cleavage products seen in figures 3.39 and 3.40 are the result of a Mg^{2+} dependent reaction.

3.2.4 Single turnover timecourse

Following the demonstration of ribozyme cleavage the rate of cleavage was determined in a timecourse experiment. A large excess of ribozyme over substrate was used to ensure single turnover conditions.

The ribozyme and substrate RNAs were pre-annealed in 1X ribozyme hybridisation buffer overnight at 37°C, to allow all the accessible ribozyme binding sites to become occupied; the cleavage reaction was started by adding $MgCl_2$ to a final concentration of 5mM. The reaction was stopped in formamide gel loading buffer and samples separated on a 12% denaturing polyacrylamide gel (figure 3.42).

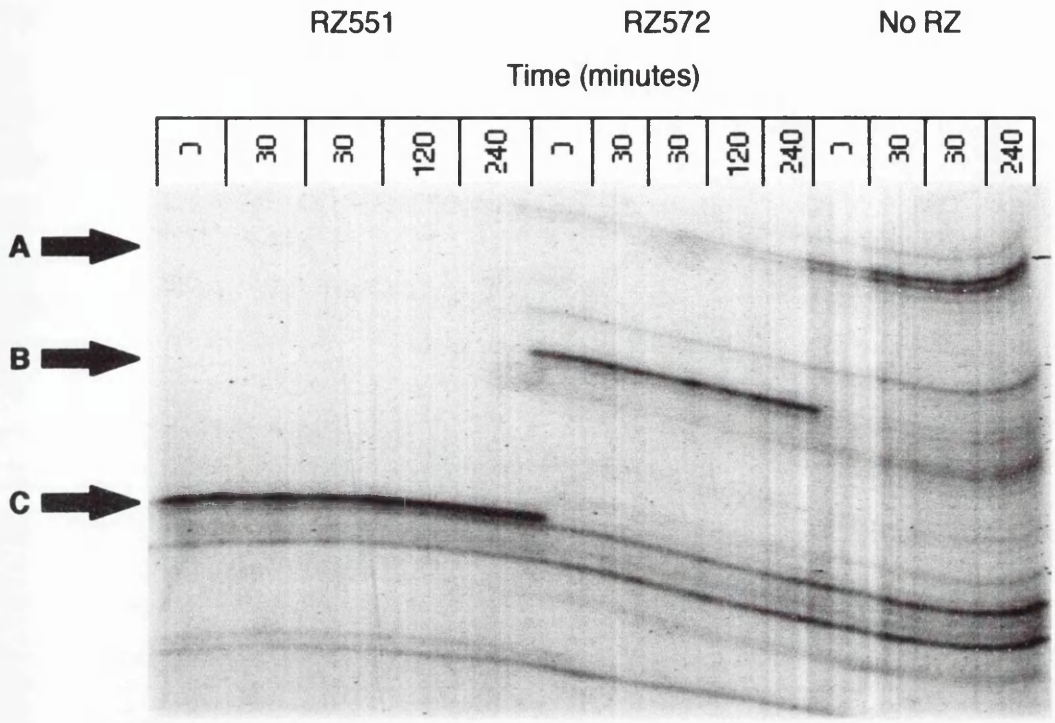

Figure 3.42. Single-turnover ribozyme cleavage timecourse performed with RZ551 and RZ572. 100-fold excess ribozyme was incubated with radiolabelled RZSUB in 1X ribozyme hybridisation buffer overnight at 37°C. Following this incubation, $MgCl_2$ was added to a final concentration of 5mM to initiate ribozyme cleavage. Aliquots were taken at various time-points and added to formamide gel-loading buffer. Samples were heated at 95°C prior to running on a 12% denaturing polyacrylamide gel. The multiple bands seen across all three samples are the result of non-specific RNase degradation of RZSUB. However, the strong bands unique to the ribozyme incubations (indicated by arrows) are the result of specific ribozyme-mediated cleavage. Key to bands: (**A**), undigested RZSUB; (**B**) major product of RZ572 cleavage of RZSUB; (**C**) major product of RZ551 cleavage of RZSUB.

There was the same degree of cleavage of RZSUB at the zero and end timepoints. There are three possible explanations. The first is that the reaction continued in the formamide gel loading buffer; this is unlikely given that the ribozyme-substrate complex would rapidly break down. The second is that the preannealing reaction was contaminated with Mg^{2+} left over from the *in vitro* transcription reactions, or from the gel elution buffer which was used in the purification of the radiolabelled substrate RNA. Dialysis would solve this problem, but would require large volumes, which would then need to be concentrated. Nucleic acids are generally concentrated by ethanol precipitation in the presence of high concentrations of a monovalent cation, leading to the possibility of salt contamination of the dialysed RNA. The third possibility is that the ribozyme cleavage reaction is virtually instantaneous, given that the zero time-point is actually approximately five seconds after the

true start of the reaction, as a result of the time needed to pipette Mg^{2+} into the reaction, and to take out a sample. The experiment was repeated, but with 10mM EDTA (final concentration) in the overnight preannealing reaction. This amount of EDTA was more than sufficient to bind all the Mg^{2+} in the transcription reaction. The reaction was then started by adding $MgCl_2$ to a final concentration of 20mM, resulting in a final concentration of Mg^{2+} of at least 10mM. Over a 4 hour time course at 37°C, no detectable cleavage was seen, implying that the ribozyme cleavage reaction was not instantaneous (figure 3.43).

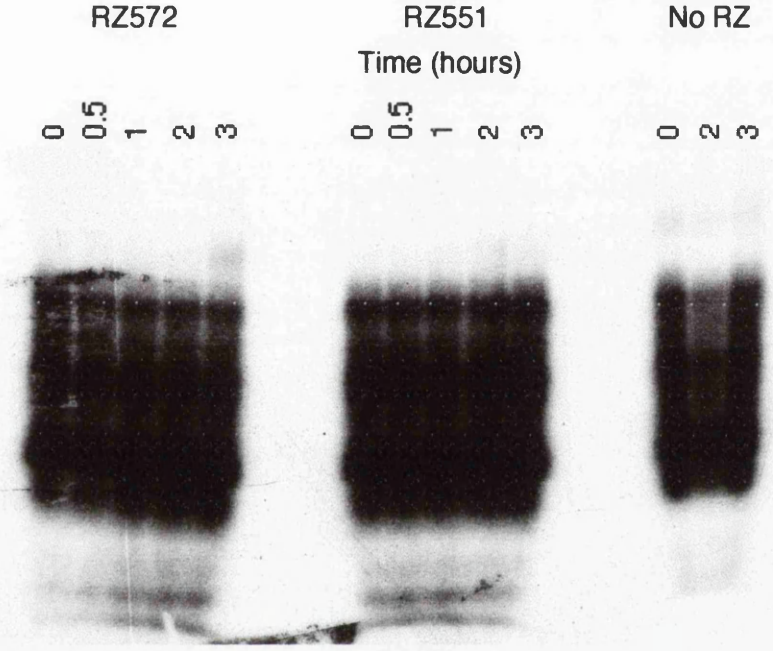

Figure 3.43. Single-turnover ribozyme cleavage timecourse performed with RZ551 and RZ572. 100-fold excess ribozyme was incubated with radiolabelled RZSUB in 1X ribozyme hybridisation buffer supplemented with EDTA (final concentration 10mM) overnight at 37°C. Following this incubation, $MgCl_2$ was added to a final concentration of 20mM to initiate ribozyme cleavage. Aliquots were taken at various time-points and added to formamide gel-loading buffer. Samples were heated at 95°C prior to running on a 12% denaturing polyacrylamide gel. The multiple bands seen across all three samples are the result of non-specific RNase degradation of RZSUB. Because of this degradation, no evidence of ribozyme cleavage can be seen.

It can be seen that there is a large amount of degradation of the radiolabelled RNA in both of these experiments. Because of exposure to RNase degradation during the overnight pre-incubation of ribozyme with substrate in the absence of Mg^{2+}, it was decided to simply start the ribozyme reactions by mixing purified ribozyme and substrate RNAs in 1X ribozyme hybridisation buffer supplemented with 5mM $MgCl_2$. This does not allow the cleavage reaction to be separated from the ribozyme-substrate hybridisation reaction. However, by performing the reactions under single turnover conditions, the only steps which could potentially influence the cleavage rate are ribozyme-substrate hybridisation and

substrate cleavage. As the rate of ribozyme-substrate hybridisation has been determined by gel-shift assay (see section 3.1.3), any differences seen between the rate of ribozyme-substrate hybridisation and the rate of cleavage, as determined under single turnover conditions, must be attributable to the phosphodiesterase reaction catalysed by the ribozyme core.

Cleavage reactions were performed with at least a 50-fold excess of ribozyme over substrate. The quantity of ribozyme was increased until the rate of cleavage did not increase with further addition of ribozyme. In all cases this was achieved with a 100-fold excess of ribozyme over substrate. Experiments were repeated in triplicate, with cleavage products being analysed by denaturing polyacrylamide gel electrophoresis (figures 3.44). Band intensities were quantified using the phosphorimager. Percentage cleavage was determined using the formula

$$\frac{\left[\frac{\text{Product 1}}{\text{no. U residues}}\right] + \left[\frac{\text{Product 2}}{\text{no. U residues}}\right]}{\left[\frac{\text{Product 1}}{\text{no. U residues}}\right] + \left[\frac{\text{Product 2}}{\text{no. U residues}}\right] + \left[\frac{\text{Uncleaved substrate}}{\text{no. U residues}}\right]} \qquad (v)$$

where the intensities of each band are normalised by dividing the intensity obtained from the phosphorimager by the number of radiolabelled U residues in the RNA. Note that only one band is visible in the RZ572 and RZ572B timecourse cleavage gels (figures 3.44b and 3.44c). This is because the smaller cleavage product only contains a single U residue, and is therefore not labelled to a sufficiently high specific activity to be detectable.

Despite repeated attempts, it was not possible to get RZ551 working in the single turnover timecourse experiments. Therefore only data is presented for RZ556, RZ572 and RZ572B (figure 3.45). It can be clearly seen that RZ556 and RZ572B have similar cleavage rates ($2X10^{-2}$ fmol/min and $3X10^{-2}$ fmol/min respectively), whilst RZ572 cleaves 5-fold faster ($14.6X10^{-2}$ fmol/min).

3.2.5 Multiple turnover

The main argument put forward favouring ribozymes over antisense is that ribozymes are predicted to be able to cleave multiple substrates through successive cycles of ribozyme-substrate hybridisation followed by substrate cleavage and the subsequent dissociation of the cleavage products. In contrast, one antisense oligonucleotide can only inactivate one target RNA. Antisense inhibition also has the potential to be reversible, with the antisense oligonucleotide dissociating from its target. The ability of ribozymes to cycle can be tested by incubating the ribozymes with an excess of substrate, and determining whether the quantity of cleaved substrate exceeds the quantity of ribozyme. In the present study it was found to be impossible to detect any cleavage products under such conditions.

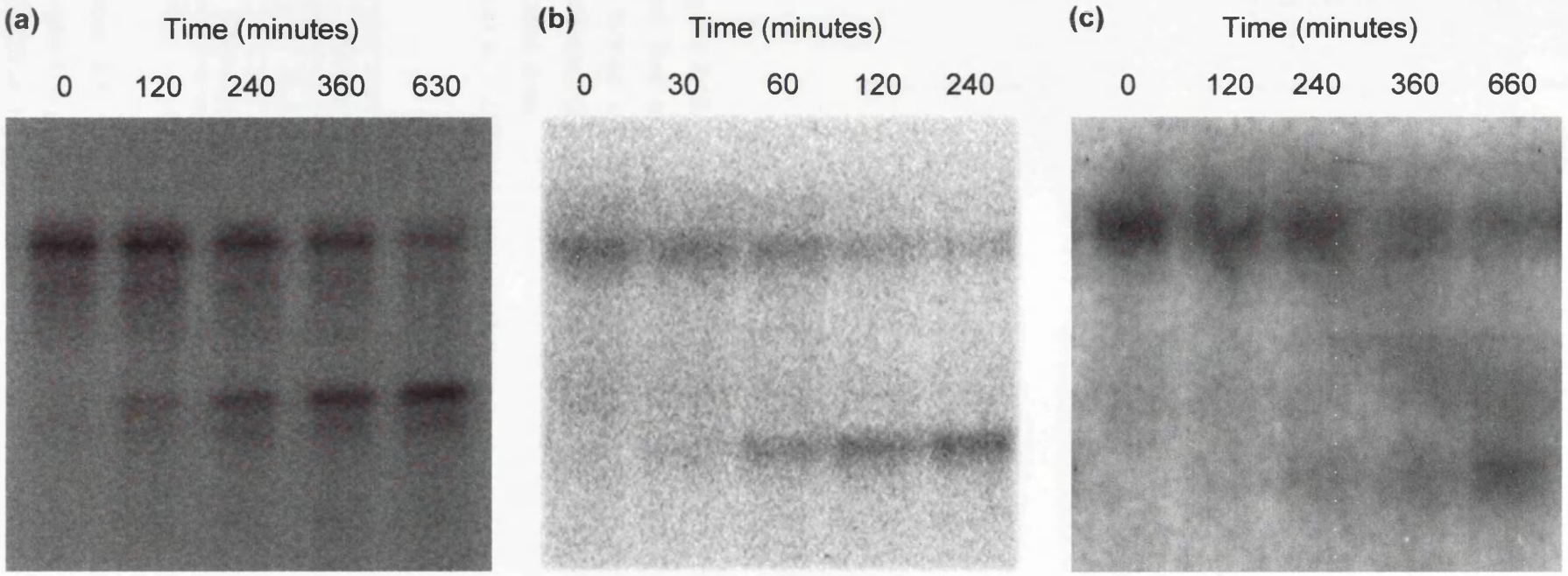

Figure 3.44. Ribozyme cleavage timecourses. Radiolabelled RZSUB was incubated with 100-fold excess of either **(a)** RZ556, **(b)** RZ572 or **(c)** RZ572B in 1X ribozyme hybridization buffer supplemented with 5mM $MgCl_2$ (final concentration). Aliquots were taken at the times shown, and placed in formamide gel loading buffer. Samples were heated to 95°C for 2 minutes before loading onto a 10% denaturing polyacrylamide gel, run in 1X TBE buffer. After electrophoresis the gels were dried and analysed by phosphorimager to determine band intensity. Results are plotted in figure 3.45. All experiments were repeated at least five times.

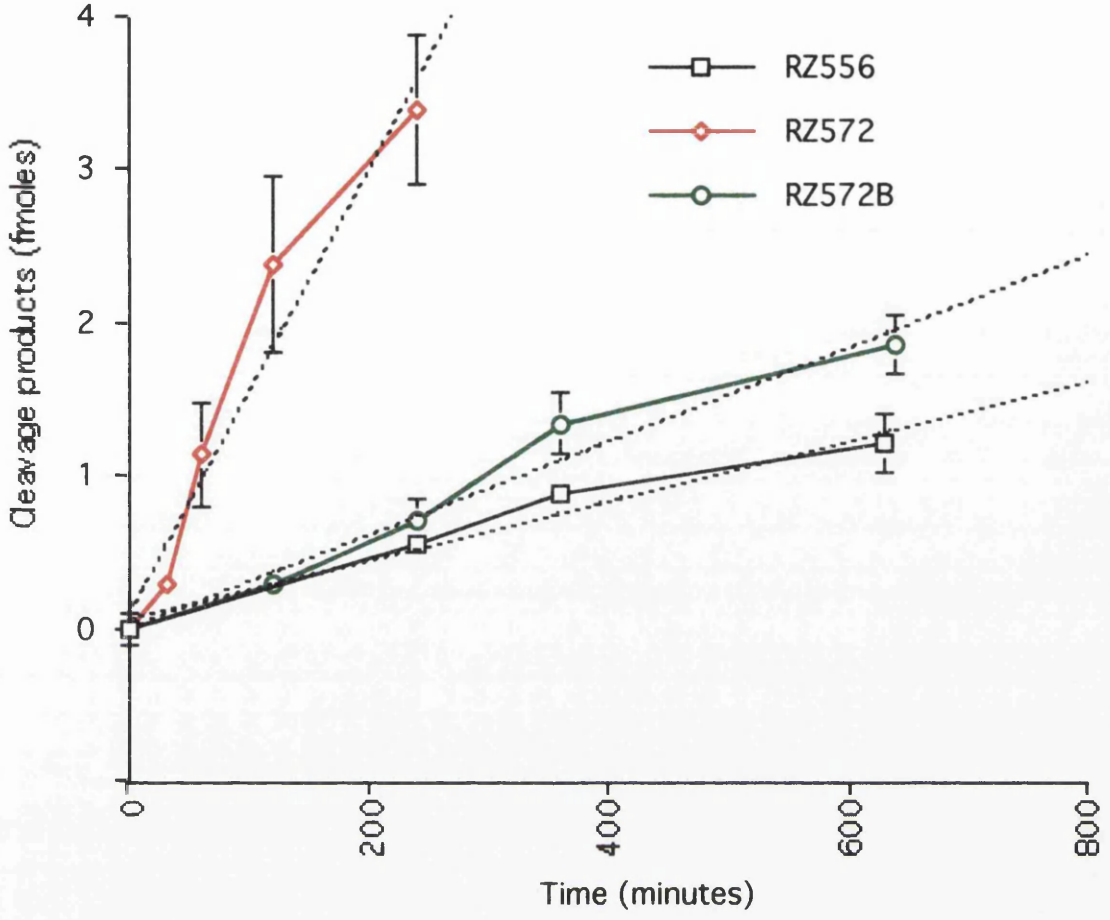

Figure 3.45. Ribozyme cleavage timecourses. The data presented are the averages of at least five experiments, with standard deviations shown. Ribozyme cleavage was performed under single-turnover conditions, with ribozymes in 100-fold excess over substrate RZSUB. Cleavage rates were determined from linear best fits made to each plot (dotted lines). Calculated cleavage rates are: RZ556, $2X10^{-2}$ fmol/min; RZ572B, $3X10^{-2}$ fmol/min; RZ572, $14.6X10^{-2}$ fmol/min.

Ribozyme	RZ556	RZ572	RZ572B
k_2	$(4.1\pm1.4)s^{-1}M^{-1}$	$3.27s^{-1}M^{-1}$	$(23.9\pm9.2)s^{-1}M^{-1}$
Cleavage rate	$2X10^{-2}$ fmol/min	$14.6X10^{-2}$ fmol/min	$3X10^{-2}$ fmol/min

Table 3.5. Comparison of pseudo-first order ribozyme-substrate hybridisation rate constant (k_2) and single-turnover cleavage rates for ribozymes RZ556, RZ572 and RZ572B and substrate RZSUB.

3.2.6 Discussion

The gel-shift assays described in section 3.1.3 showed that only ribozymes RZ534 and RZ568 failed to bind to RZSUB. These observations were supported by the 24 hour ribozyme cleavage incubations in 5mM $MgCl_2$ (figure 3.40) which showed that RZSUB was cleaved by all the ribozymes except RZ534 and RZ568. A comparison of ribozyme-substrate association constants and rates of cleavage is shown in table 3.5.

The most interesting observation made in the single-turnover timecourse experiments was the difference in cleavage rates between RZ572 and RZ572B. RZ572B was designed to cleave at the same point in RZSUB as RZ572. Despite RZ572B having a 13-fold greater affinity for RZSUB than RZ572 (see section 3.1.3c), RZ572B was only able to cleave, when in excess, 35% of RZSUB. As the catalytic core is the same in both ribozymes, and both are cutting at the same triplet (thus eliminating the variable cleavage efficiencies seen at different NUX triplets) it is surprising that there is such a large difference in cleavage efficiencies. Long-flank ribozymes have been shown to have reduced cleavage rates in multiple turnover experiments compared to short-flank ribozymes targeted against the same point. However, in the current study, a large excess of ribozyme was used. It is assumed that all accessible ribozyme binding sites in the substrate become occupied by ribozyme, after which the substrate is cleaved. As all the substrate is cleaved in one cycle of ribozyme activity, dissociation of products from the ribozyme does not influence the rate of cleavage. It is the rate of product dissociation which is reduced by lengthening the ribozyme flanking sequence.

Why should the seemingly identical catalytic cores of ribozymes RZ572 and RZ572B cleave RZSUB at different rates? Clearly the long flanking sequences of RZ572B are influencing the cleavage rate, possibly by inducing changes in the structure of RZSUB. Analysis of the three-dimensional structure of hammerhead ribozymes reveals that the scissile bond is twisted away from the normal bond angle for a phosphodiester linkage (see section 1.12.4c). It is believed that this twisting enables the hammerhead ribozyme to lower the activation energy of the phosphodiesterase reaction and, in so doing, catalyse the cleavage of the substrate RNA. It would appear that inducing mechanical stress at the scissile bond promotes cleavage.

RZ572 binds between bases 564 and 580 of RZSUB whilst RZ572B binds to the entire length of RZSUB (figure 3.46). Therefore when RZ572 binds to RZSUB the double-stranded region formed between bases 530 to 534 and bases 581 to 585 should be maintained. This will keep RZSUB in a stem loop structure. In contrast when RZ572B binds to RZSUB, the stem loop structure of RZSUB will be lost (figure 3.47). It is hypothesised that the phosphodiester linkages in the single-stranded region of the stem loop form of RZSUB will be under more strain than those in the linear form of RZSUB bound to RZ572B. This extra strain should favour an increased rate of cleavage of the stem-loop form of RZSUB.

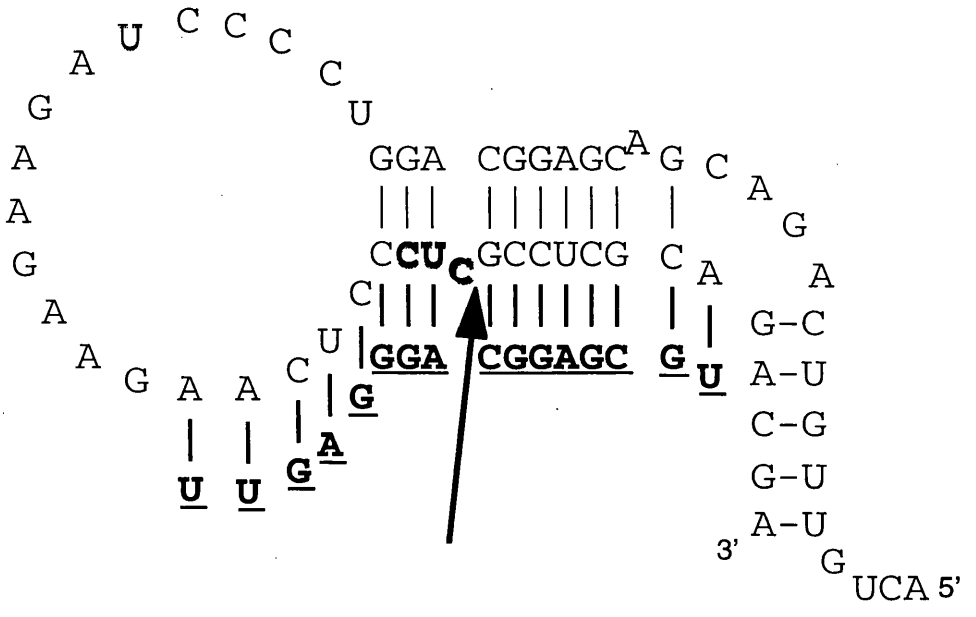

Figure 3.46. The binding of RZ572 to RZSUB. The stem-loop of RZSUB, corresponding to bases 526 to 585 of the pre-core/ core ORF is shown in light type. The flanking sequences of RZ572 (both 8 bases long) are shown in bold, underlined type. The cleavage point for ribozymes RZ572 and RZ572B is indicated by an arrow, and the target triplet, CUC, is highlighted in bold type. RZ572 binds between bases 564 and 580 of RZSUB, whilst RZ572B (total length of flanking sequences 59 bases) binds to the entire length of RZSUB.

To confirm this hypothesis it is necessary to confirm the structure of the ribozyme-substrate intermediates formed between RZ572 and RZSUB and RZ572B and RZSUB. This could be achieved by RNase mapping, as described in section 3.1.3c. However, this could be difficult because of the presence of ribozyme and substrate RNAs which are not part of a ribozyme-substrate complex. It may be necessary to stabilise any ribozyme-substrate complex using intercalating agents such as psoralen or acridine (see section 1.10), and then purify the stabilised complex by gel electrophoresis prior to RNase probing.

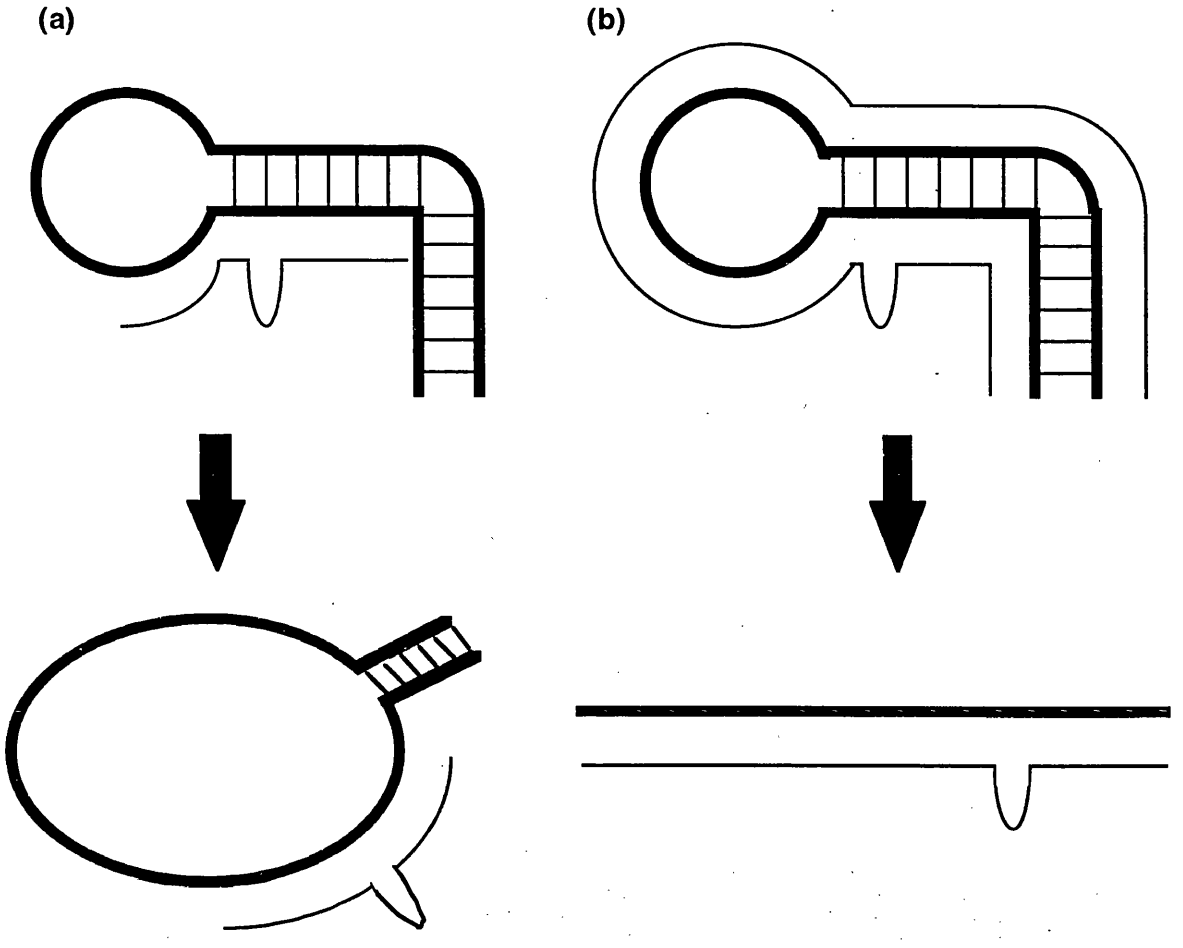

Figure 3.47. Hypothetical changes in the structure of RZSUB on the binding of ribozymes **(a)** RZ572 and **(b)** RZ572B. RZSUB (bold line) is predicted to assume a stem-loop structure (shown in detail in figures 3.3 and 3.45). The stem is kinked as the result of bases 535 to 539 being single-stranded. Both ribozymes are represented as narrow lines, with the conserved catalytic core shown as a loop. RZ572 is designed to bind between bases 564 and 580 of RZSUB. This is predicted to partially disrupt the double-stranded stem of RZSUB, though the double-stranded region formed between bases 530 to 534 and bases 580 to 585 should be maintained, with the result that the RZSUB portion of the RZ572:RZSUB complex should maintain a stem-loop structure **(a)**. In contrast, RZ572B is designed to bind to the entire length of RZSUB, between bases 526 and 585. It is predicted that this should completely destroy the stem-loop structure of RZSUB. The resulting RZ572B:RZSUB complex is predicted to be linear and completely double-stranded **(b)**. It is proposed that the differences described here between the ribozyme-substrate complexes explain the differences in cleavage rates between RZ572 and RZ572B. The increased rate of cleavage observed with RZ572 is believed to result from increased torsional stress at the scissile bond as a result of the substrate being twisted into a stem-loop.

3.3 CAN RIBOZYMES BLOCK PROTEIN SYNTHESIS?

3.3.1 Intracellular ribozyme activity.

Despite the large number of *in vitro* studies which have successfully demonstrated ribozyme-mediated cleavage of a wide variety of mRNA substrates, there has been limited success in repeating these results in cell culture. This can be attributed in part to the intracellular environment, which is very different from the conditions used *in vitro*. RNA binding proteins could block ribozyme binding sites either by blocking ribozyme target sequences, or by changing the substrate secondary structure. These proteins could also bind to the ribozyme RNA itself. Substrate and ribozyme RNAs could be localised to different intracellular compartments, though inclusion of appropriate signal sequences in the ribozyme RNA can get around this problem (see section 1.12.4f). Intracellular ribozyme activity could even be affected by the medium in which cells are cultured. *In vitro* studies have shown that hammerhead ribozyme activity can be inhibited by neomycin, an antibiotic widely used in the establishment of mammalian cell lines (Murray & Arnold, 1996).

Although many early studies claimed to have observed inhibition of protein synthesis due to intracellular ribozyme activity, the majority failed to use the correct controls to confirm that this was mediated by ribozyme cleavage. There are two methods for confirming intracellular ribozyme activity. The first is to use a ribozyme containing an inactivating point mutation in its conserved catalytic core. This inactive mutant ribozyme will still be able bind to, but not cleave, its target. Therefore any inhibition of protein synthesis observed when this mutant ribozyme is used can be attributed to an antisense mechanism. Studies utilising such controls have revealed that, across a range of substrates and cell types, some or all of a ribozyme's inhibitory potential is attributable to antisense effects. The second method to search for cleavage products. As most target mRNAs are at very low abundance, this is very difficult, and few studies have demonstrated cleavage of endogenous transcripts. It is easier to detect transcripts expressed to high copy number from transfected plasmids, or which have been transcribed *in vitro* and introduced into cells by microinjection.

Because of time constraints, it was not possible to test the efficacy of ribozymes RZ534, RZ551, RZ556, RZ568, RZ572 and RZ572B in transfected human hepatoma cells. Therefore it was decided to use the rabbit reticulocyte lysate *in vitro* coupled transcription-translation system (Promega). This allowed the constructs used for generating ribozyme and substrate RNAs for the *in vitro* ribozyme-substrate hybridisation (section 3.1) and ribozyme-mediated cleavage (section 3.2) to be used. DNA templates are transcribed in the reticulocyte lysate by T7 bacteriophage RNA polymerase, generating RNAs for translation. In addition to the plasmid p5D, which encoded HBcAg, a second plasmid pBL, encoding firefly luciferase, was used as an internal control in all ribozyme reactions.

3.3.2 Expression of ribozymes and proteins in rabbit reticulocyte lysate.

All constructs used contained a T7 bacteriophage promoter. All incubations were performed at 30°C for 2 hours in accordance with the users manual.

Ribozymes were expressed from partially single-stranded oligonucleotide templates (figure 3.13). Expression was confirmed and quantified by northern blotting (figure 3.48), with ribozyme RNA produced at a concentration of approximately 4μM in the rabbit reticulocyte lysate system when 0.11μg of oligonucleotide template was used.

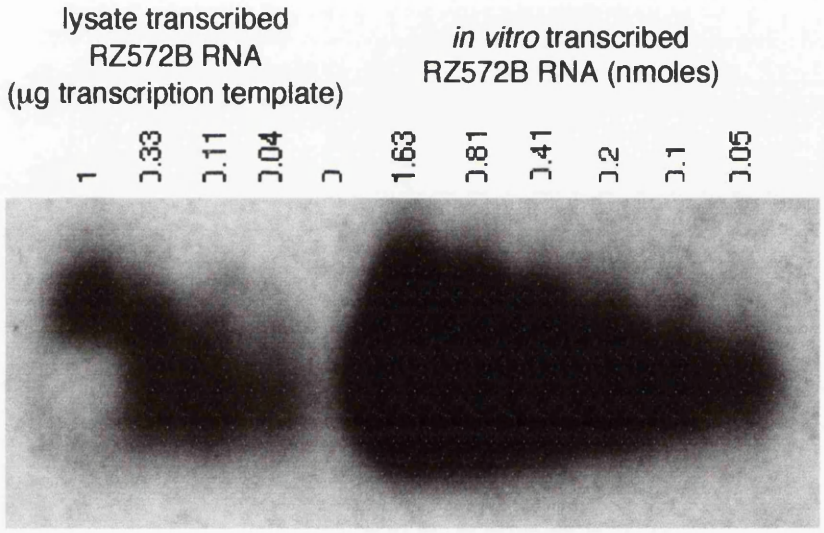

Figure 3.48. Northern blot of RZ572B RNA. Dilutions of partially single-stranded oligonucleotide transcription template RZ572B were added to 30μl rabbit reticulocyte lysate coupled transcription-translation reactions. Reactions were incubated at 30°C for 2 hours. RNA was extracted by phenol/ chloroform extraction followed by ethanol precipitation. The resulting RNA pellets were resuspended in 15μl H_2O. 5μl of the resuspended RNA was run on a 2% agarose, 1% formaldehyde gel in 1X MOPS buffer. In addition, a dilution series of RZ572B RNA generated by *in vitro* transcription was run on the same gel. The gel was blotted onto Hybond-N nylon membrane in 10X SSC buffer. The blot was probed with oligonucleotide RZ572BT 5'-endlabelled using γ^{32}P-ATP and T4 polynucleotide kinase. Band intensities were determined by phosphorimager scanning. Accurate determination was impossible due to the diffusion of the RNA bands during the blotting process. This was a result of the extremely small size of the RZ572B RNA (82 bases), which reduces the transfer and binding efficiencies of the RNA to the nylon membrane.

Production of HBcAg mRNA was confirmed and quantified by northern blotting (figure 3.49). HBcAg mRNA was produced at a concentration of approximately 0.8μM in the rabbit reticulocyte lysate system when 0.5μg of template DNA was used.

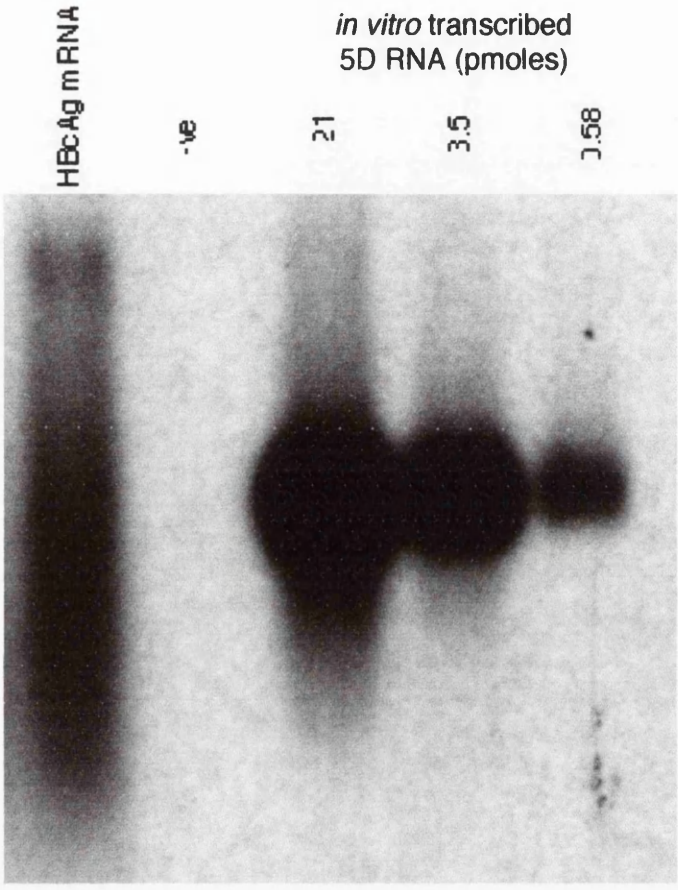

Figure 3.49. Northern blot of core mRNA. 0.5μg of p5D plasmid DNA was added to a 30μl rabbit reticulocyte lysate coupled transcription-translation reaction. Following incubation at 30°C for 2 hours, RNA was extracted by phenol/ chloroform extraction followed by ethanol precipitation. The resulting RNA pellet was resuspended in 15μl H_2O. 5μl of resuspended RNA was run on a 1% agarose, 1% formaldehyde gel in 1X MOPS buffer (HBcAg mRNA). In addition, a negative control lysate (-ve) in which no translation had occurred was phenol/ chloroform extracted, and a dilution series of *in vitro* transcribed 5D RNA were run on the same gel. The gel was blotted onto Hybond-N nylon membrane in 10X SSC buffer. The blot was probed with core ORF PCR product, labelled by nick translation with α^{32}P-dCTP. Despite RNase degradation, HBcAg mRNA could be detected in rabbit reticulocyte lysate following coupled transcription-translation reactions. The greater size of the transcripts in the lysate reactions results from the template being a circular plasmid rather than a linearized plasmid as in *in vitro* run-off transcription. With a circular template the T7 polymerase has to scan further along the plasmid to reach the transcription termination signal.

Is this mRNA translated to produce protein? Addition of ^{35}S-L-methionine to the rabbit reticulocyte lysate reaction allows the radiolabelling of proteins, and their subsequent detection by SDS-PAGE and autoradiography. Bands corresponding to the correct sizes for HBcAg and luciferase were detected (figure 3.50). Western blotting was used to confirm the identity of the postulated HBcAg band. No band was visible when a rabbit anti-HBcAg polyclonal antibody was used (figure 3.51). Instead, a broad, pale band was visible at the same point where HBcAg was expected to lie. This broad band is due to globin from the rabbit reticulocyte lysate which has a similar molecular weight to HBcAg (24kD). The great excess of globin over HBcAg blocks the anti-HBcAg antibody from binding to the HBcAg.

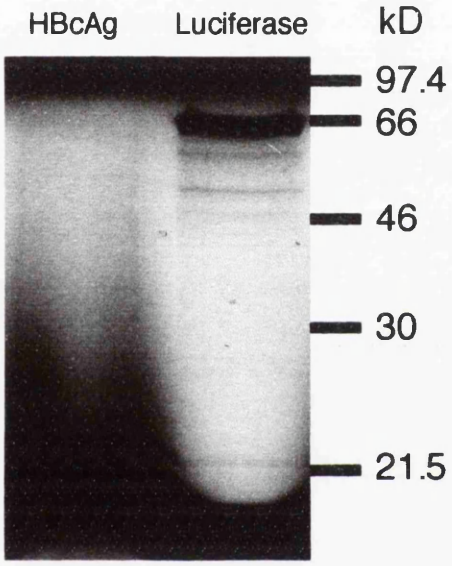

Figure 3.50. Expression of HBcAg and luciferase in rabbit reticulocyte lysate coupled transcription-translation system. 1μg of plasmid DNA template (p5D encoding HBcAg, pBL encoding luciferase) were added to rabbit reticulocyte lysate supplemented with ^{35}S-L-methionine. Reactions were incubated at 30°C for 2 hours. Samples were separated by SDS-PAGE and visualised by autoradiography. The bands shown are of the sizes expected for HBcAg and luciferase.

In order to separate any HBcAg away from the globin background immunoprecipitation was used. Anti-HBcAg polyclonal antibody was added to rabbit reticulocyte lysate following completion of the transcription-translation reaction. The resulting antibody-antigen complexes were pulled down using protein A-sepharose beads. Protein A is a bacterial protein which binds the F_c portion of IgG antibodies. The radiolabelled protein is removed from the beads by boiling, and is visualised by SDS-PAGE followed by autoradiography. Use of this technique allowed the detection of HBcAg (figure 3.52). The presence of luciferase was confirmed by performing an enzyme activity assay (figure 3.53)

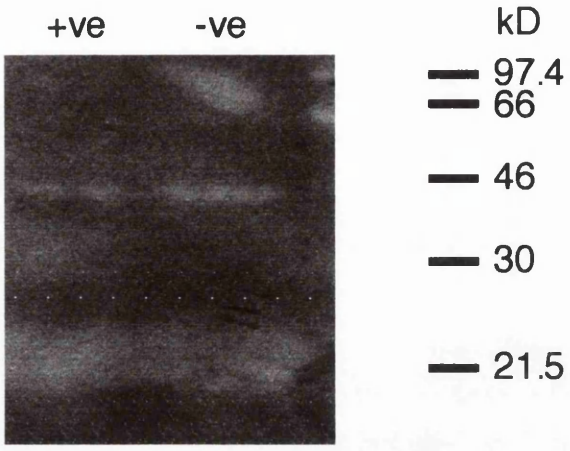

Figure 3.51. Western blot of HBcAg produced in rabbit reticulocyte lysate coupled transcription-translation system. Samples were separated by SDS-PAGE in Tris-glycine buffer. The gel was blotted onto Hybond-N nylon membrane in Towbin buffer using a Biorad electroblotter. The blot was probed with a rabbit anti-HBcAg polyclonal primary antibody and a sheep anti-rabbit secondary antibody/ peroxidase conjugate. The blot was developed using the ECL chemiluminescent system (Amersham). The long exposure used here (1 minute) shows pale regions at 46 and 21.5 kD in both the positive and negative lanes. These are regions were protein in the sample has blocked the antibodies used to probe the blot from binding non-specifically to the membrane. The region at 21.5 kD can be attributed to globin from the reticulocyte lysate. This is approximately the same relative molecular weight as HBcAg, and masks any HBcAg present.

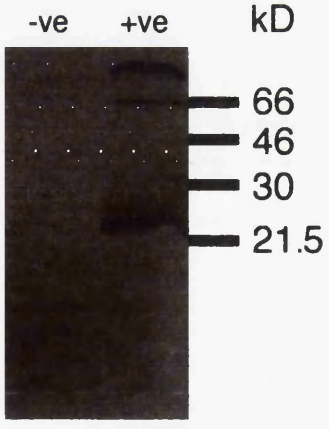

Figure 3.52. Immunoprecipitation of HBcAg from rabbit reticulocyte lysate coupled transcription-translation reactions confirms HBcAg is being produced. Radiolabelled HBcAg was expressed from the p5D plasmid during a 2 hour incubation at 30°C in rabbit reticulocyte lysate supplemented with ^{35}S-L-methionine. On completion, the lysate was cleared with protein A-sepharose beads. The beads were removed by centrifugation, and rabbit anti-HBcAg polyclonal antibody was added and incubated at 4°C for 3 hours. The resulting antibody-HBcAg complexes were pulled down with fresh protein A-sepharose beads. HBcAg was removed from the beads by boiling. Samples were separated by SDS-PAGE, and visualised by autoradiography.

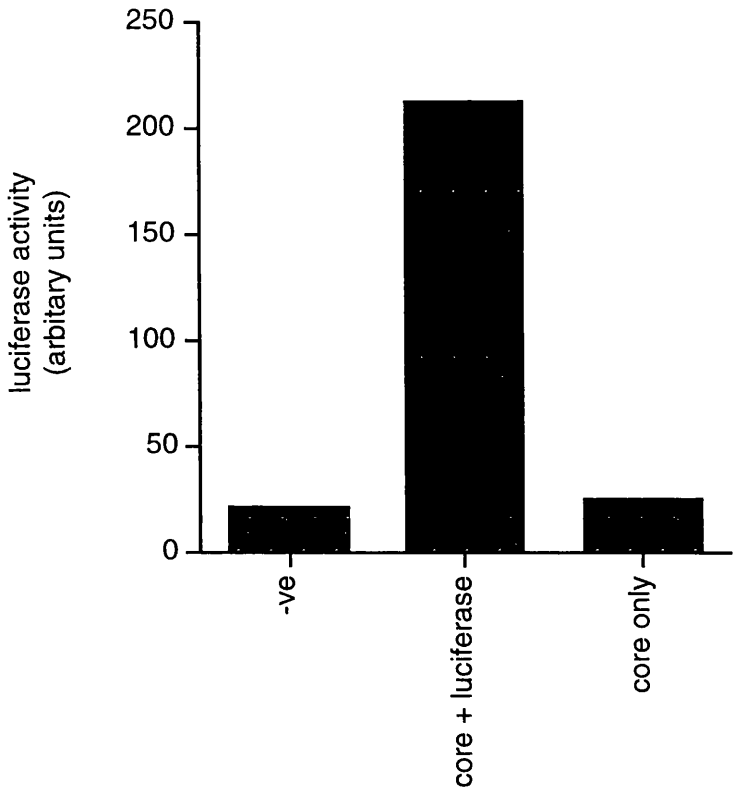

Figure 3.53. Confirmation of luciferase activity after *in vitro* translation reactions. Rabbit reticulocyte lysate reactions were set up with either no DNA template (-ve), plasmids p5D and pBL (HBcAg and luciferase templates respectively) and p5D only. Active luciferase is clearly produced during cotranslation of p5D and pBL. Luciferase activity is measured in arbitrary luminescence units.

After demonstrating that all the constructs were being expressed in the rabbit reticulocyte lysate, reactions were set up containing plasmids p5D and pBL, plus individual ribozyme templates. 0.25µg of each template DNA were added to each reaction. In addition to the ribozyme reactions, a control reaction containing only p5D and pBL with no ribozyme template plus a negative control containing no added DNA were also set up. Reactions were incubated at 30°C for 2 hours, with samples being visualised by SDS-PAGE (figure 3.54). It was necessary to limit the amount of ribozyme template DNA, as translation appeared to be sensitive to high concentrations of oligonucleotide. This effect may be sequence dependent, as it was particularly pronounced with oligonucleotide RZ572BT (figure 3.55). However, this inhibition of translation was not a result of an antisense effect, as both luciferase and HBcAg production were inhibited.

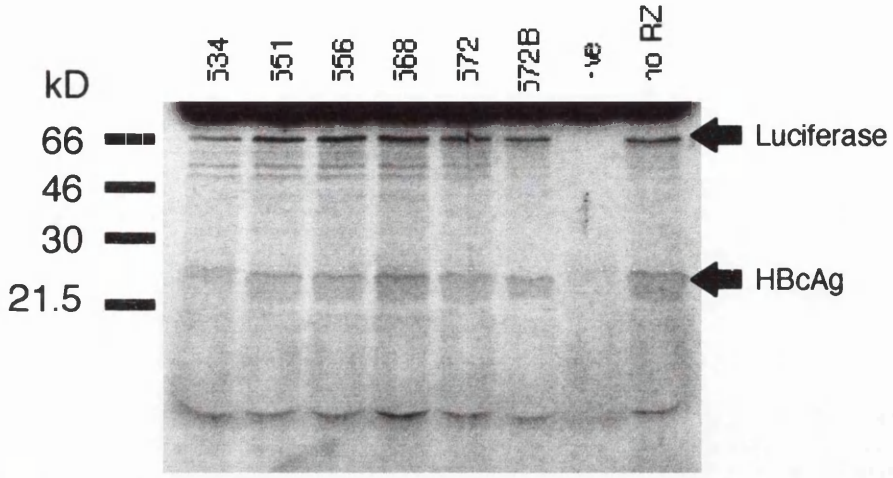

Figure 3.54 SDS-polyacrylamide gel of rabbit reticulocyte lysate reactions producing ^{35}S-L-methionine labelled luciferase and HBcAg. HBcAg was co-expressed with ribozymes RZ534, RZ551, RZ556, RZ568, RZ572 and RZ572B. Luciferase was used as an internal control. Band intensities were quantified by phosphorimager scanning.

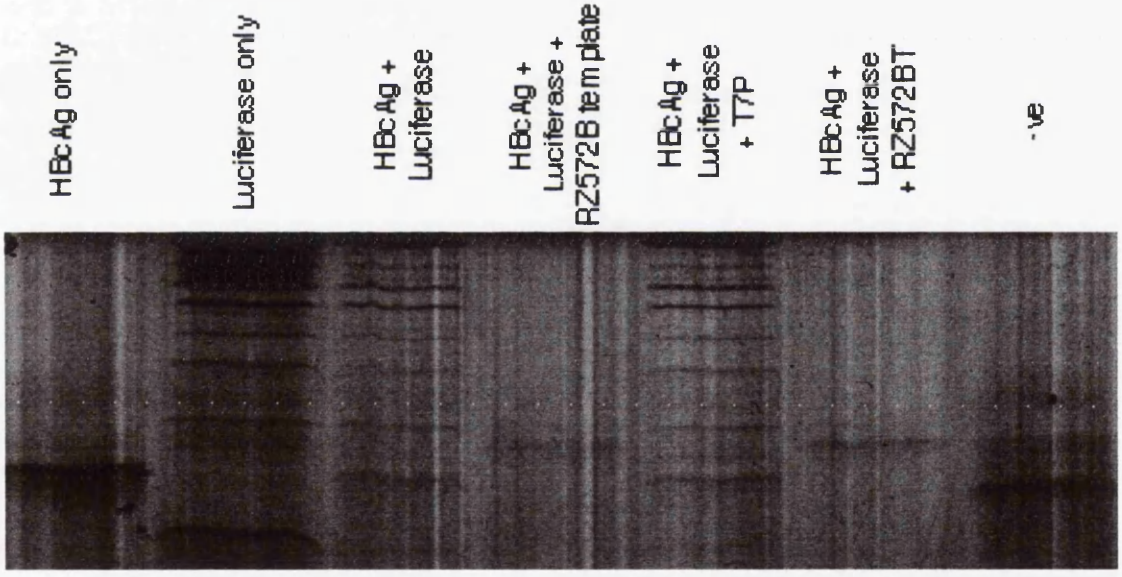

Figure 3.55. Inhibition of translation by oligonucleotide RZ572BT. Initial experiments showed a loss of both HBcAg and luciferase expression in rabbit reticulocyte lysates when the partially single-stranded oligonucleotide template for RZ572B (composed of annealed oligonucleotides T7P and RZ572BT) was used. Coupled transcription-translation reactions were performed using both HBcAg and luciferase templates. In addition, the partially single-stranded template for RZ572B and oligonucleotides T7P and RZ572BT were added. A negative control in which no DNA was added was also included (-ve). Translation of both HBcAg and luciferase were inhibited when either the partially single-stranded template or oligonucleotide RZ572BT were used. Lowering the concentration of the partially single-stranded template allowed translation to proceed. Addition of RZ572B RNA did not affect translation.

Gels were scanned with the phosphorimager, and the band intensities quantified as previously described (see section 3.1.3b). The level of HBcAg was expressed as the ratio between the intensity of the HBcAg band to the intensity of the luciferase band. These results were then expressed as a percentage of the control (luciferase and HBcAg only, no ribozyme). The mean results obtained from five experiments are shown in figure 3.55. The only significant variation is seen with RZ534 ($p<0.05$, Student's t-test).

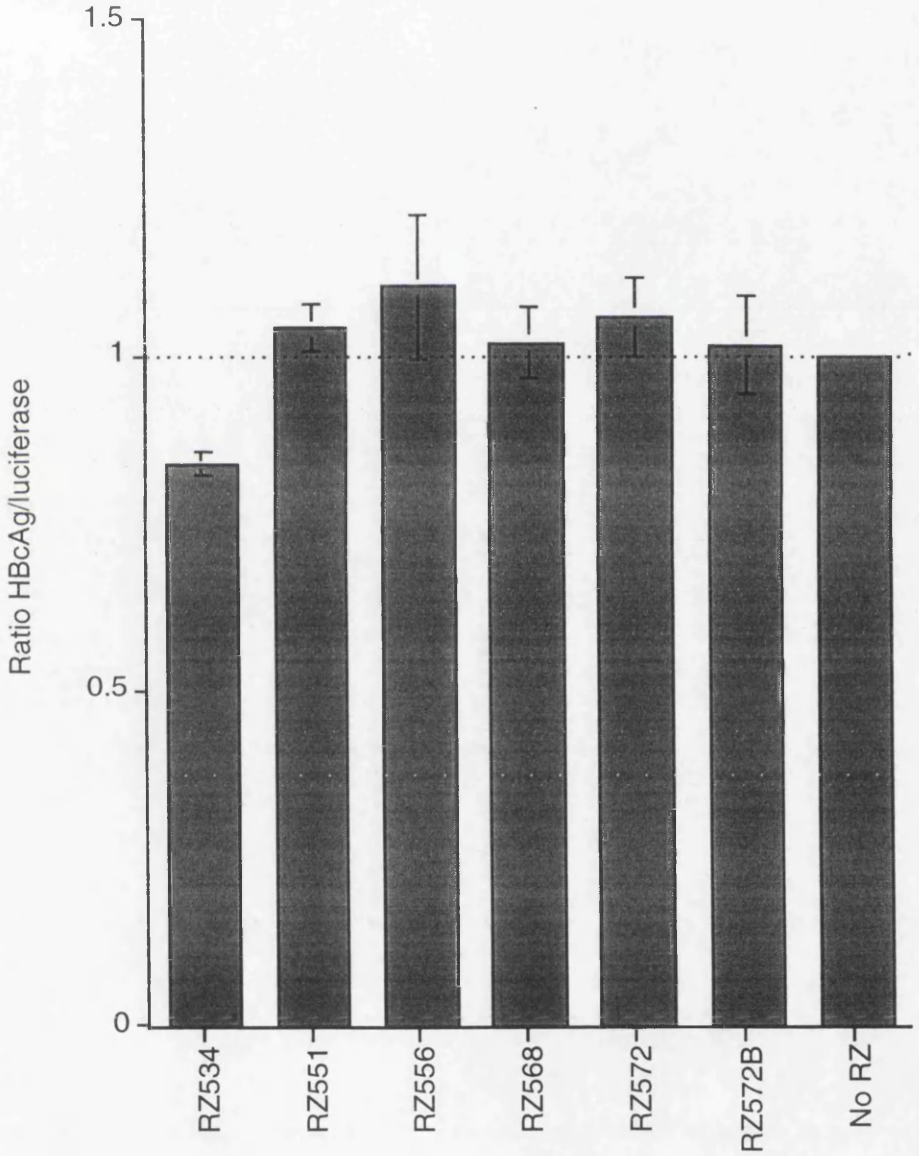

Figure 3.56. Mean results from five ribozyme/ rabbit reticulocyte lysate reactions. The quantity of HBcAg is expressed as the ratio of HBcAg to luciferase, as determined by phosphorimager scanning. The data from all five experiments was normalised relative to the negative control (no RZ). The only significant variation was seen with RZ534 ($p<0.05$, Student's t-test).

Is this variation the result of ribozyme activity? Primer extension analysis was used to detect the presence of cleavage products. This method utilises a radiolabelled oligonucleotide primer which binds to the 3' region of an RNA. Reverse transcriptase is used to extend from the primer to the 5'-end of the RNA. If the RNA has been cleaved by a ribozyme then the primer extension should be prematurely terminated (figure 3.56).

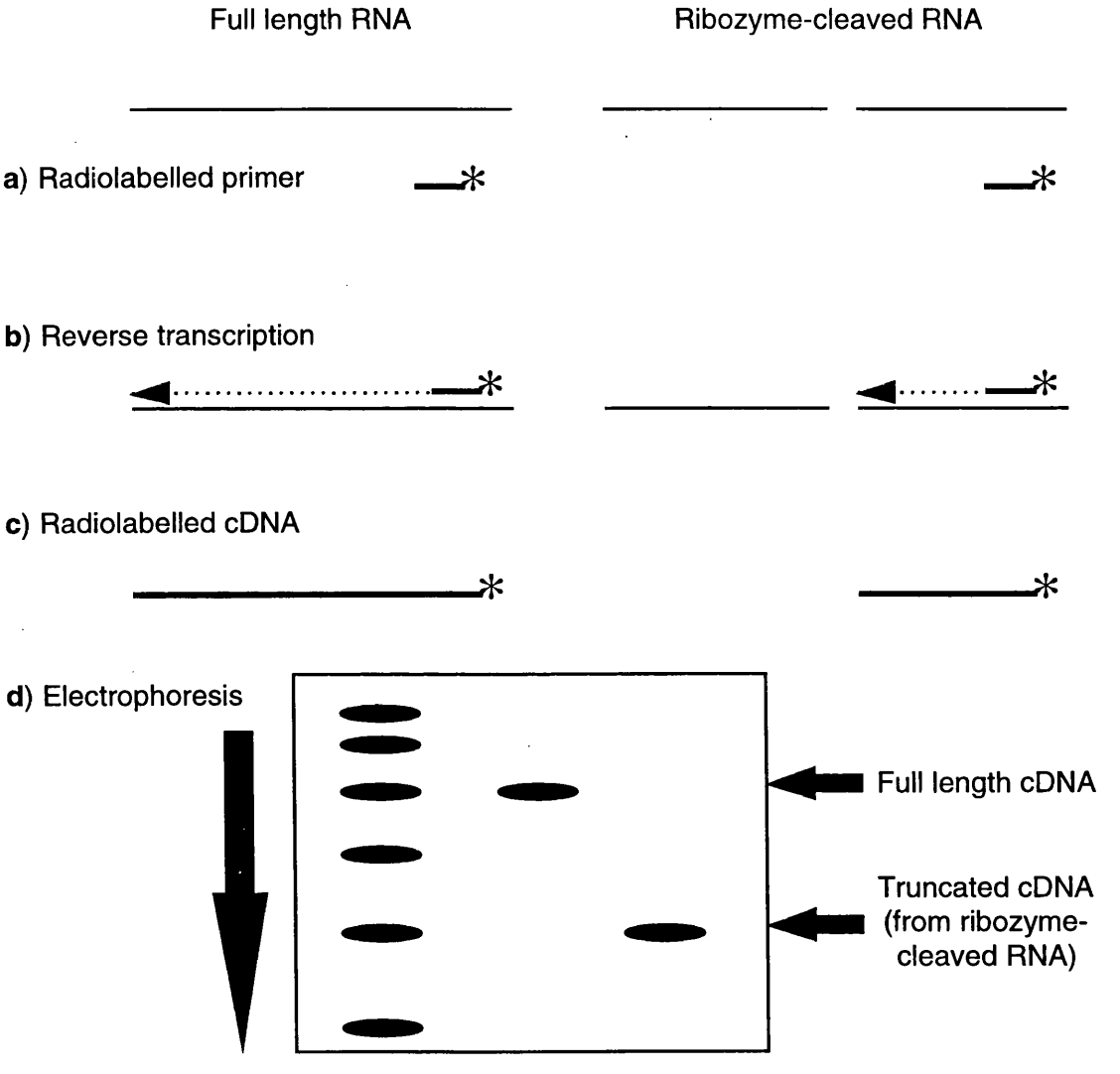

Figure 3.57. Detection of ribozyme cleavage products using primer extension analysis. Primer extension analysis allows the precise mapping of the 5' ends of RNA molecules. (**a**) A radiolabelled oligonucleotide primer is annealed near the 3' end of the RNA of interest. In order to detect ribozyme cleavage products the oligonucleotide must bind on the 3' side of the putative ribozyme cleavage point. (**b**) Reverse transcriptase is used to extend from the primer, using the RNA as a template. (**c**) Extension terminates at the 5' end of the RNA. If the RNA has been cleaved by a ribozyme, then the resulting cDNA is shorter than that produced from full length RNA. (**d**) Resolution of radiolabelled cDNAs by polyacrylamide gel electrophoresis.

RNA was acid-phenol extracted from rabbit reticulocyte lysate ribozyme reactions, and annealed to radiolabelled C2 primer. This primer, obtained from laboratory stocks, is designed to bind to the extreme 3'-end of the core ORF. Extension was performed using MMLV reverse transcriptase, and the products were separated by SDS-PAGE (figure 3.58). No ribozyme cleavage product was seen, only radiolabelled cDNA corresponding to the complete HBcAg mRNA as generated from the plasmid DNA template p5D.

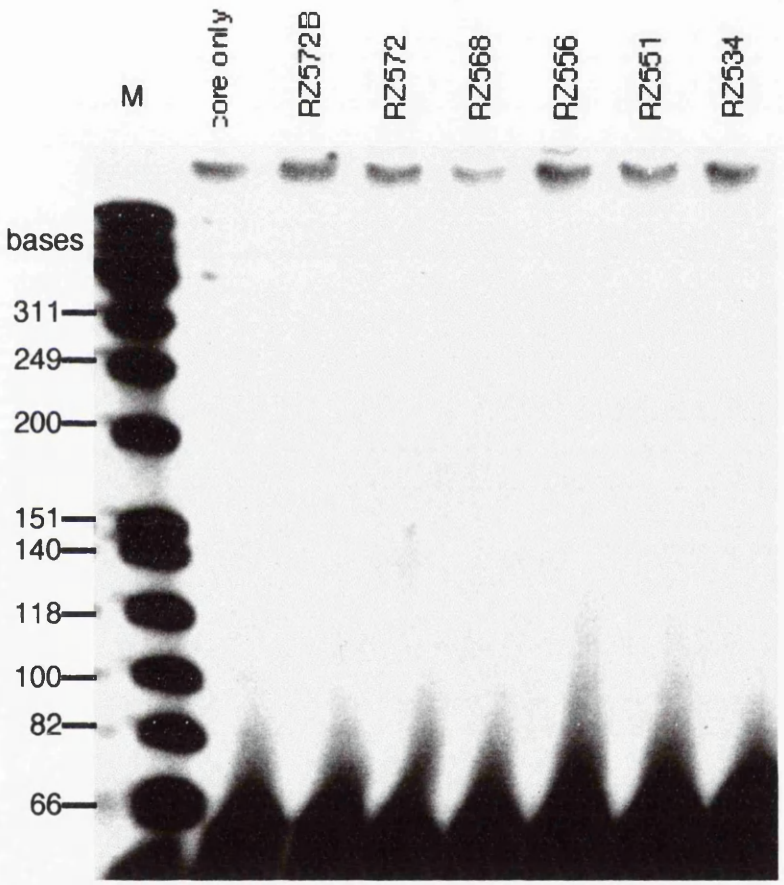

Figure 3.58. Primer extension of HBcAg mRNA extracted from rabbit reticulocyte lysate ribozyme reactions, using radiolabelled primer C2. In all lanes the expected cDNA product from full-length HBcAg mRNA is seen (approximately 640 bases). If ribozyme cleavage had occurred it would be expected that a product of approximately 100 bases in length would be seen. This is not the case. The dense band at the bottom of the gel is due to unextended primer. This band is higher up the gel than would be expected for a 28-base long primer. This is possibly due to there being too much primer added to the reaction, causing the primer in the sample to smear on the gel.

It was considered that perhaps this experiment was asking too much of the ribozymes. Rather than transcribing both the ribozymes and substrate simultaneously in the rabbit reticulocyte lysate it was decided to add ribozymes previously prepared by run-off *in vitro* transcription to rabbit reticulocyte lysate reactions in which HBcAg and the luciferase control were being transcribed and translated. Based on the estimated levels of HBcAg mRNA in the lysate reactions (0.8μM, see figure 3.49), a forty-fold excess of each individual ribozyme over substrate was added to the reticulocyte transcription-translation reactions. Initial reactions showed poor levels of HBcAg. This was thought to be due to insufficient non-coding sequence at the 5'-end of the HBcAg transcript. A second core construct containing a 5' untranslated region was obtained (pZeo-5D), and was found to express large quantities of HBcAg (figure 3.59). This construct was used in subsequent ribozyme reactions. Following a 90 minute incubation at 30°C, the reactions were analysed by SDS-PAGE (figure 3.60). No inhibition of HBcAg production on addition of the ribozymes to the coupled transcription-translation can be seen. As a result of this it was decided not to proceed with analysis of the HBcAg mRNA.

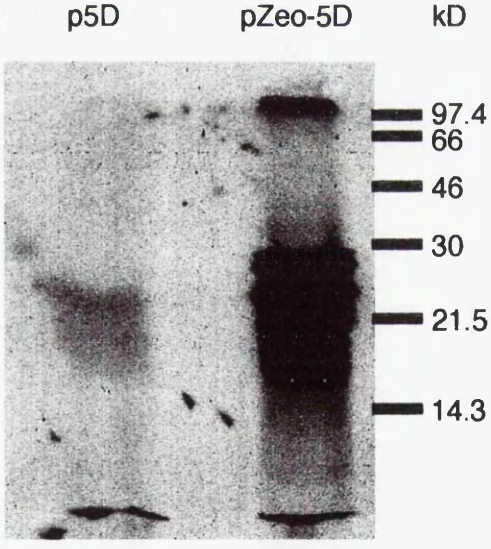

Figure 3.59. Comparison of expression of ^{35}S-methionine labelled HBcAg from p5D and pZeo-5D in rabbit reticulocyte lysate coupled transcription-translation reactions. 0.5μg of each plasmid was added to a 12.5μl reaction, which was incubated at 30°C for 90 minutes. Samples were analysed by SDS-PAGE, using a 17.5% polyacrylamide gel. The wide protein band is the result of translation being initiated from multiple start codons.

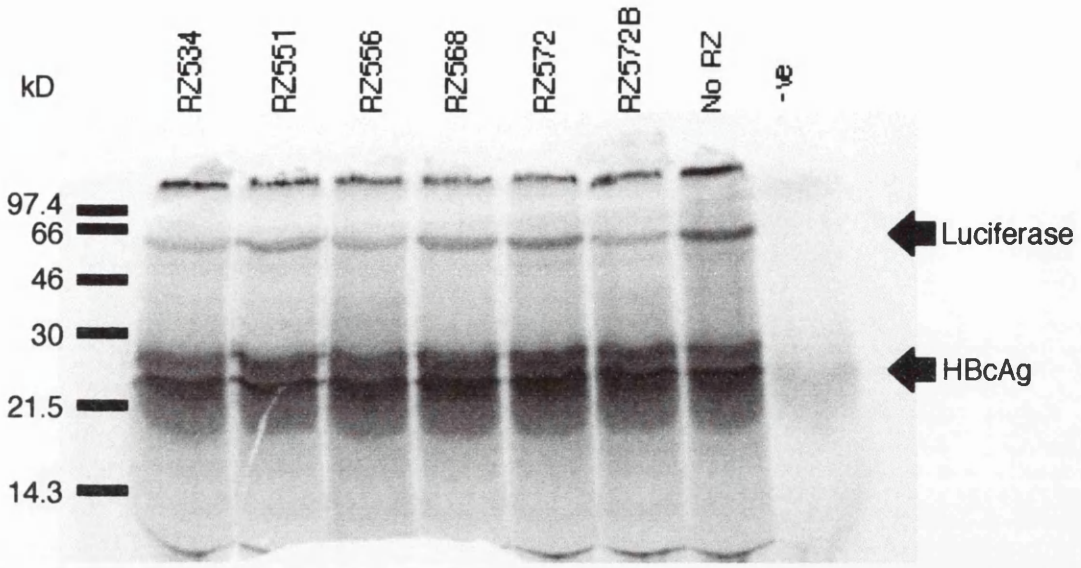

Figure 3.60. 17.5% SDS-polyacrylamide gel of luciferase and HBcAg expressed in rabbit reticulocyte lysate coupled transcription-translation reactions in the presence of 40μM anti-HBcAg ribozymes. The ribozymes were generated by in vitro transcription from partially single-stranded oligonucleotide templates, and were purified by phenol-chloroform extraction followed by ethanol precipitation. Individual ribozymes were added to transcription-translation reactions to a final concentration of 40μM. Reactions contained 0.5μg pZeo-5D (HBcAg template) and 0.025μg luciferase template. Reactions were incubated at 30°C for 90 minutes.

3.3.3 Discussion

Of the six ribozymes used in the current study, only RZ534 appeared to produce a reduction in HBcAg levels in the rabbit reticulocyte lysate *in vitro* translation system. Although overloading the translation reactions with partially single-stranded oligonucleotide template was shown to reduce translation (figure 3.55), this was not the case with RZ534, as the luciferase internal control was not affected (figure 3.56).

Was this reduction in HBcAg expression by RZ534 the result of ribozyme cleavage of the 5D RNA. Primer extension analysis failed to detect any cleavage products in RNA extracted from any of the rabbit reticulocyte lysate ribozyme reactions (figure 3.58). On the basis of this data it appeared that RZ534 was functioning by an antisense mechanism. However, repeating this experiment with pre-synthesised ribozyme RNA, rather than transcribing the ribozyme in the coupled transcription- translation reaction, showed that non of the ribozymes caused a significant decrease in HBcAg production. Therefore the reduction seen with RZ534 in the initial set of reticulocyte reactions was probably a result of the oligonucleotide template.

The rabbit reticulocyte lysate system is not an ideal system for studying ribozyme activity. *In vitro* translation systems are designed to rapidly produce large quantities of

protein. It has already been shown in sections 3.1 and 3.2 that the ribozymes used in this study have slow rates of hybridisation and cleavage. Northern blotting suggests that the ribozymes could be expressed from the partially single-stranded templates to give a five-fold excess of ribozyme over substrate. However, it is possible that the ribozymes, even when in excess over the substrate, are not being transcribed at a sufficient rate to enable them to keep up with the rapid rate of transcription and translation of HBcAg in the reticulocyte lysate system, and therefore cannot cause an appreciable reduction in protein synthesis. Even so, adding a large excess of pre-synthesised ribozyme RNA to the reticulocyte lysate reactions did not have any effect on HBcAg production (figure 3.60). The *in vitro* translation reactions only last for 90 minutes and are incubated at 30°C, whilst in section 3.2 it was shown that appreciable cleavage of the truncated substrate RZSUB took up to 10 hours at 37°C. It is possible that the ribozymes used here may cause appreciable reduction of HBcAg synthesis in cell culture, as such experiments are likely to take at least 24 hours, and levels of target RNA are likely to be lower than those seen in the reticulocyte lysate system. However, such studies would have to take into account the problems associated with intracellular localisation and processing of RNAs.

CHAPTER 4 CONCLUSIONS

Despite the availability of an efficacious vaccine for twenty years, hepatitis B is still a major public health problem. Although the introduction of global vaccination would eventually lead to the eradication of HBV, there are still over 300 million chronic carriers around the world. There is an urgent need for cheap, efficacious antiviral agents to either clear the virus from these carriers, or to reduce their infectivity. Current antivirals, reviewed in sections 1.7 and 1.8, include immune system modulators and inhibitors of HBV polymerase. This study has investigated an alternative approach using hammerhead ribozymes to specifically cleave HBV transcripts. The main goal was to try and deduce how substrate secondary structure is involved in determining the susceptibility of different regions of RNA to ribozyme cleavage. Although there have been a number of studies addressing this question in the past, the current study has divided the ribozyme reaction into two parts; ribozyme-substrate hybridisation, and substrate cleavage, and investigated how substrate secondary structure affects both of these steps in turn.

4.1 DOES SUBSTRATE SECONDARY STRUCTURE AFFECT RIBOZYME ACTIVITY?

Previous studies performed with both antisense and ribozymes have come up with varying answers, due in part to differences in the reaction conditions used. Nucleic acid hybridisation is particularly sensitive to ionic concentrations (Wang *et al.*, 1995). Also, ribozymes may bind to, but fail to cleave, their substrate. This does not mean that they will fail to work as gene-silencing agents, as they may still function *in vivo* as antisense agents. This has been observed in some studies in which ribozymes have failed to work *in vitro* but have inhibited protein synthesis in cell culture (Crisell *et al.*, 1993), though of course the converse is also true (Cotten & Birnstiel, 1989, Cameron & Jennings, 1994). For this reason it was decided to look at the two steps of the ribozyme reaction separately *in vitro*, then to see if these results could be duplicated in a cell-free translation system. In order to determine the effects of substrate secondary structure, a stem-loop was identified using computer modelling in the pre-core/core ORF which contained five potential ribozyme cleavage sites.

Ribozyme-substrate hybridisation was studied using a gel-shift assay system. Two different substrates were used: 5D RNA, corresponding to the entire pre-core/ core ORF, and RZSUB, a truncated substrate corresponding to the stem-loop to which the ribozymes were targeted. A truncated substrate was used as this was less prone to RNase degradation. As described in section 3.1, the accuracy of this technique was very poor. The hybridisation constants differed between the two substrates used, with much stronger binding being seen when 5D RNA was used. This does contradict earlier observations in which ribozymes

cleave shorter substrates more readily than longer substrates (Campbell *et al.*, 1997), which does lead to questions about the validity of the data. However, the initial experiments do suggest that RZSUB tends to associate with itself to form aggregates rather than binding the ribozyme, which could have played a part in producing this unusual observation. Even with the large inaccuracies in the current study, this does have interesting implications for much of the *in vitro* work that has been performed with ribozymes. Many studies have utilised truncated substrates rather than full-length mRNAs simply due to ease of handling shorter RNAs. The differences observed here in the hybridisation constants of the ribozymes with each substrate (for example, RZ534 fails to bind to RZSUB, but binds strongly to 5D RNA) obtained in this study implies that the conclusions reached in earlier studies are questionable in their relevance to physiological conditions. The current study is also flawed in this respect as it has not used the full-length substrate for these ribozymes. In an HBV infected cell, the core protein is translated from the 3.5kb pgRNA, which contains the 639 base pre-core/ core ORF. It was not possible to use the pgRNA as a substrate, as it is necessary to work in category 3 containment facilities when using this potentially infectious RNA and such facilities were not available.

The inaccuracies arising in the quantification of the gel-shifts led to a large amount of variability between repeated assays performed with the same ribozyme and substrate. This lack of reproducibility was cause for concern. In addition to analytical problems, the RNA-RNA gel-shift assay system is very sensitive to fluctuations in experimental conditions. The biggest problem in this area lies with variability between different batches of RNA generated by *in vitro* transcription. This arises from salt contamination during the purification process. Although much care was taken with repeated ethanol washes of the precipitated RNA, it would probably have been better to use one of the ion exchange resin spin-column systems which are now available for purifying and desalting the RNA. Another problem arose from repeating the gel-shifts with different concentrations of unlabelled substrate. As the substrate was in excess over the radiolabelled ribozyme the hybridisation reaction should have been under pseudo-first order kinetics, and the resulting hybridisation constants should have been virtually the same. However, this was not the case (figures 3.20, 3.22, and 3.23). This suggests that the reaction was still following second-order kinetics (i.e. was dependent on the concentrations of both components) and a higher concentration of unlabelled RNA was needed for pseudo-first-order kinetics to be achieved. Many of the graphs produced from the gel-shift data (figures 3.18 to 3.27) do not follow straight lines. This suggests an initial phase of rapid hybridisation followed by a period of slower binding. This could occur as a result of one or both of the RNAs assuming more than one conformation. Although, again, many of these problems can be attributed to the inaccuracies of the technique, this is unlikely to be the sole cause of the non-linearity of the data sets, or the variability of the hybridisation constants. Given that the non-linearity was seen in multiple data sets, and that the errors

associated with hybridisation constants within each group of experiments with the same RNA concentrations were small, it is unlikely that the observations described are artifactual.

With the problems arising from the gel-shift assay system, it was decided to develop an ELISA-based RNA-RNA hybridisation system (section 3.1.4). This would have the advantage of being able to screen many ribozymes at once, or a single ribozyme in a variety of reaction conditions. However, the ELISA failed to have sufficient sensitivity or reproducibility to serve as a successful assay system.

Do the results obtained in the gel-shift assays correlate to ribozyme-mediated cleavage activity? Only the truncated substrate, RZSUB, was used in the cleavage experiments due to the instability of the 5D RNA. An excess of ribozyme over substrate was used to ensure single-turnover conditions. Under such conditions the cleavage reaction, rather than hybridisation, would be the rate determining step. The results showed that a high hybridisation constant did not necessarily guarantee rapid substrate cleavage (table 3.5). The variation between RZ556 and RZ572 cleavage rates can be attributed to the differences in the target NUX triplet (CUA for RZ556 and CUC for RZ572), which has already been shown to affect ribozyme activity (Zoumadakis *et al.*, 1995). However, the difference in cleavage rates between RZ572 and RZ572B is more interesting. Both ribozymes were designed to cleave at the same target triplet. RZ572 has total flanking sequences of 16 bases, whilst RZ572B has total flanking sequences of 60 bases. Because of its longer flanking sequences, RZ572B binds more strongly to RZSUB than does RZ572. It has long been known that ribozymes with longer flanking sequences bind more strongly than those with shorter flanks; this observation is not dependent on the gel-shift assays described earlier. However, RZ572 cleaves RZSUB more rapidly under single-turnover conditions. This eliminates the problem, seen with ribozymes with long flanking sequences, of slow product dissociation reducing cleavage rate. As described in section 3.2.6, it is hypothesised that the flanking sequences alter the secondary structure of the substrate, and in doing so alter the rate of cleavage. This implies that a highly structured substrate may be beneficial to ribozyme activity, provided that the ribozyme is able to hybridize with the substrate. The phosphodiester bonds in RNA stem-loops are under considerable torsional stress, which it is proposed makes them more susceptible to ribozyme cleavage.

4.2 DO RESULTS OBTAINED *IN VITRO* CORRELATE WITH THOSE OBTAINED IN A CELL-FREE TRANSLATION SYSTEM?

As described previously, many studies have failed to convincingly duplicate *in vitro* results in cell culture. Either ribozymes which cleaved their substrate *in vitro* failed to function in cell culture, or else inhibition of protein synthesis was observed but the lack of adequate controls made it impossible to attribute this inhibition to ribozyme cleavage. Due to time constraints it was not possible to test the ribozymes designed in this study in cell culture. Instead it was decided to use the rabbit reticulocyte lysate coupled transcription-

translation system, which would enable the same constructs used in the earlier part of the study to be used.

A plasmid expressing firefly luciferase was used as an internal control to ensure that any inhibition of protein synthesis by the constructs used was specific to HBcAg. Following the reticulocyte ribozyme reactions, ^{35}S-L-methionine labelled proteins were visualised by SDS-PAGE and the bands quantified by phosphorimager scanning. The quantity of HBcAg was expressed as the ratio of HBcAg band intensity to luciferase band intensity. Initially non-specific inhibition of all protein synthesis was observed if too much oligonucleotide transcription template was used. However, once the system was optimised it was seen that only RZ534 caused a significant drop (20%) in HBcAg levels. Primer extension analysis of the RNA from these reactions failed to detect any ribozyme cleavage products in any of the reactions. This suggests that the reduction seen with RZ534 is the result of an antisense mechanism. As RZ534 is an RNA, it may be assumed that protein synthesis is stopped prematurely by the ribosome stalling on the mRNA when it reaches the ribozyme. If this hypothesis is correct then an inactive mutant RZ534 should produce the same effects, though lack of time prevented this experiment from being performed. However, it is difficult to draw any realistic conclusions from this work, as the hybridisation and cleavage kinetics of the ribozymes used in this study may prevent them from causing any appreciable inhibition of HBcAg expression in the rabbit reticulocyte lysate system, which is designed to rapidly produce very large quantities of mRNA and protein. It was decided to add ribozyme RNA synthesised by *in vitro* transcription to the reticulocyte lysate reactions. Under these conditions no inhibition of protein synthesis was seen with any of the ribozymes. This suggests that the inhibition seen with RZ534 was caused by the oligonucleotide transcription template for this ribozyme. It would be preferable to study ribozyme activity in cell culture, with HBcAg being expressed under the control of its endogenous promoter, in order to determine if these ribozymes are efficient enough to affect a natural HBV infection.

4.3 FUTURE PROSPECTS FOR RIBOZYMES

Will ribozymes live up to their early high expectations and find a place in medicine? Antisense oligonucleotides have survived the recent questions surrounding their safety and mechanism of action (see section 1.11.5), with a number of protocols currently in clinical trials. However, these antisense protocols are all based on chemically modified oligonucleotides which are synthesised exogenously and delivered as conventional pharmaceuticals (Bayever & Iversen, 1994, Bishop *et al.*, 1996). Although chemically modified active ribozymes have been constructed, it will be preferable for many applications to express unmodified ribozymes from genes delivered to the target tissue.

Despite early enthusiasm, the field of human gene therapy has stalled due to the requirements for safe, efficient vectors. A number of different approaches have been

investigated. These can be divided into non-viral and viral methods. Non-viral methods have focused on cationic liposomes (Song *et al.*, 1997). The DNA of interest wraps around the liposome. The lipid component of the DNA-liposome complex fuses with the plasma membrane and deposits the DNA into the endosome. Because of the digestive enzymes in the endosome most of the DNA delivered in this fashion is destroyed. Therefore this method has very low efficiency *in vivo* as demonstrated in early trials of corrective gene therapy for cystic fibrosis (Caplen *et al.*, 1995). Liposomes also have no target cell specificity, though current studies are attempting to target liposomes by embedding ligands for cell surface receptors into the liposome (Felgner, 1996). An alternative cationic DNA carrier is poly-L-lysine (Martinez-Fong *et al.*, 1994). This can be covalently linked to proteins to enable cell targeting. Numerous experiments have utilized poly-L-lysine-asialoglycoprotein conjugates, which are targeted to hepatocytes. This has enabled antisense oligonucleotides (both unmodified and with phosphorothioate backbones) to be successfully targeted against transient transfections of HBsAg in hepatocytes (Wu & Wu, 1991) and against WHV in woodchucks (Bartholomew *et al.*, 1995). Another alternative is to conjugate DNA to native lipoproteins called chylomicrons which are targeted to the liver (Rensen *et al.*, 1995).

Viral vectors come in several categories; retroviruses, adenoviruses and adeno-associated virus. Retroviruses are widely used for transduction of mammalian cells, though they do have a limited coding capacity (though this is not a problem for small antisense and ribozyme constructs) and concerns have been raised about the possibility of recombination with endogenous human retroviruses. Because of this only murine retroviruses have been used for human applications to date, and these are only licensed for *ex vivo* use, as in the trials of the anti-HIV-1 hairpin ribozyme (section 1.12.3b) (Ho *et al.*, 1994, Rosenzweig *et al.*, 1997). Although retroviruses can integrate into the host chromosomes, thus stably transducing target cells, they can only do this in dividing cells. Future protocols are likely to be based on lentiviruses which are capable of infecting non-dividing cells. Target specificity can be altered either by chemical modification of surface glycoproteins (Neda *et al.*, 1991) or by generating pseudotyped viruses containing surface proteins from a source other than the parent retroviral strain (Freedman & Yee, 1995). Adenoviruses have a large coding capacity, and the ability to efficiently infect a wide variety of cell types. The penton base protein in the viral capsid allows viral DNA to be delivered into the cytoplasm from the endosome (Seth, 1994). Adenovirus vectors have been successfully used to transfect human hepatocytes with anti-HCV ribozymes (Lieber *et al.*, 1996a) and to target anti-human growth hormone ribozymes to the livers of transgenic mice (Lieber *et al.*, 1996b). However, safety issues concerning lack of tissue specificity and possible immune reaction make adenoviruses unattractive vectors. This follows the development of pneumonia in a number of patients in a phase I clinical trial utilizing adenovirus vectors in corrective therapy for cystic fibrosis (Wilmott *et al.*, 1994, Wilmott *et al.*, 1996). There is also the possibility of an immune response being raised against the vector. This is likely to be mediated by memory cells as

the vast majority of the population has been infected at one time or another with at least one strain of human adenovirus. Because of this it is likely that adenoviruses from other mammalian species will be used in future (Klonjkowski *et al.*, 1997). The adeno-associated virus, which is a satellite virus of human adenoviruses, is able to insert into a specific site in chromosome 19, which does not disrupt any proto-oncogenes (which is a risk of using randomly integrating retroviruses). Adeno-associated virus is not associated with any disease. However, the limited coding capacity and also the potential to recombine with other parts of the host DNA at low frequency do pose problems (Linden *et al.*, 1996).

The problems of delivery mean that initial ribozyme therapy protocols (and indeed gene therapy protocols in general) are likely to fall into three groups. The first involves *ex vivo* modification of tissues which are then replaced into the patient. The most obvious application is in the area of haematological disorders. This is already happening with the anti-HIV-1 hairpin ribozyme trial. It has been proposed to use antisense oligonucleotides to purge the bone marrow of leukaemia patients of malignant cells (Bishop *et al.*, 1997). The treated bone marrow would then be returned in an autologous transplant back to the patient. The *ex vivo* approach allows a specific cell population to be exposed to a vector which may not have a high tissue specificity without exposing non-target tissues to transduction. The modified cells can be screened before return to ensure all vector has been removed. The second area concerns the treatment of solid tumours. Vectors can be injected directly into the tumour, removing the need for the vector to circulate around the body searching for its target. This approach has already been used with E1-negative adenoviruses (Kirn *et al.*, 1997). These are only able to grow in cells where the p53 tumour suppressor is inactive, producing a lytic infection which destroys tumour cells, but leaves healthy tissue untouched. The final area involves treatments of external disorders. These are almost entirely dermatological, and could include papillomavirus infection and melanoma. Antisense oligonucleotides targeted against human papillomavirus strains 16 and 18 (implicated in cervical cancer) have blocked viral expression in cultured cells taken from genital warts (Baker & Tyring, 1997). Such therapies are likely to be delivered in a liposome cream preparation, with uptake possibly enhanced by the addition of dimethylsulphoxide.

Clearly none of these approaches are suitable for the long-term treatment of viral hepatitis. As described above, both viral and non-viral delivery systems have been used in animal models to target ribozymes or antisense to the liver. Whether these approaches would be suitable for long-term treatment is unknown. Repeated administration with such vectors could lead to an immune response which could at best lead to failure of therapy or, at worst, lead to a range of immune complex disorders. It would be more desirable to use a retroviral or lentiviral vector which could stably integrate into hepatocytes and produce a population of HBV-resistant hepatocytes. An alternative approach would be to use HBV itself as a vector. Inclusion of an HBV encapsidation signal and direct repeats DR1 and DR2, into a vector construct would enable the therapeutic RNA to be encapsidated by viral proteins present in

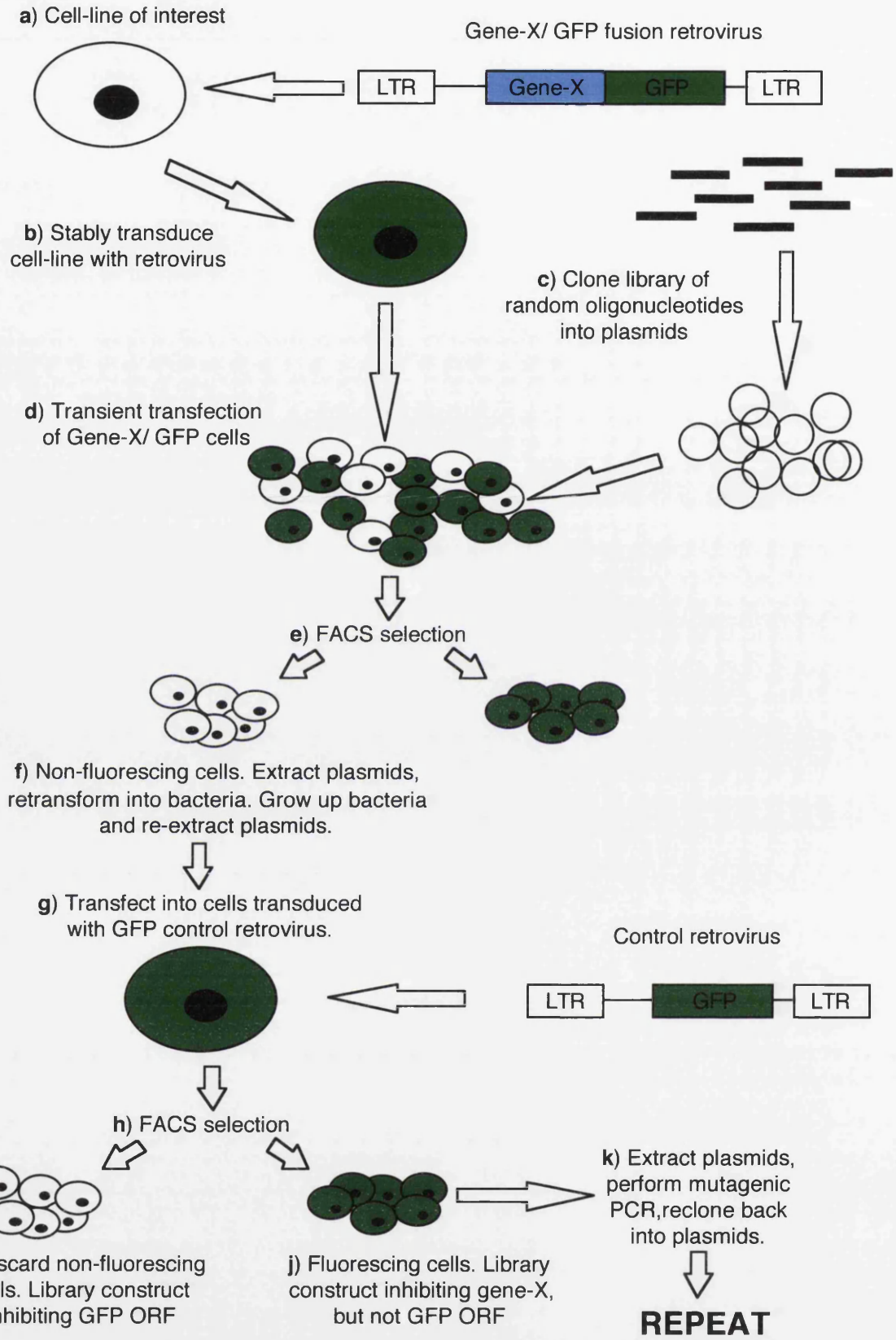
a) Cell-line of interest
Gene-X/ GFP fusion retrovirus
LTR
Gene-X
GFP
LTR
b) Stably transduce cell-line with retrovirus
c) Clone library of random oligonucleotides into plasmids
d) Transient transfection of Gene-X/ GFP cells
e) FACS selection
f) Non-fluorescing cells. Extract plasmids, retransform into bacteria. Grow up bacteria and re-extract plasmids.
g) Transfect into cells transduced with GFP control retrovirus.
Control retrovirus
LTR
GFP
LTR
h) FACS selection
i) Discard non-fluorescing cells. Library construct inhibiting GFP ORF
j) Fluorescing cells. Library construct inhibiting gene-X, but not GFP ORF
k) Extract plasmids, perform mutagenic PCR,reclone back into plasmids.
REPEAT

Figure 4.1. Proposed scheme for intracellular selection of gene-silencing RNAs. **a**) For the initial round of selection the cell-line of interest must be stably transduced with an appropriate reporter construct (**b**). This can be rapidly acheived using a retrovirus containing a fusion of the gene of interest (gene-X) and the jellyfish green fluorescent protein (GFP) ORFs. It must be ensured that such a fusion protein still has the GFP fluorescence activity.

c) A library of random synthetic double-stranded oligonucleotides is cloned into plasmids under the control of an appropriate mammalian promoter. The oligonucleotides could have either an entirely random sequence, or a ribozyme catalytic domain could be included in the centre of the oligonucleotide and be flanked by random sequences. **d**) The library is transiently transfected into the gene-X/ GFP cells. The amount of plasmid DNA added to the cells should be such that on average each transfected cell contains one plasmid. **e**) Some of the cells will contain plasmids which are expressing RNAs that block expression of the gene-X/ GFP fusion protein. These cells will fail to fluoresce, and can be separated from the rest of the cells by fluorescence activated cell sorting (FACS) scanning. **f**) Plasmids are extracted from the non-fluorescing cells. These can be amplified by retransforming the plasmids back into bacteria, growing up the bacteria, then re-extracting the plasmids.

Some of the constructs which inhibited fluorescence in the first round of selection could have been acting by ribozyme or antisense mechanisms on the GFP ORF rather than the gene-X ORF. These must be removed from the selected plasmids. **g**) The plasmids are transfected into cells stably transduced with a retrovirus only expressing GFP. **h**) The transfected cells are again sorted by FACS. **I**) The non-fluorescing cells are discarded. The constructs in these cells are inhibiting GFP directly rather than by targeting the gene-X portion of the fusion transcript. **j**) The fluorescing cells have been transfected with constructs which, although they can target the gene-X ORF, do not affect the GFP transcript directly. **k**) The plasmids are extracted from the fluorescing cells. The selected plasmids can be further enriched by repeating the process back at step (**d**). The selected plasmids can be mutagenized by PCR, enabling mutations with enhanced inhibitory activity to be evolved. Selection pressure can be increased by increasing the stringency of selection by FACS. This can be done by altering the cut-off point between fluorescing and non-fluorescing cells.

the patient's liver. It would be necessary to include the polymerase gene, as the polymerase becomes associated with the encapsidation signal in the pgRNA from which it was translated, though the core, surface and X ORFs would be truncated, and therefore inactive. This would ensure that the vector could only be propagated in cells already infected with wild-type HBV. Once the vector construct was in the liver, it would produce a second generation of vectors which would go on to infect more HBV-infected hepatocytes. Such an approach is attractive in that only one initial injection of vector is required, after which the vector continues to multiply in the patient until all the wild-type HBV is cleared. Once the wild-type virus has been cleared there are no more proteins to package the vector, and the vector disappears. The main concern with this approach is that of safety, as the vector could foreseeably spread from the patient and infect other people. Although the vector should only replicate in people infected with HBV, such a possibility is not likely to be entertained by the current legislation concerning the release of genetically modified organisms. Although ribozymes and antisense could rapidly suppress HBV gene expression, the cccDNA would still be present. There are no therapies currently available which target the cccDNA. The only potential treatment would be triplex forming oligonucleotides, especially those conjugated to a chemically modifying group (see section 1.10). Initial cell culture studies utilizing HBV promoter/ luciferase reporter constructs have been encouraging (Ito *et al.*, 1997), though care would be needed to ensure that such oligonucleotides had sufficient specificity. It is unlikely that any form of gene therapy will be used in the foreseeable future for the treatment of chronic HBV given the current therapies available. Combination therapies consisting of such treatments as interferon, lamivudine, famciclovir and ganciclovir are proven to be effective, and are cheaper than a potential gene therapy treatment. Given that vector production would need to be closely monitored, would require extensive mammalian cell culture (if a viral method was used), and that patients would need close observation, it is unlikely that gene therapy would be practical outside of the developed world. As most of the world's HBV carriers are in the developing world a cheap treatment requiring a minimum of doses is required. From this standpoint it appears that therapeutic vaccination is probably the most cost-effective and practical method of managing chronic HBV infection (section 1.7.7).

Although ribozymes are probably not going to find a place treating HBV, they could still be used in a variety of other applications. These are likely to be in dominant negative genetic disorders such as osteogenesis imperfecta (Marini & Gerber, 1997), where genes need to be silenced rather than replaced and in the treatment of tumours. An important factor to consider is the choice of ribozyme target site. It is clear from many studies, including this one, that *in vitro* studies do not necessarily correlate with those seen in cell-free translation systems and in cell culture. It can also be seen from the present study that ribozyme activity and substrate accessibility (as predicted by computer modelling) do not correlate. Therefore it is proposed that in future ribozymes should be designed by a method of intracellular

selection, as detailed in figure 4.1. This method enables inhibitory RNAs to be selected in the environment in which they are ultimately supposed to function. By using a library of entirely randomised sequence not only ribozymes, but antisense and RNase P external guide sequences could potentially be selected. By performing multiple rounds of selection interspersed with rounds of mutagenic PCR, the initial selection from the library can be evolved through several generations to obtain the optimum inhibitor.

It is rapidly becoming clear that designing ribozymes purely by guesswork, as has been the case in nearly all ribozyme research to date, is far from being the best approach to coming up with gene-silencing tools. *In vitro* work has failed to progress successfully to cell culture and *in vivo* applications, leaving many groups disheartened with the ribozyme approach and writing it off as a dead end. Ribozymes will in the future have a place in the gene therapy armoury, though probably only in certain applications. The use of intracellular selection procedures will allow the rapid screening of RNA libraries and the identification of effective gene-silencing RNAs. However, for these constructs to become useful therapies, it will be necessary for safe and efficient delivery systems to be developed.

REFERENCES

Abe, J., Zhou, W., Taguchi, J., Takuwa, N., Miki, K., Okazaki, H., Kurokawa, K., Kumada, M. & Takuwa, Y. (1994). Suppression of neointimal smooth-muscle cell accumulation *in vivo* by antisense CDC2 and CDK2 oligonucleotides in rat carotid-artery. *Biochemical and Biophysical Research Communications* **198**, 16-24.

Agrawal, S., Tan, W. T., Cai, Q. Y., Xie, X. W. & Zhang, R. W. (1997). *In vivo* pharmacokinetics of phosphorothioate oligonucleotides containing contiguous guanosines. *Antisense & Nucleic Acid Drug Development* **7**, 245-249.

Akbar, S. M. F., Inaba, K. & Onji, M. (1996). Up-regulation of MHC class-II antigen on dendritic cells from hepatitis B virus transgenic mice by interferon-gamma - abrogation of immune-response defect to a T-cell-dependent antigen. *Immunology* **87**, 519-527.

Aldershvile, J., Frosner, G. G., Nielsen, J. O., Hardt, F., Dienhardt, F. & Skinhoj, P. (1980). Hepatitis B e-antigen and antibody measured by radioimmunoassay in acute hepatitis B surface antigen-positive hepatitis. *Journal of Infectious Disease* **141**, 293-298.

Altman, S. (1993). RNA enzyme-directed gene-therapy. *Proceedings Of the National Academy of Sciences of the United States of America* **90**, 10898-10900.

Altman, S., Baer, M., Cudny, H. & McCorkle, G. (1981). RNase-P and transfer-RNA processing. *Federation Proceedings* **40**, 1651-1651.

Altman, S., Baer, M. F., Bartkiewicz, M., Gold, H., Guerriertakada, C., Kirsebom, L. A., Lumelsky, N. & Peck, K. (1989). Catalysis by the RNA subunit of RNase-P - a minireview. *Gene* **82**, 63-64.

Altman, S. & Guerrier-Takada, C. (1986). M1-RNA, the RNA subunit of *Escherichia coli* ribonuclease-P, can undergo a pH-sensitive conformational change. *Biochemistry* **25**, 1205-1208.

Altman, S., Vioque, A., Kirsebom, L., Baer, M. & Guerriertakada, C. (1987). Interactions of the protein subunit of *Escherichia coli* ribonuclease P with the catalytic RNA subunit. *Federation Proceedings* **46**, 2052-2052.

Andreone, P., Cursaro, C., Gramenzi, A., Miniero, R., Manzin, A., Severini, R., Franzone, J. S., Clementi, M., Sprovieri, G. & Gasbarrini, G. (1993). Preliminary results of thymosin-alpha-1 versus IFN-alpha treatment in patients with HBeAg negative and HBV-DNA positive chronic active hepatitis. *International Journal of Immunotherapy* **9**, 201-205.

Anonymous. (1997). Banana vaccines and other developments - The Jordan Report. *Public Health Reports* **112**, 93-93.

Araki, K., Miyazaki, J.-I., Hino, O., Tomita, N., Chisaka, O., Matsubara, K. & Yamamura, K.-I. (1989). Expression and replication of hepatitis B virus genome in transgenic mice. *Proceedings of the National Academy of Sciences of the United States of America* **86**, 207-211.

Arii, M., Takada, S. & Koike, K. (1992). Identification of 3 essential regions of hepatitis B virus X-protein for transactivation function. *Oncogene* **7**, 397-403.

Arnold, L. (1996). High affinity antisense oligonucleotides and their application to disease targets. *Antisense Therapeutics: International Business Communications Conference Proceedings, Coronado, CA, February 1996.*

Baker, G. E. & Tyring, S. K. (1997). Therapeutic approaches to papillomavirus infections. *Dermatologic Clinics* **15**, 331.

Barawkar, D. A., Kumar, V. A. & Ganesh, K. N. (1994). Triplex formation at physiological pH by oligonucleotides incorporating 5-Me-dC-(N-4-Spermine). *Biochemical and Biophysical Research Communications* **205**, 1665-1670.

Barawkar, D. A., Rajeev, K. G., Kumar, V. A. & Ganesh, K. N. (1996). Triplex formation at physiological pH by 5-Me-dC-N-4-(Spermine) [X] oligodeoxynucleotides - non protonation of N3 in X of X-*-G-C triad and effect of base mismatch ionic strength on triplex stabilities. *Nucleic Acids Research* **24**, 1229-1237.

Bartenschlager, R., Junkerniepmann, M. & Schaller, H. (1990). The P-gene product of hepatitis B virus is required as a structural component for genomic RNA encapsidation. *Journal of Virology* **64**, 5324-5332.

Bartenschlager, R. & Schaller, H. (1992). Hepadnaviral assembly is initiated by polymerase binding to the encapsidation signal in the viral-RNA genome. *EMBO Journal* **11**, 3413-3420.

Bartholomew, M. M., Jansen, R. W., Jeffers, L. J., Reddy, K. R., Johnson, L. C., Bunzendahl, H., Condreay, L. D., Tzakis, A. G., Schiff, E. R. & Brown, N. A. (1997). Hepatitis B-virus resistance to lamivudine given for recurrent infection after orthotopic liver transplantation. *Lancet* **349**, 20-22.

Bartholomew, R. M., Carmichael, E. P., Findeis, M. A., Wu, C. H. & Wu, G. Y. (1995). Targeted delivery of antisense DNA in woodchuck hepatitis virus- infected woodchucks. *Journal of Viral Hepatitis* **2**, 273-278.

Bass, B. L. & Cech, T. R. (1984). Specific interaction between the self-splicing RNA of *Tetrahymena* and its guanosine substrate - Implications for biological catalysis by RNA. *Nature* **308**, 820-826.

Bates, P. J., Macaulay, V. M., McLean, M. J., Jenkins, T. C., Reszka, A. P., Laughton, C. A. & Neidle, S. (1995). Characteristics of tripler-directed photoadduct formation by psoralen-linked oligodeoxynucleotides. *Nucleic Acids Research* **23**, 4283-4289.

Bayever, E. & Iversen, P. (1994). Oligonucleotides in the treatment of leukemia. *Hematological Oncology* **12**, 9-14.

Bayraktar, Y., Koseoglu, T., Temizer, A., Kayhan, B., Vanthiel, D. H. & Uzunalimoglu, B. (1996). Relationship between the serum alanine aminotransferase level at the end of interferon treatment and histologic-changes in wild-type and precore mutant hepatitis-B virus infections. *Journal of Viral Hepatitis* **3**, 137-142.

Bchini, R., Capel, F., Dauguet, C., Dubanchet, S. & Petit, M. A. (1990). *In vitro* infection of human hepatoma (HepG2) cells with hepatitis B virus. *Journal of Virology* **64**, 3025-3032.

Beck, J. & Nassal, M. (1995). Efficient hammerhead ribozyme-mediated cleavage of the structured hepatitis B virus encapsidation signal *in vitro* and in cell-extracts, but not in intact-cells. *Nucleic Acids Research* **23**, 4954-4962.

Been, M. D., Barfod, E. T., Burke, J. M., Price, J. V., Tanner, N. K., Zaug, A. J. & Cech, T. R. (1987). Structures involved in *Tetrahymena* ribosomal RNA self-splicing and RNA enzyme activity. *Cold Spring Harbor Symposia on Quantitative Biology* **52**, 147-157.

Benhamou, Y., Lunel, F., Dohin, E., Gentilini, M., Katlama, C., Huraux, J. M., Poynard, T. & Opolon, P. (1995). 3TC(TM) (lamivudine, 109714x) activity on hepatitis B virus (HBV) replication in HIV-infected patients - Preliminary results. *Gastroenterology* **108**, A1033-A1033.

Benn, J., Su, F., Doria, M. & Schneider, R. J. (1996). Hepatitis B virus HBx protein induces transcription factor AP-1 by activation of extracellular signal-regulated and *c-jun* N-terminal mitogen-activated protein kinases. *Journal Of Virology* **70**, 4978-4985.

Bennett, M. R., Anglin, S., McEwan, J. R., Jagoe, R., Newby, A. C. & Evan, G. I. (1994). Inhibition of vascular smooth-muscle cell-proliferation *in vitro* and *in vivo* by *c-myc* antisense oligodeoxynucleotides. *Journal of Clinical Investigation* **93**, 820-828.

Berting, A., Hahnen, J., Kroger, M. & Gerlich, W. H. (1995). Computer-aided studies on the spatial structure of the small hepatitis B surface protein. *Intervirology* **38**, 8-15.

Bertoletti, A., Sette, A., Chisari, F. V., Penna, A., Levrero, M., Decarli, M., Fiaccadori, F. & Ferrari, C. (1994). Natural variants of cytotoxic epitopes are T-cell receptor antagonists for antiviral cytotoxic T-cells. *Nature* **369**, 407-410.

Bertrand, E. L. & Rossi, J. J. (1994). Facilitation of hammerhead ribozyme catalysis by the nucleocapsid protein of HIV-1 and the heterogeneous nuclear ribonucleoprotein A1. *EMBO Journal* **13**, 2904-2912.

Berzalherranz, A., Joseph, S., Chowrira, B. M., Butcher, S. E. & Burke, J. M. (1993). Essential nucleotide-sequences and secondary structure elements of the hairpin ribozyme. *EMBO Journal* **12**, 2567-2574.

Bianchi, N., Rutigliano, C., Passadore, M., Tomassetti, M., Pippo, L., Mischiati, C., Feriotto, G. & Gambari, R. (1997). Targeting of the HIV-1 long terminal repeat with chromomycin potentiates the inhibitory effects of a triplex-forming oligonucleotide on Sp1-DNA interactions and in vitro transcription. *Biochemical Journal* **326**, 919-927.

Birnbaum, F. & Nassal, M. (1990). Hepatitis B virus nucleocapsid assembly - primary structure requirements in the core protein. *Journal of Virology* **64**, 3319-3330.

Bishop, M. R., Iversen, P. L., Bayever, E., Sharp, J. G., Greiner, T. C., Copple, B. L., Ruddon, R., Zon, G., Spinolo, J., Arneson, M., Armitage, J. O. & Kessinger, A. (1996). Phase-I trial of an antisense oligonucleotide Ol(1)p53 in hematologic malignancies. *Journal of Clinical Oncology* **14**, 1320-1326.

Bitter, G. A., Egan, K. M., Burnette, W. N., Samal, B., Fieschko, J. C., Peterson, D. L., Downing, M. R., Wypych, J. & Langley, K. E. (1988). Hepatitis B vaccine produced in yeast. *Journal of Medical Virology* **25**, 123-140.

Blum, H. E., Galun, E., Von Weizsacker, F. & Wands, J. R. (1991). Inhibition of hepatitis B virus by antisense oligodeoxynucleotides. *Lancet* **337**, 1230-1230.

Blum, H. E., Zhang, Z. S., Galun, E., Von Weizsacker, F., Garner, B., Liang, T. J. & Wands, J. R. (1992). Hepatitis B virus X-protein is not central to the viral life-cycle *in vitro*. *Journal of Virology* **66**, 1223-1227.

Bock, L. C., Griffin, L. C., Latham, J. A., Vermaas, E. H. & Toole, J. J. (1992). Selection of single-stranded-DNA molecules that bind and inhibit human thrombin. *Nature* **355**, 564-566.

Bockman, J. M., Narayan, P., Takle, G. B., Drivas, G. T., Siony, S., George, S. T. & Goldberg, A. R. (1993). Ribonuclease-P can cleave hepatitis B virus-RNA in the presence of External Guide Sequences. *Journal of Cellular Biochemistry*, 210-210.

Bosch, O., Moraleda, G., Castillo, I. & Carreno, V. (1993). Treatment of chronic hepatitis-B with recombinant interferon-alpha versus recombinant interferon-alpha plus levamisole. *Journal of Hepatology* **19**, 437-441.

Branch, A. D. & Robertson, H. D. (1991). Efficient *trans*-cleavage and a common structural motif for the ribozymes of the human hepatitis-delta agent. *Proceedings of the National Academy of Sciences of the United States of America* **88**, 10163-10167.

Bridgen, A. & Elliott, R. M. (1996). Rescue of a segmented negative-strand RNA virus entirely from cloned complementary DNAs. *Proceedings of the National Academy of Sciences of the United States of America* **93**, 15400-15404.

Brown, R. S., Dewan, J. C. & Klug, A. (1985). Crystallographic and biochemical investigation of the lead(II)- catalyzed hydrolysis of yeast phenylalanine transfer-RNA. *Biochemistry* **24**, 4785-4801.

Brown, R. S., Hingerty, B. E., Dewan, J. C. & Klug, A. (1983). Pb(II)-catalysed cleavage of the sugar-phosphate backbone of yeast transfer RNA^{Phe} - Implications for lead toxicity and self-splicing RNA. *Nature* **303**, 543-546.

Brunetto, M. R., Oliveri, F., Demartini, A., Calvo, P., Manzini, P., Cerenzia, M. T. & Bonino, F. (1991). Treatment with interferon of chronic hepatitis B associated with antibody to hepatitis B e-antigen. *Journal of Hepatology* **13**, S 8-S 11.

Bruss, V., Gerhardt, E., Vieluf, K. & Wunderlich, G. (1996a). Functions of the large hepatitis B virus surface protein in viral particle morphogenesis. *Intervirology* **39**, 23-31.

Bruss, V. & Gerlich, W. H. (1988). Formation of transmembraneous hepatitis B e-antigen by cotranslational *in vitro* processing of the viral precore protein. *Virology* **163**, 268-275.

Bruss, V., Hagelsten, J., Gerhardt, E. & Galle, P. R. (1996b). Myristylation of the large surface protein is required for hepatitis B virus *in vitro* infectivity. *Virology* **218**, 396-399.

Bruss, V., Lu, X. Y., Thomssen, R. & Gerlich, W. H. (1994). Post-translational alterations in transmembrane topology of the hepatitis B virus large envelope protein. *EMBO Journal* **13**, 2273-2279.

Bulla, G. A. & Siddiqui, A. (1988). The hepatitis B virus enhancer modulates transcription of the hepatitis-B virus surface-antigen gene from an internal location. *Journal of Virology* **62**, 1437-1441.

Buti, M., Rodriguezfrias, F., Genesca, J., Arranz, A., Jardi, R., Esteban, R. & Guardia, J. (1993). Disappearance of serum hepatitis B virus DNA by Polymerase Chain-Reaction after adenine arabinoside 5'-monophosphate therapy in chronic hepatitis B. *Liver* **13**, 136-140.

Campbell, T. B., McDonald, C. K. & Hagen, M. (1997). The effect of structure in a long target RNA on ribozyme cleavage efficiency. *Nucleic Acids Research* **25**, 4985-4993.

Cameron, F. H. & Jennings, P. A. (1994). Multiple domains in a ribozyme construct confer increased suppressive activity in monkey cells. *Antisense Research and Development* **4**, 87-94.

Capalbo, M., Actis, C., Maurizia, R., Brunetto, R., Poli, G., Baldi, M., Palmisano, L., Verme, G. & Bonino, F. (1992). Treatment of chronic hepatitis B with beta interferon given intramuscularly - A pilot-study. *Italian Journal of Gastroenterology* **24**, 203-205.

Caplen, N. J., Alton, E. W. F. W., Middleton, P. G., Dorin, J. R., Stevenson, B. J., Gao, X., Durham, S. R., Jeffery, P. K., Hodson, M. E., Coutelle, C., Huang, L., Porteous, D. J., Williamson, R. & Geddes, D. M. (1995). Liposome-mediated CFTR gene transfer to the nasal epithelium of patients with cystic fibrosis. *Nature Medicine* **1**, 39-46.

Carman, W. F., Boner, W., Fattovich, G., Colman, K., Dornan, E. S., Thursz, M. & Hadziyannis, S. (1997a). Hepatitis B virus core protein mutations are concentrated in B cell epitopes in progressive disease and in T helper cell epitopes during clinical remission. *Journal of Infectious Diseases* **175**, 1093-1100.

Carman, W. F., Jacyna, M. R., Karayiannis, P., Hadziyannis, S., McGarvey, M. J., Makris, A. & Thomas, H. C. (1989). Occurrence of a novel translational stop codon in the pre-core core gene of HBV in anti-HBe positive patients with chronic hepatitis and persistent HBV replication. *Hepatology* **10**, 582-582.

Carman, W. F., Thursz, M., Hadziyannis, S., McIntyre, G., Colman, K., Gioustoz, A., Fattovich, G., Alberti, A. & Thomas, H. C. (1995). Hepatitis B e-antigen negative chronic active hepatitis - Hepatitis B virus core mutations occur predominantly in known antigenic determinants. *Journal of Viral Hepatitis* **2**, 77-84.

Carman, W. F., van Deursen, F. J., Mimms, L. T., Hardie, D., Coppola, R., Decker, R. & Sanders, R. (1997b). The prevalence of surface antigen variants of hepatitis B virus in Papua New Guinea, South Africa and Sardinia. *Hepatology* **26**, 1658-1666.

Carman, W. F., Zanetti, A., Karayiannis, P., Manzillo, G., Tanzi, E., Zuckerman, A. J. & Thomas, H. C. (1990a). A vaccine induced surface mutant of HBV that is replication competent. *Gut* **31**, A 591-A 591.

Carman, W. F., Zanetti, A. R., Karayiannis, P., Waters, J., Manzillo, G., Tanzi, E., Zuckerman, A. J. & Thomas, H. C. (1990b). Vaccine-induced escape mutant of hepatitis B virus. *Lancet* **336**, 325-329.

Cattaneo, R., Will, H., Hernandez, N. & Schaller, H. (1983). Signals regulating hepatitis B surface-antigen transcription. *Nature* **305**, 336-338.

Cavanaugh, V. J., Guidotti, L. G. & Chisari, F. V. (1997). Interleukin-12 inhibits hepatitis B virus replication in transgenic mice. *Journal of Virology* **71**, 3236-3243.

Chapman, K. B. & Szostak, J. W. (1994). *In vitro* selection of catalytic RNAs. *Current Opinion in Structural Biology* **4**, 618-622.

Chen, C. J., Banerjea, A. C., Haglund, K., Harmison, G. G. & Schubert, M. (1992). Inhibition of HIV-1 replication by novel multitarget ribozymes. *Annals of the New York Academy of Sciences* **660**, 271-273.

Chen, M., Hieng, S., Qian, X. B., Costa, R. & Ou, J. H. (1994). Regulation of hepatitis B virus EnhI enhancer activity by hepatocyte-enriched transcription factor HNF3. *Virology* **205**, 127-132.

Cherrington, J., Russnak, R. & Ganem, D. (1992). Upstream sequences and cap proximity in the regulation of polyadenylation in ground-squirrel hepatitis virus. *Journal of Virology* **66**, 7589-7596.

Chisari, F. V. (1989). Hepatitis B virus gene-expression in transgenic mice. *Molecular Biology & Medicine* **6**, 143-149.

Chisari, F. V. (1996). Hepatitis B virus transgenic mice - Models of viral immunobiology and pathogenesis. *Current Topics In Microbiology and Immunology* **206**, 149-173.

Chisari, F. V., Filippi, P., McLachlan, A., Milich, D. R., Riggs, M., Lee, S., Palmiter, R. D., Pinkert, C. A. & Brinster, R. L. (1986). Expression of hepatitis B virus large envelope polypeptide inhibits hepatitis B surface antigen secretion in transgenic mice. *Journal of Virology* **60**, 880-887.

Chisari, F. V., Milich, D. R., McLachlan, A., Filippi, P., Buras, J., Pinkert, C. A., Palmiter, R. D. & Brinster, R. L. (1987). Intracellular accumulation of the hepatitis

B virus large envelope polypeptide induces hepatocellular injury in transgenic mice. *Journal of Cellular Biochemistry*, 4-4.

Chisari, F. V., Milich, D. R., Tiollais, P., Pourcel, C., Palmiter, R., Pinkert, C. & Brinster, R. (1985). Development and preliminary characterization of transgenic mice carrying integrated hepatitis B virus-DNA. *Federation Proceedings* **44**, 992-992.

Chou, C. K., Wang, L. H., Lin, H. M. & Chi, C. W. (1992). Glucocorticoid stimulates hepatitis B viral gene-expression in cultured human hepatoma-cells. *Hepatology* **16**, 13-18.

Chowrira, B. M., Berzalherranz, A., Keller, C. F. & Burke, J. M. (1993). 4 ribose 2'-hydroxyl groups essential for catalytic function of the hairpin ribozyme. *Journal of Biological Chemistry* **268**, 19458-19462.

Christian, E. L. & Yarus, M. (1993). Metal coordination sites that contribute to structure and catalysis in the group-I intron from *Tetrahymena*. *Biochemistry* **32**, 4475-4480.

Cirelli, R., Herne, K., McCrary, M., Lee, P. & Tyring, S. K. (1996). Famciclovir - Review of clinical efficacy and safety. *Antiviral Research* **29**, 141-151.

Civitico, G., Shaw, T. & Locarnini, S. (1996). Interaction between ganciclovir and foscarnet as inhibitors of duck hepatitis B virus-replication *in vitro*. *Antimicrobial Agents and Chemotherapy* **40**, 1180-1185.

Colacino, J. M. (1996). Mechanisms for the anti-hepatitis B virus activity and mitochondrial toxicity of fialuridine (Fiau). *Antiviral Research* **29**, 125-139.

Colledge, D., Locarnini, S. & Shaw, T. (1997). Synergistic inhibition of hepadnaviral replication by lamivudine in combination with penciclovir *in vitro*. *Hepatology* **26**, 216-225.

Cotten, M. & Birnstiel, M. L. (1989). Ribozyme mediated destruction of RNA *in vivo*. *EMBO Journal* **8**, 3861-3866.

Crisell, P., Thompson, S. & James, W. (1993). Inhibition of HIV-1 replication by ribozymes that show poor activity *in vitro*. *Nucleic Acids Research* **21**, 5251-5255.

Crooke, R. M., Graham, M. J., Cooke, M. E. & Crooke, S. T. (1995). *In vitro* pharmacokinetics of phosphorothioate antisense oligonucleotides. *Journal of Pharmacology and Experimental Therapeutics* **275**, 462-473.

Daikoku, M., Nakata, K., Hamasaki, K., Ido, A., Nakao, K., Kato, Y. J., Koga, M., Yano, M. & Nagataki, S. (1995). Analysis of wild-type and e-antigen defective hepatitis B viruses during the course of a short-term corticosteroid therapy in chronic hepatitis B. *Journal of Medical Virology* **47**, 184-188.

Dannaoui, E., Trepo, C. & Zoulim, F. (1997). Inhibitory effect of penciclovir-triphosphate on duck hepatitis B virus reverse transcription. *Antiviral Chemistry & Chemotherapy* **8**, 38-46.

Daros, J. A., Marcos, J. F., Hernandez, C. & Flores, R. (1994). Replication of avocado sunblotch viroid - Evidence for a symmetrical pathway with 2 rolling circles and hammerhead ribozyme processing. *Proceedings of the National Academy of Sciences of the United States of America* **91**, 12813-12817.

Davis, H. L. (1996). DNA-based vaccination against hepatitis B virus. *Advanced Drug Delivery Reviews* **21**, 33-47.

Davis, H. L., Millan, C. L. B., Mancini, M., McCluskie, M. J., Hadchouel, M., Comanita, L., Tiollais, P., Whalen, R. G. & Michel, M. L. (1997). DNA based immunization against hepatitis B surface antigen (HBsAg) in normal and HBsAg-transgenic mice. *Vaccine* **15**, 849-852.

Debruin, W. C. C., Hertogs, K., Leenders, W. P. J., Depla, E. & Yap, S. H. (1995). Hepatitis B virus - Specific binding and internalization of small HBsAg by human hepatocytes. *Journal of General Virology* **76**, 1047-1050.

Delcanho, R., Grosheide, P. M., Schalm, S. W., Devries, R. R. P. & Heijtink, R. A. (1994). Failure of neonatal hepatitis B vaccination - The role of HBV-DNA levels in hepatitis B carrier mothers and HLA antigens in neonates. *Journal of Hepatology* **20**, 483-486.

Denman, R. B. (1996). Facilitator oligonucleotides increase ribozyme RNA-binding to full-length RNA substrates *in vitro*. *FEBS Letters* **382**, 116-120.

Denman, R. B., Purow, B., Rubenstein, R. & Miller, D. L. (1992). Hammerhead ribozyme cleavage of hamster prion pre-messenger RNA in complex cell-free model systems. *Biochemical and Biophysical Research Communications* **186**, 1171-1177.

Dikstein, R., Faktor, O., Benlevy, R. & Shaul, Y. (1990a). Functional organization of the hepatitis B virus enhancer. *Molecular and Cellular Biology* **10**, 3683-3689.

Dikstein, R., Faktor, O. & Shaul, Y. (1990b). Hierarchical and cooperative binding of the rat liver nuclear protein C/EBP at the hepatitis B virus enhancer. *Molecular and Cellular Biology* **10**, 4427-4430.

Dimartino, V., Lunel, F., Cadranel, J. F., Hoang, C., Parlier, Y., Lecharpentier, Y. & Opolon, P. (1996). Long-term effects of interferon alpha in 5 HIV-positive patients with chronic hepatitis B. *Journal of Viral Hepatitis* **3**, 253-260.

Dopheide, T. A. A. & Azad, A. A. (1996). The hepatitis B virus X protein is a potent AMP kinase. *Journal of General Virology* **77**, 173-176.

Durrenberger, F. & Rochaix, J. D. (1991). Chloroplast ribosomal intron of *Chlamydomonas reinhardtii - in vitro* self-splicing, DNA endonuclease activity and *in vivo* mobility. *EMBO Journal* **10**, 3495-3501.

Emerick, V. L. & Woodson, S. A. (1993). Self-splicing of the *Tetrahymena* pre-ribosomal RNA is decreased by misfolding during transcription. *Biochemistry* **32**, 14062-14067.

Escude, C., Nguyen, C. H., Mergny, J. L., Sun, J. S., Bisagni, E., Garestier, T. & Helene, C. (1995). Selective stabilization of DNA triple helices by benzopyridoindole derivatives. *Journal of the American Chemical Society* **117**, 10212-10219.

Espinas, M. L., Jimenezgarcia, E., Martinezbalbas, A. & Azorin, F. (1996). Formation of triple-stranded DNA at D(GA-*-TC)(N) sequences prevents nucleosome assembly and is hindered by nucleosomes. *Journal of Biological Chemistry* **271**, 31807-31812.

Farza, H., Salmon, A. M., Hadchouel, M., Moreau, Babinet, C., Tiollais, P. & Pourcel, C. (1987). Hepatitis B surface antigen gene expression is regulated by sex steroids and glucocorticoids in transgenic mice. *Proceedings of the National Academy of Sciences of the United States of America* **84**, 1187-1191.

Fattovich, G., Giustina, G., Alberti, A., Guido, M., Pontisso, P., Favarato, S., Benvegnu, L. & Ruol, A. (1994). A randomized controlled trial of thymopentin therapy in patients with chronic hepatitis B. *Journal of Hepatology* **21**, 361-366.

Fauzi, H., Kawakami, J., Nishikawa, F. & Nishikawa, S. (1997). Analysis of the cleavage reaction of a *trans*-acting human hepatitis delta virus ribozyme. *Nucleic Acids Research* **25**, 3124-3130.

Fedor, M. J. & Uhlenbeck, O. C. (1990). Substrate sequence effects on hammerhead RNA catalytic efficiency. *Proceedings of the National Academy of Sciences of the United States of America* **87**, 1668-1672.

Feldherr, C. M., Kallenbach, E. & Schultz, N. (1984). Nucleocytoplasmic exchanges of endogenous proteins. *Journal of Cell Biology* **99**, A136-A136.

Feldstein, P. A. & Bruening, G. (1993). Catalytically active geometry in the reversible circularization of minimonomer RNAs derived from the complementary strand of tobacco ringspot virus satellite RNA. *Nucleic Acids Research* **21**, 1991-1998.

Felgner, P. L. (1996). Improvements in cationic liposomes for *in vivo* gene transfer. *Human Gene Therapy* **7**, 1791-1793.

Felsenfeld, G., Davies, D. R., Rich, A. (1957). *Journal of the American Chemical Society* **79**, 2023-2024.

Ferat, J. L. & Michel, F. (1993). Group-II self-splicing introns in bacteria. *Nature* **364**, 358-361.

Fischer, M., Runkel, L. & Schaller, H. (1995). HBx protein of hepatitis B virus interacts with the C-terminal portion of a novel human proteasome alpha subunit. *Virus Genes* **10**, 99-102.

Fischer, T., Aman, J., Vanderkuip, H., Rudolf, G., Peschel, C., Aulitzky, W. E. & Huber, C. (1996). Induction of interferon regulatory factors, 2'-5'-oligoadenylate synthetase, p68 kinase and RNase-L in chronic myelogenous leukemia- cells and its relationship to clinical responsiveness. *British Journal of Haematology* **92**, 595-603.

Fisher, T. L., Terhorst, T., Cao, X. D. & Wagner, R. W. (1993). Intracellular disposition and metabolism of fluorescently labeled unmodified and modified oligonucleotides microinjected into mammalian-cells. *Nucleic Acids Research* **21**, 3857-3865.

Forster, A. C. & Altman, S. (1990). External Guide Sequences for an RNA enzyme. *Science* **249**, 783-786.

Fowler, M. J. F., Monjardino, J. P., Weller, I., Tsiquaye, K. N., Zuckerman, A. & Thomas, H. C. (1982). Hepatitis B virus-replication in chronic chimpanzee carriers. *Biology of the Cell* **45**, 309-309.

Franco, A., Alvarado, V., Guidotti, L. G. & Chisari, F. V. (1996). T-helper 1 lymphocytes mediate liver-disease in hepatitis B virus transgenic mice. *FASEB Journal* **10**, 1830-1830.

Frank-Kamenetskii, M. D. & Mirkin, S. M. (1995). Triplex DNA structures. *Annual Review of Biochemistry* **64**, 65-95.

Franzen, J. S., Zhang, M. C., Chay, T. R. & Peebles, C. L. (1994). Thermal activation of a group-II intron ribozyme reveals multiple conformational states. *Biochemistry* **33**, 11315-11326.

Friedman, T. & Yee, J-K. (1995). Pseudotyped retroviral vectors for studies of human gene therapy. *Nature Medicine* **1**, 275-278.

Gallina, A., Bonelli, F., Zentilin, L., Rindi, G., Muttini, M. & Milanesi, G. (1989). A recombinant hepatitis B core antigen polypeptide with the protamine-like domain deleted self assembles into capsid particles but fails to bind nucleic acids. *Journal of Virology* **63**, 4645-4652.

Gallina, A., Dekoning, A., Rossi, F. & Milanesi, G. (1994). Intracellular retention of hepatitis B virus surface protein mutants devoid of amino-terminal pre-S1 sequences. *Journal of General Virology* **75**, 449-455.

Ganem, D. (1991). Assembly of hepadnaviral virions and subviral particles. *Current Topics in Microbiology and Immunology* **168**, 61-83.

Ganem, D. & Varmus, H. E. (1987). The molecular-biology of the hepatitis B viruses. *Annual Review of Biochemistry* **56**, 651-693.

Gao, W. Y., Han, F. S., Storm, C., Egan, W. & Cheng, Y. C. (1992). Phosphorothioate oligonucleotides are inhibitors of human DNA polymerases and RNaseH - Implications for antisense technology. *Molecular Pharmacology* **41**, 223-229.

Garcia, P. D., Ou, J. H., Rutter, W. J. & Walter, P. (1988). Targeting of the hepatitis B virus precore protein to the endoplasmic-reticulum membrane - After signal peptide cleavage translocation can be aborted and the product released into the cytoplasm. *Journal of Cell Biology* **106**, 1093-1104.

Geissler, M., Tokushige, K., Chante, C. C., Zurawski, V. R. & Wands, J. R. (1997). Cellular and humoral immune response to hepatitis B virus structural proteins in mice after DNA-based immunization. *Gastroenterology* **112**, 1307-1320.

George, S. T., Shih, A., Takle, G. B., Siony, S. & Goldberg, A. R. (1993). Ribozyme mediated cleavage of hepatitis B virus surface-antigen messenger RNA. *Journal of Cellular Biochemistry*, 212-212.

Gerlich, W. H. (1993a). Hepatitis B virus. Structure and molecular virology. In: *Viral Hepatitis*. Zuckerman, A. J. & Thomas, H. C., eds., Churchill Livingstone, New York.

Gerlich, W. H., Lu, X. & Heermann, K. H. (1993b). Studies on the attachment and penetration of hepatitis B virus. *Journal of Hepatology* **17**, S 10-S 14.

Ghosh, M. K., Ghosh, K., Dahl, O. & Cohen, J. S. (1993). Evaluation of some properties of a phosphorodithioate oligodeoxyribonucleotide for antisense application. *Nucleic Acids Research* **21**, 5761-5766.

Gilles, P. N., Guerrette, D. L., Ulevitch, R. J., Schreiber, R. D. & Chisari, F. V. (1992). HBsAg retention sensitizes the hepatocyte to injury by physiological concentrations of interferon gamma. *Hepatology* **16**, 655-663.

Giovannangeli, C., Diviacco, S., Labrousse, V., Gryaznov, S., Charneau, P. & Helene, C. (1997). Accessibility of nuclear DNA to triplex-forming oligonucleotides: The integrated HIV-1 provirus as a target. *Proceedings of the National Academy of Sciences of the United States of America* **94**, 79-84.

Giovannangeli, C., Perrouault, L., Escude, C., Thuong, N. & Helene, C. (1996). Specific inhibition of *in vitro* transcription elongation by triplex-forming oligonucleotide-intercalator conjugates targeted to HIV proviral DNA. *Biochemistry* **35**, 10539-10548.

Gish, R. G., Keeffe, E. B., Fang, J. W. S., Garcia-Kennedy, R. & Lau, J. Y. N. (1994). Ganciclovir treatment of recurrent hepatitis B virus (HBV) infection in orthotopic liver transplant (OLT) recipients. *Gastroenterology* **106**, A 899-A 899.

Gong, Z. J., DeMeyer, S., Verslype, C., Roskams, T., vanPelt, J. F., Soumillion, A., Crabbe, M. & Yap, S. H. (1997). Chronic HBV infection model *in vitro* using susceptible cells cultured in molecularporous membrane bags. *Hepatology* **26**, 740-740.

Goodarzi, G., Gross, S. C., Tewari, A. & Watabe, K. (1990). Antisense oligodeoxyribonucleotides inhibit the expression of the gene for hepatitis B virus surface antigen. *Journal of General Virology* **71**, 3021-3025.

Goodchild, J. & Kohli, V. (1991). Ribozymes that cleave an RNA sequence from human immunodeficiency virus - The effect of flanking sequence on rate. *Archives of Biochemistry and Biophysics* **284**, 386-391.

Griffin, L. C. & Dervan, P. B. (1989). Recognition of thymine-adenine base-pairs by guanine in a pyrimidine triple helix motif. *Science* **245**, 967-971.

Griffin, L. C., Kiessling, L. L., Beal, P. A., Gillespie, P. & Dervan, P. B. (1992). Recognition of all 4 base-pairs of double-helical DNA by triple-helix formation - Design of non-natural deoxyribonucleosides for pyrimidine-purine base pair binding. *Journal of the American Chemical Society* **114**, 7976-7982.

Gripon, P., Diot, C., Theze, N., Fourel, I., Loreal, O., Brechot, C. & Guguen-Guillouzo, C. (1988). Hepatitis B virus infection of adult human hepatocytes cultured in the presence of dimethylsulfoxide. *Journal of Virology* **62**, 4136-4143.

Guerrier-Takada, C., Gardiner, K., Marsh, T., Pace, N. & Altman, S. (1983). The RNA moiety Of Ribonuclease-P is the catalytic subunit of the enzyme. *Cell* **35**, 849-857.

Guerrier-Takada, C., Lumelsky, N. & Altman, S. (1989). Specific interactions in RNA enzyme-substrate complexes. *Science* **246**, 1578-1584.

Guidotti, L. G., Guilhot, S. & Chisari, F. V. (1994a). Interleukin-2 and alpha/beta interferon down-regulate hepatitis B virus gene expression *in vivo* by tumor necrosis factor-dependent and factor-independent pathways. *Journal of Virology* **68**, 1265-1270.

Guidotti, L. G., Ishikawa, T., Hobbs, M. V., Matzke, B., Schreiber, R. & Chisari, F. V. (1996a). Intracellular inactivation of the hepatitis B virus by cytotoxic T-lymphocytes. *Immunity* **4**, 25-36.

Guidotti, L. G., Martinez, V., Loh, Y. T., Rogler, C. E. & Chisari, F. V. (1994b). Hepatitis B virus nucleocapsid particles do not cross the hepatocyte nuclear-membrane in transgenic mice. *Journal of Virology* **68**, 5469-5475.

Guidotti, L. G., Matzke, B., Pasquinelli, C., Shoenberger, J. M., Rogler, C. E. & Chisari, F. V. (1996b). Hepatitis B virus (HBV) precore protein inhibits HBV replication in transgenic mice. *Journal of Virology* **70**, 7056-7061.

Guo, W. T., Chen, M., Yen, T. S. B. & Ou, J. H. (1993). Hepatocyte-specific expression of the hepatitis B virus core promoter depends on both positive and negative regulation. *Molecular and Cellular Biology* **13**, 443-448.

Hager, A. J. & Szostak, J. W. (1997). Isolation of novel ribozymes that ligate AMP-activated RNA substrates. *Chemistry & Biology* **4**, 607-617.

Hampel, A. & Cowan, J. A. (1997). A unique mechanism for RNA catalysis: the role of metal cofactors in hairpin ribozyme cleavage. *Chemistry & Biology* **4**, 513-517.

Hampel, K. J., Crosson, P. & Lee, J. S. (1991). Polyamines favor DNA triplex formation at neutral pH. *Biochemistry* **30**, 4455-4459.

Haseloff, J. & Gerlach, W. L. (1988). Simple RNA enzymes with new and highly specific endoribonuclease activities. *Nature* **334**, 585-591.

Haseloff, J. & Gerlach, W. L. (1989). Sequences required for self-catalyzed cleavage of the satellite RNA of tobacco ringspot virus. *Gene* **82**, 43-52.

Heermann, K. H., Goldmann, U., Schwartz, W., Seyffarth, T., Baumgarten, H. & Gerlich, W. H. (1984). Large surface proteins of hepatitis B virus containing the pre-S sequence. *Journal of Virology* **52**, 396-402.

Heermann, K. H., Kruse, F., Seifer, M. & Gerlich, W. H. (1987). Immunogenicity of the gene-S and pre-S domains in hepatitis B virions and HBsAg filaments. *Intervirology* **28**, 14-25.

Heidenreich, O., Benseler, F., Fahrenholz, A. & Eckstein, F. (1994). High activity and stability of hammerhead ribozymes containing 2'-modified pyrimidine nucleosides and phosphorothioates. *Journal of Biological Chemistry* **269**, 2131-2138.

Herschlag, D. (1991). Implications of ribozyme kinetics for targeting the cleavage of specific RNA molecules *in vivo* - More isn't always better. *Proceedings of the National Academy of Sciences of the United States of America* **88**, 6921-6925.

Herschlag, D., Khosla, M., Tsuchihashi, Z. & Karpel, R. L. (1994). An RNA chaperone activity of nonspecific RNA-binding proteins in hammerhead ribozyme catalysis. *EMBO Journal* **13**, 2913-2924.

Herschlag, D., Piccirilli, J. A. & Cech, T. R. (1991). Ribozyme catalyzed and nonenzymatic reactions of phosphate diesters - Rate effects upon substitution of sulfur for a nonbridging phosphoryl oxygen atom. *Biochemistry* **30**, 4844-4854.

Heusch, M., Kraus, G., Johnson, P. & Wongstaal, F. (1996). Intracellular immunization against SIV-Mac utilizing a hairpin ribozyme. *Virology* **216**, 241-244.

Hiller, B., Schlayer, H. J., Peters, T., Fehr, J., Blum, H. E. & Rasenack, J. (1995). Replication-defective HBV mutants in an immunologically negative patient. *Hepatology* **22**, 1290-1290.

Hirschman, S. Z. & Chen, C. W. (1996). Peptide nucleic acids stimulate gamma-interferon and inhibit the replication of the human immunodeficiency virus. *Journal of Investigative Medicine* **44**, 347-351.

Ho, A. D., Yu, M., Leavitt, M., Maruyama, M., Yamada, O., Young, D. & Wongstaal, F. (1994). Efficient transduction of CD34+ cells with an anti-HIV-1 ribozyme-bearing retroviral vector. *Blood* **84**, A 248.

Holland, P. V. (1996). Strategies for prevention of viral hepatitis in the United States. *International Hepatology Communications* **5**, 3-9.

Homann, M., Tzortzakaki, S., Rittner, K., Sczakiel, G. & Tabler, M. (1993). Incorporation of the catalytic domain of a hammerhead ribozyme into antisense RNA enhances its inhibitory effect on the replication of human immunodeficiency virus type 1. *Nucleic Acids Research* **21**, 2809-2814.

Honkoop, P., Deman, R. A., Francke, J., Vandeberg, J. W. O., Zondervan, P. E. & Schalm, S. W. (1996). Lack of toxicity in patients with chronic HBV infection treated with a 6 months course of lamivudine. *Hepatology* **23**, 130-P 130.

Hoofnagle, J. H. & Di Bisceglie, A. M. (1997). The treatment of chronic viral hepatitis. *New England Journal of Medicine* **336**, 347-356.

Hormes, R., Homann, M., Oelze, I., Marschal, P., Tabler, M., Eckstein, F. & Sczakiel, G. (1997). The subcellular localization and length of hammerhead ribozymes determines efficiency in human cells. *Nucleic Acids Research* **25**, 769-775.

Hourvitz, A., Mosseri, R., Solomon, A., Yehezkelli, Y., Atsmon, J., Danon, Y. L., Koren, R. & Shouval, D. (1996). Reactogenicity and immunogenicity of a new recombinant hepatitis B vaccine containing pre-S antigens - A preliminary report. *Journal of Viral Hepatitis* **3**, 37-42.

Hu, P. S. & Peterson, D. L. (1988). Location of the polymerized human serum albumin binding site on hepatitis B surface antigen (HBsAg). *FASEB Journal* **2**, A1371-A1371.

Huang, Z. & Yen, T. S. B. (1995). Role of the hepatitis B virus posttranscriptional regulatory element in export of intronless transcripts. *Molecular and Cellular Biology.* **15**, 3864-3869.

Inoue, I. (1990). Fundamental structure of group-I intron ribozyme. *Seikagaku* **62**, 338-343.

Isaacs, A. & Lindenmann, J. (1957). *Proceedings of the Royal Society B* **147**, 258.

Ishihara, K., Waters, J. A., Pignatelli, M. & Thomas, H. C. (1987). Characterization of the polymerized and monomeric human serum albumin binding sites on hepatitis B surface antigen. *Journal of Medical Virology* **21**, 89-95.

Ishikawa, T. & Ganem, D. (1995). The pre-S domain of the large viral envelope protein determines host range in avian hepatitis B viruses. *Proceedings of the National Academy of Sciences of the United States of America* **92**, 6259-6263.

Ito, Y., Asahina, Y., Wu, C. H. & Wu, G. Y. (1997). Suppression of HBV-core promoter activity by a triple-helix forming oligonucleotide. *Hepatology* **26**, 221A.

Jaeger, J. A., Turner, D. H. & Zuker, M. (1989). Improved predictions of secondary structures for RNA. *Proceedings of the National Academy of Sciences of the United States of America* **86**, 7706-7710.

Jaeger, L., Westhof, E. & Michel, F. (1993). Monitoring of the cooperative unfolding of the State University of New York group-I intron of bacteriophage T4 - The active form of the State University of New York ribozyme is stabilized by multiple interactions with 3' terminal intron components. *Journal of Molecular Biology* **234**, 331-346.

Jameel, S. & Siddiqui, A. (1986). The human hepatitis B virus enhancer requires *trans*-acting cellular factor(s) for activity. *Molecular and Cellular Biology* **6**, 710-715.

Jankowsky, E. & Schwenzer, B. (1996a). Efficient improvement of hammerhead ribozyme mediated cleavage of long substrates by oligonucleotide facilitators. *Biochemistry* **35**, 15313-15321.

Jankowsky, E. & Schwenzer, B. (1996b). Oligonucleotide facilitators may inhibit or activate a hammerhead ribozyme. *Nucleic Acids Research* **24**, 423-429.

Ji, W. & Si, C. W. (1997). Inhibition of hepatitis B virus by retroviral vectors expressing antisense RNA. *Journal of Viral Hepatitis* **4**, 167-173.

Joseph, S. & Burke, J. M. (1993). Optimization of an anti-HIV hairpin ribozyme by *in vitro* selection. *Journal of Biological Chemistry* **268**, 24515-24518.

Joshi, R. R. & Ganesh, K. N. (1994). Duplex and tripler directed DNA cleavage by oligonucleotide Cu(II)/Co(III) metallodesferal conjugates. *Biochimica Et Biophysica Acta-General Subjects* **1201**, 454-460.

Kahle, D., Kust, B. & Krupp, G. (1993). Phosphorothioates in pre-transfer RNAs can change the specificities of RNases P or reduce the cleavage efficiencies. *Biochimie* **75**, 955-962.

Kakumu, S., Ishikawa, T., Mizokami, M., Orido, E., Yoshioka, K., Wakita, T. & Yamamoto, M. (1991). Treatment with human gamma-interferon of chronic hepatitis B - Comparative study with alpha interferon. *Journal of Medical Virology* **35**, 32-37.

Kandimalla, E. R., Manning, A., Zhao, Q. Y., Shaw, D. R., Byrn, R. A., Sasisekharan, V. & Agrawal, S. (1997). Mixed backbone antisense oligonucleotides: Design, biochemical and biological properties of oligonucleotides containing 2'-5'-ribo- and 3'-5'-deoxyribonucleotide segments. *Nucleic Acids Research* **25**, 370-378.

Kane, S. A., Natrajan, A. & Hecht, S. M. (1994). On the role of the bithiazole moiety in sequence-selective DNA cleavage by Fe(II)-*-bleomycin. *Journal of Biological Chemistry* **269**, 10899-10904.

Kann, M., Thomssen, R., Kochel, H. G. & Gerlich, W. H. (1993). Characterization of the endogenous protein kinase activity of the hepatitis B virus. *Archives of Virology*, 53-62.

Karayiannis, P., Novick, D., Lok, A. S. F., Fowler, M., Monjardino, J. & Thomas, H. C. (1985). Hepatitis B virus DNA in saliva, urine, and seminal fluid of carriers of hepatitis B e-antigen. *British Medical Journal* **291**, 482-482.

Kirn, D., Heise, C., Sampson-Johannes, A., Williams, A., Munn, M., Trown, P. W. & McCormick, F. (1997). ONYX-015: An adenovirus with a deletion in the E1B 55kD gene replicates in, and causes lysis of, p53- tumor cells. *European Journal of Cancer* **33**, 119.

Klein, N. P. & Schneider, R. J. (1997). Activation of Src family kinases by hepatitis B virus HBx protein and coupled signaling to Ras. *Molecular and Cellular Biology* **17**, 6427-6436.

Klonjkowski, B., Gilardi-Hebenstreit, P., Hadchouel, J., Randrianarison, V., Boutin, S., Yeh, P., Perricaudet, M. & Kremer, E. J. (1997). A recombinant E1-deleted canine

adenoviral vector capable of transduction and expression of a transgene in human-derived cells and *in vivo*. *Human Gene Therapy* **8**, 2103-2115.

Knaus, T. & Nassal, M. (1993). The encapsidation signal on the hepatitis B virus RNA pregenome forms a stem-loop structure that is critical for its function. *Nucleic Acids Research* **21**, 3967-3975.

Knudsen, H. & Nielsen, P. E. (1996). Antisense properties of duplex-forming and triplex-forming PNAs. *Nucleic Acids Research* **24**, 494-500.

Koike, K., Moriya, K., Iino, S., Yotsuyanagi, H., Endo, Y., Miyamura, T. & Kurokawa, K. (1994). High level expression of hepatitis B virus HBx gene and hepatocarcinogenesis in transgenic mice. *Hepatology* **19**, 810-819.

Koizumi, M. & Ohtsuka, E. (1991). Effects of phosphorothioate and 2-amino groups in hammerhead ribozymes on cleavage rates and Mg^{2+} binding. *Biochemistry* **30**, 5145-5150.

Korba, B. E. (1996). *In vitro* evaluation of combination therapies against hepatitis B virus replication. *Antiviral Research* **29**, 49-51.

Korba, B. E. & Boyd, M. R. (1996). Penciclovir is a selective inhibitor of hepatitis B virus replication in cultured human hepatoblastoma cells. *Antimicrobial Agents and Chemotherapy* **40**, 1282-1284.

Korenman, J., Baker, B., Waggoner, J., Everhart, J. E., DiBisceglie, A. M. & Hoofnagle, J. H. (1991). Long-term remission of chronic hepatitis B after alpha interferon therapy. *Annals of Internal Medicine* **114**, 629-634.

Krieg, A. M., Matson, S. & Fisher, E. (1996). Oligodeoxynucleotide modifications determine the magnitude of B-cell stimulation by CpG motifs. *Antisense & Nucleic Acid Drug Development* **6**, 133-139.

Krogsgaard, K., Marcellin, P., Trepo, C., Berthelot, P., SanchezTapias, J. M., Bassendine, M., Tran, A., Ouzan, D., RingLarsen, H., Lindberg, J., Enriquez, J., Benhamou, J. P., Bindslev, N., Bertet, S., Boyer, N., Brind, A., Civeira, M. P., Housset, C., LundLaursen, A., Mas, A., Pol, S., Prieto, J., Quedens, J., Rampal, P., Schlichting, P., Soriano, G., Spacey, B. E. M., Hawley, S., Brand, C. & Howe, I. (1996). Prednisolone withdrawal therapy enhances the effect of human lymphoblastoid interferon in chronic hepatitis B. *Journal of Hepatology* **25**, 803-813.

Krone, B., Lenz, A., Heermann, K. H., Seifer, M., Lu, X. Y. & Gerlich, W. H. (1990). Interaction between hepatitis B surface proteins and monomeric human serum albumin. *Hepatology* **11**, 1050-1056.

Kruger, K., Grabowski, P. J., Zaug, A. J., Sands, J., Gottschling, D. E. & Cech, T. R. (1982). Self-splicing RNA - Auto-excision and auto-cyclization of the ribosomal-rna intervening sequence of *Tetrahymena*. *Cell* **31**, 147-157.

Kuhns, M. C., Bartholomew, M., Demedina, M., McNamara, A., Olson, J., Green, P. & Schiff, E. R. (1995). HBV marker kinetics during therapy of chronic hepatitis-B - Comparing interferon (IFN) and lamivudine (3TC). *Hepatology* **22**, 884-884.

Kuhrober, A., Wild, J., Pudollek, H. P., Chisari, F. V. & Reimann, J. (1997). DNA vaccination with plasmids encoding the intracellular (HBcAg) or secreted (HBeAg) form of the core protein of hepatitis B virus primes T cell responses to two overlapping K-b- and K-d-restricted epitopes. *International Immunology* **9**, 1203-1212.

Kuimelis, R. G. & McLaughlin, L. W. (1997). Application of a 5'-bridging phosphorothioate to probe divalent metal and hammerhead ribozyme mediated RNA cleavage. *Bioorganic & Medicinal Chemistry* **5**, 1051-1061.

Kumar, P. K. R., Suh, Y. A., Miyashiro, H., Nishikawa, F., Kawakami, J., Taira, K. & Nishikawa, S. (1992). Random mutations to evaluate the role of bases at 2 important single-stranded regions of genomic HDV ribozyme. *Nucleic Acids Research* **20**, 3919-3924.

Kumar, P. K. R., Machida, K., Urvil P. T., Kakiuchi, N., Vishnuvardhan, D., Shimotohno, K., Taira, K. & Nishikawa, S. (1997). Isolation of RNA aptamers specific to the NS3 protein of hepatitis C from a pool of completely random RNA. *Virology* **237**, 270-282.

Lai, C. L., Ching, C. K., Tung, A., Hill, A. M., Wong, B. C. Y., Lim, S. P., Dent, J. C. & Wu, P. C. (1994). Short-term lamivudine suppresses HBV DNA in Chinese HBsAg carriers. *Hepatology* **20**, A 298-A 298.

Lai, C. L., Ching, C. K., Tung, A. K. M., Li, E., Young, J., Hill, A., Wong, B. C. Y., Dent, J. & Wu, P. C. (1997). Lamivudine is effective in suppressing hepatitis B virus DNA in Chinese hepatitis B surface antigen carriers: A placebo controlled trial. *Hepatology* **25**, 241-244.

Lau, J. Y. N., Bain, V. G., Smith, H. M., Alexander, G. J. M. & Williams, R. (1992). Modulation of hepatitis B viral antigen expression by immunosuppressive drugs in primary hepatocyte culture. *Transplantation* **53**, 894-898.

Lederman, S., Sullivan, G., Benimetskaya, L., Lowy, I., Land, K., Khaled, Z., Cleary, A. M., Yakubov, L. & Stein, C. A. (1996). Polydeoxyguanine motifs in a 12-mer phosphorothioate oligodeoxynucleotide augment binding to the V3 loop of HIV-1

gp120 and potency of HIV-1 inhibition independently of G-tetrad formation. *Antisense & Nucleic Acid Drug Development* **6**, 281-289.

Lederman, S., Sullivan, G., Benimetskaya, L., Lowy, I., Land, K., Khaled, Z., Cleary, A. M., Yakubov, L. & Stein, C. A. (1997). Polydeoxyguanine motifs in a 12-mer phosphorothioate oligodeoxynucleotide augment binding to the V3loop of HIV-I gp 120 and potency of HIV-1 inhibition in dependently of G-tetrad formation (vol 6, pg 286, 1996). *Antisense & Nucleic Acid Drug Development* **7**, 131.

Lee, J. S., Latimer, L. J. P. & Hampel, K. J. (1993). Coralyne binds tightly to both T.A.T-containing and C.G.C+-containing DNA triplexes. *Biochemistry* **32**, 5591-5597.

Leenders, W. P. J., Hertogs, K., Moshage, H. & Yap, S. H. (1992). Host and tissue tropism of hepatitis B virus. *Liver* **12**, 51-55.

Lehmann, T. E., Greenberg, W. A., Liberles, D. A., Wada, C. K. & Dervan, P. B. (1997). Triple-helix formation by pyrimidine oligonucleotides containing nonnatural nucleosides with extended aromatic nucleobases: Intercalation from the major groove as a method for recognizing C* G and T*A base pairs. *Helvetica Chimica Acta* **80**, 2002-2022.

Lieber, A., He, C. Y., Polyak, S. J., Gretch, D. R., Barr, D. & Kay, M. A. (1996a). Elimination of hepatitis C virus RNA in infected human hepatocytes by adenovirus-mediated expression of ribozymes. *Journal of Virology* **70**, 8782-8791.

Lieber, A. & Kay, M. A. (1996b). Adenovirus-mediated expression of ribozymes in mice. *Journal Of Virology* **70**, 3153-3158.

Linden, R. M., Ward, P., Giraud, C., Winocour, E. & Berns, K. L. (1996). Site-specific integration by adeno-associated virus. *Proceedings of the National Academy of Sciences of the United States of America* **93**, 11288-11294.

Lo, W. Y. & Ting, L. P. (1994). Repression of enhancer-II activity by a negative regulatory element in the hepatitis B virus genome. *Journal of Virology* **68**, 1758-1764.

Locarnini, S., Guo, K., Lucas, R. & Gust, I. (1989). Inhibition of HBV DNA replication by ganciclovir in patients with AIDS. *Lancet* **2**, 1225-1226.

Lohse, P. A. & Szostak, J. W. (1996). Ribozyme-catalyzed amino acid transfer reactions. *Nature* **381**, 442-444.

Lok, A. S. F., Lai, C. L. & Leung, E. K. Y. (1990). Interferon antibodies may negate the antiviral effects of recombinant alpha-interferon treatment in patients with chronic hepatitis B virus infection. *Hepatology* **12**, 1266-1270.

Lorsch, J. R. & Szostak, J. W. (1995). *In vitro* evolution of polynucleotide kinase ribozymes. *FASEB Journal* **9**, A1422-A1422.

Lu, X. Y., Block, T. M. & Gerlich, W. H. (1996). Protease-induced infectivity of hepatitis B virus for a human hepatoblastoma cell line. *Journal of Virology* **70**, 2277-2285.

Luber, B., Hammann, C., Tabler, M. & Brechot, C. (1997). Efficiency of a hammerhead ribozyme directed against the X region of the hepatitis B virus *in vitro* and *in vivo*. *Journal of Hepatology* **26**, S68.

Luscombe, C., Pedersen, J., Uren, E. & Locarnini, S. (1996). Long-term ganciclovir chemotherapy for congenital duck hepatitis B virus infection *in vivo* - Effect on intrahepatic-viral DNA, RNA, and protein expression. *Hepatology* **24**, 766-773.

Luzi, E., Denti, M., Casarosa, S. & Barsacchi, G. (1995). The newt hammerhead ribozyme - Structure and applications. *Journal of Cellular Biochemistry*, 211-211.

Luzi, E., Eckstein, F. & Barsacchi, G. (1997). The newt ribozyme is part of a riboprotein complex. *Proceedings of the National Academy of Sciences of the United States of America* **94**, 9711-9716.

Macaya, R. F., Gilbert, D. E., Malek, S., Sinsheimer, J. S. & Feigon, J. (1991). Structure and stability of X.G.C mismatches in the 3rd strand of intramolecular triplexes. *Science* **254**, 270-274.

Machida, A., Ohnuma, H., Tsuda, F., Yoshikawa, A., Hoshi, Y., Tanaka, T., Kishimoto, S., Akahane, Y., Miyakawa, Y. & Mayumi, M. (1991). Phosphorylation in the carboxyl-terminal domain of the capsid protein of hepatitis B virus - Evaluation with a monoclonal antibody. *Journal of Virology* **65**, 6024-6030.

Machida, A., Okamoto, H., Tsuda, F., Tanaka, T., Domoto, K. & Mishiro, S. (1994). Anti-preS2 neutralizes the hepatitis B virus variant with a vaccine-escape mutation at the amino acid position-126 or position-145 within the S-gene. *International Hepatology Communications* **2**, 186-189.

Marcellin, P., Pouteau, M., Loriot, M. A., Boyer, N., Degos, F., Cales, P., Bettau, L., Bacq, Y., Coppere, H., Grange, J. D., Bernard, P. H., Degott, C., Erlanger, S. & Benhamou, J. P. (1995). Adenine arabinoside 5'-monophosphate in patients with chronic hepatitis B - Comparison of the efficacy in patients with high and low viral replication. *Gut* **36**, 422-426.

Marini, J. C. & Gerber, N. L. (1997). Osteogenesis Imperfecta- Rehabilitation and prospects for gene therapy. *Journal of the American Medical Association* **277**, 746-750.

Marinos, G., Torre, F., Gunther, S., Thomas, M. G., Will, H., Williams, R. & Naoumov, N. V. (1996). Hepatitis B virus variants with core gene deletions in the evolution of chronic hepatitis B infection. *Gastroenterology* **111**, 183-192.

Martinez-Fong, D., Mullersman, J. E., Purchio, A. F., Armendariz-Borunda, J. & Martinez-Hernandez, A. (1994). Nonenzymatic glycosylation of poly-L-lysine: A new tool for targeted gene delivery. *Hepatology* **20**, 1602-1608.

McShan, W. M. & Kinsey, B. M. (1993). Site-specific cleavage of target DNA by a triplex forming oligonucleotide conjugate containing an Auger-electron emitting atom. *FASEB Journal* **7**, A1088-A1088.

Mergny, J. L., Sun, J. S., Rougee, M., Montenay-Garestier, T., Barcelo, F., Chomilier, J. & Helene, C. (1991). Sequence specificity in triple-helix formation - Experimental and theoretical studies of the effect of mismatches on triplex stability. *Biochemistry* **30**, 9791-9798.

Michalak, T. I., Pasquinelli, C., Guilhot, S. & Chisari, F. V. (1994a). Hepatitis B virus persistence after recovery from acute viral-hepatitis. *Journal of Clinical Investigation* **93**, 230-239.

Michalak, T. I., Pasquinelli, C., Guilhot, S. & Chisari, F. V. (1994b). Hepatitis B virus persistence after recovery from acute viral-hepatitis (Vol 93, Pg 230, 1994). *Journal of Clinical Investigation* **94**, 907-907.

Milich, D. R., Jones, J. E., Hughes, J. L., Price, J., Raney, A. K. & McLachlan, A. (1990). Is a function of the surface hepatitis B antigen to induce immunologic tolerance *in utero*? *Proceedings of the National Academy of Sciences of the United States of America* **87**, 659-665.

Milich, D. R., Jones, J., Hughes, J. & Maruyama, T. (1993a). Role of T-cell tolerance in the persistence of hepatitis B virus-infection. *Journal of Immunotherapy* **14**, 226-233.

Milich, D. R., Maruyama, T., Jones, J. & Hughes, J. (1993b). Role of T-cell tolerance in the persistence of hepatitis B virus-infection. *Journal of Cellular Biochemistry*, 95-95.

Milich, D. R., Jones, J. E., Hughes, J. L., Maruyama, T., Price, J., Melhado, I. & Jirik, F. (1994). Extracellular expression of the intracellular hepatitis B core antigen results in T-cell tolerance in transgenic mice. *Journal of Immunology* **152**, 455-466

Milich, D. R., Peterson, D. L., Schodel, F., Jones, J. E. & Hughes, J. L. (1995). Preferential recognition of hepatitis B nucleocapsid antigens by Th-1 or Th-2 cells is epitope and major histocompatibility complex-dependent. *Journal of Virology* **69**, 2776-2785.

Miller, D. M., Shrestha, K. N., Rodu, B. K., Mayfield, C. A. & Gee, J. E. (1991). Intracellular triplex formation by an acridine-oligonucleotide conjugate targeted to the

c-myc promoter inhibits *c-myc* expression and proliferation of Hl-60 cells. *Clinical Research* **39**, A 863-A 863.

Miller, P. S. (1991). Oligonucleoside methylphosphonates as antisense reagents. *Bio-Technology* **9**, 358-362.

Miller, P. S. (1996). Development of antisense and antigene oligonucleotide analogs. *Progress in Nucleic Acid Research and Molecular Biology* **52**, 261-291.

Miller, W. A. & Silver, S. L. (1991). Alternative tertiary structure attenuates self-cleavage of the ribozyme in the satellite RNA of barley yellow dwarf virus. *Nucleic Acids Research* **19**, 5313-5320.

Milligan, J. F., Groebe, D. R., Witherell, G. W., Uhlenbeck, O. C. (1987). Oligoribonucleotide synthesis using T7 RNA-polymerase and synthetic DNA templates. *Nucleic Acids Research* **15**, 8783-8798.

Mishra, A., Durgapal, H., Manivel, V., Acharya, S. K., Rao, K. V. S. & Panda, S. K. (1992). Immune response to hepatitis B virus surface antigen peptides during HBV infection. *Clinical and Experimental Immunology* **90**, 194-198.

Monteith, D. K., Henry, S. P., Howard, R. B., Flournoy, S., Levin, A. A., Bennett, C. F. & Crooke, S. T. (1997). Immune stimulation - A class effect of phosphorothioate oligodeoxynucleotides in rodents. *Anti-Cancer Drug Design* **12**, 421-432.

Morishita, R., Gibbons, G. H., Ellison, K. E., Nakajima, M., Zhang, L., Kaneda, Y., Ogihara, T. & Dzau, V. J. (1993). Single intraluminal delivery of antisense cdc2 kinase and proliferating-cell nuclear antigen oligonucleotides results in chronic inhibition of neointimal hyperplasia. *Proceedings of the National Academy of Sciences of the United States of America* **90**, 8474-8478.

Morishita, R., Gibbons, G. H., Kaneda, Y., Ogihara, T. & Dzau, V. J. (1994). Pharmacokinetics of antisense oligodeoxyribonucleotides (cyclin-B-1 and cdc-2 Kinase) in the vessel wall *in vivo* - Enhanced therapeutic utility for restenosis by HVJ-liposome delivery. *Gene* **149**, 13-19.

Moriyama, T., Guilhot, S., Klopchin, K., Moss, B., Pinkert, C. A., Palmiter, R. D., Brinster, R. L., Kanagawa, O. & Chisari, F. V. (1990). Immunobiology and pathogenesis of hepatocellular injury in hepatitis B virus transgenic mice. *Science* **248**, 361-364

Moshier, J. A., Mutchnick, M. G., Dosescu, J., Holtz, T. K., Akkary, S., Mahakala, K., Merline, J. R. & Naylor, P. H. (1996). Thymosin-alpha(1), but not interferon-alpha, specifically inhibits anchorage-independent growth of hepatitis B viral transfected HepG2 cells. *Journal of Hepatology* **25**, 814-820.

Mphahlele, M. J., Shattock, A. G., Boner, W., Quinn, J., McCormick, P. A. & Carman, W. F. (1997). Transmission of a homogeneous hepatitis B virus population of A(1896)-containing strains leading to mild resolving acute hepatitis and seroconversion to hepatitis B e antigen antibodies in an adult. *Hepatology* **26**, 743-746.

Murray, J. B. & Arnold, J. R. P. (1996). Antibiotic interactions with the hammerhead ribozyme - Tetracyclins as a new class of hammerhead inhibitor. *Biochemical Journal* **317**, 855-860.

Narayan, P., Pace, U., George, S. T. & Goldberg, A. R. (1993). Nuclease resistant ribozymes against hepatitis B surface antigen messenger RNA. *Journal of Cellular Biochemistry*, 213-213.

Nassal, M. (1992a). The arginine-rich domain of the hepatitis B virus core protein is required for pregenome encapsidation and productive viral positive-strand DNA synthesis but not for virus assembly. *Journal of Virology* **66**, 4107-4116.

Nassal, M. (1992b). Conserved cysteines of the hepatitis B virus core protein are not required for assembly of replication-competent core particles nor for their envelopment. *Virology* **190**, 499-505.

Nassal, M. & Schaller, H. (1996). Hepatitis B virus replication - An update. *Journal of Viral Hepatitis* **3**, 217-226.

Naylor, P. H., Nathani, M. G. & Mutchnick, M. G. (1996). Thymosin alpha-1 associated clearance of serum HBV DNA occurs in patients with chronic hepatitis B (CHB) who have DNA levels less than 2500 pg/ml and is accompanied by a flare in serum ALT. *FASEB Journal* **10**, 33-33.

Neda, H., Wu, C. H. & Wu G. Y. (1991). Chemical modification of an ecotropic murine leukaemia virus results in redirection of its target cell specificity. *Journal of Biological Chemistry* **266**, 14143-14146.

Nedbal, W., Frey, M., Willemann, B., Zentgraf, H. & Sczakiel, G. (1997). Mechanistic insights into p53-promoted RNA-RNA annealing. *Journal of Molecular Biology* **266**, 677-687.

Nesbitt, S. & Goodchild, J. (1994). Further studies on the use of oligonucleotide facilitators to increase ribozyme turnover. *Antisense Research and Development* **4**, 243-249.

Neurath, A. R., Kent, S. B. H., Strick, N. & Parker, K. (1986). Identification and chemical synthesis of a host-cell receptor binding site on hepatitis B virus. *Cell* **46**, 429-436.

Neurath, A. R., Strick, N. & Sproul, P. (1992). Search for hepatitis B virus cell receptors reveals binding sites for interleukin-6 on the virus envelope protein. *Journal of Experimental Medicine* **175**, 461-469.

Nicklin, P. L., Ambler, J., Mitchelson, A., Bayley, D., Phillips, J. A., Craig, S. J. & Monia, B. P. (1997). Preclinical profiling of modified oligonucleotides: Anticoagulation and pharmacokinetic properties. *Nucleosides & Nucleotides* **16**, 1145-1153.

Noto, H., Fujii, Y., Takahashi, K., Kishimoto, S. & Mishiro, S. (1997). Therapeutic effect of preS2-containing vaccine in an infant infected with a vaccine-escape variant (Thr(127)) of hepatitis B virus. *International Hepatology Communications* **6**, 158-165.

Obert, S., Zachmannbrand, B., Deindl, E., Tucker, W., Bartenschlager, R. & Schaller, H. (1996). A spliced hepadnavirus RNA that is essential for virus replication. *EMBO Journal* **15**, 2565-2574.

Ochiya, T., Tsurimoto, T., Ueda, K., Okubo, K., Shiozawa, M. & Matsubara, K. (1989). An *in vitro* system for infection with hepatitis B virus that uses primary human fetal hepatocytes. *Proceedings of the National Academy of Sciences of the United States of America* **86**, 1875-1879.

Ohkawa, J., Yuyama, N., Takebe, Y., Nishikawa, S. & Taira, K. (1993). Importance of independence in ribozyme reactions - Kinetic behavior of trimmed and of simply connected multiple ribozymes with potential activity against human immunodeficiency virus. *Proceedings Of the National Academy Of Sciences Of the United States Of America* **90**, 11302-11306.

Ojwang, J. O., Hampel, A., Looney, D. J., Wongstaal, F. & Rappaport, J. (1992). Inhibition of human immunodeficiency virus type-1 expression by a hairpin ribozyme. *Proceedings of the National Academy of Sciences of the United States of America* **89**, 10802-10806.

Ou, J. H., Laub, O. & Rutter, W. J. (1986). Hepatitis B virus gene function - The precore region targets the core antigen to cellular membranes and causes the secretion of the e-antigen. *Proceedings of the National Academy of Sciences of the United States of America* **83**, 1578-1582.

Paes, H. M. & Fox, K. R. (1997). Kinetic studies on the formation of intermolecular triple helices. *Nucleic Acids Research* **25**, 3269-3274.

Pasek, M., Goto, T., Gilbert, W., Zink, B., Schaller, H., MacKay, P., Leadbetter, G. & Murray, K. (1979). Hepatitis B virus genes and their expression in *E. coli*. *Nature* **282**, 575-579.

Patzel, V., Putlitz, J. Z., Wieland, S., Blum, H. E. & Sczakiel, G. (1997). Theoretical and experimental selection parameters for HBV-directed antisense RNA are related to increased RNA-RNA annealing. *Biological Chemistry* **378**, 539-543.

Penna, A., Artini, M., Cavalli, A., Levrero, M., Bertoletti, A., Pilli, N., Chisari, F. V., Rehermann, B., Delprete, G., Fiaccadori, F. & Ferrari, C. (1996). Long-lasting memory T-cell responses following self-limited acute hepatitis B. *Journal Of Clinical Investigation* **98**, 1185-1194.

Perrotta, A. T. & Been, M. D. (1990). The self-cleaving domain from the genomic RNA of hepatitis-delta virus - Sequence requirements and the effects of denaturant. *Nucleic Acids Research* **18**, 6821-6827.

Perrotta, A. T. & Been, M. D. (1992). Cleavage of oligoribonucleotides by a ribozyme derived from the hepatitis delta virus RNA sequence. *Biochemistry* **31**, 16-21.

Persson, C., Wagner, T. H. & Nordstrom, K. (1990). Control of replication of plasmid R1: Structures and sequences of the antisense RNA, CopA, required for its binding to the target RNA, CopT. *EMBO Journal* **9**, 3767-3775.

Peterson, D. L., Nath, N. & Gavilanes, F. (1982). Structure of hepatitis B surface antigen - Correlation of subtype with amino acid sequence and location of the carbohydrate moiety. *Journal of Biological Chemistry* **257**, 414-420.

Pley, H. W., Flaherty, K. M. & McKay, D. B. (1994). 3-dimensional structure of a hammerhead ribozyme. *Nature* **372**, 68-74.

Pley, H. W., Flaherty, K. M. & McKay, D. B. (1995). 3-dimensional structure of a hammerhead ribozyme. *Journal of Cellular Biochemistry*, 204-204.

Pley, H. W., Lindes, D. S., Deluca-Flaherty, C. & McKay, D. B. (1993). Crystals of a hammerhead ribozyme. *Journal of Biological Chemistry* **268**, 19656-19658.

Plum, G. E., Pilch, D. S., Singleton, S. F. & Breslauer, K. J. (1995). Nucleic acid hybridization - Triplex stability and energetics. *Annual Review of Biophysics and Biomolecular Structure* **24**, 319-350.

Pollack, J. R. & Ganem, D. (1993). An RNA stem-loop structure directs hepatitis B virus genomic RNA encapsidation. *Journal of Virology* **67**, 3254-3263.

Postel, E. H., Flint, S. J., Kessler, D. J. & Hogan, M. E. (1991). Evidence that a triplex-forming oligodeoxyribonucleotide binds to the *c-myc* promoter in HeLa cells, thereby reducing *c-myc* messenger RNA levels. *Proceedings of the National Academy of Sciences of the United States of America* **88**, 8227-8231.

Potaman, V. N. & Sinden, R. R. (1995). Stabilization of triple-helical nucleic acids by basic oligopeptides. *Biochemistry* **34**, 14885-14892.

Prieto, M., Cordoba, J., Berenguer, M., Rayon, M., Carrasco, D., Olaso, V., Mir, J. & Berenguer, J. (1996). Famciclovir treatment of hepatitis-Bvirus (HBV) infection after liver-transplantation (OLT) - A pilot-study. *Hepatology* **24**, 1169-1169.

Qiao, M., Macnaughton, T. B. & Gowans, E. J. (1994). Adsorption and penetration of hepatitis B virus in a nonpermissive cell-line. *Virology* **201**, 356-363.

Radziwill, G., Tucker, W. & Schaller, H. (1990). Mutational analysis of the hepatitis B virus P-gene product - Domain structure and RNaseH activity. *Journal of Virology* **64**, 613-620.

Rajeev, K. G., Jadhav, V. R. & Ganesh, K. N. (1997). Triplex formation at physiological pH: Comparative studies on DNA triplexes containing 5-Me-dC tethered at N-4 with spermine and tetraethyleneoxyamine. *Nucleic Acids Research* **25**, 4187-4193.

Rao, T. S., Hogan, M. E. & Revankar, G. R. (1994). Synthesis of triple-helix forming oligonucleotides containing 2'-deoxyformycin-A. *Nucleosides and Nucleotides* **13**, 95-107.

Rappaport, J., Wongstaal, F., Ojwang, J. O., Looney, D. J., Franks, R., Richardson, M. W., Hampel, A., Notkins, A. L. & Klotman, P. E. (1993). HIV-1 targeted hairpin ribozyme - Antiviral effects and potential application to gene therapy. *Journal of Acquired Immune Deficiency Syndromes* **6**, 675-675.

Rasi, G., Mutchnick, M. G., Divirgilio, D., Sinibaldivallebona, P., Pierimarchi, P., Colella, F., Favalli, C. & Garaci, E. (1996). Combination low-dose lymphoblastoid interferon and thymosin alpha(1) therapy in the treatment of chronic hepatitis B. *Journal of Viral Hepatitis* **3**, 191-196.

Rastogi, T., Beattie, T. L., Olive, J. E. & Collins, R. A. (1996). A long-range pseudoknot is required for activity of the *Neurospora* VS ribozyme. *EMBO Journal* **15**, 2820-2825.

Rehermann, B., Lau, D., Hoofnagle, J. H. & Chisari, F. V. (1996). Cytotoxic T-lymphocyte responsiveness after resolution of chronic hepatitis B virus infection. *Journal of Clinical Investigation* **97**, 1655-1665.

Rensen, P. C. N., van Dijk, M. C. M., Havenaar, E. C., Bijsterbosch, M. K., Kruijt, J. K. & van Berkel, T. J. C. (1995). Selective targeting of antivirals by recombinant chylomicrons - A new therapeutic approach to hepatitis B. *Nature Medicine* **1**, 221-225.

Rigg, R. J. & Schaller, H. (1992). Duck hepatitis B virus infection of hepatocytes is not dependent on low pH. *Journal of Virology* **66**, 2829-2836.

Rizzetto, M. (1990). Hepatitis delta - The virus and the disease. *Journal of Hepatology* **11**, S 145-S 148.

Roggendorf, M. & Tolle, T. K. (1995). The Woodchuck - An animal model for hepatitis B virus infection in man. *Intervirology* **38**, 100-112.

Roossinck, M. J. & Siddiqui, A. (1987). *In vivo* phosphorylation and protein analysis of hepatitis B virus core antigen. *Journal of Virology* **61**, 955-961.

Rosenzweig, M., Marks, D. F., Hempel, D., Heusch, M., Kraus, G., WongStaal, F. & Johnson, R. P. (1997). Intracellular immunization of rhesus CD34(+) hematopoietic progenitor cells with a hairpin ribozyme protects T cells and macrophages from simian immunodeficiency virus infection. *Blood* **90**, 4822-4831.

Rossi, J. J., Larson, G. P., Bertrand, E., Carbonelle, C., Zhou, C. & Kohn, D. (1993). New strategies for ribozyme therapies against human retroviruses. *Journal of Cellular Biochemistry*, 194-194.

Rossol, S., Marinos, G., Carucci, P., Singer, M. V., Williams, R. & Naoumov, N. V. (1997). Interleukin-12 induction of Th1 cytokines is important for viral clearance in chronic hepatitis B. *Journal of Clinical Investigation* **99**, 3025-3033.

Roychoudhury, R., Jay, E. & Wu, R. (1976). Terminal labelling and addition of homopolymer tracts to duplex DNA fragments by terminal deoxynucleotidyl transferase. *Nucleic Acids Research* **3**, 101-116.

Ruiz, J., Wu, C. H., Ito, Y. & Wu, G. Y. (1997). Design and preparation of a multimeric self-cleaving hammerhead ribozyme. *Biotechniques* **22**, 338-345.

Saville, B. J. & Collins, R. A. (1991). RNA-mediated ligation of self-cleavage products of a *Neurospora* mitochondrial plasmid transcript. *Proceedings of the National Academy of Sciences of the United States of America* **88**, 8826-8830.

Scaglioni, P., Melegari, M., Takahashi, M., Chowdhury, J. R. & Wands, J. (1996). Use of dominant-negative mutants of the hepadnaviral core protein as antiviral agents. *Hepatology* **24**, 1010-1017.

Scaglioni, P. P., Melegari, M. & Wands, J. R. (1997). Biologic properties of hepatitis B viral genomes with mutations in the precore promoter and precore open reading frame. *Virology* **233**, 374-381.

Schaller, H. & Fischer, M. (1991). Transcriptional control of hepadnavirus gene-expression. *Current Topics In Microbiology and Immunology* **168**, 21-39.

Schalm, S. W. (1997). Clinical implications of lamivudine resistance by HBV. *Lancet* **349**, 3-4.

Schirmbeck, R., Bohm, W., Ando, K., Chisari, F. V. & Reimann, J. (1995). Nucleic acid vaccination primes hepatitis B virus surface antigen- specific cytotoxic T-lymphocytes in nonresponder mice. *Journal of Virology* **69**, 5929-5934.

Schlicht, H. J. & Schaller, H. (1988). The synthesis of e-antigens is not essential for the generation of hepatitis B virus infection. *Zentralblatt Fur Bakteriologie Mikrobiologie Und Hygiene Series A- Medical Microbiology Infectious Diseases Virology Parasitology* **269**, 114-114.

Schodel, F., Milich, D. R. & Will, H. (1990). Hepatitis B Virus nucleocapsid pre-S2 fusion proteins expressed in attenuated salmonella for oral vaccination. *Journal of Immunology* **145**, 4317-4321.

Schodel, F., Peterson, D., Hughes, J. & Milich, D. R. (1993). Avirulent salmonella expressing hybrid hepatitis B virus core/pre-S genes for oral vaccination. *Vaccine* **11**, 143-148.

Schweisguth, D. C. & Moore, P. B. (1997). On the conformation of the anticodon loops of initiator and elongator methionine tRNAs. *Journal of Molecular Biology* **267**, 505-519.

Scott, W. G., Finch, J. T. & Klug, A. (1995). The crystal structure of an all-RNA hammerhead ribozyme - A proposed mechanism for RNA catalytic cleavage. *Cell* **81**, 991-1002.

Scott, W. G., Murray, J. B., Arnold, J. R. P., Stoddard, B. L. & Klug, A. (1996). Capturing the structure of a catalytic RNA intermediate - The hammerhead ribozyme. *Science* **274**, 2065-2069.

Seeger, C., Summers, J. & Mason, W. S. (1991). Viral DNA Synthesis. *Current Topics In Microbiology and Immunology* **168**, 41-60.

Seifer, M., Heermann, K. H. & Gerlich, W. H. (1990). Expression pattern of the hepatitis B virus genome in transfected mouse fibroblasts. *Virology* **179**, 287-299.

Seifer, M., Hohne, M., Schaefer, S. & Gerlich, W. H. (1991). *In vitro* tumorigenicity of hepatitis B virus DNA and HBx protein. *Journal of Hepatology* **13**, S 61-S 65.

Seifer, M. & Standring, D. N. (1993). Recombinant human hepatitis B virus reverse transcriptase is active in the absence of the nucleocapsid or the viral replication origin, DR1. *Journal of Virology* **67**, 4513-4520.

Seifer, M. & Standring, D. N. (1995). Assembly and antigenicity of hepatitis B virus core particles. *Intervirology* **38**, 47-62.

Seth, P. (1994). Mechanism of adenovirus-mediated endosome lysis - Role of the intact adenovirus capsid structure. *Biochemical and Biophysical Research Communications* **205**, 1318-1324.

Shaw, D. R., Rustagi, P. K., Kandimalla, E. R., Manning, A. N., Jiang, Z. W. & Agrawal, S. (1997). Effects of synthetic oligonucleotides on human complement and coagulation. *Biochemical Pharmacology* **53**, 1123-1132.

Shaw, T., Mok, S. S. & Locarnini, S. A. (1996). Inhibition of hepatitis B virus DNA polymerase by enantiomers of penciclovir triphosphate and metabolic basis for selective inhibition of HBV replication by penciclovir. *Hepatology* **24**, 996-1002.

Shih, A., Mackay, B., Goldberg, A. R. & George, S. T. (1993). A novel clamp-like structure enables retargeting of a ribozyme derived from the antigenome of hepatitis delta virus and *trans*-cleavage of heterologous RNA. *Journal of Cellular Biochemistry*, 214-214.

Shimayama, T., Nishikawa, F., Nishikawa, S. & Taira, K. (1993). Nuclease resistant chimeric ribozymes containing deoxyribonucleotides and phosphorothioate linkages. *Nucleic Acids Research* **21**, 2605-2611.

Siddiqui, A., Bulla, G. & Jameel, S. (1987). Regulation of HBV gene expression. *Journal of Medical Virology* **21**, A 51-A 51.

Simon, K., Lingappa, V. R. & Ganem, D. (1988). Secreted hepatitis B surface antigen polypeptides are derived from a transmembrane precursor. *Journal of Cell Biology* **107**, 2163-2168.

Simons, M., Edelman, E. R., Dekeyser, J. L., Langer, R. & Rosenberg, R. D. (1992). Antisense *c-myb* oligonucleotides inhibit intimal arterial smooth-muscle cell accumulation *in vivo*. *Nature* **359**, 67-70.

Simons, M., Edelman, E. R. & Rosenberg, R. D. (1994). Antisense proliferating cell nuclear antigen oligonucleotides inhibit intimal hyperplasia in a rat carotid artery injury model. *Journal of Clinical Investigation* **93**, 2351-2356.

Singh, N., Gayowski, T., Wannstedt, C. F., Wagener, M. M. & Marino, I. R. (1997). Pretransplant famciclovir as prophylaxis for hepatitis B virus recurrence after liver transplantation. *Transplantation* **63**, 1415-1419.

Sioud, M. (1994). Interaction between tumor necrosis factor alpha ribozyme and cellular proteins - Involvement in ribozyme stability and activity. *Journal of Molecular Biology* **242**, 619-629.

Solinas, A., Cossu, P., Poddighe, P., Tocco, A., Deplano, A., Garrucciu, G. & Diana, M. S. A. (1993). Changes of serum 2',5'-oligoadenylate synthetase activity during interferon treatment of chronic hepatitis-C. *Liver* **13**, 253-258.

Song, Y. K., Liu, F., Chu, S. Y. & Liu, D. X. (1997). Characterization of cationic liposome-mediated gene transfer *in vivo* by intravenous administration. *Human Gene Therapy* **8**, 1585-1594.

Soni, P. N., Brown, D., Saffie, R., Moore, D., Gregoriadis, G. & Dusheiko, G. M. (1995). Pharmacokinetics of free and liposome-entrapped phosphorothioate antisense oligonucleotides in ducks - A model for antisense therapy of hepatitis B. *Hepatology* **22**, 889-889.

Soni, P. N., Brown, D., Saffie, R., Moore, D., Gregoriadis, G. & Dusheiko, G. M. (1997). Antiviral efficacy of liposome-entrapped antisense oligodeoxynucleotides for the in vivo inhibition of duck hepatitis B virus infection. *Hepatology* **26**, 1183-1183.

Soni, P. N., Brown, D., Saffie, R., Moore, D., Savage, K., Gregoriadis, G. & Dusheiko, G. M. (1996). Plasma-clearance, organ uptake, urine excretion and hepatic distribution of free and liposome-entrapped phosphorothioate antisense oligonucleotides in ducks. *Hepatology* **23**, T 61-T 61.

Steinecke, P., Steger, G. & Schreier, P. H. (1994). A stable hammerhead structure is not required for endonucleolytic activity of a ribozyme *in vivo*. *Gene* **149**, 47-54.

Stephenson, M. L. & Zamecnik, P. C. (1978). Inhibition of Rous sarcoma viral RNA translation by a specific oligodeoxyribonucleotide. *Proceedings of the National Academy of Sciences of the United States of America* **75**, 285-288.

Stibbe, W. & Gerlich, W. H. (1983a). Characterization of pre-S gene products in hepatitis B surface antigen. *Developments In Biological Standardization* **54**, 33-43.

Stibbe, W. & Gerlich, W. H. (1983b). Structural relationships between minor and major proteins of hepatitis B surface antigen. *Journal of Virology* **46**, 626-628.

Stilz, H. U. & Dervan, P. B. (1993). Specific recognition of CG base-pairs by 2-deoxynebularine within the purine.purine.pyrimidine triple-helix motif. *Biochemistry* **32**, 2177-2185.

Stirk, H. J., Thornton, J. M. & Howard, C. R. (1992). A topological model for hepatitis B surface antigen. *Intervirology* **33**, 148-158.

StollBecker, S., Repp, R., Glebe, D., Schaeffer, S., Kreuder, J., Kann, M., Lampert, F. & Gerlich, W. H. (1997). Transcription of hepatitis B virus in peripheral blood mononuclear cells from persistently infected patients. *Journal of Virology* **71**, 5399-5407.

Su, F. & Schneider, R. J. (1997). Hepatitis B virus HBx protein sensitizes cells to apoptotic killing by tumor necrosis factor alpha. *Proceedings of the National Academy of Sciences of the United States of America* **94**, 8744-8749.

Su, T. S., Lai, C. J., Huang, J. L., Lin, L. H., Yauk, Y. K., Chang, C. M., Lo, S. J. & Han, S. H. (1989). Hepatitis B virus transcript produced by RNA splicing. *Journal of Virology* **63**, 4011-4018.

Suh, E. & Waring, R. B. (1992). A phosphorothioate at the 3' splice-site inhibits the 2nd splicing step in a group-I intron. *Nucleic Acids Research* **20**, 6303-6309.

Sullenger, B. & Cech, T. (1994a). Space and time considerations for ribozyme cleavage of viral RNAs *in vivo*. *Aids Research and Human Retroviruses* **10**, S 30-S 30.

Sullenger, B. A. & Cech, T. R. (1994b). Ribozyme-mediated repair of defective messenger RNA by targeted *trans*-splicing. *Nature* **371**, 619-622.

Summerfield, J. A., Ryder, S., Sumiya, M., Thursz, M., Gorchein, A., Monteil, M. A. & Turner, M. W. (1995). Mannose binding protein gene mutations associated with unusual and severe infections in adults. *Lancet* **345**, 886-889.

Svinarchuk, F., Nagibneva, I., Chern, D., AitSiAli, S., Pritchard, L. L., Robin, P., Malvy, C. & HarelBellan, A. (1997). Recruitment of transcription factors to the target site by triplex-forming oligonucleotides. *Nucleic Acids Research* **25**, 3459-3464.

Symons, R. H., Hutchins, C. J., Forster, A. C., Rathjen, P. D., Keese, P. & Visvader, J. E. (1987). Self-cleavage of RNA in the replication of viroids and virusoids. *Journal of Cell Science*, 303-318.

Takahara, T., Hayashi, N., Katayama, K., Ueda, K., Towata, T., Kasahara, A., Fusamoto, H. & Kamada, T. (1992). Enhanced expression of HLA class I by inhibited replication of hepatitis B virus. *Journal of Hepatology* **14**, 232-236.

Takayama, K. M. & Inouye, M. (1990). Antisense RNA. *Critical Reviews in Biochemistry and Molecular Biology* **25**, 155-184.

Tallsjo, A. (1996). On the kinetics of *Escherichia coli* ribonuclease P. *University of Uppsala PhD Thesis.*

Tamizawa, J. & Som, T. (1984). Control of ColE1 plasmid replication: Enhancement of binding of RNA I to the primer transcript by the Rom protein. *Cell* **38**, 871-878.

Tang, J. & Breaker, R. R. (1997). Rational design of allosteric ribozymes. *Chemistry & Biology* **4**, 453-459.

Thomas, H. C., Weller, I. V. D., Fowler, M. & Monjardino, J. P. (1982). Analysis of hepatitis B virus replication in chronic chimpanzee carriers. *Gastroenterologie Clinique Et Biologique* **6**, 827-827.

Thomas, C. M. (1992). Regulation of gene expression by antisense RNA in bacteria. In: *Antisense RNA and DNA*. Murray, J. A. H., ed., Wiley-Liss, New York.

Thomas, T. J., Faaland, C. A., Gallo, M. A. & Thomas, T. (1995). Suppression of *c-myc* oncogene expression by a polyamine-complexed triplex-forming oligonucleotide in MCF-7 breast cancer cells. *Nucleic Acids Research* **23**, 3594-3599.

Thursz, M. R. (1997). Host genetic factors influencing the outcome of hepatitis. *Journal of Viral Hepatitis* **4**, 215-220.

Thursz, M. R., Kwiatkowski, D., Allsopp, C. E. M., Greenwood, B. M., Thomas, H. C. & Hill, A. V. S. (1995). Association between an MHC class-II allele and clearance of hepatitis-B virus in the Gambia. *New England Journal of Medicine* **332**, 1065-1069.

Tipples, G. A., Ma, M. M., Fischer, K. P., Bain, V. G., Kneteman, N. M. & Tyrrell, D. L. J. (1996). Mutation in HBV RNA-dependent DNA polymerase confers resistance to lamivudine *in vivo*. *Hepatology* **24**, 714-717.

Toulme, J. J. & Helene, C. (1988). Antimessenger oligodeoxyribonucleotides - An alternative to antisense RNA for artificial regulation of gene expression - A review. *Gene* **72**, 51-58.

Trepo, C., Hantz, O., Coupier, D., Chossegros, P., Chevallier, P. & Brette, R. (1983). Comparative tolerance and efficacy studies of ARA-A, ARA-AMP and Acyclovir on HBV replication. *Hepatology* **3**, 846-846.

Trepo, C., Jezek, P., Atkinson, G. F. & Boon, R. J. (1997). Long term efficacy of famciclovir (FCV) in chronic hepatitis B: Results of a phase IIB study. *Journal of Hepatology* **26**, S74.

Trepo, C., Ouzan, D., Fontanges, T., Chevallier, M., Chossegros, P., Degos, F., Chevallier, P. & Hantz, O. (1986). Therapeutic potential of acyclovir and of the interferons in HBV-related chronic active hepatitis due to HBV with or without HDV superinfection. *Journal of Hepatology* **3**, S 129-S 135.

Tritz, R. & Hampel, A. (1988). RNA catalytic fragments of a plant satellite RNA. *FASEB Journal* **2**, A 539-A 539.

Truant, R., Antunovic, J., Greenblatt, J., Prives, C. & Cromlish, J. A. (1995). Direct interaction of the hepatitis B virus HBx protein with p53 leads to inhibition by HBx

Wallace, L. A. & Carman, W. F. (1997). Surface gene variation of HBV: Scientific and medical relevance. *Viral Hepatitis Reviews* **3**, 5-16.

Wang, S. H., Friedman, A. E. & Kool, E. T. (1995). Origins of high sequence selectivity - A stopped flow kinetics study of DNA-RNA hybridization by duplex-forming and triplex-forming oligonucleotides. *Biochemistry* **34**, 9774-9784.

Wasenauer, G., Kock, J. & Schlicht, H. J. (1992). A cysteine and a hydrophobic sequence in the noncleaved portion of the pre-C leader peptide determine the biophysical properties of the secretory core protein (HBe protein) of human hepatitis B virus. *Journal Of Virology* **66**, 5338-5346.

Watanabe, S., Saito, S., Kojima, H., Yoshikawa, A., Suzuki, S. & Ichida, F. (1982a). Antiviral effect on chronic HBV infection by oral administration of adenine arabinoside. *Hepatology* **2**, 163-163.

Watanabe, S., Saito, S., Yoshikawa, A., Shibayama, T., Kamimura, T., Suzuki, S. & Ischida, F. (1982b). Evaluation of the antiviral effects of adenine arabinoside on chronic HBV infection. *Hepato-Gastroenterology* **29**, 102-105.

Welch, P. J., Tritz, R., Yei, S., Barber, J. & Yu, M. (1997). Intracellular application of hairpin ribozyme genes against hepatitis B virus. *Gene Therapy* **4**, 736-743.

Weller, I. V. D., Carreno, V., Fowler, M. J. F., Monjardino, J., Makinen, D., Thomas, H. C. & Sherlock, S. (1982). Acyclovir inhibits hepatitis B virus replication in Man. *Lancet* **1**, 273-273.

Weller, I. V. D., Carreno, V., Fowler, M. J. F., Monjardino, J., Makinen, D., Varghese, Z., Sweny, P., Thomas, H. C. & Sherlock, S. (1983). Acyclovir in hepatitis-B antigen-positive chronic liver disease - Inhibition of viral replication and transient renal impairment with IV bolus administration. *Journal of Antimicrobial Chemotherapy* **11**, 223-231.

Weller, I. V. D., Tedder, R. S., Karayiannis, P., Thomas, H. C. & Fiddian, A. P. (1986). A pilot study of BWA515V (6-deoxyacyclovir) in chronic hepatitis B virus infection. *Journal of Hepatology* **3**, S119-S122.

Werner, M. & Uhlenbeck, O. C. (1995). The effect of base mismatches in the substrate recognition helices of hammerhead ribozymes on binding and catalysis. *Nucleic Acids Research* **23**, 2092-2096.

Williams, D. J. (1997) Hepatitis B virus core gene deletions. *University of Glasgow PhD Thesis.*

Wilmott, R. W., Whitsett, J. A., Trapnell, B., Wert, S., Baughman, R., Cuppoletti, J. & Tolstohev, P. (1994). Gene therapy for cystic fibrosis utilizing a replication deficient

recombinant adenovirus vector to deliver the human cystic fibrosis transmembrane conductance regulator cDNA to the airways - a phase I study. *Human Gene Therapy* **5**, 1019-1057.

Wilmott, R. W., Amin, R. S., Perez, C. R., Wert, S. E., Keller, G., Boivin, G. P., Hirsch, R., Deincencio, J., Lu, P. R., Reising, S. F., Yei, S. P., Whitsett, J. A. & Trapnell, B. C. (1996). Safety of adenovirus-mediated transfer of the human cystic fibrosis transmembrane conductance regulator cDNA to the lungs of non-human primates. *Human Gene Therapy* **7**, 301-318.

Wilson, J. N., Nokes, D. J. & Carman, W. F. (1997). The evolution of vaccine resistant strains of hepatitis B virus: Predicted patterns of emergence. *Hepatology* **26**, 2004-2004.

Wolff, J. A., Malone, R. W., Williams, P., Chong, W., Acsadi, G., Jani, A. & Felgner, P. L. (1990). Direct gene transfer into mouse muscle*in vivo*. *Science* **247**, 1465-1468.

Wu, G. Y. & Wu, C. H. (1991). Inhibition of hepatitis-B viral gene-expression *in vitro* by targeted delivery of antisense oligonucleotides. *Hepatology* **14**, A 125-A 125.

Wu, H. N., Hua, Y. S. & Shueh, T. G. (1992). Mutational analysis of an ribozyme derived from hepatitis-delta virus genomic RNA. *FASEB Journal* **6**, A 490-A 490.

Wu, J. W. & Gerber, M. A. (1997). The inhibitory effects of antisense RNA on hepatitis B virus surface antigen synthesis. *Journal of General Virology* **78**, 641-647.

Wu, J. Y., Zhou, Z. Y., Judd, A., Cartwright, C. A. & Robinson, W. S. (1990). The hepatitis B virus-encoded transcriptional transactivator HBx appears to be a novel protein serine-threonine kinase. *Cell* **63**, 687-695.

Xing, Z., Mahadeviah, S. & Whitton, J. L. (1995). Antiviral activity of RNA molecules containing self-releasing ribozymes targeted to lymphocytic choriomeningitis virus. *Antisense Research and Development* **5**, 203-212.

Xing, Z. & Whitton, J. L. (1992). Ribozymes which cleave arenavirus RNAs: Identification of susceptible target sites and inhibition by target site secondary structure. *Journal of Virology*. **66**, 1361-1369.

Yaginuma, K. & Koike, K. (1989). Identification of a promoter region for 3.6-kilobase messenger-RNA of hepatitis B virus and specific cellular binding protein. *Journal of Virology* **63**, 2914-2920.

Yakubov, L., Khaled, Z., Zhang, L. M., Truneh, A., Vlassov, V. & Stein, C. A. (1993). Oligodeoxynucleotides interact with recombinant CD4 at multiple sites. *Journal of Biological Chemistry* **268**, 18818-18823.

Yamada, O., Kraus, G., Leavitt, M. C., Yu, M. & Wongstaal, F. (1994a). Activity and cleavage site-specificity of an anti-HIV-1 hairpin ribozyme in human T-cells. *Virology* **205**, 121-126.

Yamada, O., Yu, M., Yee, J. K., Kraus, G., Looney, D. & Wongstaal, F. (1994b). Intracellular immunization of human T-cells with a hairpin ribozyme against human immunodeficiency virus type-1. *Gene Therapy* **1**, 38-45.

Yao, Z. Q., Zhou, Y. X., Feng, X. M., Chen, C. X. & Guo, J. (1996a). *In vivo* inhibition of hepatitis B viral gene expression by antisense phosphorothioate oligodeoxynucleotides in athymic nude mice. *Journal of Viral Hepatitis* **3**, 19-22.

Yao, Z. Q., Zhou, Y. X., Guo, J., Feng, Z. H., Feng, X. M., Chen, C. X., Jiao, J. Z. & Wang, S. Q. (1996b). Inhibition of hepatitis B virus *in vitro* by antisense oligonucleotides. *Acta Virologica* **40**, 35-39.

Yasmin, M. (1997). The molecular biology of fulminant hepatitis B viruses. *University of Glasgow PhD Thesis.*

Yeh, C. T., Liaw, Y. F. & Ou, J. H. (1990). The arginine rich domain of hepatitis B virus pre-core and core proteins contains a signal for nuclear transport. *Journal of Virology* **64**, 6141-6147.

Yu, M., Ojwang, J., Yamada, O., Hampel, A., Rapapport, J., Looney, D. & Wongstaal, F. (1993). A hairpin ribozyme inhibits expression of diverse strains of human immunodeficiency virus type-1. *Proceedings of the National Academy of Sciences of the United States of America* **90**, 6340-6344.

Yuan, Y. & Altman, S. (1994). Selection of guide sequences that direct efficient cleavage of messenger RNA by human ribonuclease-P. *Science* **263**, 1269-1273.

Yuh, C. H., Chang, Y. L. & Ting, L. P. (1992). Transcriptional regulation of pre-core and pregenomic RNAs of hepatitis B virus. *Journal of Virology* **66**, 4073-4084.

Yuh, C. H. & Ting, L. P. (1990). The genome of hepatitis B virus contains a 2nd enhancer - Cooperation of 2 elements within this enhancer is required for its function. *Journal of Virology* **64**, 4281-4287.

Yuh, C. H. & Ting, L. P. (1991). C/EBP-like proteins binding to the functional box-alpha and box-alpha of the 2nd enhancer of hepatitis B virus. *Molecular and Cellular Biology* **11**, 5044-5052.

Yuh, C. H. & Ting, L. P. (1993). Differentiated liver cell specificity of the 2nd enhancer of hepatitis-B virus. *Journal Of Virology* **67**, 142-149.

Zaug, A. J., Been, M. D. & Cech, T. R. (1986). The *Tetrahymena* ribozyme acts like an RNA restriction endonuclease. *Nature* **324**, 429-433.

Zaug, A. J. & Cech, T. R. (1986). The *Tetrahymena* intervening sequence ribonucleic acid enzyme is a phosphotransferase and an acid phosphatase. *Biochemistry* **25**, 4478-4482.

Zhang, R. W., Lu, Z. H., Zhao, H., Zhang, X. S., Diasio, R. B., Habus, I., Jiang, Z. W., Iyer, R. P., Yu, D. & Agrawal, S. (1995). *In vivo* stability, disposition and metabolism of a hybrid oligonucleotide phosphorothioate in rats. *Biochemical Pharmacology* **50**, 545-556.

Zhou, S. & Standring, D. N. (1992a). Hepatitis B virus capsid particles are assembled from core protein dimer precursors. *Proceedings of the National Academy of Sciences of the United States of America* **89**, 10046-10050.

Zhou, S. L., Shu, Q. Y. & Standring, D. N. (1992). Characterization of hepatitis B virus capsid particle assembly in *Xenopus* oocytes. *Journal of Virology* **66**, 3086-3092.

Zhou, S. L. & Standring, D. N. (1991). Production of hepatitis B virus nucleocapsidlike core particles in *Xenopus* oocytes - Assembly occurs mainly in the cytoplasm and does not require the nucleus. *Journal of Virology* **65**, 5457-5464.

Zhou, S. L. & Standring, D. N. (1992b). Cys residues of the hepatitis B virus capsid protein are not essential for the assembly of viral core particles but can influence their stability. *Journal of Virology* **66**, 5393-5398.

Zhu, Q. R., Lu, Q., Gu, X. H., Xu, H. F. & Duan, S. C. (1997). A preliminary study on interruption of HBV transmission in uterus. *Chinese Medical Journal* **110**, 145-147.

Zignego, A. L., Fontana, R., Puliti, S., Barbagli, S., Monti, M., Careccia, G., Giannelli, F., Giannini, C., Buzzelli, G., Brunetto, M. R., Bonino, F. & Gentilini, P. (1997). Impaired response to alpha interferon in patients with an inapparent hepatitis B and hepatitis C virus coinfection. *Archives of Virology* **142**, 535-544.

Zoulim, F., Saputelli, J. & Seeger, C. (1994). Woodchuck hepatitis virus X protein is required for viral infection *in vivo*. *Journal of Virology* **68**, 2026-2030.

Zoumadakis, M. & Tabler, M. (1995). Comparative analysis of cleavage rates after systematic permutation of the NUX consensus target motif for hammerhead ribozymes. *Nucleic Acids Research* **23**, 1192-1196.